Science
AAAS

Supplementary Materials for

Synthesis and isolation of a triplet bismuthinidene with a quenched magnetic response

Yue Pang *et al*.

Corresponding authors: Frank Neese, neese@kofo.mpg.de; Josep Cornella, cornella@kofo.mpg.de

Science **380**, 1043 (2023)
DOI: 10.1126/science.adg2833

The PDF file includes:

Materials and Methods
Supplementary Text
Figs. S1 to S57
Tables S1 to S27
References

Contents

1. Materials and Methods **3**
2. Synthesis and Characterization of S1−S3, 1−4 ..... **4**
2.1. Synthesis and characterization of [M^{s}Fluind-Bi(I)]$_2$ (**S2**) 4
2.2. Synthesis and characterization of ^{t}Bu-M^{s}Fluind-Bi(I) (**2**) 10
2.3. The reaction of **2** with MeI and *N*-Me-maleimide 22
3. X-ray Crystal Structure Analysis of S1−S3, 1−3 ..... **31**
3.1. Single crystal structure analysis of M^{s}Fluind-BiCl$_2$ (**S1**) · THF solvate 31
3.2. Single crystal structure analysis of [M^{s}Fluind-Bi(I)]$_2$ (**S2**) 39
3.3. Single crystal structure analysis of ^{t}Bu-M^{s}Fluind-Br (**S3**) · cyclopentane 51
3.4. Single crystal structure analysis of ^{t}Bu-M^{s}Fluind-BiBr$_2$ (**1**) · THF 63
3.5. Single crystal structure analysis of ^{t}Bu-M^{s}Fluind-Bi(I) (**2**) 74
3.6. Single crystal structure analysis of ^{t}Bu-M^{s}Fluind- Bi(Me)I (**3**) 84
3.7. Structure search in the Cambridge Structural Database (CSD) 96
3.8. Geometry comparison of **2**: between X-ray crystal structure and DFT calculations 97
3.8.1. X-ray crystal structure of **2** versus DFT calculations on the Bi closed-shell system 97
3.8.2. X-ray crystal structure of **2** versus DFT calculations on the Bi open-shell singlet 98
3.8.3. X-ray crystal structure of **2** versus DFT calculations on the Bi-triplet 99
3.9. XRD comparison of **2** with **S2** and **S3** 101
3.9.1. Intramolecular interactions 102
3.9.2. Intermolecular interactions 103
3.9.3. Analysis of voids 105
4. X-ray absorption spectroscopy (XAS) **106**
4.1. XAS Data Collection 106
4.2. XAS Data Processing 107
5. Computational Studies of 2 ..... **110**
5.1. Computational methods 110
5.2. Computational details 111
5.3. Methods for X-ray absorption calculations 115
5.4. Computational insights into the interaction between the Bi(I) center and the ligand in **2** 116
5.5. Coordinates of the optimized structures of **2** 118
5.5.1. Coordinates of the optimized closed-shell singlet structure of **2** 118
5.5.2. Coordinates of the optimized open-shell singlet structure of **2** 121
5.5.3. Coordinates of the optimized triplet structure of **2** 124
6. References **127**

1. Materials and Methods

All experiments were conducted in flame-dried glassware under argon atmosphere by using standard Schlenk techniques or an MBraun glovebox and freshly dried and degassed solvents. All solvents (THF, THF-d_8, benzene, toluene and *n*-pentane) were distilled from sodium and stored over 4 Å molecular sieves (activated at 200 °C under a high vacuum of 1×10^{-4} bar for three days) under argon prior to use. Anhydrous $BiCl_3$ (99.9%, trace metal basis) was purchased from Alfa Aesar. Anhydrous $BiBr_3$ (97%) and cobaltocene (min. 98%) were purchased from Strem Chemicals, and cobaltocene was stored in the freezer of the glove box prior to use. All other reagents were obtained from commercial suppliers and used without further purification. ^{t}Bu-bisimine-Bi(I) (*30*), Phebox-$BiCl_2$ and Phebox-Bi(I) (*32*) for XAS studies were synthesized according to the literature methods.

NMR data were recorded using a Bruker AVIII HD 300 MHz, Bruker AVIII HD 400 MHz, Bruker AVIII 500 MHz or Bruker AVNeo 600 MHz NMR spectrometer. ^{1}H and ^{13}C chemical shifts are reported relative to the solvent residual peaks as an internal reference. For ^{1}H NMR the following residual proton peaks of the deuterated solvents were used: $CDCl_3$, $\delta_H(CHCl_3)$ 7.260; THF-d_8, $\delta_H[(CD_2)_3CHDO]$ 1.720. For ^{13}C NMR: $CDCl_3$, δ 77.16; THF-d_8, δ 25.31.

ESI-MS: ESQ 3000 (Bruker). Accurate mass determinations: Bruker APEX III FT-MS (7 T magnet) or MAT 95 (Finnigan). Melting points were measured with an EZ-Melt Automated Melting Point Apparatus from Standford Research Systems. UV-vis-NIR measurements were performed at room temperature under argon using a Cary6000i spectrophotometer equipped with an InGaAs detector. Elemental analyses (C, H, Bi) were performed by the Microanalytical Laboratory Kolbe. IR spectra were measured by using a Thermo Scientific NicoletTM iS5 Spectrometer with an ID7 ATRaccessory in a glovebox. The details of X-ray diffraction analysis, SQUID, EPR, XAS and computational studies are described in the following sections.

2. Synthesis and Characterization of S1−S3, 1−4

2.1. Synthesis and characterization of $[M^sFluind\text{-}Bi(I)]_2$ (**S2**)

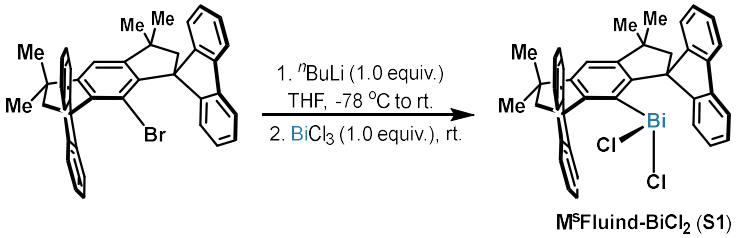

Procedure: to a solution of M^sFluind-Br (*27*) (900 mg, 1.52 mmol, in 20 mL THF), ^{n}BuLi (2.5 M in hexane, 608 μL, 1.52 mmol, 1.0 equiv.) was added dropwise at –78 °C under argon. The reaction mixture was allowed to reach to room temperature, during which the white aryllithium salt precipitated. After stirring for 2 h, $BiCl_3$ (478 mg, 1.52 mmol, 1.0 equiv., in 9 mL THF) was added into the reaction mixture, and the reaction mixture turned into a bright yellow suspension. After stirring at room temperature for 24 h, the reaction mixture was evaporated to dryness and purified by column chromatography on silica gel (*iso*-hexane/CH_2Cl_2 = 4:1, *v*/*v*, to CH_2Cl_2) to afford 772 mg M^sFluind-$BiCl_2$ (**S1**) as a yellow solid in 64% yield. **S1** was further purified by recrystallization in *n*-pentane/THF.

Characterization data of **S1**

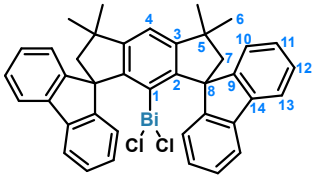

^{1}H NMR (600 MHz, THF-d_8, 298 K): δ 7.67 (s, 1H, H-4), 7.62 – 7.59 (m, 4H, H-13), 7.24 – 7.18 (m, 8H, H-10 and H-12), 7.14 (td, *J* = 7.4, 1.1 Hz, 4H, H-11), 2.34 (s, 4H, H-7), 1.57 ppm (s, 12H, H-6).

^{13}C NMR (151 MHz, THF-d_8, 298 K): δ 221.5 (C-1, br.), 161.9 (C-3), 155.5 (C-9), 155.1 (C-2), 140.5 (C-14), 128.8 (C-11), 128.6 (C-12), 126.4 (C-10), 121.5 (C-13), 119.9 (C-4), 66.6 (C-8), 60.1 (C-7), 45.0 (C-5), 32.9 ppm (C-6).

M.p.: turn red at ca. 265 °C in an argon-filled capillary.

HRMS (APPI): calc'd for $C_{40}H_{33}BiCl_2^+$ $[M]^+$ 792.17577; found 792.175190.

Anal. calc'd for $C_{40}H_{33}BiCl_2$: C, 60.54; H, 4.19; Bi, 26.33; found C, 60.79; H, 4.23; Bi, 25.87.

Stability: slightly moisture-sensitive.

XRD: single crystals of **S1** suitable for X-ray diffraction analysis were obtained by layer diffusion of *n*-hexane into a concentrated THF solution of **S1** at room temperature under argon.

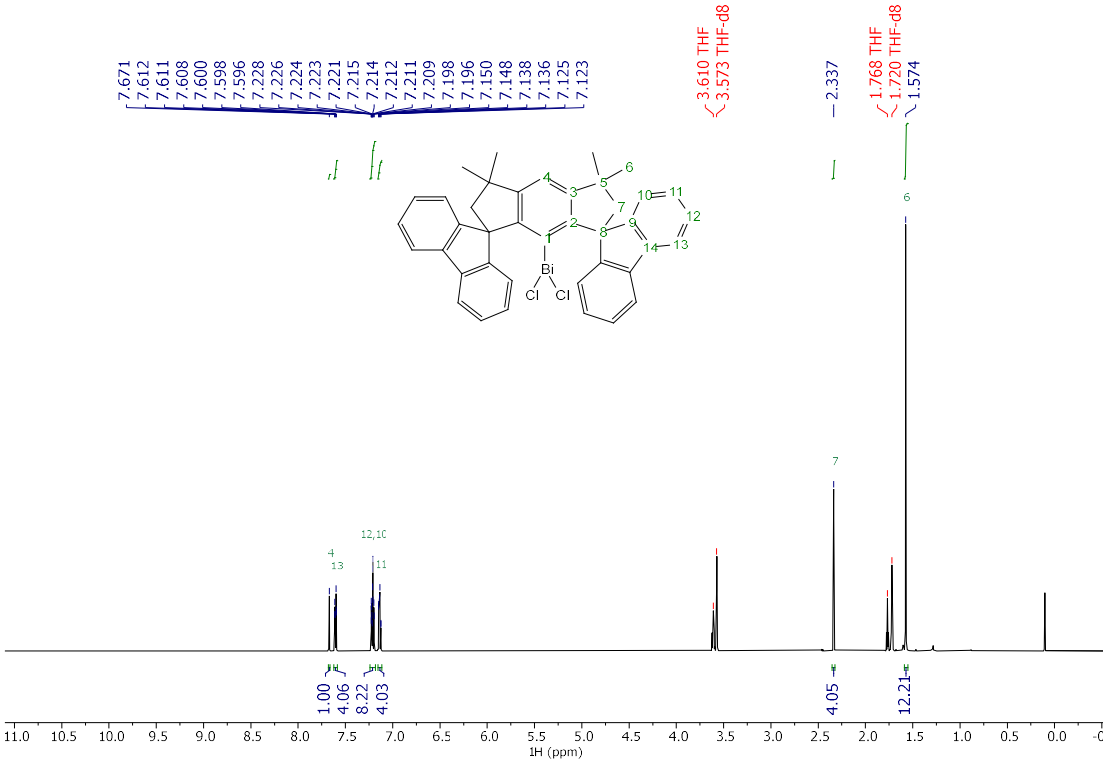

Fig. S1. ^{1}H NMR of **S1** (THF-d_8, 600 MHz, 298 K).

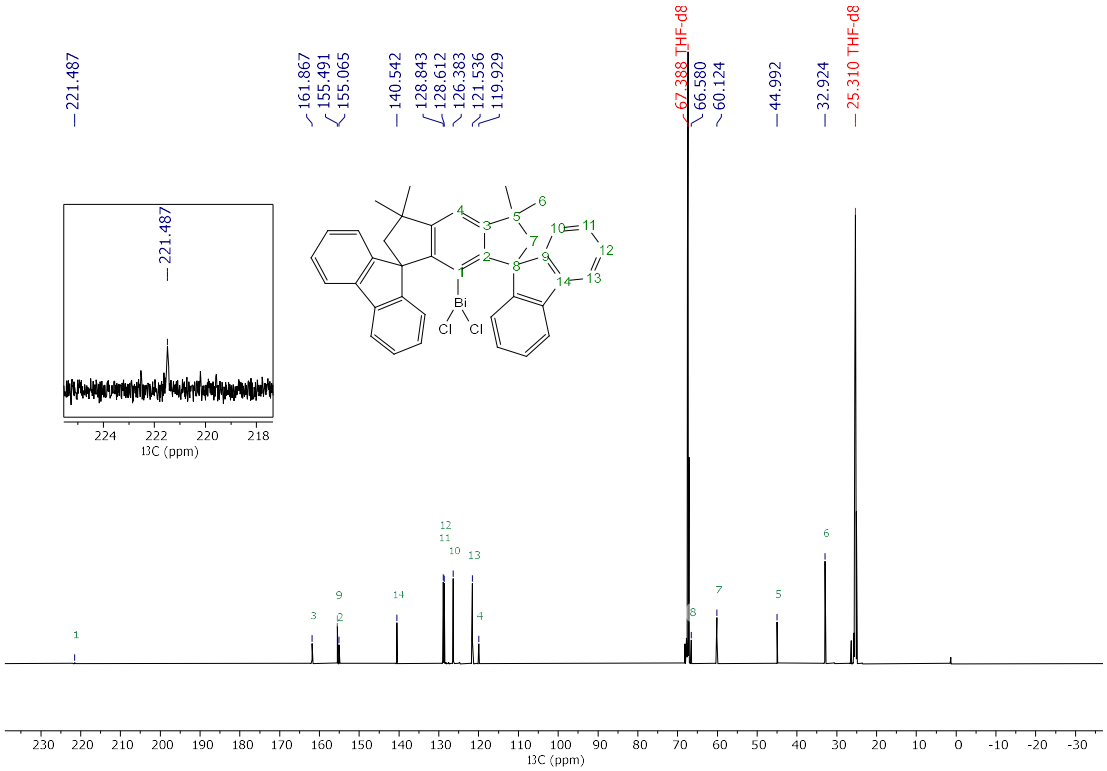

Fig. S2. ^{13}C NMR of **S1** (THF-d_8, 151 MHz, 298 K).

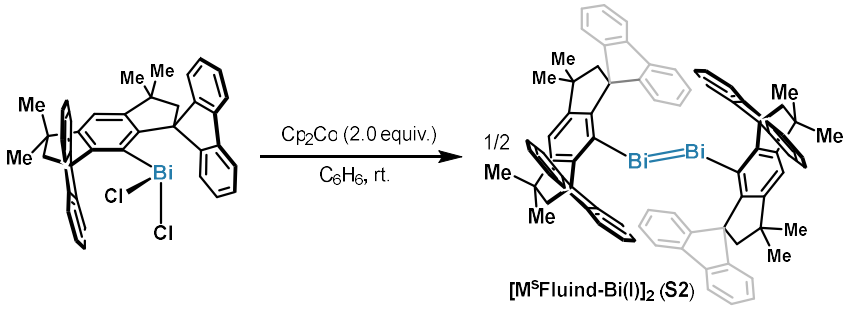

Procedure: in the glovebox, cobaltocene (286 mg, 1.51 mmol, 2.0 equiv.) was added to a suspension of **S1** (600 mg, 0.76 mmol) in 20 mL benzene under stirring, during which the solution turned dark purple and yellow cobaltocenium chloride precipitated. The reaction mixture was allowed to react for 18 h. The insoluble salt was filtered off under argon, and the solvent was removed *in vacuo*. The crude product was washed with *n*-pentane (4×15 mL) under argon and dried under high vacuum overnight, yielding 419 mg $[M^sFluind\text{-}Bi(I)]_2$ (**S2**) as a dark purple powder in 77% yield.

Characterization data of **S2**

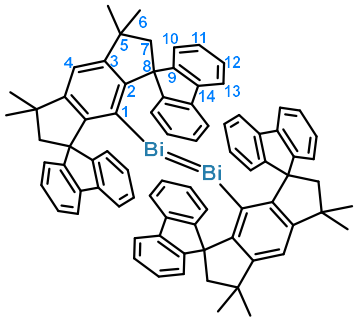

Due to dynamic behavior of **S2** (as revealed by XRD, *vide infra*), H-4 and a majority of carbons are broadened. Therefore, characterization of **S2** was performed at 233 K.

^{1}H NMR (600 MHz, THF-d_8, 233 K): δ 7.46 (d, J = 6.4 Hz, 4H, H-13), 6.97 (dd, J = 7.4, 1.3 Hz, 4H, H-12), 6.96 – 6.92 (m, 5H, H-4 and H-11), 6.74 (d, J = 7.6 Hz, 4H, H-10), 2.07 (s, 4H, H-7), 1.47 ppm (s, 12H, H-6).

^{13}C NMR (151 MHz, THF-d_8, 233 K): δ 156.3 (C-9), 155.1 (C-2), 154.3 (C-3), 142.3 (C-14), 141.9 (C-1, br.), 128.4 (C-11), 127.6 (C-12), 126.5 (C-10), 121.2 (C-13), 117.7 (C-4), 69.7 (C-8), 58.9 (C-7), 42.9 (C-5), 32.8 ppm (C-6).

M.p.: turn yellow at ca. 200 °C in an argon-filled capillary.

HRMS (APPI): calc'd for $C_{80}H_{66}Bi_2^+$ $[M]^+$ 1444.47667; found 1444.476250.

Anal. calc'd for $C_{80}H_{66}Bi_2$: C, 66.48; H, 4.60; Bi, 28.92; found C, 66.01; H, 4.59; Bi, 28.75.

Stability: The solid sample of **S2** is *gradually* oxidized in air.

XRD: single crystals of **S2** suitable for X-ray diffraction analysis were obtained by slow diffusion of *n*-pentane into a THF solution of **S2** at room temperature under argon.

DOSY-NMR:

Table S1. DOSY-NMR experiments of **S1**, **S2** and **M^{s}Fluind-Br** in THF-d_8 at 298 K.

	type	D_{pred} (SEGWE method)	D_{exp} (m^2/s)				$\frac{D_{exp}-D_{pred}}{D_{pred}}$
			$D_{exp,1}$	$D_{exp,2}$	$D_{exp,3}$	$D_{average}$	
PAY-PA-115-01	Dimer	5.81E-10 ± 1.7E-10	7.75E-10	7.66E-10	7.63E-10	**7.68E-10**	32.06%
[M^{s}Fluind-Bi(I)]$_2$	Monomer	7.89E-10 ± 2.3E-10					-2.71%
PAY-PA-115-02	Dimer	5.59E-10 ± 1.6E-10	9.20E-10	9.22E-10	9.52E-10	**9.31E-10**	66.70%
M^{s}Fluind-BiCl$_2$	Monomer	7.57E-10 ± 2.2E-10					23.09%
PAY-PA-115-03	Dimer	6.33E-10 ± 1.8E-10	9.41E-10	9.46E-10	9.43E-10	**9.43E-10**	48.99%
M^{s}Fluind-Br	Monomer	8.63E-10 ± 2.5E-10					9.24%
M^{s}Fluind-H	Dimer	6.74E-10 ± 2.0E-10	-				
	Monomer	9.22E-10 ± 2.7E-10					

The diffusion data for the measured compounds do not match the predicted values from the SEGWE method (*41, 42*). Qualitatively, the self-diffusion-coefficients of M^{s}Fluind-Br and M^{s}Fluind-BiCl$_2$ (**S1**) are on the same order of magnitude, both of which are known to be monomeric from X-ray single crystal structures. By comparison, [M^{s}Fluind-Bi(I)]$_2$ (**S2**) has a significant lower diffusion coefficient, although its molecular weight is smaller than that of **S1**. This suggests that **S2** could be dimeric in solution, as the substitution at C_{ipso} did not have a significant influence on the diffusion coefficient in the other components for the other ones. The origin of the similar self-diffusion coefficient for M^{s}Fluind-Br and **S1** could be a similar hydrodynamic radius of both species, due to the spatial shielding of the ligand scaffold. Interestingly, the predicted self-diffusion value for M^{s}Fluind-H is close to the values measured for M^{s}Fluind-Br and **S1**, which would further support this hypothesis.

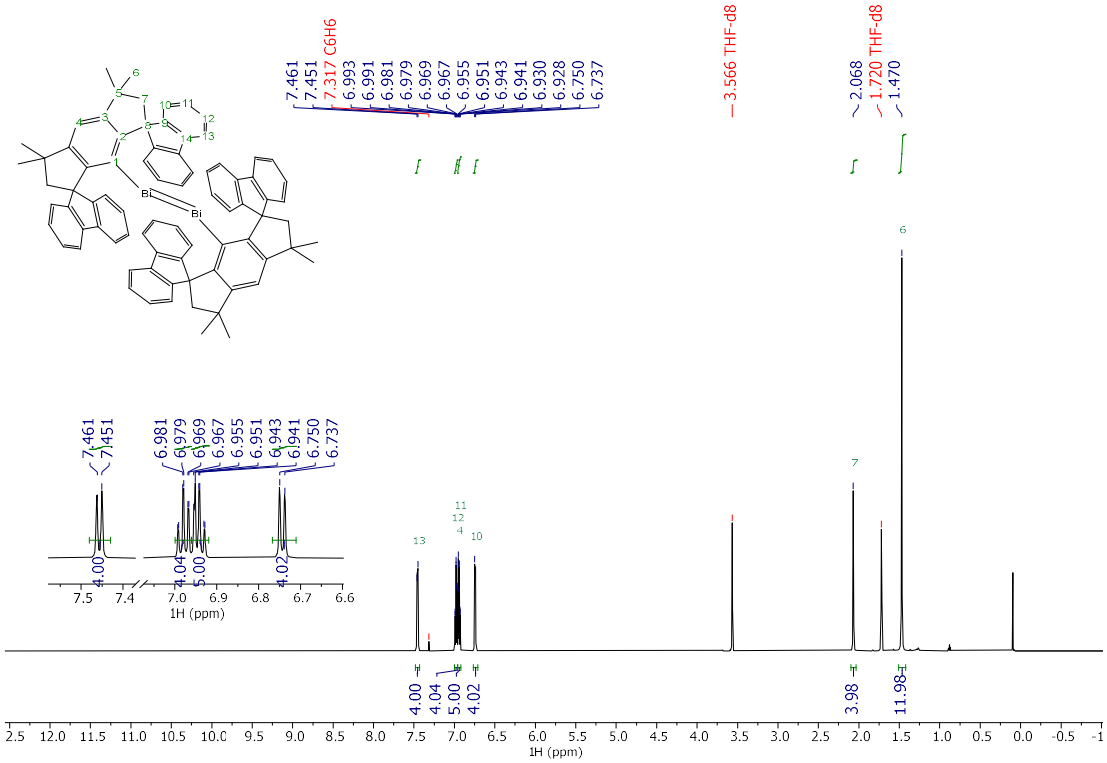

Fig. S3. ^{1}H NMR of **S2** (THF-d_8, 600 MHz, 233 K).

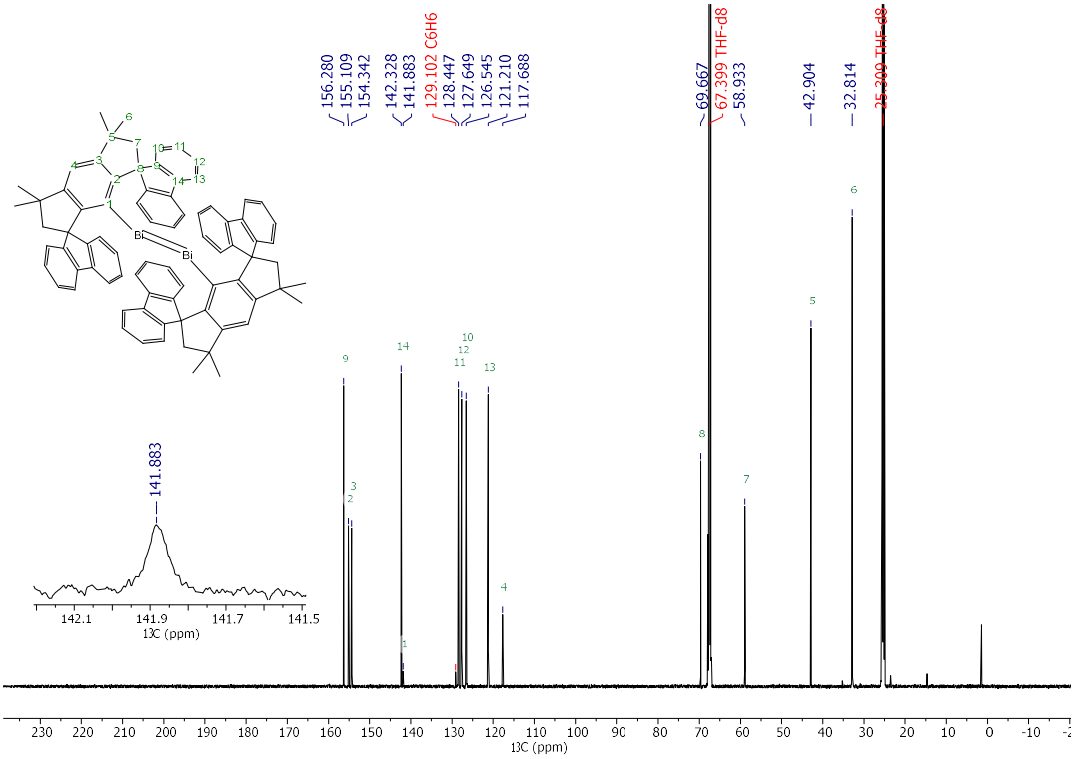

Fig. S4. ^{13}C NMR of **S2** (THF-d_8, 151 MHz, 233 K).

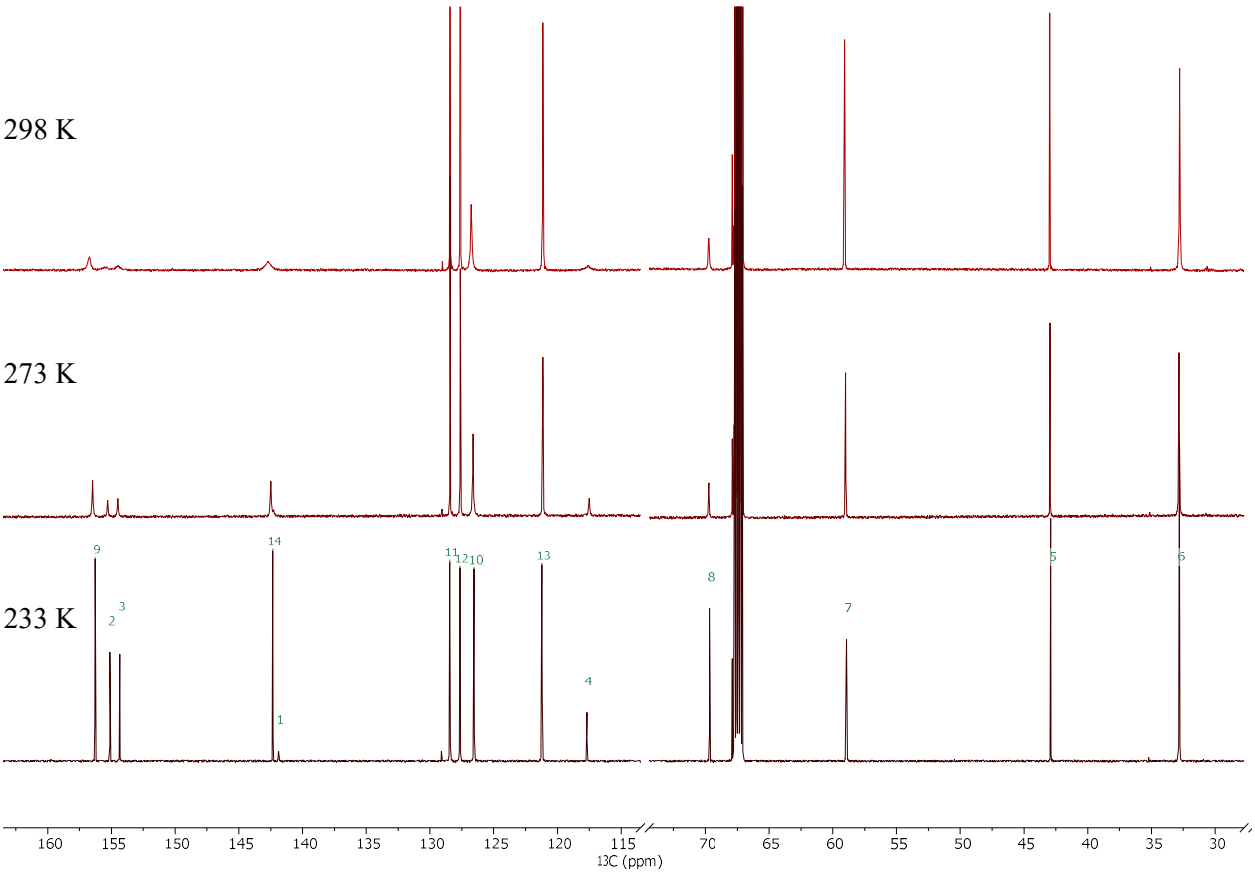

Fig. S5. VT ^{13}C NMR of **S2** (THF-d_8, 151 MHz).

2.2. Synthesis and characterization of ^{t}Bu-M^{s}Fluind-Bi(I) (**2**)

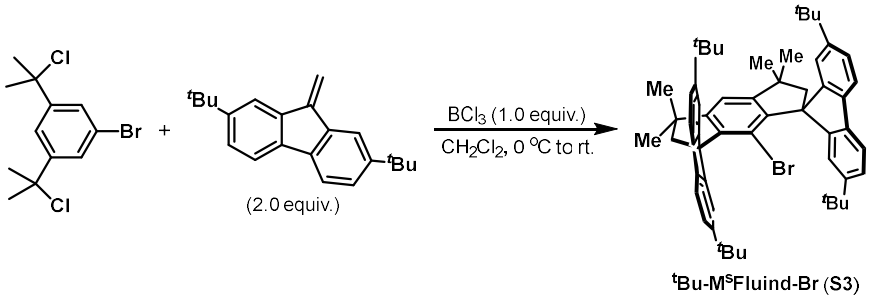

Procedure: at 0 °C, BCl_3 (1M in CH_2Cl_2, 9.7 mmol, 9.7 mL, 1.0 equiv.) was added dropwise to a solution of 1-bromo-3,5-bis(2-chloropropan-2-yl)benzene (3.0 g, 9.7 mmol) and 2,7-di-*tert*-butyl-9-methylene-9*H*-fluorene (5.62 g, 19.4 mmol, 2.0 equiv.) in 180 mL of dry CH_2Cl_2 under argon, during which the solution turned blood red. After stirring for 12 h at room temperature, the reaction mixture was quenched with 1M aq. NaOH (50 mL). After the organic layer was separated, the aqueous layer was extracted with 100 mL CH_2Cl_2. The combined organic layer was filtered through a Celite pad. After evaporation of the solvent, the crude product was washed with *n*-pentane (ca. 250 to 300 mL), yielding ^{t}Bu-M^{s}Fluind-Br (**S3**) as a white solid (6.28 g, 79%).

Characterization data of **S3**

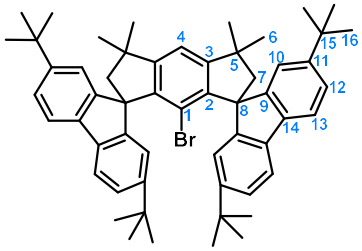

The spectral data in $CDCl_3$ match with those reported in the literature (*43*).

^{1}H NMR (600 MHz, THF-*d*$_8$, 298 K): δ 7.41 (dd, *J* = 7.9, 0.6 Hz, 4H, H-13), 7.40 (s, 1H, H-4), 7.18 (dd, *J* = 8.0, 1.8 Hz, 4H, H-12), 7.05 (dd, *J* = 1.8, 0.6 Hz, 4H, H-10), 2.42 (s, 4H, H-7), 1.61 (s, 12H, H-6), 1.20 ppm (s, 36H, H-16).

^{13}C NMR (151 MHz, THF-*d*$_8$, 298 K): δ 157.7 (C-3), 154.0 (C-9), 150.7 (C-11), 144.4 (C-2), 139.1 (C-14), 124.5 (C-12), 120.8 (C-10), 119.3 (C-13), 118.9 (C-1), 116.4 (C-4), 64.9 (C-8), 58.3 (C-7), 44.0 (C-5), 35.4 (C-15), 33.0 (C-6), 32.1 ppm (C-16).

M.p.: turn red at ca. 390 °C.

HRMS (ESI): calc'd for $C_{56}H_{65}BrNa^{+}$ $[M+Na]^{+}$ 839.416194; found 839.416010.

XRD: single crystals of **S3** suitable for X-ray diffraction analysis were obtained by slow evaporation of a diethyl ether/*iso*-hexane solution of **S3** at room temperature. *Iso*-hexane contains 0.5%-18% cyclopentane.

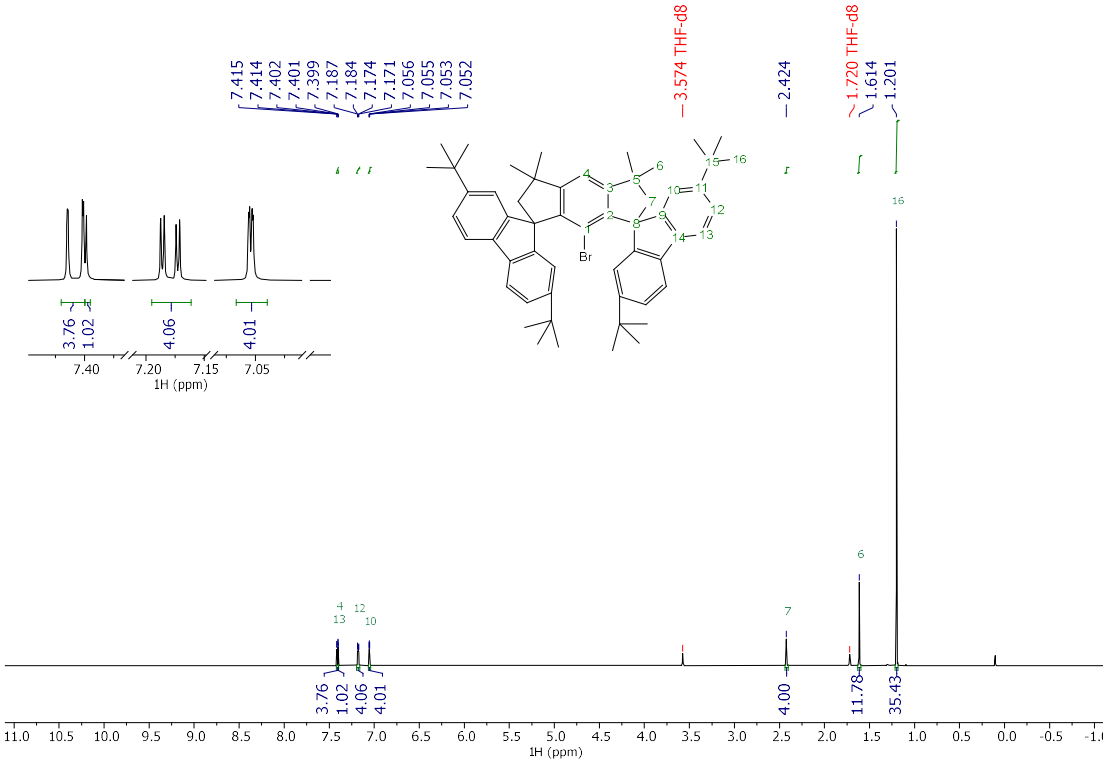

Fig. S6. ^{1}H NMR of **S3** (THF-d_8, 600 MHz, 298 K).

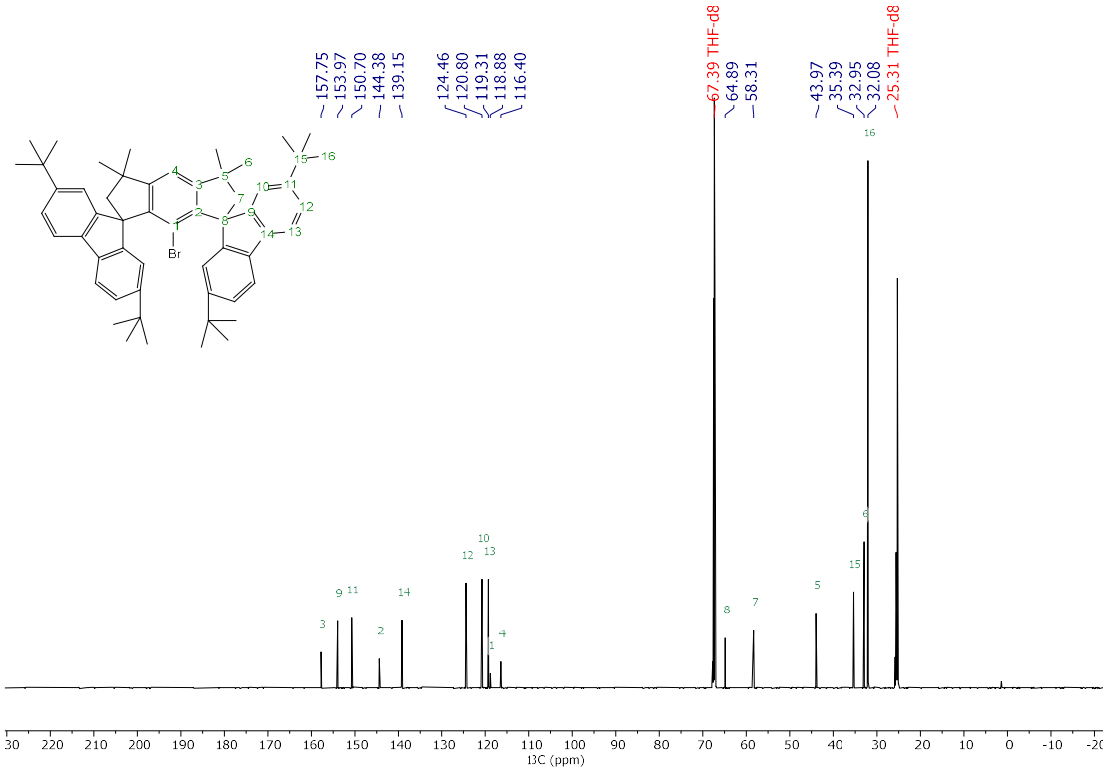

Fig. S7. ^{13}C NMR of **S3** (THF-d_8, 151 MHz, 298 K).

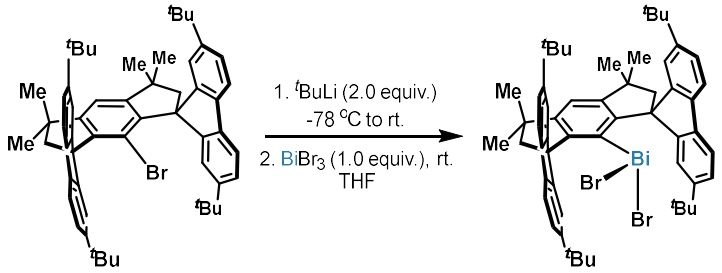

Procedure: to a suspension of **S3** (2.00 g, 2.44 mmol, 40 mL THF) at –78 °C, ^{t}BuLi (1.7 M in pentane, 2.9 mL, 4.89 mmol, 2.0 equiv.) was added dropwise under argon. The suspension was allowed to reach to room temperature. After 1 h, the reaction mixture turned into a pale brown solution. In the glovebox, $BiBr_3$ (1.10 g, 2.44 mmol, 1.0 equiv., in 20 mL THF) was added into the reaction mixture, and the reaction mixture turned into a bright yellow suspension.

After stirring at room temperature for 18h, the reaction mixture was evaporated to dryness and further purified by column chromatography on silica gel (*iso*-hexane/CH_2Cl_2 = 4:1, *v*/*v*, to CH_2Cl_2), affording 1.74 g ^{t}Bu-M^{s}Fluind-$BiBr_2$ (**1**) as a bright yellow solid in 64% yield.

Characterization data of **1**

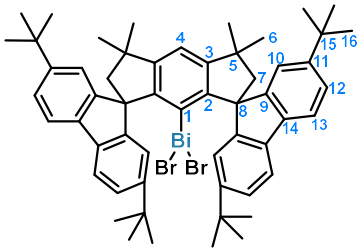

^{1}H NMR (600 MHz, THF-*d*$_8$, 298 K): δ 7.69 (s, 1H, H-4), 7.51 (d, *J* = 7.9 Hz, 4H, H-13), 7.30 (dd, *J* = 7.9, 1.9 Hz, 4H, H-12), 7.23 (d, *J* = 1.9 Hz, 4H, H-10), 2.34 (s, 4H, H-7), 1.61 (s, 12H, H-6), 1.24 ppm (s, 36H, H-16).

^{13}C NMR (151 MHz, THF-*d*$_8$, 298 K): δ 208.9 (C-1, br.), 161.5 (C-3, br.), 155.6 (C-9), 154.9 (C-2), 151.8 (C-11, br.), 137.7 (C-14, br.), 126.3 (C-12, br.), 122.9 (C-10), 121.4 (C-13, br.), 119.8 (C-4), 66.5 (C-8, br.), 60.5 (C-7. br.), 45.0 (C-5, br.), 35.6 (C-15), 32.9 (C-6), 32.0 ppm (C-16).

M.p.: turn dark yellow-green at ca. 294 °C in an argon-filled capillary.

HRMS (ESI): calc'd for $C_{56}H_{65}BiBr^+$ $[M\text{-}Br]^+$ 1025.40681; found 1025.40643.

Anal. calc'd for $C_{56}H_{65}BiBr_2$: C, 60.76; H, 5.92; Bi, 18.88; found C, 60.67; H, 5.95; Bi, 18.82.

Stability: slightly moisture- and light-sensitive.

XRD: single crystals of **1** suitable for X-ray diffraction analysis were obtained by slow diffusion of *n*-hexane into a THF solution of **1** at room temperature under argon.

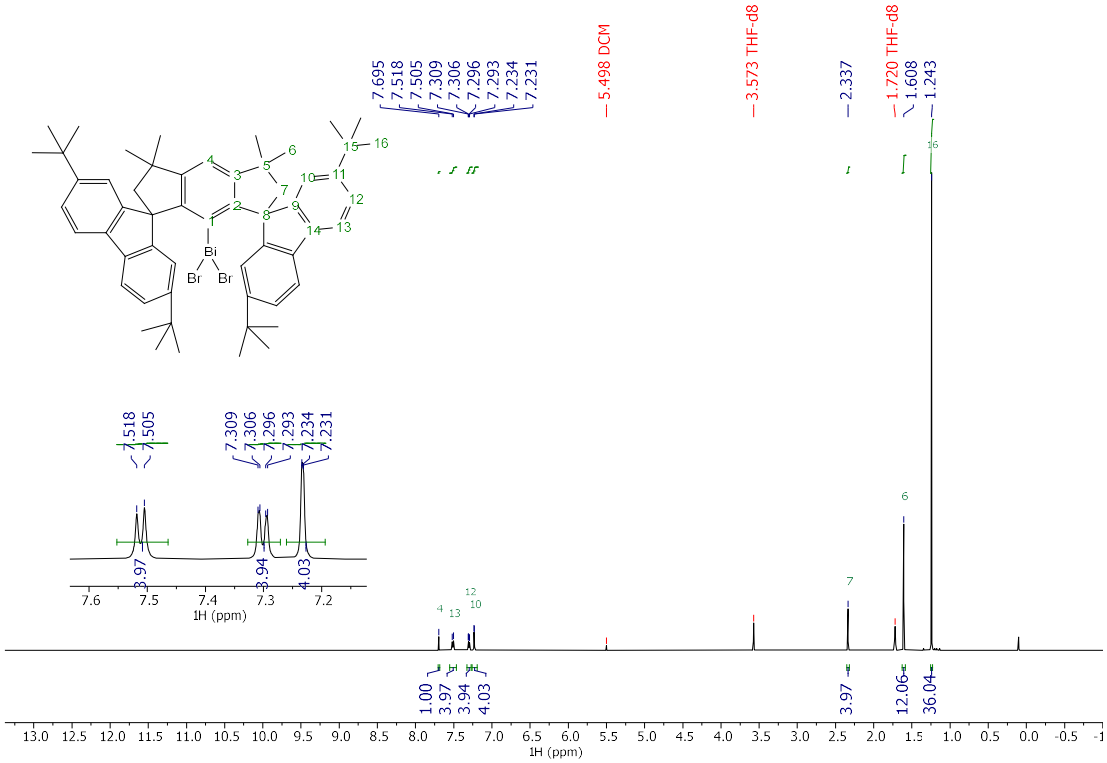

Fig. S8. ^{1}H NMR of **1** (THF-d_8, 600 MHz, 298 K)

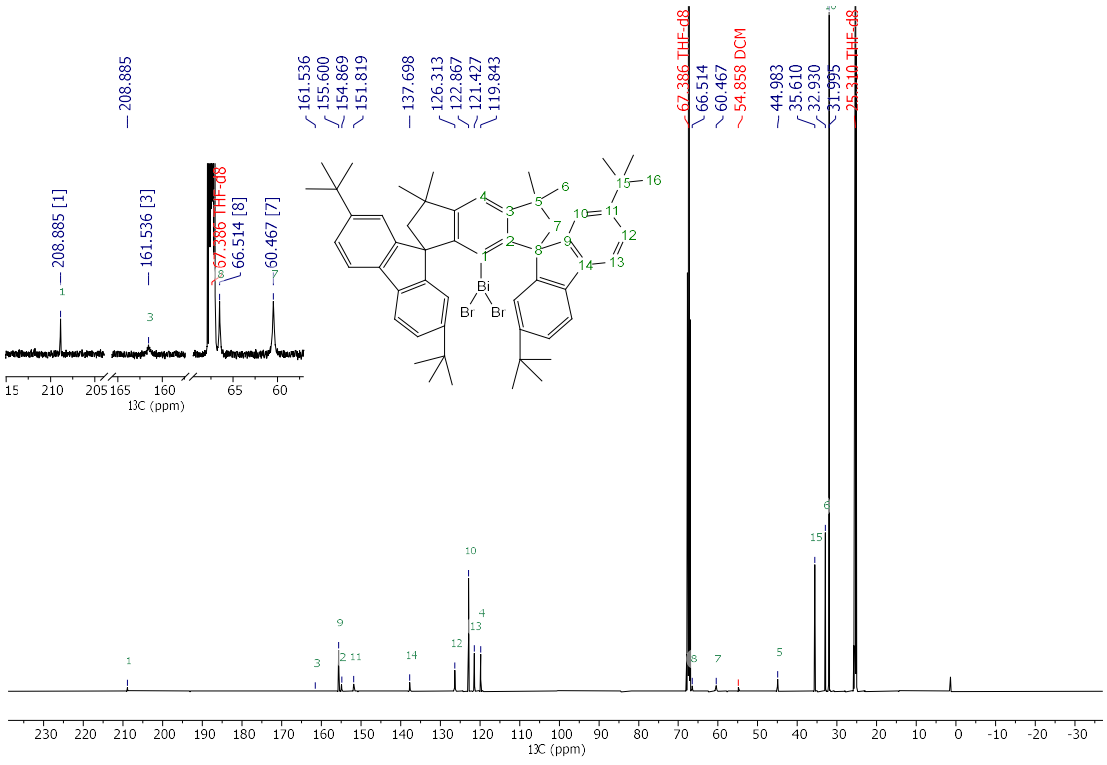

Fig. S9. ^{13}C NMR of **1** (THF-d_8, 151 MHz, 298 K)

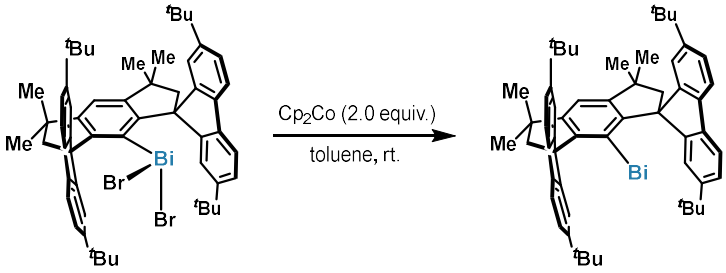

NMR scale reaction: in the glovebox, cobaltocene (10.3 mg, 54.2 µmol, 2.0 equiv.) was added to a suspension of **1** (30 mg, 27.1 µmol, 1.2 mL THF-d_8). After stirring for 10 min, the reaction mixture was filtered into a J. Young NMR tube for NMR studies.

^{1}H and ^{13}C NMR at 298 K showed a clean formation of ^{t}Bu-M^{s}Fluind-Bi(I) (**2**), and residual Cp_2Co was not detected [^{1}H NMR: δ –50.75 ppm (br.); ^{13}C NMR: δ 610.3 ppm (br.)], suggesting a two-electron reduction at the Bi center.

Preparative reaction: in the glovebox, a solution of cobaltocene (478 mg, 2.53 mmol, 2.0 equiv., in 16 mL toluene) was added dropwise to a suspension of **1** (1.40 g, 1.26 mmol, in 90 mL toluene) under stirring. The reaction mixture was allowed to react for 18 h at room temperature, during which the solution turned pale yellow and cobaltocenium bromide precipitated. The insoluble salt was filtered off under argon, and the solvent was removed *in vacuo*. The crude product was washed with *n*-pentane (4×15 mL) under argon and dried under high vacuum overnight, yielding ^{t}Bu-M^{s}Fluind-Bi(I) (**2**) as a bright yellow powder (970 mg, 81%). **2** contains 3%-5% oxo-bismuth impurities, and can be further purified by slow diffusion of *n*-pentane into a THF solution of **2** under argon over ten days, yielding **2** in the pure form as single crystals.

Characterization data of **2**

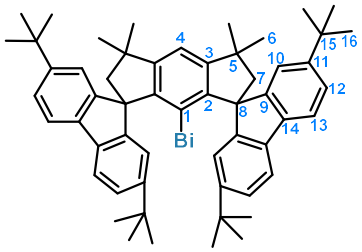

^{1}H NMR (600 MHz, THF-d_8, 298 K): δ 8.05 (dd, J = 7.8, 0.5 Hz, 4H, H-13), 7.50 (dd, J = 7.9, 1.9 Hz, 4H, H-12), 6.73 (dd, J = 1.9, 0.5 Hz, 4H, H-10), 1.69 (s, 4H, H-7), 1.67 (s, 36H, H-16), 1.04 (s, 12H, H-6), –1.06 ppm (s, 1H, H-4).

^{13}C NMR (151 MHz, THF-d_8, 298 K): δ 234.0 (C-2), 177.7 (C-9), 176.9 (C-14), 160.0 (C-4), 151.8 (C-11), 135.6 (C-10), 127.0 (C-12), 123.8 (C-13), 114.5 (C-3), 62.2 (C-8), 57.2 (C-7), 44.8 (C-5), 35.8 (C-15), 33.6 (C-16), 26.9 (C-6), –203.8 ppm (C-1, br.).

M.p.: turn off white at ca. 240 °C in an argon-filled capillary.

HRMS (APPI): calc'd for $C_{56}H_{65}Bi^+$ $[M]^+$ 946.48848; found 946.48818.

Anal. calc'd for $C_{56}H_{65}Bi$: C, 71.02; H, 6.92; Bi, 22.06; found C, 70.36; H, 6.57; Bi, 21.84.

Stability: **2** is highly air-sensitive but not light-sensitive. The solid sample of **2** is stable at room temperature under argon for months. The THF-d_8 solution of **2** is stable for at least two weeks at room temperature, and no noticeable decomposition was observed at 100 ºC for ca. one day (in toluene-d_8).

XRD: single crystals of **2** suitable for X-ray diffraction analysis were obtained by slow diffusion of *n*-pentane into a THF solution of **1** at room temperature under argon.

DOSY-NMR:

Table S2. DOSY-NMR experiments of **1**, **2** and **S3** in THF-d_8 at 298 K.

	type	D_{pred} (SEGWE method)		D_{exp} (m^2/s)				$\frac{D_{exp}-D_{pred}}{D_{pred}}$
				D1	D2	D3	average	
PAY-PA-168-01	Dimer	5.18E-10	± 1.5E-10	8.49E-10	8.44E-10	8.41E-10	**8.44E-10**	62.91%
^{t}Bu-M^{s}Fluind-Bi(I)	Monomer	6.99E-10	± 2.0E-10					20.78%
PAY-PA-234-01	Dimer	4.86E-10	± 1.4E-10	8.32E-10	8.36E-10	8.06E-10	**8.25E-10**	69.79%
^{t}Bu-M^{s}Fluind-BiBr$_2$	Monomer	6.53E-10	± 1.9E-10					26.32%
PAY-PA-168-03	Dimer	5.51E-10	± 1.6E-10	8.23E-10	8.24E-10	8.19E-10	**8.22E-10**	49.04%
^{t}Bu-M^{s}Fluind-Br	Monomer	7.46E-10	± 2.2E-10					10.13%
^{t}Bu-M^{s}Fluind-H	Dimer	6.33E-10	± 1.8E-10	-				
	Monomer	8.59E-10	± 2.5E-10					

The diffusion data for the measured compounds do not match the predicted values from the SEGWE method. Qualitatively, the self-diffusion-coefficients of the **S3**, **1** and **2** are on the same order of magnitude, suggesting that **2** could be monomeric in solution. The origin of similar self-diffusion coefficients of all the species could be similar hydrodynamic radii due to the spatial shielding of the aryl rings.

Evans method (^{1}H NMR): no shift was observed when comparing pure THF-d_8 with a sample of **2** inside.

EPR: no EPR signal was detected for **2** in the following measurements.

CW EPR spectra of **2** at X-band were recorded on a Bruker Elexsys 500 CW EPR spectrometer equipped with an ER4116DM resonator and an ESR900 Oxford Helium Flow Cryostat. The modulation amplitude was set to 7.4 Gauss (maximum available for the employed resonator). The microwave power was set to 2 mW. EPR Spectra were recorded at 7K and 77K in the range between 20mT and 500 mT.

W-band pulse EPR measurements of **2** were performed using a Bruker Elexsys E680 spectrometer equipped with a homebuilt W-band extension and a cryogen free Cryogenic 6 T magnet with a variable temperature insert. ESE-detected field-swept spectra between 2.5 T and 5.5 T were measured at 10 K using the pulse sequence: t_p–τ–2t_p–τ–echo with typical values t_p = 20 ns, τ = 260 ns, and a repetition time of 1 ms.

SQUID: magnetic susceptibility data were measured with powder samples of **2** in the temperature range 1.8 – 300 K by using a SQUID magnetometer with a field of 1.0 T (MPMS-3, Quantum Design). The instrument was calibrated with a standard palladium reference sample (error <2%). The samples were filled in a glovebox into air-tight sample holders of quartz with O-ring sealed caps, and the SQUID response curves (raw data) were corrected for holder contributions by subtracting the corresponding response curves obtained from separate measurements of the holder without sample material. The experimental magnetization data obtained from independent simulation of the corrected SQUID response curves were corrected for underlying diamagnetism by the following formula –(MW/2)•10–6 cm^3 mol^{-1}, as well as for

a small amount of unaccounted for diamagnetism in the sample (using a negative value for the temperature-independent magnetism (TIP) parameter). The magnetic susceptibility was defined as $\chi_M = M_M/B$, where M_M is the molar magnetization and B is the field. Handling and simulation of the SQUID raw data as well as spin-Hamiltonian simulation of the susceptibility and magnetization data were done with our own package julX.SL (written by E.B. and available by email to daniel.santalucia@cec.mpg.de).

UV-vis-NIR:

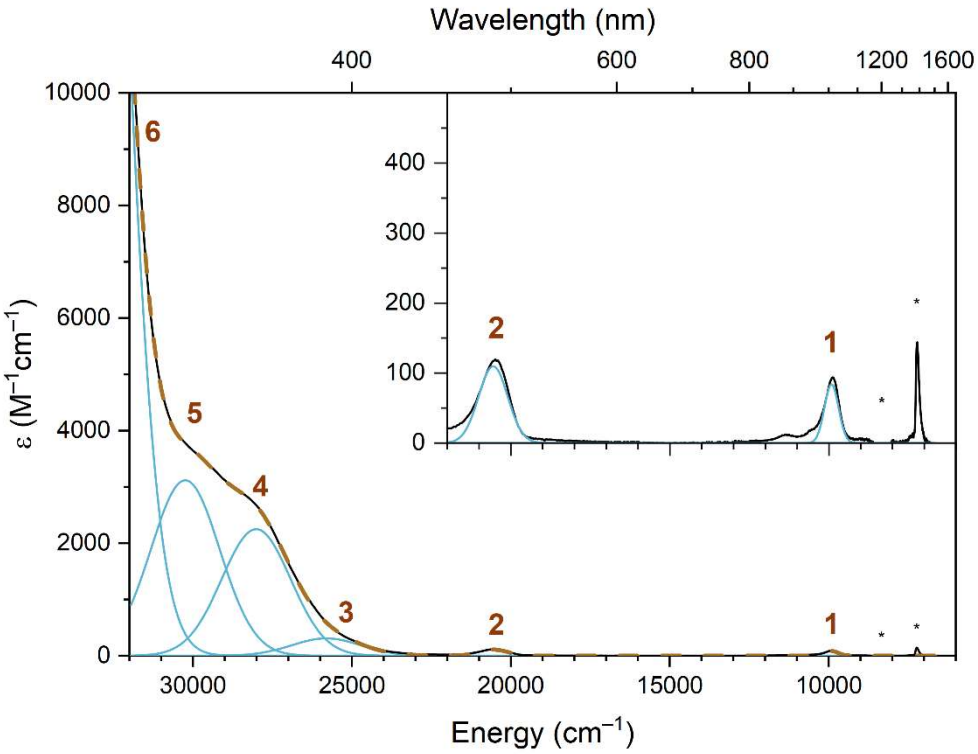

Fig. S10. UV-vis-NIR (0.352 mM of **2** in THF). Experimental data (black trace); overall fit (dashed light-brown trace); six individual Gaussian bands fit to the data (blue traces). Asterisks indicate peaks corresponding to a minor water impurity.

IR:

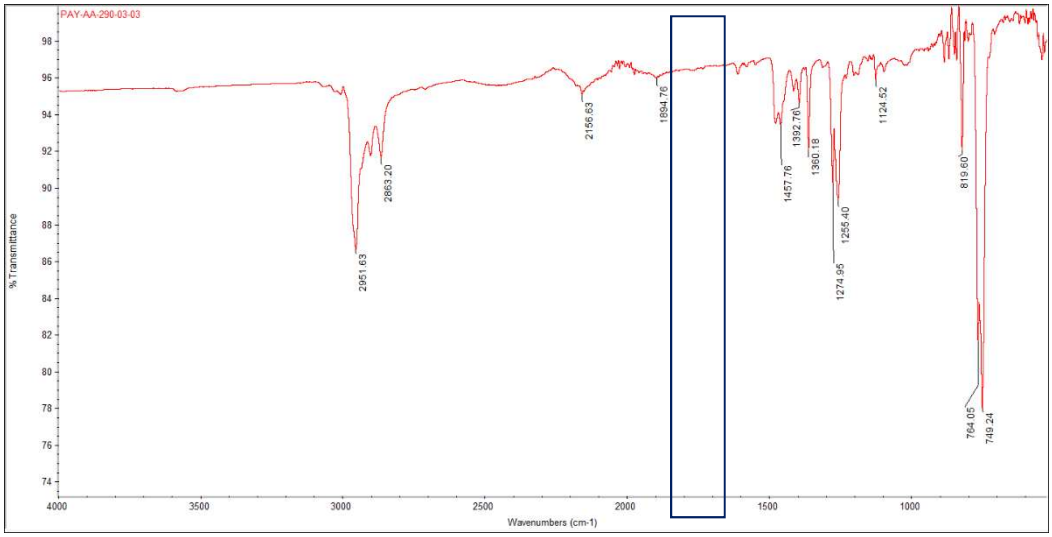

Fig. S11. IR of **2** (the expected region of the stretching band of the Bi−H bond is shown in the bracket).

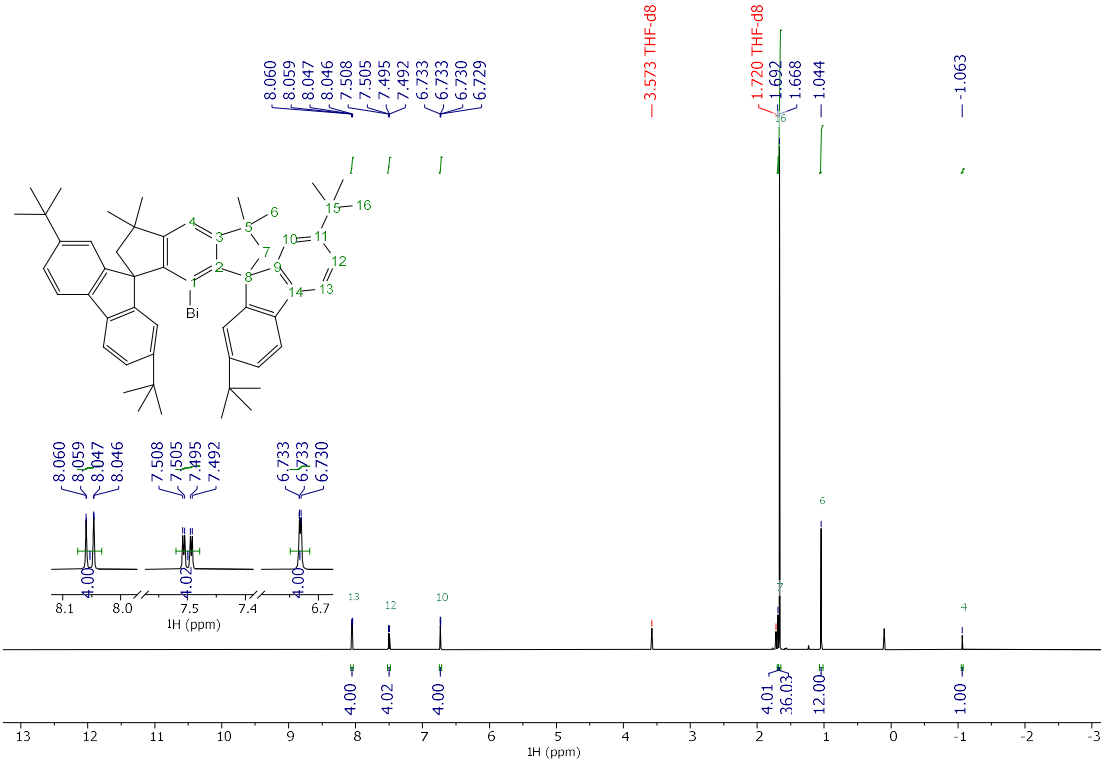

Fig. S12. [1]H NMR of **2** (THF-d_8, 600 MHz, 298 K).

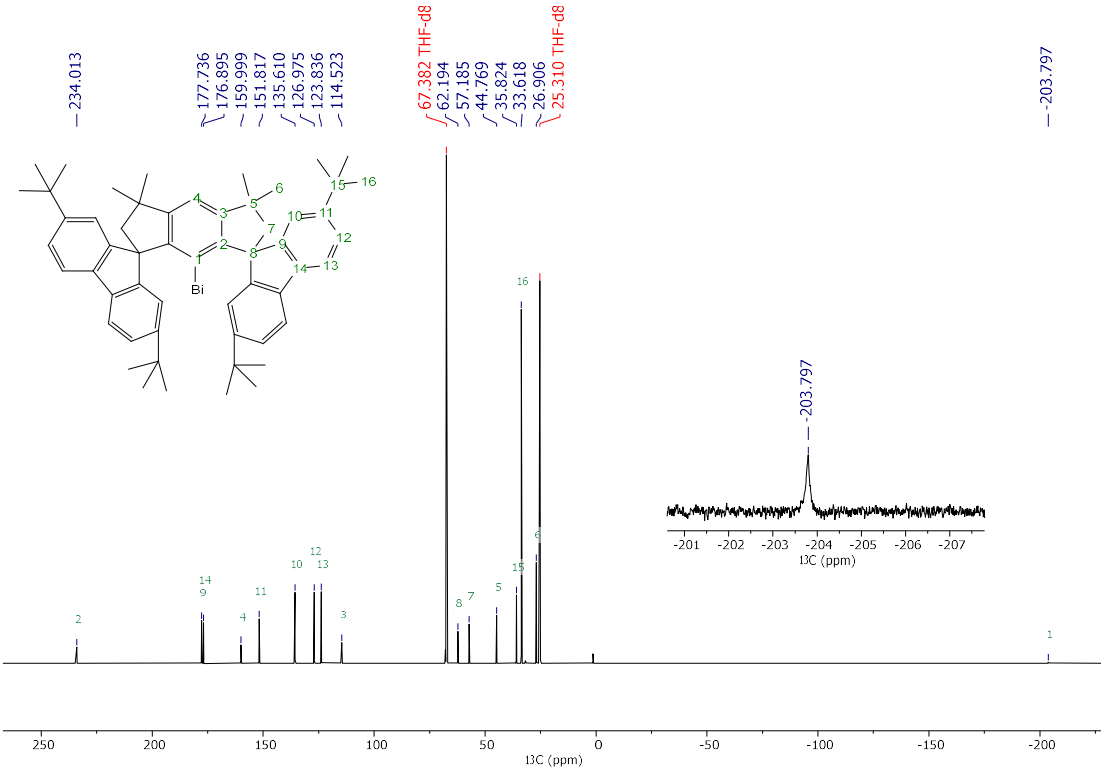

Fig. S13. [13]C NMR of **2** (THF-d_8, 151 MHz, 298 K).

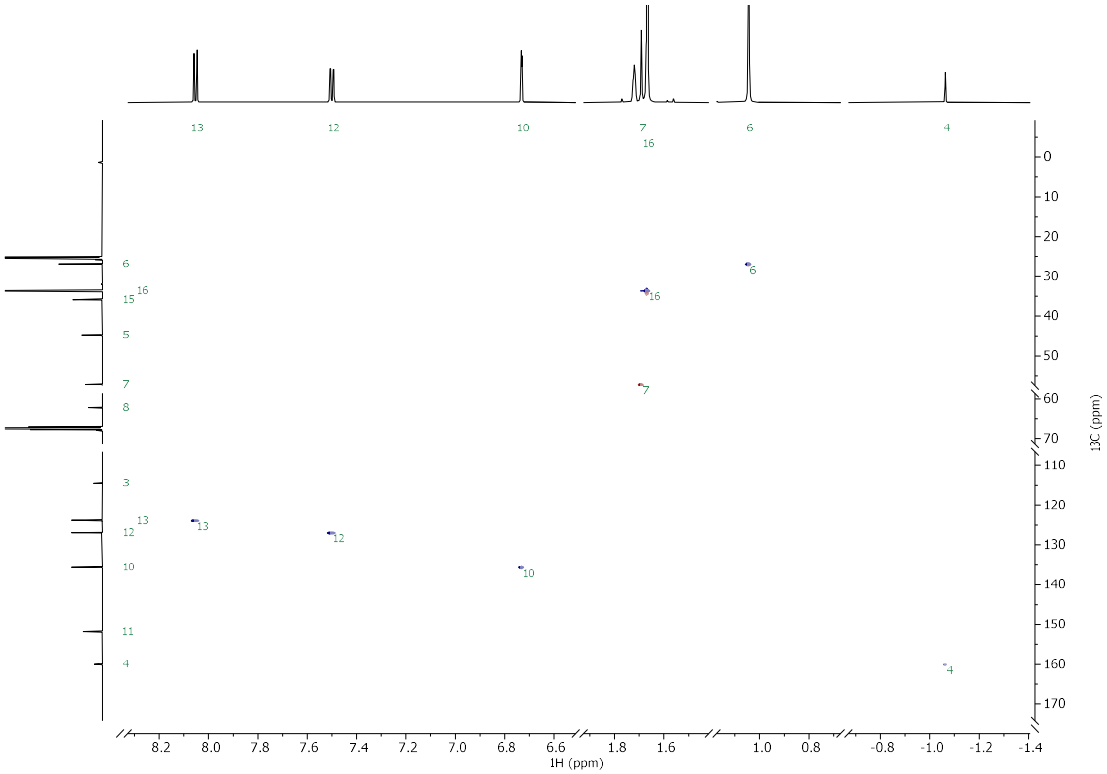

Fig. S14. ^{1}H-^{13}C HSQC of **2**.

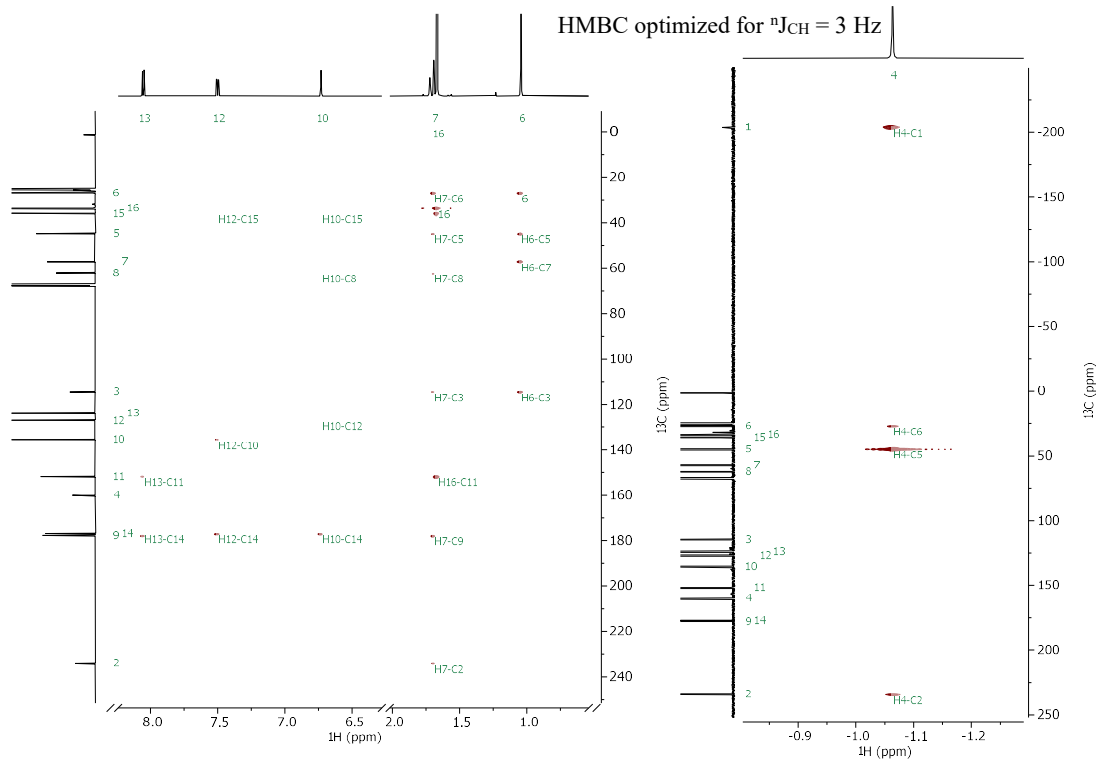

Fig. S15. ^{1}H-^{13}C HMBC of **2**.

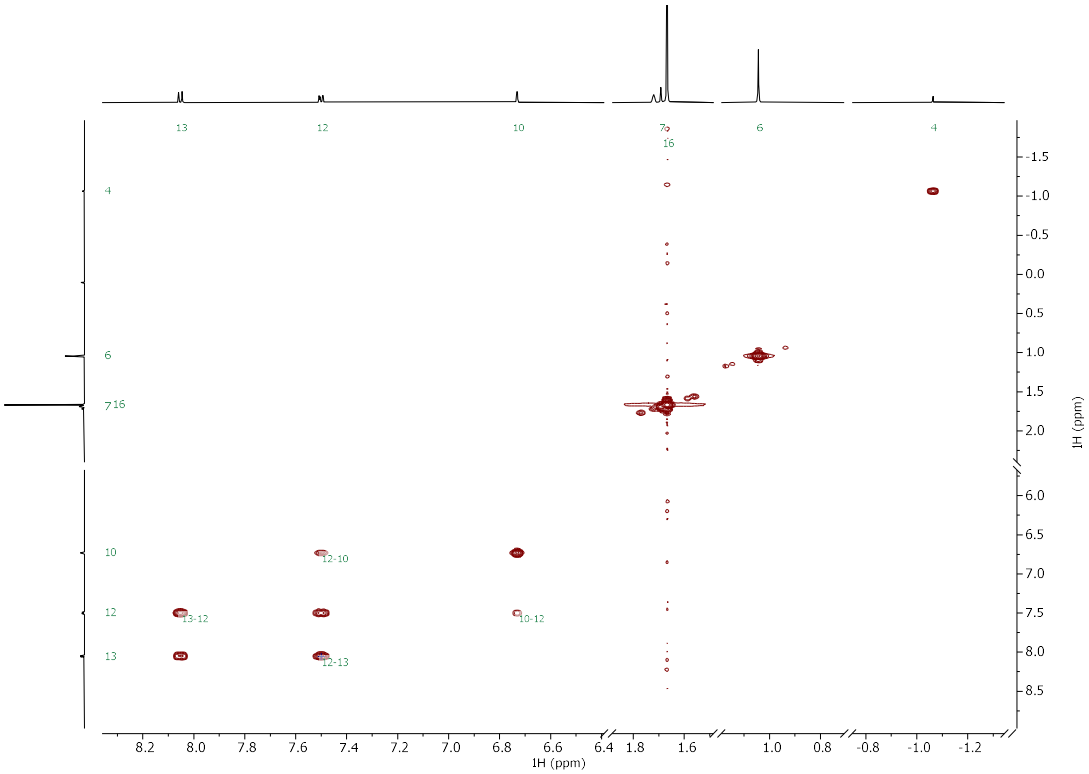

Fig. S16. ^{1}H-^{1}H COSY of **2**.

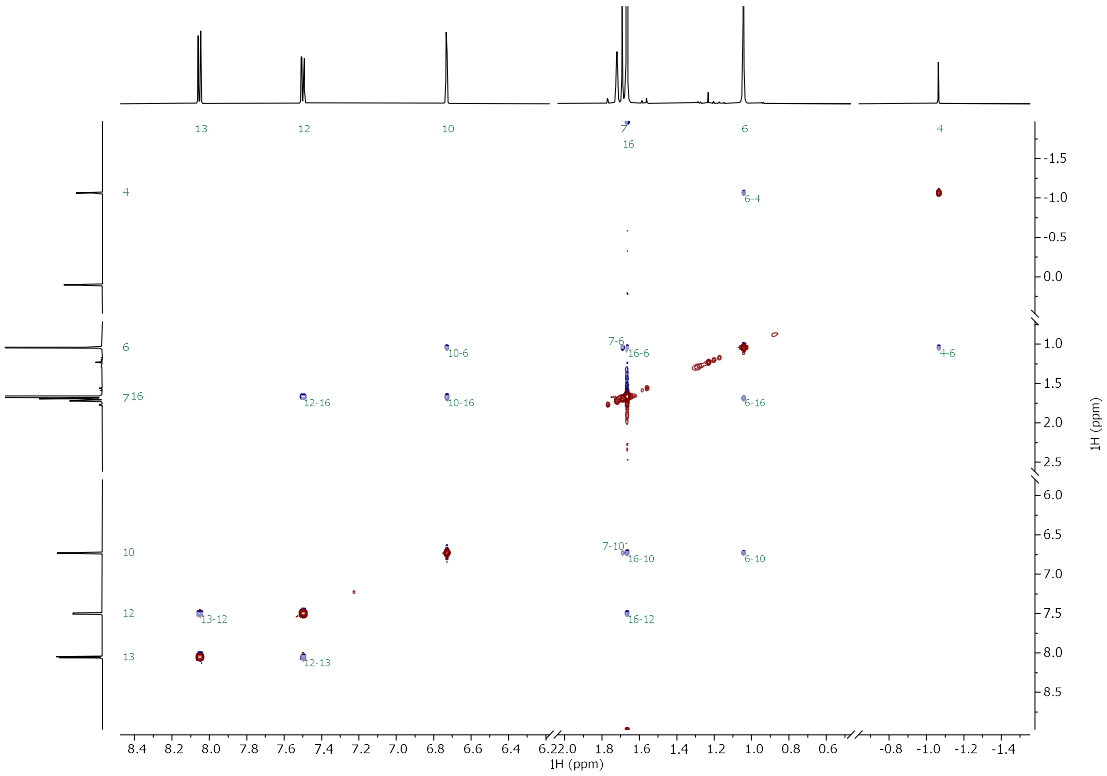

Fig. S17. NOESY of **2**.

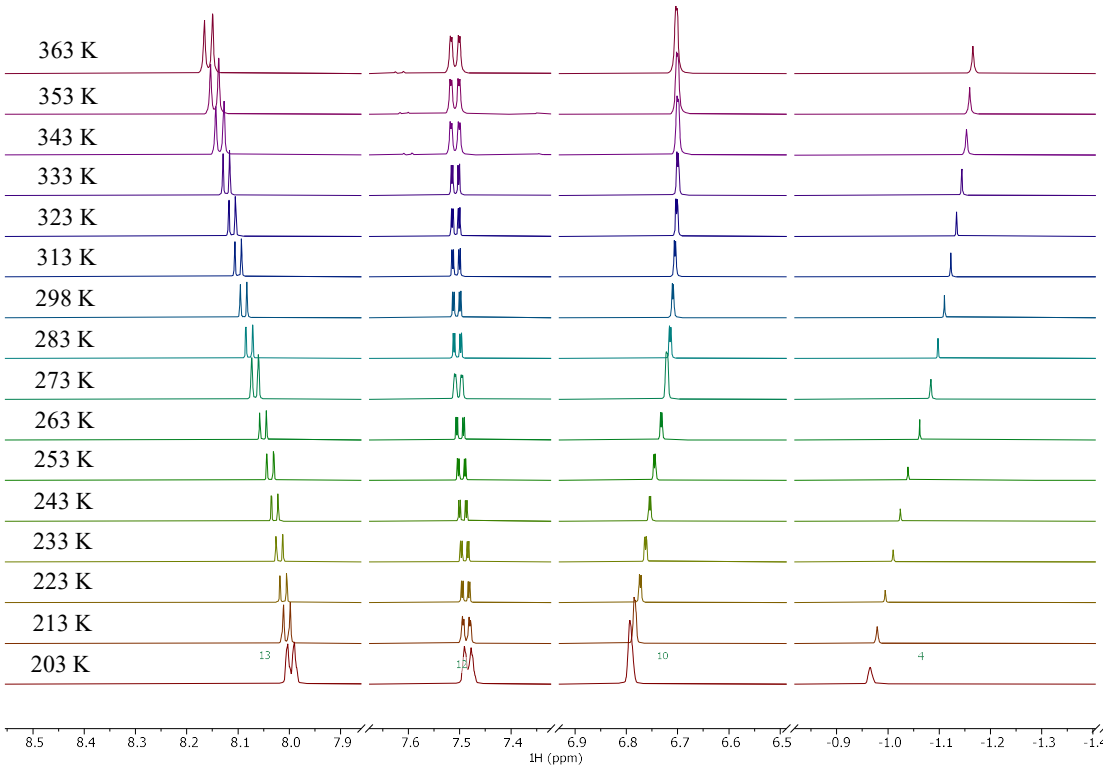

Fig. S18. VT ^{1}H NMR of **2**.

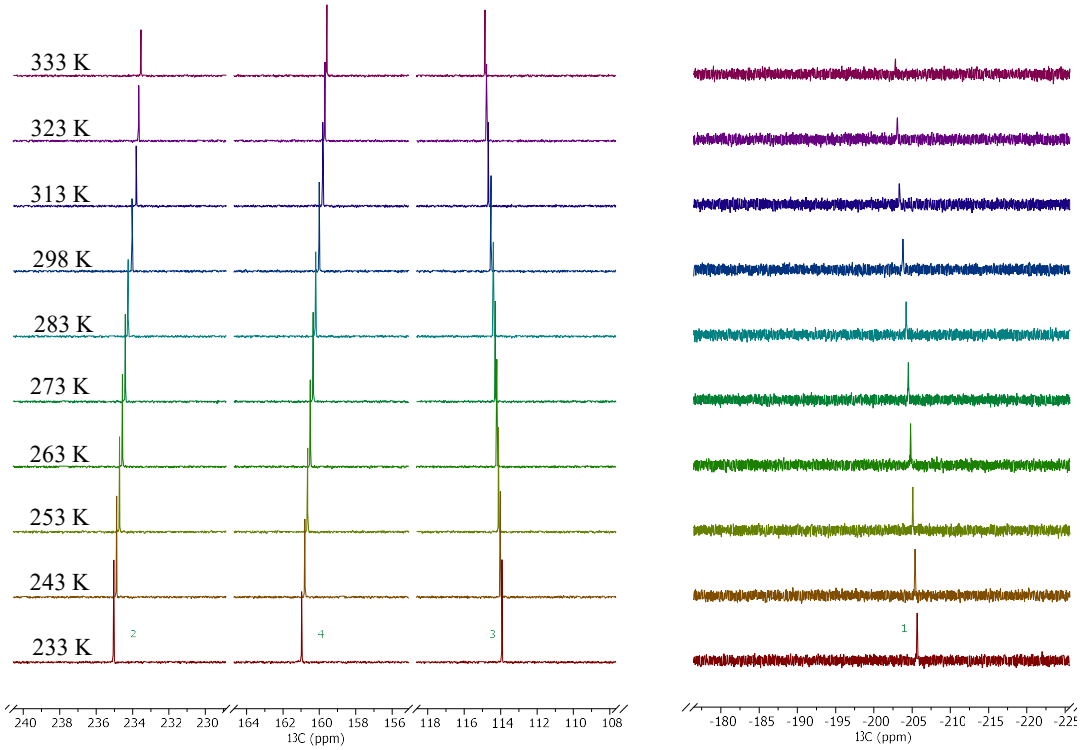

Fig. S19. VT ^{13}C NMR of **2**.

2.3. The reaction of **2** with MeI and *N*-Me-maleimide

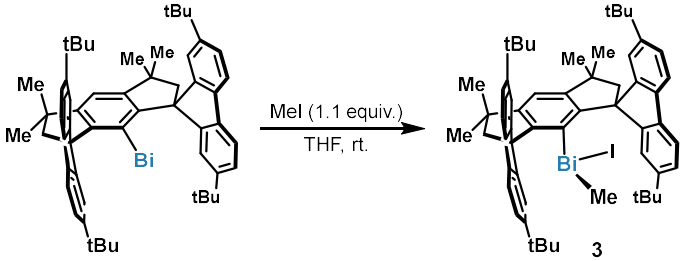

Procedure: in a glovebox, fresh-distilled MeI (33 mg, 232 μmol, 1.1 equiv.) in 1 mL THF was added dropwise into a THF solution of **2** (200 mg, 211 μmol) under stirring, during which the solution turned orange-yellow. After stirring for 10 min, the reaction mixture was evaporated to dryness. The crude product was further purified by recrystallization in THF/*n*-hexane, affording ^{t}Bu-M^{s}Fluind-Bi(Me)I (**3**) as an orange crystalline solid (192 mg, 84%).

Note: Some typical unsaturated compounds (cyclopentene, styrene, phenylacetylene and 2,3-dimethyl-1,3-butadiene) were tested in the cycloaddition reactions with **2**, and no reactivity was observed as judged by ^{1}H NMR.

Characterization data of **3**

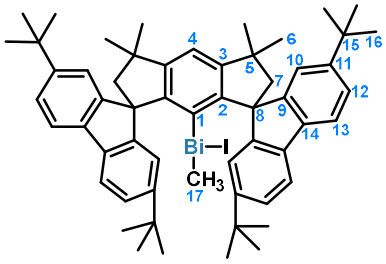

^{1}H NMR (600 MHz, THF-d_8, 298 K): δ 7.52 (s, 1H, H-4), 7.51 (d, J = 8.0 Hz, 4H, H-13), 7.29 (dd, J = 8.0, 1.8 Hz, 4H, H-12), 7.20 (br. s, 4H, H-10), 2.29 (s, 4H, H-7), 1.56 (s, 12H, H-6), 1.25 (s, 36H, H-16), 0.33 ppm (s, 3H, H-17).

^{13}C NMR (151 MHz, THF-d_8, 298 K): δ 158.0 (C-3), 156.5 (C-2), 155.2 (br, C-1), 153.5 (C-9), 151.3 (C-11), 138.3 (C-14), 125.5 (C-12), 122.2 (C-10), 121.2 (C-13), 119.2 (C-4), 67.9 (C-8), 60.9 (C-7), 43.9 (C-5), 35.6 (C-15), 32.9 (C-6), 32.1 (C-16), 24.1 ppm (C-17).

At room temperature, the dataset of **3** is pseudo C_2 symmetric, likely due to a fast rotation around the C1–Bi bond or an ionic character of the Bi–I bond. At lower temperatures, a C_s symmetry is observed. The top- and bottom-faces of the backbone of **3** gives two sets of signals in ^{1}H and ^{13}C NMR, which is in line with the asymmetric structure of **3** in XRD.

M.p.: turn red at ca. 220 °C in an argon-filled capillary.

HRMS (ESI-positive): calc'd for $C_{57}H_{69}BiI^{+}$ $[M+H]^{+}$ 1089.42425; found 1089.4236. **MS (ESI-negative)**: $[I]^{-}$ 127.

Stability: slightly light-sensitive.

XRD: single crystals of **3** suitable for X-ray diffraction analysis were obtained by slow diffusion of Et_2O into a THF solution of **3** at room temperature under argon.

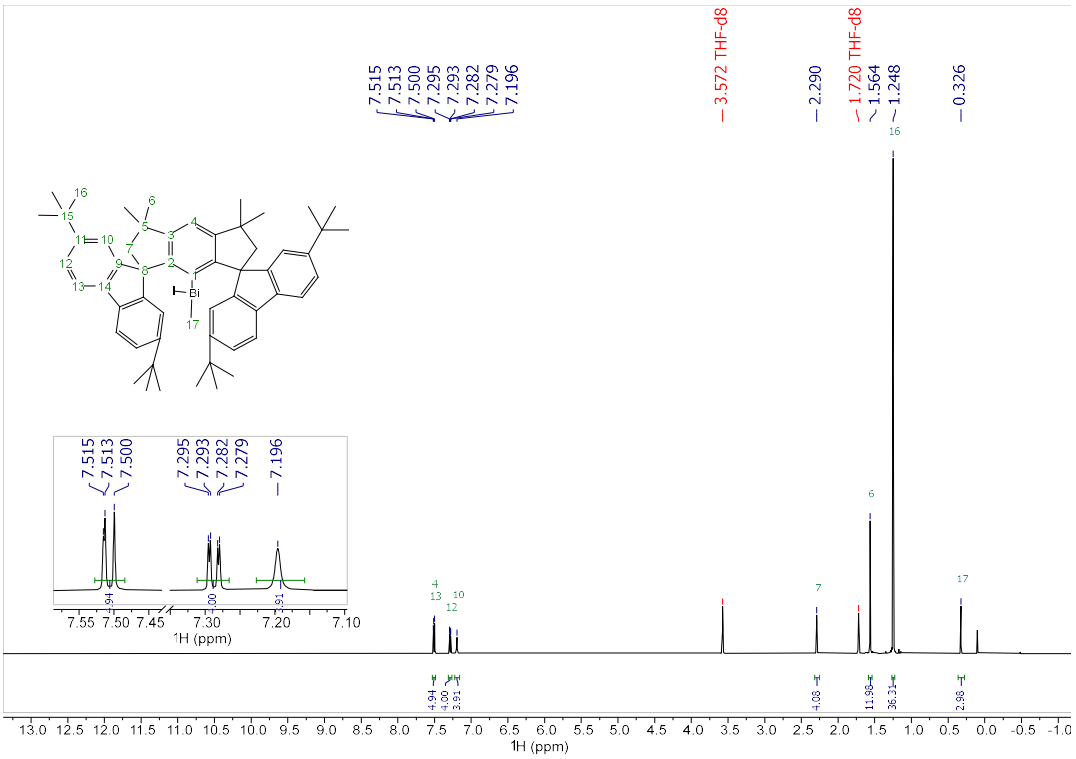

Fig. S20. ^{1}H NMR of **3** (THF-d_8, 600 MHz, 298 K).

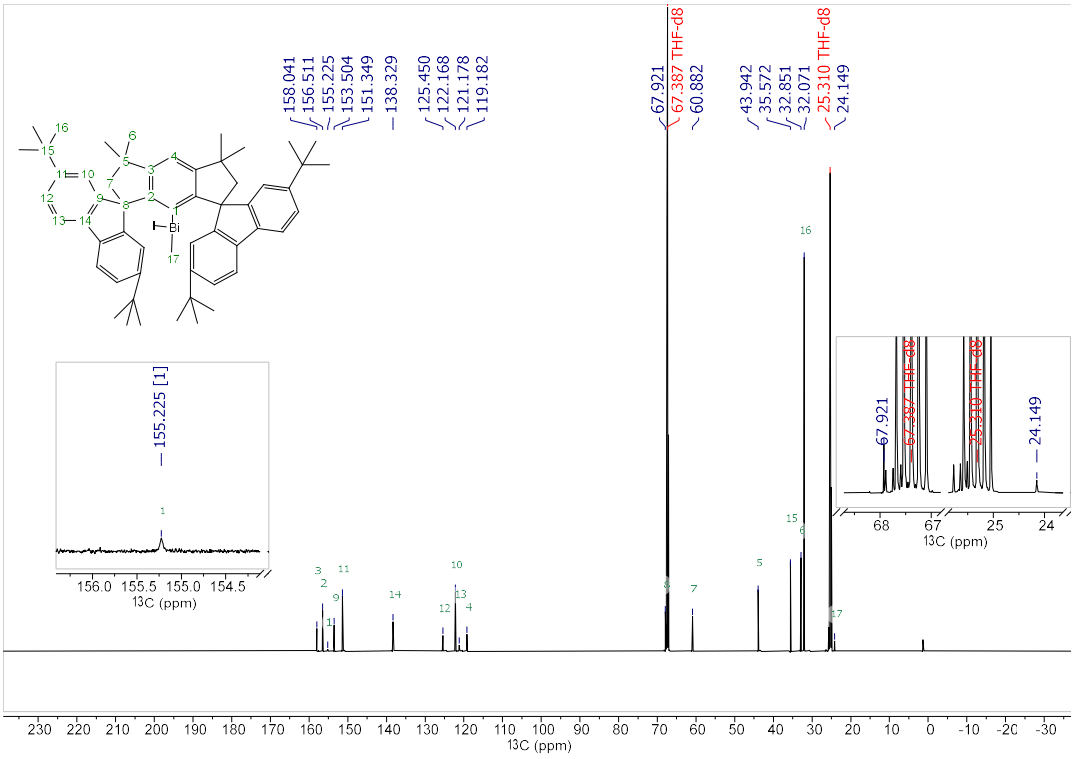

Fig. S21. ^{13}C NMR of **3** (THF-d_8, 151 MHz, 298 K).

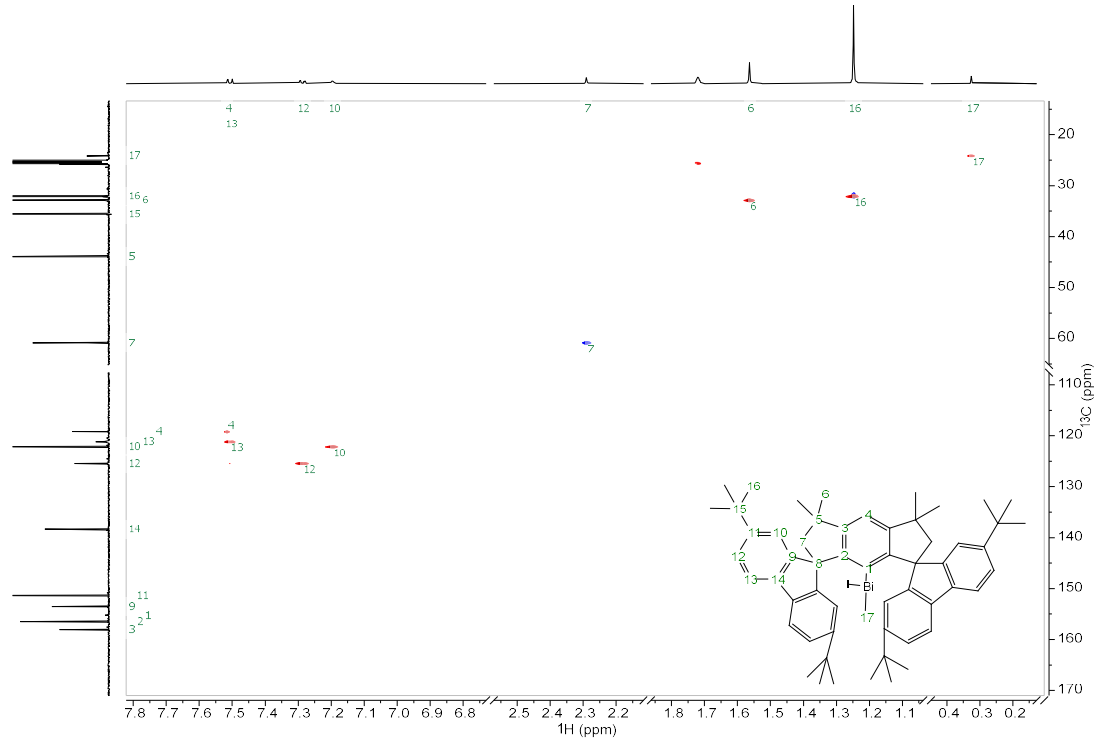

Fig. S22. ^{1}H-^{13}C HSQC of **3**.

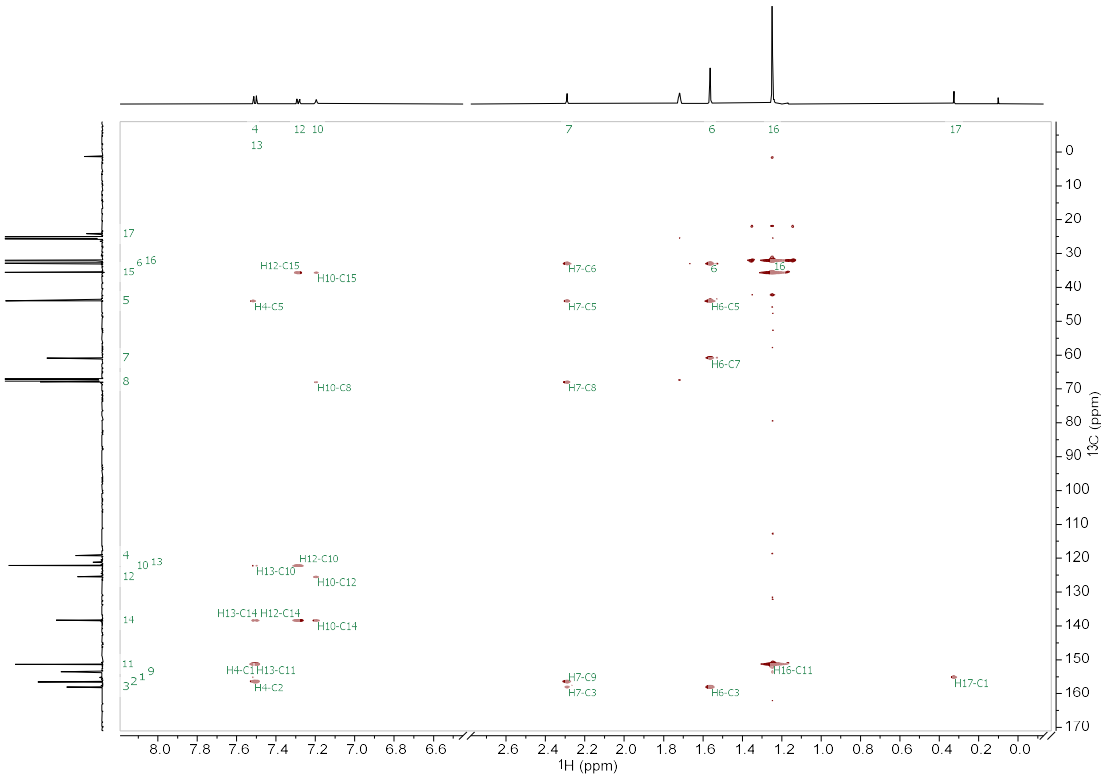

Fig. S23. ^{1}H-^{13}C HMBC of **3**.

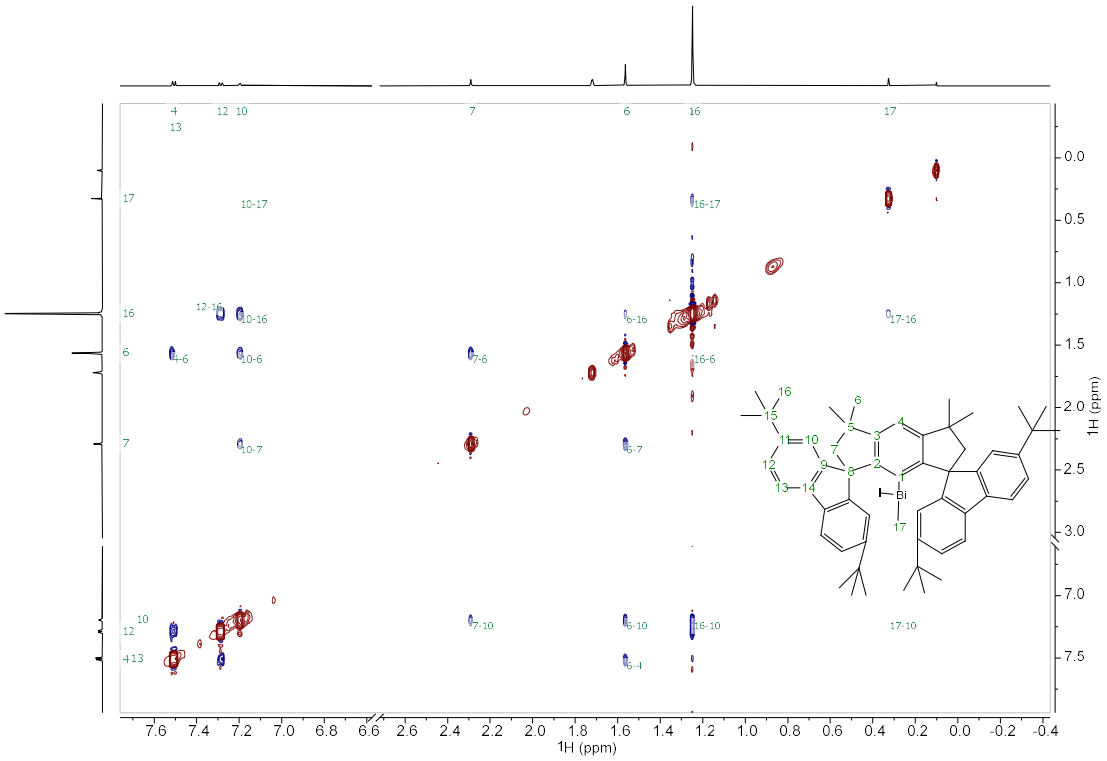

Fig. S24. NOESY of **3**.

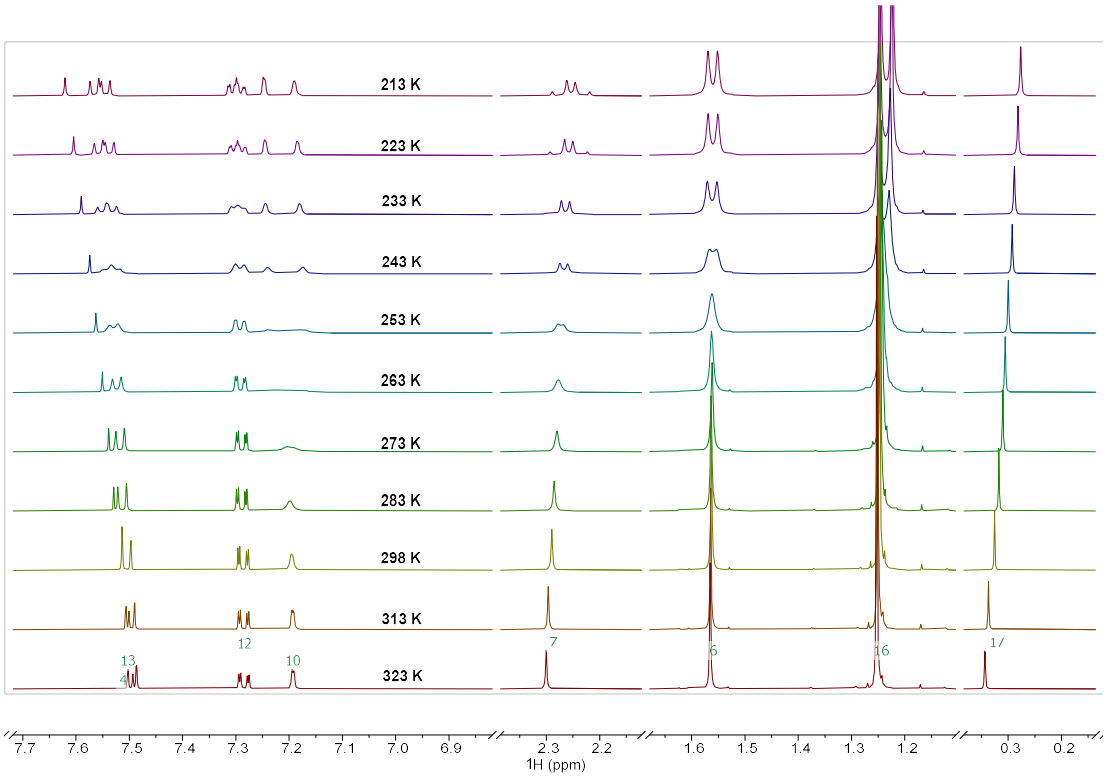

Fig. S25. VT ^{1}H NMR of **3**.

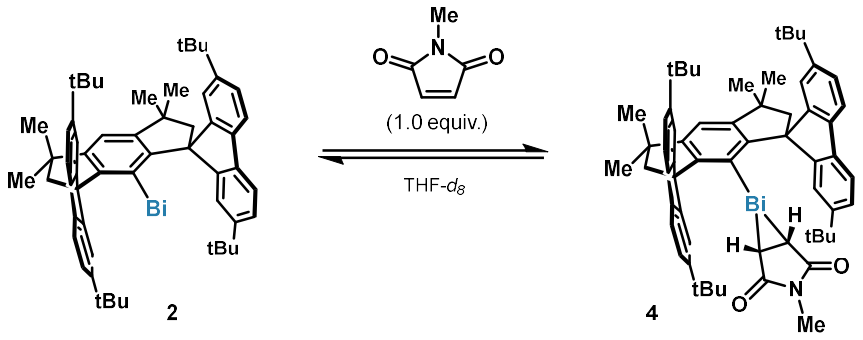

In the glovebox, ^{t}Bu-M^{s}Fluind-Bi(I) (10 mg, 10.6 µmol), *N*-Me-maleimide (THF-d_8 stock solution, 105 µM, 100 µL) and 0.5 mL THF-d_8 were added to an oven-dried J. Young NMR tube. VT ^{1}H NMR studies revealed an equilibrium between **4** and the starting material **2**. At lower temperature, the major species was **4**. The NMR characterization of **4** was performed at –90 °C.

Note: no reactivity of **2** with phenyl iodide was observed up to 100 °C.

Characterization data of **4**

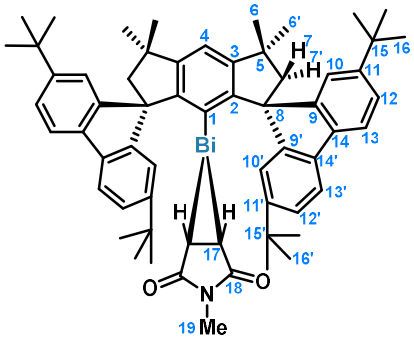

^{1}H NMR (500 MHz, THF-d_8, 183 K): δ 7.91 (d, J = 8.0 Hz, 2H, H-13), 7.69 (s, 1H, H-4), 7.59 (d, J = 8.0 Hz, 2H, H-13'), 7.35 (s, 2H, H-10'), 7.34 (d, J = 9.1 Hz, 2H, H-12), 7.29 (d, J = 8.1 Hz, 2H, H-12'), 6.94 (s, 2H, H-10), 2.54 (d, J = 13.4 Hz, 2H, H-7), 2.29 (s, 3H, H-19), 2.17 (d, J = 13.3 Hz, 2H, H-7'), 1.65 (s, 6H, H-6'), 1.54 (s, 6H, H-6), 1.25 (s, 18H, H-16'), 1.15 (s, 18H, H-16), 0.14 ppm (s, 2H, H-17).

^{13}C NMR (126 MHz, THF-d_8, 183 K): δ 169.0 (C-18), 157.4 (C-1), 156.2 (C-3), 155.2 (C-2), 154.5 (C-9), 154.5 (C-9'), 152.1 (C-11'), 150.8 (C-11), 141.3 (C-14'), 138.7 (C-14), 125.6 (C-12'), 124.4 (C-12), 123.6 (C-13), 121.4 (C-13'), 121.1 (C-10'), 121.0 (C-10), 120.1 (C-4), 67.3 (C-8), 57.5 (C-7), 49.3 (C-17), 44.0 (C-5), 35.8 (C-15'), 35.5 (C-15), 33.6 (C-6), 32.1 (C-16'), 32.0 (C-16), 31.8 (C-6'), 23.3 ppm (C-19).

The backbone of **4** is diastereotopic at –90 °C as indicated by the numberings. The equivalent positions show EXSY cross peaks in ROESY. The origin could be a hindered rotation around the C1–Bi bond, or association/dissociation of *N*-Me-maleimide.

VT NMR data of the reaction mixture suggest that *N*-Me-maleimide reversibly dissociates from the Bi center. As a result, the relative amount of free Bi(I) **2** decreases at lower temperatures.

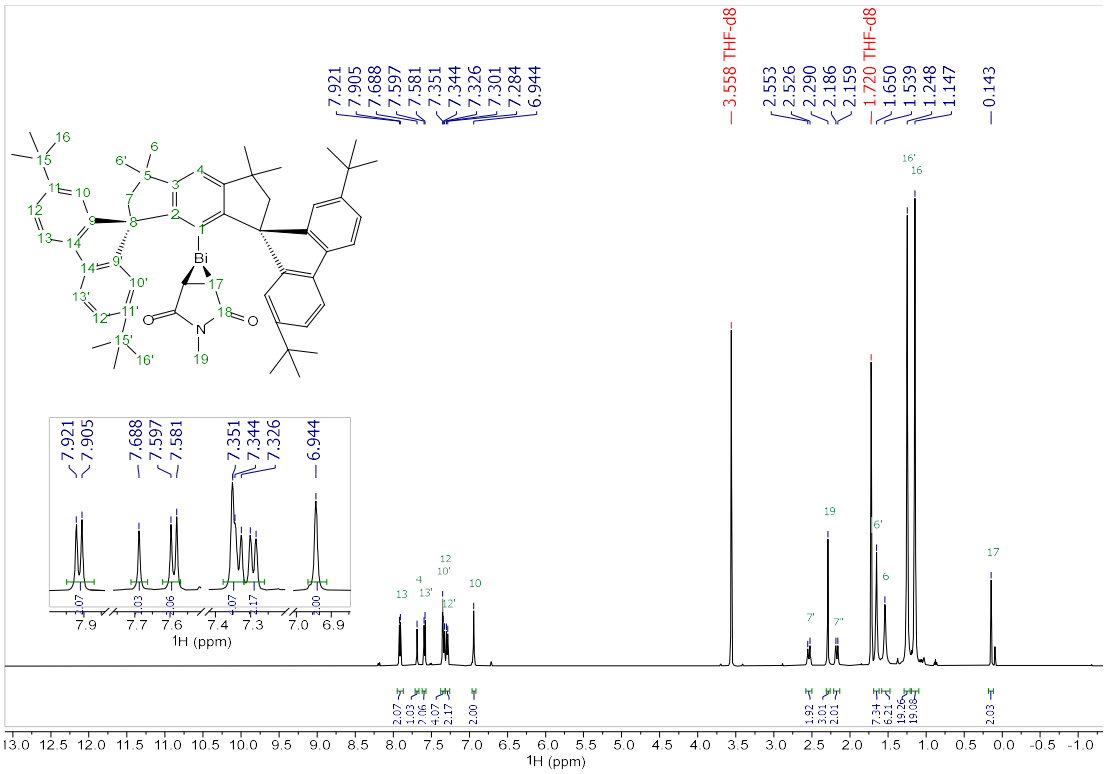

Fig. S26. ^{1}H NMR of **4** (THF-d_8, 500 MHz, 183 K).

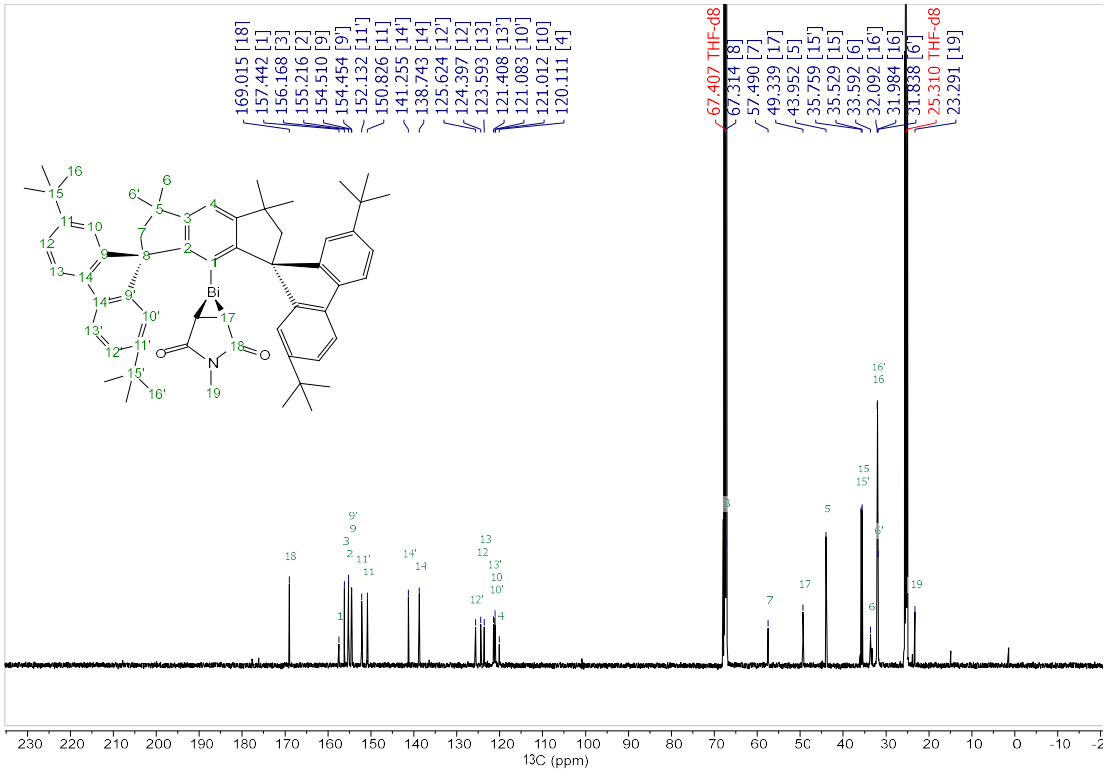

Fig. S27. ^{13}C NMR of **4** (THF-d_8, 126 MHz, 183 K).

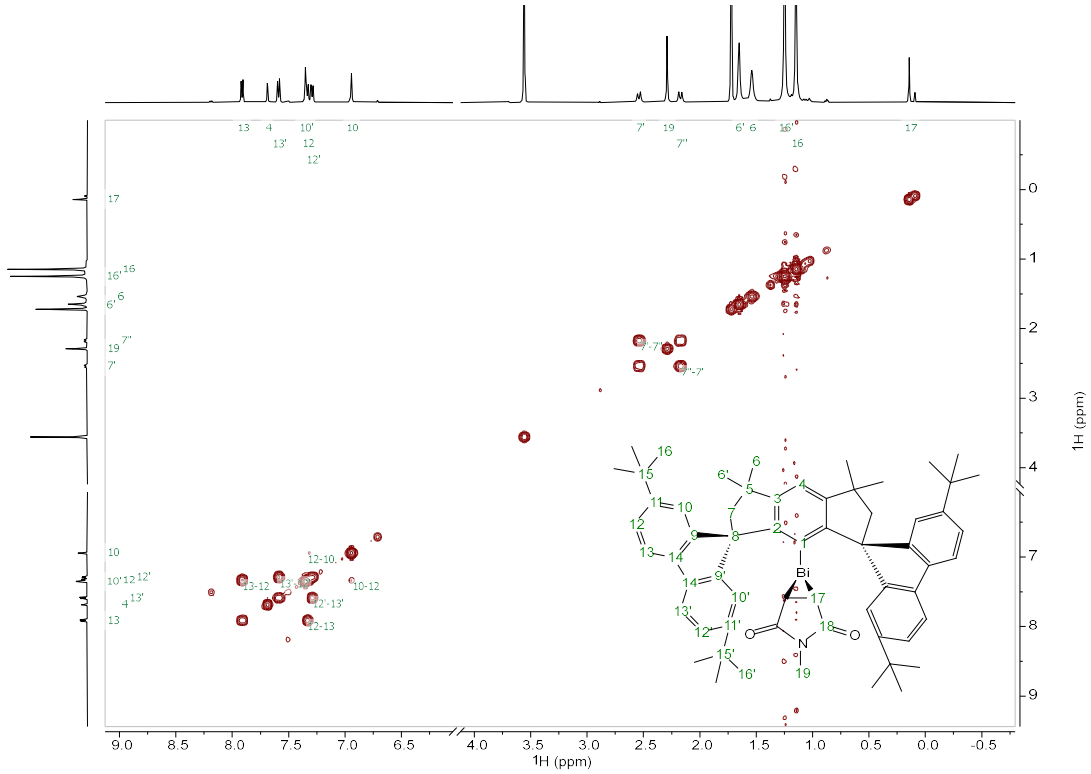

Fig. S28. ^{1}H-^{1}H COSY of **4** (183 K).

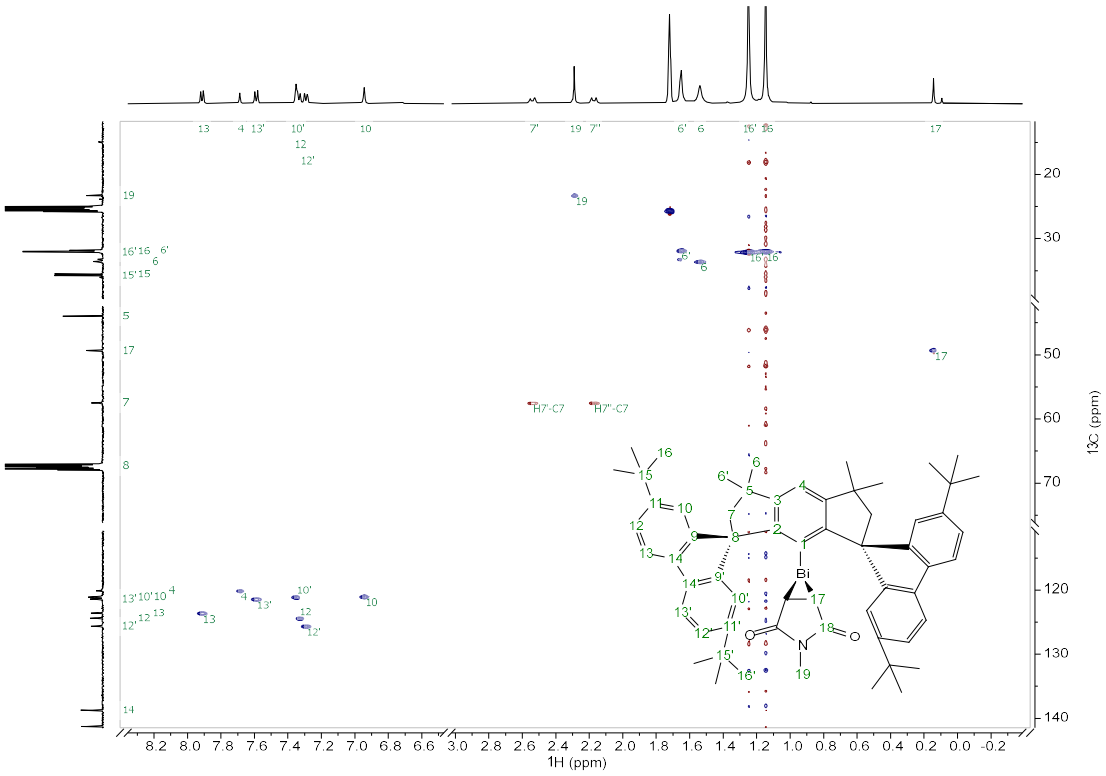

Fig. S29. ^{1}H-^{13}C HSQC of **4** (183 K).

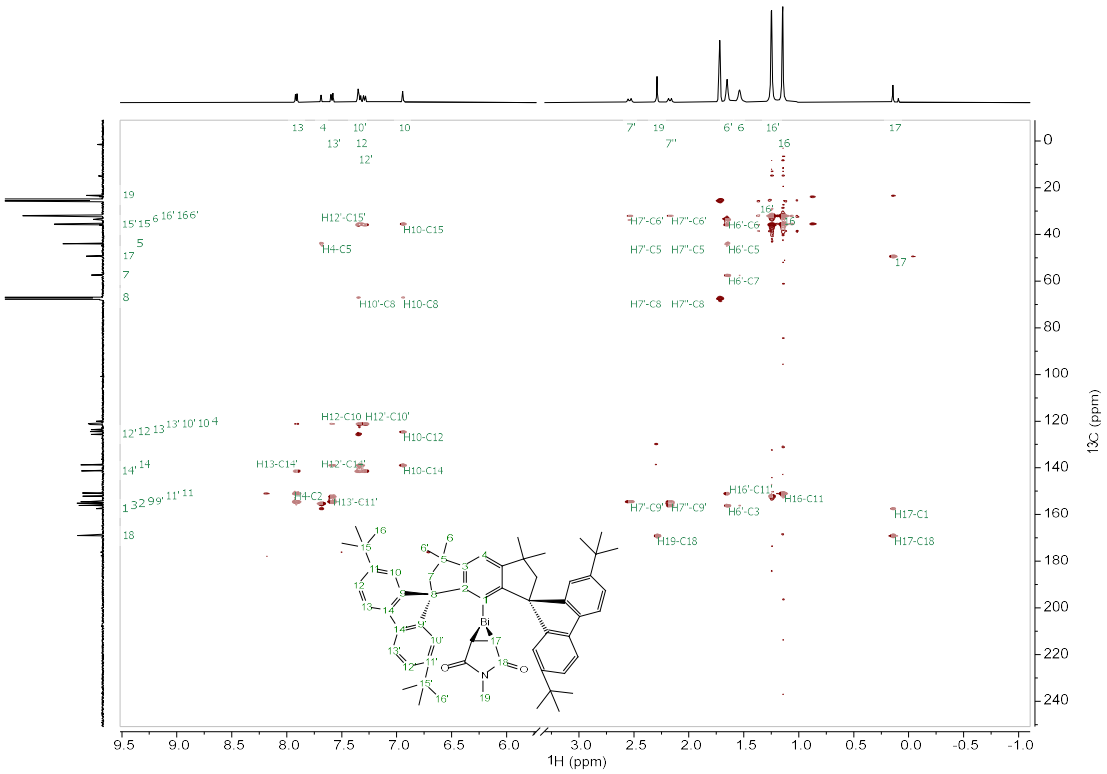

Fig. S30. ^{1}H-^{13}C HMBC of **4** (183 K).

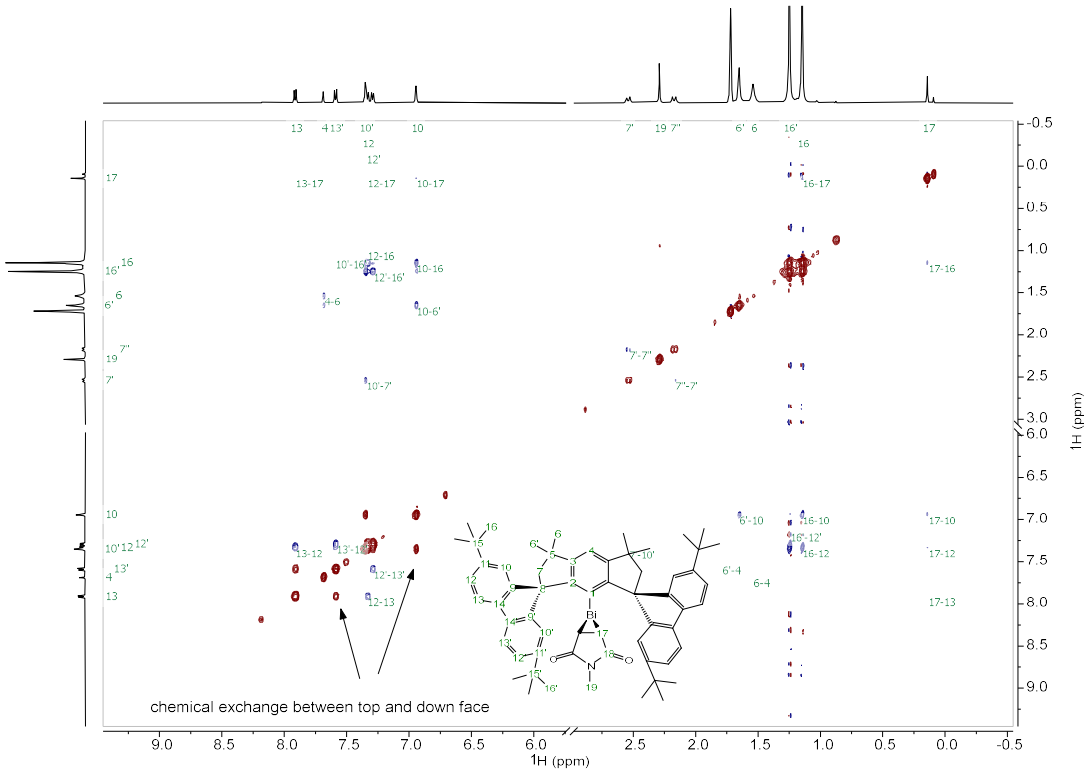

Fig. S31. ROESY of **4** (183 K).

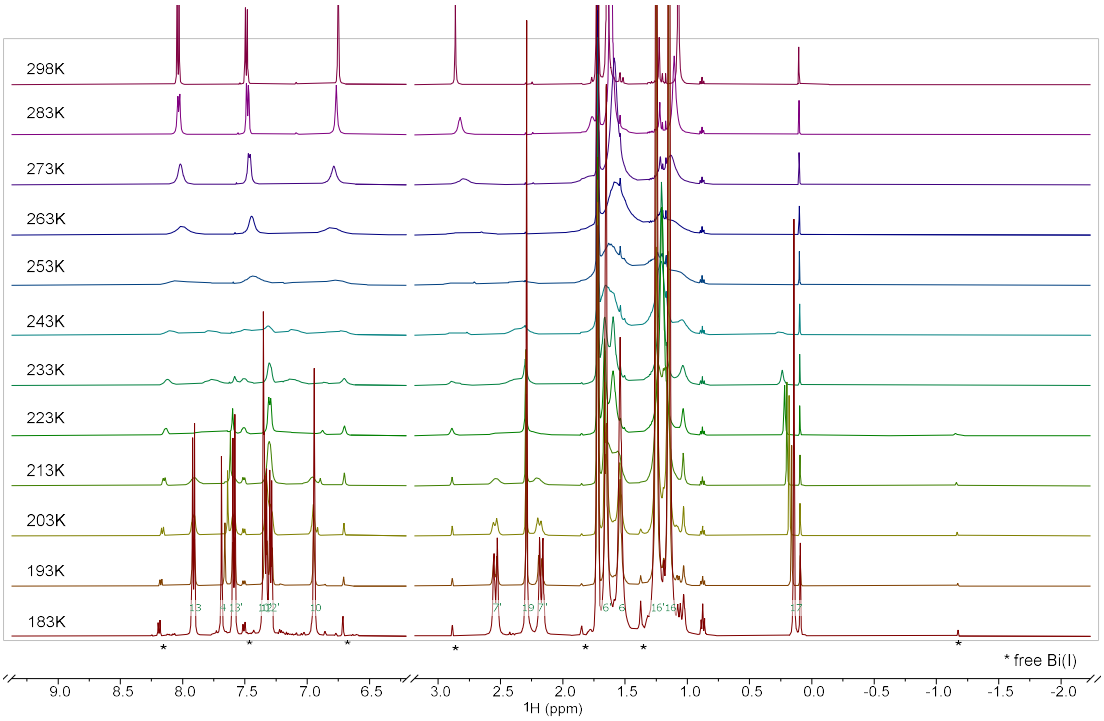

Fig. S32. VT ^{1}H NMR of **4**.

3. X-ray Crystal Structure Analysis of S1−S3, 1−3

3.1. Single crystal structure analysis of M^{s}Fluind-BiCl$_2$ (**S1**) · THF solvate

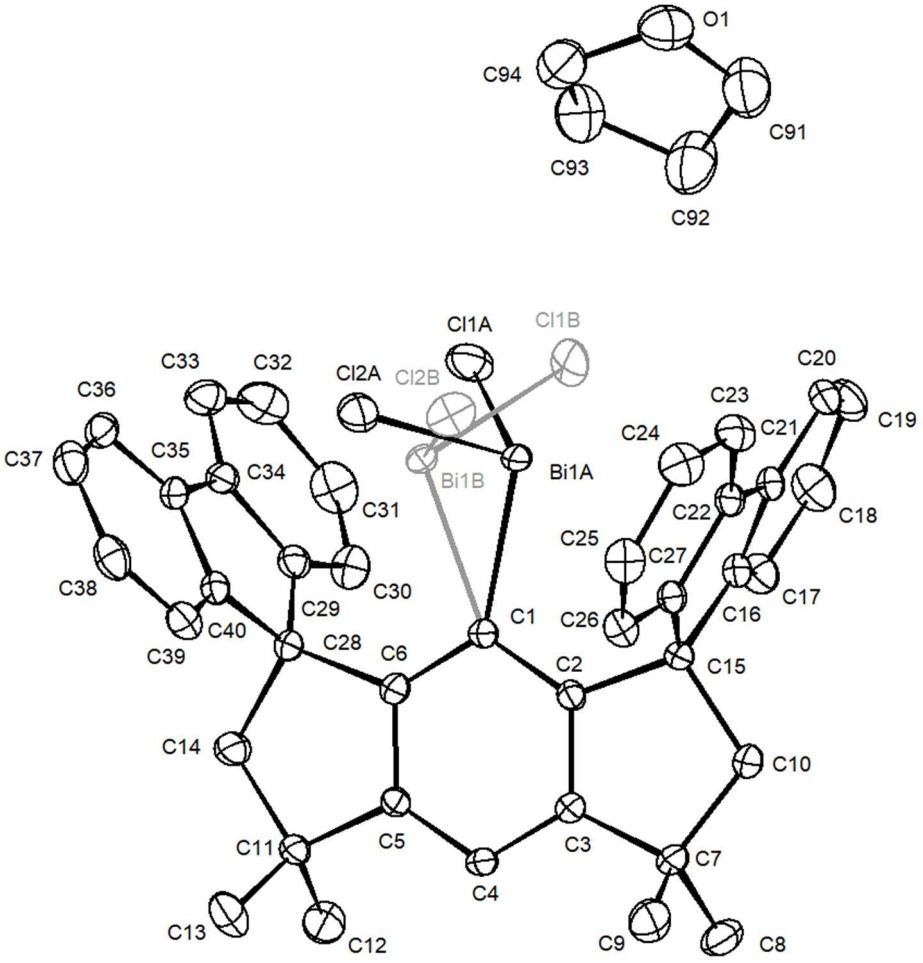

Fig. S33. The molecular structure of M^{s}Fluind-BiCl$_2$ (**S1**) · THF solvate. H atoms have been removed for clarity. Main structure shown in black and disordered parts shown in grey.

X-ray Crystal Structure Analysis of M^{s}Fluind-BiCl$_2$ (**S1**) · THF solvate:

C_{44} H_{41} Bi Cl_2 O, M_r = 865.65 g mol^{-1}, yellow plate, crystal size 0.07 x 0.07 x 0.02 mm^3, triclinic, space group *P*-1 [2], *a* = 9.6953(8) Å, b = 11.2424(8) Å, *c* = 17.8508(14) Å, α= 104.694(5)°, β= 94.393(7)°, γ = 104.682(7)°, *V* = 1799.9(3) Å^3, *T* = 150(2) K, *Z* = 2, D_{calc} = 1.597 g·cm^3, λ = 0.71073 Å, μ(*Mo-K*$_\alpha$) = 5.080 mm^{-1}, Gaussian absorption correction (T_{min} = 0.68457, T_{max} = 0.92919), Bruker-AXS Kappa Mach3 with KappaCCD detector and FR591 rotating Mo anode X-ray source, 2.621 < θ < 33.089°, 62621 measured reflections, 13633 independent reflections, 11542 reflections with $I > 2\sigma(I)$, R_{int} = 0.0613. The structure was solved by *SHELXS* and refined by full-matrix least-squares (*SHELXL*) against F^2 to R_1 = 0.0317 [$I > 2\sigma(I)$], wR_2 = 0.0658 [all data], 464 parameters and 0 restraints.

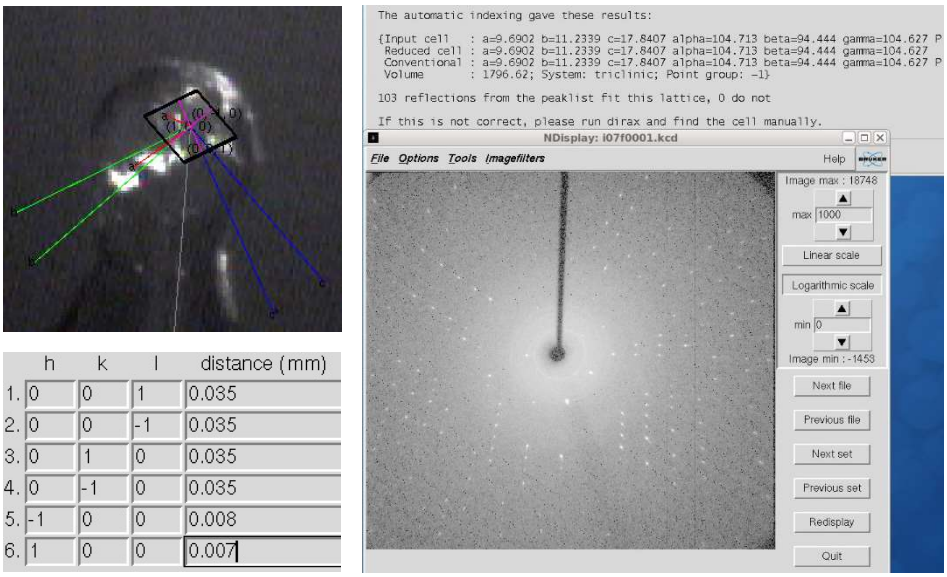

	h	k	l	distance (mm)
1.	0	0	1	0.035
2.	0	0	-1	0.035
3.	0	1	0	0.035
4.	0	-1	0	0.035
5.	-1	0	0	0.008
6.	1	0	0	0.007

Fig. S34. Crystal faces and unit cell determination/refinement of M^{s}Fluind-BiCl$_2$ (**S1**) · THF solvate.

INTENSITY STATISTICS FOR DATASET

Resolution	#Data	#Theory	%Complete	Redundancy	Mean I	Mean I/s	Rmerge	Rsigma
Inf - 2.60	206	214	96.3	9.33	162.97	52.13	0.0469	0.0169
2.60 - 1.76	491	491	100.0	6.86	122.60	39.71	0.0462	0.0211
1.76 - 1.39	682	682	100.0	6.39	76.95	34.10	0.0453	0.0242
1.39 - 1.22	689	689	100.0	6.08	61.02	30.51	0.0471	0.0270
1.22 - 1.11	681	681	100.0	5.73	50.35	26.99	0.0503	0.0300
1.11 - 1.03	694	694	100.0	5.59	44.71	24.87	0.0528	0.0323
1.03 - 0.97	681	681	100.0	5.26	36.84	21.81	0.0580	0.0369
0.97 - 0.92	710	710	100.0	5.05	29.86	18.71	0.0633	0.0423
0.92 - 0.88	683	683	100.0	4.83	25.60	16.76	0.0681	0.0480
0.88 - 0.85	618	618	100.0	4.64	23.23	15.04	0.0742	0.0533
0.85 - 0.82	687	687	100.0	4.43	20.03	13.35	0.0825	0.0609
0.82 - 0.79	824	824	100.0	4.25	18.54	12.43	0.0862	0.0673
0.79 - 0.77	616	616	100.0	4.02	16.77	11.09	0.0945	0.0754
0.77 - 0.75	645	645	100.0	3.86	15.30	9.90	0.1084	0.0848
0.75 - 0.73	792	792	100.0	3.78	14.37	9.10	0.1107	0.0920
0.73 - 0.71	816	816	100.0	3.58	12.34	7.88	0.1241	0.1092
0.71 - 0.70	466	466	100.0	3.50	10.53	6.79	0.1440	0.1291
0.70 - 0.68	1008	1009	99.9	3.31	9.97	6.22	0.1516	0.1439
0.68 - 0.67	542	542	100.0	3.25	9.03	5.56	0.1723	0.1656
0.67 - 0.66	575	577	99.7	3.16	8.02	4.70	0.1928	0.1996
0.66 - 0.65	527	541	97.4	2.99	8.37	4.60	0.1919	0.2087
0.75 - 0.65	4726	4743	99.6	3.39	10.65	6.61	0.1435	0.1367
Inf - 0.65	13633	13658	99.8	4.58	31.64	16.35	0.0605	0.0465

Complete .cif-data of M^{s}Fluind-BiCl$_2$ (**S1**) · THF solvate are available under the CCDC number CCDC-**2225003**.

The central Bi-Cl$_2$ entity of M^{s}Fluind-BiCl$_2$ (**S1**) · THF solvate is disordered over two positions. It was described by fixed occupancies of 95:5%.

Table S3. Crystal data and structure refinement of compound M^{s}Fluind-$BiCl_2$ (**S1**) · THF

Identification code	14130	
Empirical formula	C_{44} H_{41} Bi Cl_2 O	
Color	yellow	
Formula weight	865.65 g·mol^{-1}	
Temperature	150(2) K	
Wavelength	0.71073 Å	
Crystal system	Triclinic	
Space group	*P*-1, (no. 2)	
Unit cell dimensions	a = 9.6953(8) Å	α= 104.694(5)°.
	b = 11.2424(8) Å	β= 94.393(7)°.
	c = 17.8508(14) Å	γ = 104.682(7)°.
Volume	1799.9(3) Å^3	
Z	2	
Density (calculated)	1.597 Mg·m^{-3}	
Absorption coefficient	5.080 mm^{-1}	
F(000)	860 e	
Crystal size	0.07 x 0.07 x 0.02 mm^3	
θ range for data collection	2.621 to 33.089°.	
Index ranges	$-14 \le h \le 14$, $-17 \le k \le 17$, $-27 \le l \le 27$	
Reflections collected	62621	
Independent reflections	13633 [R_{int} = 0.0613]	
Reflections with I>2σ(I)	11542	
Completeness to θ = 25.242°	99.9 %	
Absorption correction	Gaussian	
Max. and min. transmission	0.92919 and 0.68457	
Refinement method	Full-matrix least-squares on F^2	
Data / restraints / parameters	13633 / 0 / 464	
Goodness-of-fit on F^2	1.047	
Final R indices [I>2σ(I)]	R_1 = 0.0317	wR^2 = 0.0617
R indices (all data)	R_1 = 0.0455	wR^2 = 0.0658
Extinction coefficient	n/a	
Largest diff. peak and hole	0.835 and –1.644 e·Å^{-3}	

Table S4. Bond lengths [Å] and angles [°] of M^{s}Fluind-$BiCl_2$ (**S1**) · THF

Bi(1A)-Cl(1A)	2.4699(7)	Bi(1A)-Cl(2A)	2.4877(8)
Bi(1A)-C(1)	2.280(2)	Bi(1B)-Cl(1B)	2.458(12)
Bi(1B)-Cl(2B)	2.477(12)	Bi(1B)-C(1)	2.305(3)
C(1)-C(2)	1.408(3)	C(1)-C(6)	1.409(3)
C(2)-C(3)	1.396(3)	C(2)-C(15)	1.537(3)
C(3)-C(4)	1.389(3)	C(3)-C(7)	1.516(3)
C(4)-H(4)	0.9500	C(4)-C(5)	1.388(3)
C(5)-C(6)	1.403(3)	C(5)-C(11)	1.514(3)
C(6)-C(28)	1.534(3)	C(7)-C(8)	1.533(4)
C(7)-C(9)	1.531(4)	C(7)-C(10)	1.547(3)
C(8)-H(8A)	0.9800	C(8)-H(8B)	0.9800
C(8)-H(8C)	0.9800	C(9)-H(9A)	0.9800
C(9)-H(9B)	0.9800	C(9)-H(9C)	0.9800
C(10)-H(10A)	0.9900	C(10)-H(10B)	0.9900
C(10)-C(15)	1.563(3)	C(11)-C(12)	1.533(3)
C(11)-C(13)	1.531(3)	C(11)-C(14)	1.543(3)
C(12)-H(12A)	0.9800	C(12)-H(12B)	0.9800
C(12)-H(12C)	0.9800	C(13)-H(13A)	0.9800
C(13)-H(13B)	0.9800	C(13)-H(13C)	0.9800
C(14)-H(14A)	0.9900	C(14)-H(14B)	0.9900
C(14)-C(28)	1.567(3)	C(15)-C(16)	1.529(3)
C(15)-C(27)	1.533(3)	C(16)-C(17)	1.383(3)
C(16)-C(21)	1.406(3)	C(17)-H(17)	0.9500
C(17)-C(18)	1.392(4)	C(18)-H(18)	0.9500
C(18)-C(19)	1.395(4)	C(19)-H(19)	0.9500
C(19)-C(20)	1.385(4)	C(20)-H(20)	0.9500
C(20)-C(21)	1.388(3)	C(21)-C(22)	1.465(3)
C(22)-C(23)	1.388(3)	C(22)-C(27)	1.414(3)
C(23)-H(23)	0.9500	C(23)-C(24)	1.390(4)
C(24)-H(24)	0.9500	C(24)-C(25)	1.394(4)
C(25)-H(25)	0.9500	C(25)-C(26)	1.390(4)
C(26)-H(26)	0.9500	C(26)-C(27)	1.379(3)
C(28)-C(29)	1.522(3)	C(28)-C(40)	1.524(3)

C(29)-C(30)	1.390(4)	C(29)-C(34)	1.399(3)
C(30)-H(30)	0.9500	C(30)-C(31)	1.393(4)
C(31)-H(31)	0.9500	C(31)-C(32)	1.391(5)
C(32)-H(32)	0.9500	C(32)-C(33)	1.389(4)
C(33)-H(33)	0.9500	C(33)-C(34)	1.393(3)
C(34)-C(35)	1.465(3)	C(35)-C(36)	1.392(3)
C(35)-C(40)	1.401(3)	C(36)-H(36)	0.9500
C(36)-C(37)	1.383(4)	C(37)-H(37)	0.9500
C(37)-C(38)	1.396(4)	C(38)-H(38)	0.9500
C(38)-C(39)	1.387(4)	C(39)-H(39)	0.9500
C(39)-C(40)	1.391(3)	O(1)-C(91)	1.420(4)
O(1)-C(94)	1.431(4)	C(91)-H(91A)	0.9900
C(91)-H(91B)	0.9900	C(91)-C(92)	1.497(5)
C(92)-H(92A)	0.9900	C(92)-H(92B)	0.9900
C(92)-C(93)	1.514(5)	C(93)-H(93A)	0.9900
C(93)-H(93B)	0.9900	C(93)-C(94)	1.497(5)
C(94)-H(94A)	0.9900	C(94)-H(94B)	0.9900

Cl(1A)-Bi(1A)-Cl(2A)	100.38(3)	C(1)-Bi(1A)-Cl(1A)	103.63(6)
C(1)-Bi(1A)-Cl(2A)	100.88(6)	Cl(1B)-Bi(1B)-Cl(2B)	102.2(5)
C(1)-Bi(1B)-Cl(1B)	102.2(3)	C(1)-Bi(1B)-Cl(2B)	99.0(3)
C(2)-C(1)-Bi(1A)	108.28(15)	C(2)-C(1)-Bi(1B)	140.71(17)
C(2)-C(1)-C(6)	117.8(2)	C(6)-C(1)-Bi(1A)	133.84(16)
C(6)-C(1)-Bi(1B)	101.31(15)	C(1)-C(2)-C(15)	128.3(2)
C(3)-C(2)-C(1)	121.5(2)	C(3)-C(2)-C(15)	110.20(19)
C(2)-C(3)-C(7)	113.5(2)	C(4)-C(3)-C(2)	120.4(2)
C(4)-C(3)-C(7)	126.1(2)	C(3)-C(4)-H(4)	120.6
C(5)-C(4)-C(3)	118.8(2)	C(5)-C(4)-H(4)	120.6
C(4)-C(5)-C(6)	121.7(2)	C(4)-C(5)-C(11)	124.5(2)
C(6)-C(5)-C(11)	113.83(19)	C(1)-C(6)-C(28)	130.4(2)
C(5)-C(6)-C(1)	119.8(2)	C(5)-C(6)-C(28)	109.82(19)
C(3)-C(7)-C(8)	111.2(2)	C(3)-C(7)-C(9)	110.8(2)
C(3)-C(7)-C(10)	102.42(18)	C(8)-C(7)-C(10)	110.1(2)
C(9)-C(7)-C(8)	109.3(2)	C(9)-C(7)-C(10)	113.0(2)
C(7)-C(8)-H(8A)	109.5	C(7)-C(8)-H(8B)	109.5
C(7)-C(8)-H(8C)	109.5	H(8A)-C(8)-H(8B)	109.5

H(8A)-C(8)-H(8C)	109.5	H(8B)-C(8)-H(8C)	109.5
C(7)-C(9)-H(9A)	109.5	C(7)-C(9)-H(9B)	109.5
C(7)-C(9)-H(9C)	109.5	H(9A)-C(9)-H(9B)	109.5
H(9A)-C(9)-H(9C)	109.5	H(9B)-C(9)-H(9C)	109.5
C(7)-C(10)-H(10A)	109.9	C(7)-C(10)-H(10B)	109.9
C(7)-C(10)-C(15)	108.93(18)	H(10A)-C(10)-H(10B)	108.3
C(15)-C(10)-H(10A)	109.9	C(15)-C(10)-H(10B)	109.9
C(5)-C(11)-C(12)	111.0(2)	C(5)-C(11)-C(13)	111.69(19)
C(5)-C(11)-C(14)	102.72(18)	C(12)-C(11)-C(14)	111.0(2)
C(13)-C(11)-C(12)	109.3(2)	C(13)-C(11)-C(14)	111.0(2)
C(11)-C(12)-H(12A)	109.5	C(11)-C(12)-H(12B)	109.5
C(11)-C(12)-H(12C)	109.5	H(12A)-C(12)-H(12B)	109.5
H(12A)-C(12)-H(12C)	109.5	H(12B)-C(12)-H(12C)	109.5
C(11)-C(13)-H(13A)	109.5	C(11)-C(13)-H(13B)	109.5
C(11)-C(13)-H(13C)	109.5	H(13A)-C(13)-H(13B)	109.5
H(13A)-C(13)-H(13C)	109.5	H(13B)-C(13)-H(13C)	109.5
C(11)-C(14)-H(14A)	109.8	C(11)-C(14)-H(14B)	109.8
C(11)-C(14)-C(28)	109.24(19)	H(14A)-C(14)-H(14B)	108.3
C(28)-C(14)-H(14A)	109.8	C(28)-C(14)-H(14B)	109.8
C(2)-C(15)-C(10)	103.05(17)	C(16)-C(15)-C(2)	114.75(18)
C(16)-C(15)-C(10)	110.73(19)	C(16)-C(15)-C(27)	100.77(18)
C(27)-C(15)-C(2)	115.60(19)	C(27)-C(15)-C(10)	112.27(18)
C(17)-C(16)-C(15)	128.0(2)	C(17)-C(16)-C(21)	120.7(2)
C(21)-C(16)-C(15)	111.3(2)	C(16)-C(17)-H(17)	120.9
C(16)-C(17)-C(18)	118.2(2)	C(18)-C(17)-H(17)	120.9
C(17)-C(18)-H(18)	119.4	C(17)-C(18)-C(19)	121.1(3)
C(19)-C(18)-H(18)	119.4	C(18)-C(19)-H(19)	119.7
C(20)-C(19)-C(18)	120.7(2)	C(20)-C(19)-H(19)	119.7
C(19)-C(20)-H(20)	120.7	C(19)-C(20)-C(21)	118.6(2)
C(21)-C(20)-H(20)	120.7	C(16)-C(21)-C(22)	108.2(2)
C(20)-C(21)-C(16)	120.7(2)	C(20)-C(21)-C(22)	130.9(2)
C(23)-C(22)-C(21)	130.5(2)	C(23)-C(22)-C(27)	120.7(2)
C(27)-C(22)-C(21)	108.7(2)	C(22)-C(23)-H(23)	120.7
C(22)-C(23)-C(24)	118.6(2)	C(24)-C(23)-H(23)	120.7
C(23)-C(24)-H(24)	119.7	C(23)-C(24)-C(25)	120.6(2)
C(25)-C(24)-H(24)	119.7	C(24)-C(25)-H(25)	119.6

C(26)-C(25)-C(24)	120.7(2)	C(26)-C(25)-H(25)	119.6
C(25)-C(26)-H(26)	120.3	C(27)-C(26)-C(25)	119.3(2)
C(27)-C(26)-H(26)	120.3	C(22)-C(27)-C(15)	110.5(2)
C(26)-C(27)-C(15)	129.5(2)	C(26)-C(27)-C(22)	120.0(2)
C(6)-C(28)-C(14)	103.41(18)	C(29)-C(28)-C(6)	118.46(19)
C(29)-C(28)-C(14)	107.98(19)	C(29)-C(28)-C(40)	100.96(18)
C(40)-C(28)-C(6)	115.02(19)	C(40)-C(28)-C(14)	111.01(19)
C(30)-C(29)-C(28)	128.5(2)	C(30)-C(29)-C(34)	120.3(2)
C(34)-C(29)-C(28)	110.8(2)	C(29)-C(30)-H(30)	120.5
C(29)-C(30)-C(31)	119.0(3)	C(31)-C(30)-H(30)	120.5
C(30)-C(31)-H(31)	119.7	C(32)-C(31)-C(30)	120.6(3)
C(32)-C(31)-H(31)	119.7	C(31)-C(32)-H(32)	119.6
C(33)-C(32)-C(31)	120.8(2)	C(33)-C(32)-H(32)	119.6
C(32)-C(33)-H(33)	120.7	C(32)-C(33)-C(34)	118.6(3)
C(34)-C(33)-H(33)	120.7	C(29)-C(34)-C(35)	108.4(2)
C(33)-C(34)-C(29)	120.8(2)	C(33)-C(34)-C(35)	130.8(2)
C(36)-C(35)-C(34)	131.1(2)	C(36)-C(35)-C(40)	120.6(2)
C(40)-C(35)-C(34)	108.3(2)	C(35)-C(36)-H(36)	120.5
C(37)-C(36)-C(35)	119.1(2)	C(37)-C(36)-H(36)	120.5
C(36)-C(37)-H(37)	119.8	C(36)-C(37)-C(38)	120.4(2)
C(38)-C(37)-H(37)	119.8	C(37)-C(38)-H(38)	119.6
C(39)-C(38)-C(37)	120.8(2)	C(39)-C(38)-H(38)	119.6
C(38)-C(39)-H(39)	120.5	C(38)-C(39)-C(40)	119.0(2)
C(40)-C(39)-H(39)	120.5	C(35)-C(40)-C(28)	110.8(2)
C(39)-C(40)-C(28)	129.0(2)	C(39)-C(40)-C(35)	120.1(2)
C(91)-O(1)-C(94)	108.7(3)	O(1)-C(91)-H(91A)	110.1
O(1)-C(91)-H(91B)	110.1	O(1)-C(91)-C(92)	108.0(3)
H(91A)-C(91)-H(91B)	108.4	C(92)-C(91)-H(91A)	110.1
C(92)-C(91)-H(91B)	110.1	C(91)-C(92)-H(92A)	111.1
C(91)-C(92)-H(92B)	111.1	C(91)-C(92)-C(93)	103.2(3)
H(92A)-C(92)-H(92B)	109.1	C(93)-C(92)-H(92A)	111.1
C(93)-C(92)-H(92B)	111.1	C(92)-C(93)-H(93A)	111.3
C(92)-C(93)-H(93B)	111.3	H(93A)-C(93)-H(93B)	109.2
C(94)-C(93)-C(92)	102.2(3)	C(94)-C(93)-H(93A)	111.3
C(94)-C(93)-H(93B)	111.3	O(1)-C(94)-C(93)	105.7(3)
O(1)-C(94)-H(94A)	110.6	O(1)-C(94)-H(94B)	110.6

C(93)-C(94)-H(94A)	110.6	C(93)-C(94)-H(94B)	110.6
H(94A)-C(94)-H(94B)	108.7		

3.2. Single crystal structure analysis of [M^{s}Fluind-Bi(I)]$_2$ (**S2**)

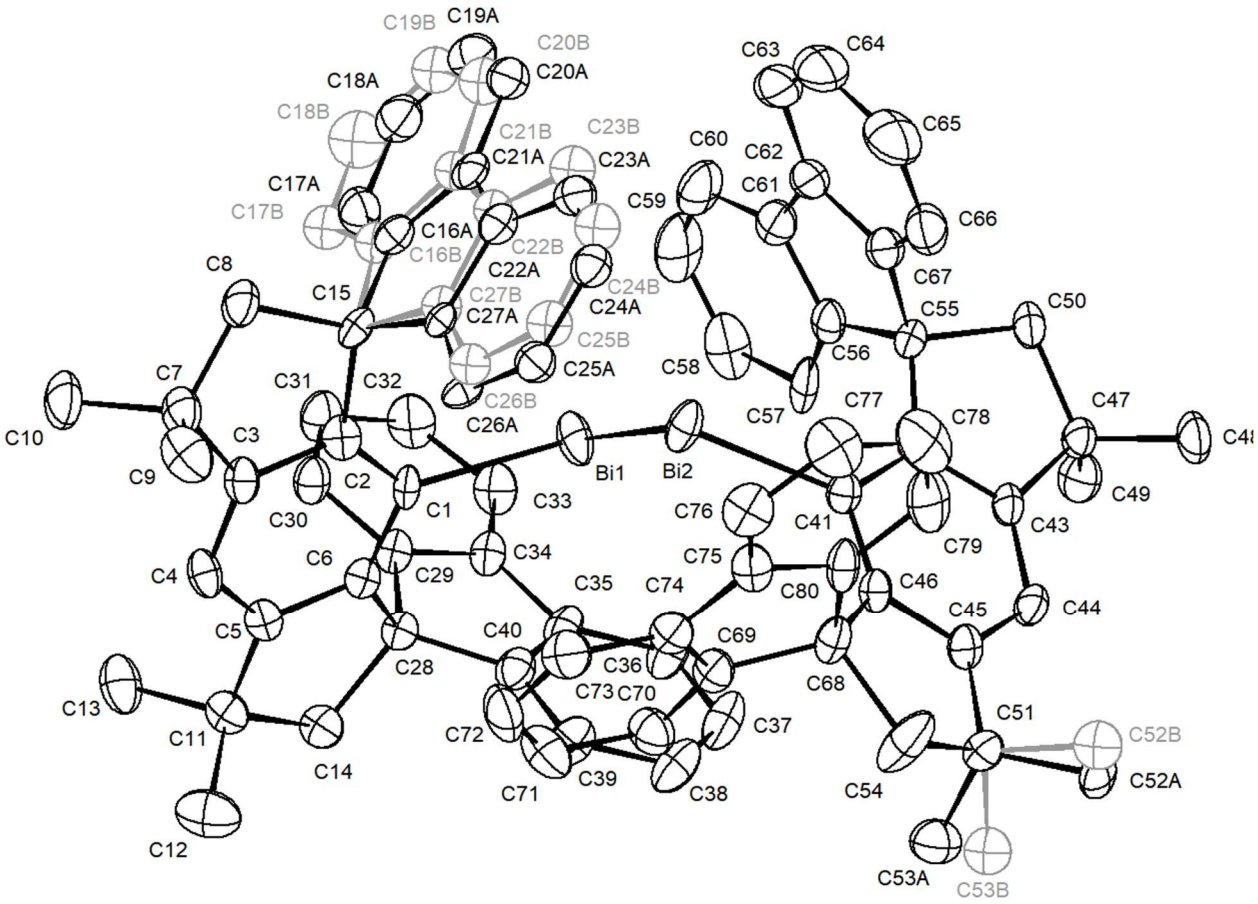

Fig. S35. The molecular structure of [M^{s}Fluind-Bi(I)]$_2$ (**S2**). H atoms have been removed for clarity. Main structure shown in black and disordered parts shown in grey.

X-ray Crystal Structure Analysis of [M^{s}Fluind-Bi(I)]$_2$ (**S2**):

C_{80} H_{66} Bi_2, M_r = 1445.28 g mol^{-1}, black prism, crystal size 0.090 x 0.086 x 0.041 mm^3, orthorhombic, space group $Pna2_1$ [33], a = 29.075(2) Å, b = 12.2171(10) Å, c = 17.4760(14) Å, V = 6207.6(9) Å^3, T = 150(2) K, Z = 4, D_{calc} = 1.546 g·cm^3, λ = 0.71073 Å, μ(*Mo-K*$_\alpha$) = 5.707 mm^{-1}, Gaussian absorption correction (T_{min} = 0.67071, T_{max} = 0.85916), Bruker-AXS Kappa Mach3 with APEX-II detector and IμS microfocus Mo-anode X-ray source, 1.401 < θ < 30.508°, 197345 measured reflections, 18656 independent reflections, 13871 reflections with $I > 2\sigma(I)$, R_{int} = 0.0889. The structure was solved by *SHELXT* and refined by full-matrix least-squares (*SHELXL*) against F^2 to R_1 = 0.0390 [$I > 2\sigma(I)$], wR_2 = 0.0702 [all data], 807 parameters, 163 restraints and absolute structure parameter Flack x = 0.171(6).

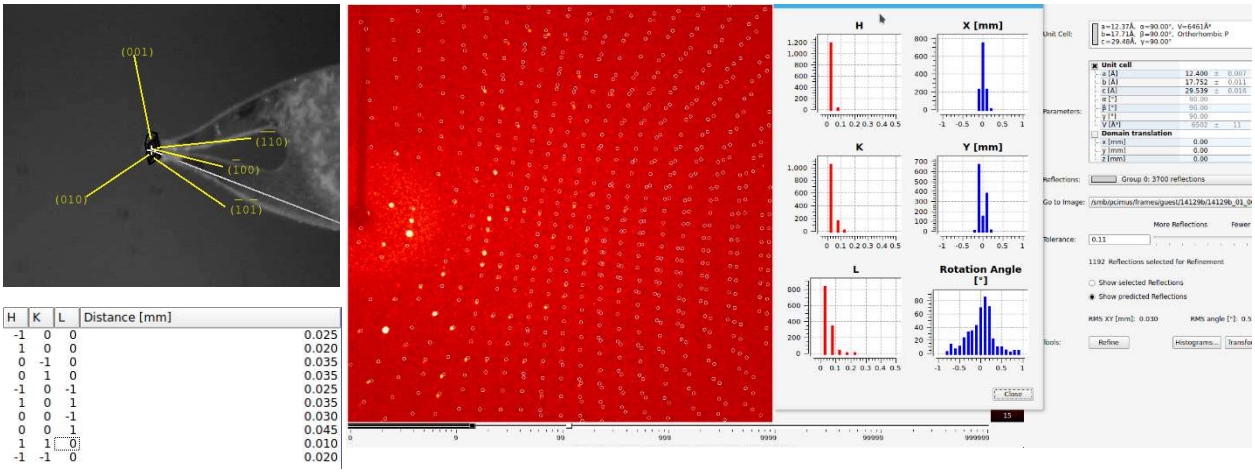

H	K	L	Distance [mm]
-1	0	0	0.025
1	0	0	0.020
0	-1	0	0.035
0	1	0	0.035
-1	0	-1	0.025
1	0	1	0.035
0	0	-1	0.030
0	0	1	0.045
1	1	0	0.010
-1	-1	0	0.020

Fig. S36. Crystal faces and unit cell determination/refinement of compound [M^{s}Fluind-Bi(I)]$_2$ (**S2**).

INTENSITY STATISTICS FOR DATASET

Resolution	#Data	#Theory	%Complete	Redundancy	Mean I	Mean I/s	Rmerge	Rsigma
Inf - 2.95	314	316	99.4	14.73	77.85	34.76	0.0273	0.0224
2.95 - 1.93	746	746	100.0	16.74	59.35	36.65	0.0322	0.0219
1.93 - 1.52	1028	1028	100.0	17.07	36.12	34.11	0.0459	0.0232
1.52 - 1.32	1066	1066	100.0	17.26	25.44	30.51	0.0615	0.0258
1.32 - 1.19	1106	1106	100.0	16.93	20.64	26.62	0.0757	0.0291
1.19 - 1.10	1093	1093	100.0	16.15	17.12	23.13	0.0921	0.0339
1.10 - 1.04	938	959	97.8	12.77	13.46	17.93	0.1131	0.0460
1.04 - 0.98	1162	1196	97.2	10.70	10.55	14.12	0.1382	0.0595
0.98 - 0.94	916	952	96.2	9.22	9.42	11.81	0.1605	0.0729
0.94 - 0.90	1134	1173	96.7	8.42	7.88	9.46	0.1871	0.0907
0.90 - 0.87	965	999	96.6	7.67	6.82	7.87	0.2073	0.1095
0.87 - 0.84	1112	1146	97.0	7.47	5.97	6.80	0.2377	0.1285
0.84 - 0.81	1278	1320	96.8	7.08	5.12	5.64	0.2677	0.1569
0.81 - 0.79	960	979	98.1	7.00	4.38	4.84	0.3109	0.1871
0.79 - 0.77	1074	1103	97.4	6.70	3.62	4.02	0.3646	0.2338
0.77 - 0.75	1236	1261	98.0	6.51	3.31	3.56	0.3978	0.2667
0.75 - 0.74	646	661	97.7	6.43	2.64	2.90	0.4584	0.3337
0.74 - 0.72	1380	1408	98.0	6.15	2.61	2.67	0.4825	0.3609
0.72 - 0.71	765	777	98.5	6.16	2.18	2.27	0.5308	0.4343
0.71 - 0.69	1666	1698	98.1	5.43	1.91	1.70	0.5913	0.5739
0.69 - 0.68	289	505	57.2	1.38	1.71	0.97	0.6179	1.0820
0.78 - 0.68	6490	6830	95.0	5.76	2.55	2.59	0.4738	0.3915
Inf - 0.68	20874	21492	97.1	9.71	12.44	12.53	0.0865	0.0673

Complete .cif-data of **S2** are available under the CCDC number CCDC-**2225005**.

A resolution cut off (SHEL 999 0.7) was applied to exclude poorly determined reflections at high diffraction angles. The investigated crystal appears to be twinned by inversion (TWIN -1 0 0 0 -1 0 0 0 -1) with a BASF of 0.171(6). A positional disorder over two positions of one fluorene arm could be found. It was refined using a free variable (FVAR) and occupancies of 58:42% have been determined. The ISOR instruction was used to equalize thermal ellipsoids of the main part. Isotropic displacement parameters have

been used for the description of minor parts. A second disorder was found at the terminal methyl groups (C52 and C53). This was described by fixed occupancies of 60:40%.

Table S5. Crystal data and structure refinement of compound $[M^sFluind\text{-}Bi(I)]_2$ (**S2**)

Identification code	14129	
Empirical formula	$C_{80}\ H_{66}\ Bi_2$	
Color	black	
Formula weight	1445.28 $g \cdot mol^{-1}$	
Temperature	150(2) K	
Wavelength	0.71073 Å	
Crystal system	Orthorhombic	
Space group	*Pna*2_1, (no. 33)	
Unit cell dimensions	a = 29.075(2) Å	α= 90°.
	b = 12.2171(10) Å	β= 90°.
	c = 17.4760(14) Å	γ = 90°.
Volume	6207.6(9) $Å^3$	
Z	4	
Density (calculated)	1.546 $Mg \cdot m^{-3}$	
Absorption coefficient	5.707 mm^{-1}	
F(000)	2848 e	
Crystal size	0.090 x 0.086 x 0.041 mm^3	
θ range for data collection	1.401 to 30.508°.	
Index ranges	$-41 \le h \le 41, -17 \le k \le 17, -24 \le l \le 24$	
Reflections collected	197345	
Independent reflections	18656 [R_{int} = 0.0889]	
Reflections with I>2σ(I)	13871	
Completeness to θ = 25.242°	100.0 %	
Absorption correction	Gaussian	
Max. and min. transmission	0.85916 and 0.67071	
Refinement method	Full-matrix least-squares on F^2	
Data / restraints / parameters	18656 / 163 / 807	
Goodness-of-fit on F^2	1.037	
Final R indices [I>2σ(I)]	R_1 = 0.0390	wR^2 = 0.0623
R indices (all data)	R_1 = 0.0716	wR^2 = 0.0702
Absolute structure parameter	0.171(6)	
Extinction coefficient	n/a	
Largest diff. peak and hole	1.307 and –1.561 $e \cdot Å^{-3}$	

Table S6. Bond lengths [Å] and angles [°] of compound $[M^sFluind\text{-}Bi(I)]_2$ (**S2**)

Bi(1)-Bi(2)	2.8464(4)	Bi(1)-C(1)	2.292(6)
Bi(2)-C(41)	2.287(6)	C(1)-C(2)	1.402(10)
C(1)-C(6)	1.407(9)	C(2)-C(3)	1.405(9)
C(2)-C(15)	1.523(9)	C(3)-C(4)	1.371(10)
C(3)-C(7)	1.506(10)	C(4)-H(4)	0.9500
C(4)-C(5)	1.386(10)	C(5)-C(6)	1.390(9)
C(5)-C(11)	1.516(10)	C(6)-C(28)	1.534(9)
C(7)-C(8)	1.537(10)	C(7)-C(9)	1.533(12)
C(7)-C(10)	1.533(10)	C(8)-H(8A)	0.9900
C(8)-H(8B)	0.9900	C(8)-C(15)	1.582(9)
C(9)-H(9A)	0.9800	C(9)-H(9B)	0.9800
C(9)-H(9C)	0.9800	C(10)-H(10A)	0.9800
C(10)-H(10B)	0.9800	C(10)-H(10C)	0.9800
C(11)-C(12)	1.524(10)	C(11)-C(13)	1.548(10)
C(11)-C(14)	1.539(9)	C(12)-H(12A)	0.9800
C(12)-H(12B)	0.9800	C(12)-H(12C)	0.9800
C(13)-H(13A)	0.9800	C(13)-H(13B)	0.9800
C(13)-H(13C)	0.9800	C(14)-H(14A)	0.9900
C(14)-H(14B)	0.9900	C(14)-C(28)	1.552(9)
C(15)-C(16A)	1.527(13)	C(15)-C(27A)	1.549(12)
C(15)-C(16B)	1.493(16)	C(15)-C(27B)	1.503(17)
C(16A)-C(17A)	1.390(11)	C(16A)-C(21A)	1.407(12)
C(17A)-H(17A)	0.9500	C(17A)-C(18A)	1.399(12)
C(18A)-H(18A)	0.9500	C(18A)-C(19A)	1.379(13)
C(19A)-H(19A)	0.9500	C(19A)-C(20A)	1.376(13)
C(20A)-H(20A)	0.9500	C(20A)-C(21A)	1.398(10)
C(21A)-C(22A)	1.458(12)	C(22A)-C(23A)	1.398(11)
C(22A)-C(27A)	1.398(11)	C(23A)-H(23A)	0.9500
C(23A)-C(24A)	1.368(12)	C(24A)-H(24A)	0.9500
C(24A)-C(25A)	1.387(13)	C(25A)-H(25A)	0.9500
C(25A)-C(26A)	1.386(11)	C(26A)-H(26A)	0.9500
C(26A)-C(27A)	1.374(12)	C(16B)-C(17B)	1.387(12)
C(16B)-C(21B)	1.404(12)	C(17B)-H(17B)	0.9500

C(17B)-C(18B)	1.395(13)	C(18B)-H(18B)	0.9500
C(18B)-C(19B)	1.378(14)	C(19B)-H(19B)	0.9500
C(19B)-C(20B)	1.373(14)	C(20B)-H(20B)	0.9500
C(20B)-C(21B)	1.399(12)	C(21B)-C(22B)	1.459(12)
C(22B)-C(23B)	1.398(12)	C(22B)-C(27B)	1.397(12)
C(23B)-H(23B)	0.9500	C(23B)-C(24B)	1.370(14)
C(24B)-H(24B)	0.9500	C(24B)-C(25B)	1.381(14)
C(25B)-H(25B)	0.9500	C(25B)-C(26B)	1.391(13)
C(26B)-H(26B)	0.9500	C(26B)-C(27B)	1.378(12)
C(28)-C(29)	1.522(9)	C(28)-C(40)	1.524(9)
C(29)-C(30)	1.382(8)	C(29)-C(34)	1.408(8)
C(30)-H(30)	0.9500	C(30)-C(31)	1.394(9)
C(31)-H(31)	0.9500	C(31)-C(32)	1.374(10)
C(32)-H(32)	0.9500	C(32)-C(33)	1.378(9)
C(33)-H(33)	0.9500	C(33)-C(34)	1.386(8)
C(34)-C(35)	1.462(8)	C(35)-C(36)	1.395(8)
C(35)-C(40)	1.393(9)	C(36)-H(36)	0.9500
C(36)-C(37)	1.371(9)	C(37)-H(37)	0.9500
C(37)-C(38)	1.383(11)	C(38)-H(38)	0.9500
C(38)-C(39)	1.392(9)	C(39)-H(39)	0.9500
C(39)-C(40)	1.380(9)	C(41)-C(42)	1.423(10)
C(41)-C(46)	1.407(9)	C(42)-C(43)	1.394(9)
C(42)-C(55)	1.511(9)	C(43)-C(44)	1.377(9)
C(43)-C(47)	1.512(10)	C(44)-H(44)	0.9500
C(44)-C(45)	1.396(10)	C(45)-C(46)	1.393(9)
C(45)-C(51)	1.504(9)	C(46)-C(68)	1.537(10)
C(47)-C(48)	1.520(10)	C(47)-C(49)	1.533(11)
C(47)-C(50)	1.551(10)	C(48)-H(48A)	0.9800
C(48)-H(48B)	0.9800	C(48)-H(48C)	0.9800
C(49)-H(49A)	0.9800	C(49)-H(49B)	0.9800
C(49)-H(49C)	0.9800	C(50)-H(50A)	0.9900
C(50)-H(50B)	0.9900	C(50)-C(55)	1.577(9)
C(51)-C(52A)	1.498(15)	C(51)-C(52B)	1.61(3)
C(51)-C(53A)	1.533(15)	C(51)-C(53B)	1.55(2)
C(51)-C(54)	1.514(10)	C(52A)-H(52A)	0.9800
C(52A)-H(52B)	0.9800	C(52A)-H(52C)	0.9800

C(52B)-H(52D)	0.9800	C(52B)-H(52E)	0.9800
C(52B)-H(52F)	0.9800	C(53A)-H(53A)	0.9800
C(53A)-H(53B)	0.9800	C(53A)-H(53C)	0.9800
C(53B)-H(53D)	0.9800	C(53B)-H(53E)	0.9800
C(53B)-H(53F)	0.9800	C(54)-H(54A)	0.9900
C(54)-H(54B)	0.9900	C(54)-C(68)	1.567(10)
C(55)-C(56)	1.525(9)	C(55)-C(67)	1.522(10)
C(56)-C(57)	1.390(11)	C(56)-C(61)	1.404(10)
C(57)-H(57)	0.9500	C(57)-C(58)	1.412(11)
C(58)-H(58)	0.9500	C(58)-C(59)	1.391(14)
C(59)-H(59)	0.9500	C(59)-C(60)	1.343(14)
C(60)-H(60)	0.9500	C(60)-C(61)	1.405(11)
C(61)-C(62)	1.441(11)	C(62)-C(63)	1.391(11)
C(62)-C(67)	1.403(10)	C(63)-H(63)	0.9500
C(63)-C(64)	1.393(14)	C(64)-H(64)	0.9500
C(64)-C(65)	1.366(13)	C(65)-H(65)	0.9500
C(65)-C(66)	1.396(11)	C(66)-H(66)	0.9500
C(66)-C(67)	1.373(11)	C(68)-C(69)	1.542(10)
C(68)-C(80)	1.510(11)	C(69)-C(70)	1.380(11)
C(69)-C(74)	1.397(10)	C(70)-H(70)	0.9500
C(70)-C(71)	1.392(11)	C(71)-H(71)	0.9500
C(71)-C(72)	1.380(12)	C(72)-H(72)	0.9500
C(72)-C(73)	1.389(12)	C(73)-H(73)	0.9500
C(73)-C(74)	1.392(10)	C(74)-C(75)	1.463(10)
C(75)-C(76)	1.364(10)	C(75)-C(80)	1.396(10)
C(76)-H(76)	0.9500	C(76)-C(77)	1.373(11)
C(77)-H(77)	0.9500	C(77)-C(78)	1.379(13)
C(78)-H(78)	0.9500	C(78)-C(79)	1.387(13)
C(79)-H(79)	0.9500	C(79)-C(80)	1.377(11)

C(1)-Bi(1)-Bi(2)	100.81(17)	C(41)-Bi(2)-Bi(1)	96.36(16)
C(2)-C(1)-Bi(1)	128.3(5)	C(2)-C(1)-C(6)	115.6(6)
C(6)-C(1)-Bi(1)	116.1(5)	C(1)-C(2)-C(3)	121.9(6)
C(1)-C(2)-C(15)	128.0(6)	C(3)-C(2)-C(15)	109.7(6)
C(2)-C(3)-C(7)	113.4(6)	C(4)-C(3)-C(2)	120.6(6)
C(4)-C(3)-C(7)	125.9(6)	C(3)-C(4)-H(4)	120.5

C(3)-C(4)-C(5)	119.0(6)	C(5)-C(4)-H(4)	120.5
C(4)-C(5)-C(6)	120.4(6)	C(4)-C(5)-C(11)	125.9(6)
C(6)-C(5)-C(11)	113.6(6)	C(1)-C(6)-C(28)	127.1(6)
C(5)-C(6)-C(1)	122.3(6)	C(5)-C(6)-C(28)	109.6(6)
C(3)-C(7)-C(8)	101.8(6)	C(3)-C(7)-C(9)	112.5(7)
C(3)-C(7)-C(10)	111.6(6)	C(9)-C(7)-C(8)	111.8(7)
C(10)-C(7)-C(8)	110.9(6)	C(10)-C(7)-C(9)	108.3(7)
C(7)-C(8)-H(8A)	110.2	C(7)-C(8)-H(8B)	110.2
C(7)-C(8)-C(15)	107.7(6)	H(8A)-C(8)-H(8B)	108.5
C(15)-C(8)-H(8A)	110.2	C(15)-C(8)-H(8B)	110.2
C(7)-C(9)-H(9A)	109.5	C(7)-C(9)-H(9B)	109.5
C(7)-C(9)-H(9C)	109.5	H(9A)-C(9)-H(9B)	109.5
H(9A)-C(9)-H(9C)	109.5	H(9B)-C(9)-H(9C)	109.5
C(7)-C(10)-H(10A)	109.5	C(7)-C(10)-H(10B)	109.5
C(7)-C(10)-H(10C)	109.5	H(10A)-C(10)-H(10B)	109.5
H(10A)-C(10)-H(10C)	109.5	H(10B)-C(10)-H(10C)	109.5
C(5)-C(11)-C(12)	111.3(6)	C(5)-C(11)-C(13)	110.8(6)
C(5)-C(11)-C(14)	102.7(5)	C(12)-C(11)-C(13)	108.1(7)
C(12)-C(11)-C(14)	111.5(6)	C(14)-C(11)-C(13)	112.4(7)
C(11)-C(12)-H(12A)	109.5	C(11)-C(12)-H(12B)	109.5
C(11)-C(12)-H(12C)	109.5	H(12A)-C(12)-H(12B)	109.5
H(12A)-C(12)-H(12C)	109.5	H(12B)-C(12)-H(12C)	109.5
C(11)-C(13)-H(13A)	109.5	C(11)-C(13)-H(13B)	109.5
C(11)-C(13)-H(13C)	109.5	H(13A)-C(13)-H(13B)	109.5
H(13A)-C(13)-H(13C)	109.5	H(13B)-C(13)-H(13C)	109.5
C(11)-C(14)-H(14A)	109.9	C(11)-C(14)-H(14B)	109.9
C(11)-C(14)-C(28)	109.0(6)	H(14A)-C(14)-H(14B)	108.3
C(28)-C(14)-H(14A)	109.9	C(28)-C(14)-H(14B)	109.9
C(2)-C(15)-C(8)	102.4(5)	C(2)-C(15)-C(16A)	118.7(8)
C(2)-C(15)-C(27A)	116.2(9)	C(16A)-C(15)-C(8)	110.6(9)
C(16A)-C(15)-C(27A)	99.4(8)	C(27A)-C(15)-C(8)	109.5(11)
C(16B)-C(15)-C(2)	111.9(11)	C(16B)-C(15)-C(8)	105.4(13)
C(16B)-C(15)-C(27B)	103.3(10)	C(27B)-C(15)-C(2)	122.1(15)
C(27B)-C(15)-C(8)	110.8(18)	C(17A)-C(16A)-C(15)	126.7(10)
C(17A)-C(16A)-C(21A)	121.9(10)	C(21A)-C(16A)-C(15)	111.4(8)
C(16A)-C(17A)-H(17A)	120.6	C(16A)-C(17A)-C(18A)	118.9(11)

C(18A)-C(17A)-H(17A)	120.6	C(17A)-C(18A)-H(18A)	120.6
C(19A)-C(18A)-C(17A)	118.8(11)	C(19A)-C(18A)-H(18A)	120.6
C(18A)-C(19A)-H(19A)	118.5	C(20A)-C(19A)-C(18A)	123.0(10)
C(20A)-C(19A)-H(19A)	118.5	C(19A)-C(20A)-H(20A)	120.4
C(19A)-C(20A)-C(21A)	119.2(11)	C(21A)-C(20A)-H(20A)	120.4
C(16A)-C(21A)-C(22A)	108.2(7)	C(20A)-C(21A)-C(16A)	118.2(10)
C(20A)-C(21A)-C(22A)	133.6(10)	C(23A)-C(22A)-C(21A)	129.5(10)
C(23A)-C(22A)-C(27A)	121.5(10)	C(27A)-C(22A)-C(21A)	108.8(8)
C(22A)-C(23A)-H(23A)	121.4	C(24A)-C(23A)-C(22A)	117.1(10)
C(24A)-C(23A)-H(23A)	121.4	C(23A)-C(24A)-H(24A)	119.0
C(23A)-C(24A)-C(25A)	122.0(10)	C(25A)-C(24A)-H(24A)	119.0
C(24A)-C(25A)-H(25A)	119.8	C(26A)-C(25A)-C(24A)	120.4(11)
C(26A)-C(25A)-H(25A)	119.8	C(25A)-C(26A)-H(26A)	120.6
C(27A)-C(26A)-C(25A)	118.8(11)	C(27A)-C(26A)-H(26A)	120.6
C(22A)-C(27A)-C(15)	110.7(9)	C(26A)-C(27A)-C(15)	129.4(10)
C(26A)-C(27A)-C(22A)	120.0(10)	C(17B)-C(16B)-C(15)	129.2(13)
C(17B)-C(16B)-C(21B)	121.0(12)	C(21B)-C(16B)-C(15)	109.8(10)
C(16B)-C(17B)-H(17B)	121.0	C(16B)-C(17B)-C(18B)	117.9(13)
C(18B)-C(17B)-H(17B)	121.0	C(17B)-C(18B)-H(18B)	119.8
C(19B)-C(18B)-C(17B)	120.4(13)	C(19B)-C(18B)-H(18B)	119.8
C(18B)-C(19B)-H(19B)	118.6	C(20B)-C(19B)-C(18B)	122.7(13)
C(20B)-C(19B)-H(19B)	118.6	C(19B)-C(20B)-H(20B)	121.3
C(19B)-C(20B)-C(21B)	117.4(13)	C(21B)-C(20B)-H(20B)	121.3
C(16B)-C(21B)-C(22B)	108.2(9)	C(20B)-C(21B)-C(16B)	120.5(12)
C(20B)-C(21B)-C(22B)	131.3(12)	C(23B)-C(22B)-C(21B)	130.5(12)
C(27B)-C(22B)-C(21B)	108.9(10)	C(27B)-C(22B)-C(23B)	120.5(12)
C(22B)-C(23B)-H(23B)	121.1	C(24B)-C(23B)-C(22B)	117.7(12)
C(24B)-C(23B)-H(23B)	121.1	C(23B)-C(24B)-H(24B)	118.8
C(23B)-C(24B)-C(25B)	122.4(13)	C(25B)-C(24B)-H(24B)	118.8
C(24B)-C(25B)-H(25B)	120.0	C(24B)-C(25B)-C(26B)	119.9(13)
C(26B)-C(25B)-H(25B)	120.0	C(25B)-C(26B)-H(26B)	120.6
C(27B)-C(26B)-C(25B)	118.8(13)	C(27B)-C(26B)-H(26B)	120.6
C(22B)-C(27B)-C(15)	109.2(11)	C(26B)-C(27B)-C(15)	130.1(12)
C(26B)-C(27B)-C(22B)	120.7(12)	C(6)-C(28)-C(14)	103.4(5)
C(29)-C(28)-C(6)	110.1(5)	C(29)-C(28)-C(14)	113.0(6)
C(29)-C(28)-C(40)	100.3(5)	C(40)-C(28)-C(6)	120.4(6)

C(40)-C(28)-C(14)	110.0(6)	C(30)-C(29)-C(28)	127.9(6)
C(30)-C(29)-C(34)	120.7(6)	C(34)-C(29)-C(28)	111.4(5)
C(29)-C(30)-H(30)	120.7	C(29)-C(30)-C(31)	118.6(6)
C(31)-C(30)-H(30)	120.7	C(30)-C(31)-H(31)	119.8
C(32)-C(31)-C(30)	120.5(7)	C(32)-C(31)-H(31)	119.8
C(31)-C(32)-H(32)	119.3	C(31)-C(32)-C(33)	121.4(7)
C(33)-C(32)-H(32)	119.3	C(32)-C(33)-H(33)	120.4
C(32)-C(33)-C(34)	119.2(6)	C(34)-C(33)-H(33)	120.4
C(29)-C(34)-C(35)	107.8(5)	C(33)-C(34)-C(29)	119.6(6)
C(33)-C(34)-C(35)	132.6(6)	C(36)-C(35)-C(34)	130.0(6)
C(40)-C(35)-C(34)	108.6(5)	C(40)-C(35)-C(36)	121.2(6)
C(35)-C(36)-H(36)	121.1	C(37)-C(36)-C(35)	117.8(7)
C(37)-C(36)-H(36)	121.1	C(36)-C(37)-H(37)	119.2
C(36)-C(37)-C(38)	121.6(7)	C(38)-C(37)-H(37)	119.2
C(37)-C(38)-H(38)	119.8	C(37)-C(38)-C(39)	120.5(7)
C(39)-C(38)-H(38)	119.8	C(38)-C(39)-H(39)	120.6
C(40)-C(39)-C(38)	118.8(7)	C(40)-C(39)-H(39)	120.6
C(35)-C(40)-C(28)	111.5(6)	C(39)-C(40)-C(28)	128.4(6)
C(39)-C(40)-C(35)	120.0(6)	C(42)-C(41)-Bi(2)	129.0(4)
C(46)-C(41)-Bi(2)	115.2(5)	C(46)-C(41)-C(42)	115.7(6)
C(41)-C(42)-C(55)	126.6(6)	C(43)-C(42)-C(41)	120.9(6)
C(43)-C(42)-C(55)	112.2(6)	C(42)-C(43)-C(47)	111.8(6)
C(44)-C(43)-C(42)	121.8(6)	C(44)-C(43)-C(47)	126.2(6)
C(43)-C(44)-H(44)	120.9	C(43)-C(44)-C(45)	118.3(6)
C(45)-C(44)-H(44)	120.9	C(44)-C(45)-C(51)	126.1(6)
C(46)-C(45)-C(44)	120.3(6)	C(46)-C(45)-C(51)	113.5(6)
C(41)-C(46)-C(68)	126.9(6)	C(45)-C(46)-C(41)	122.4(6)
C(45)-C(46)-C(68)	109.8(6)	C(43)-C(47)-C(48)	110.5(6)
C(43)-C(47)-C(49)	113.1(6)	C(43)-C(47)-C(50)	102.3(5)
C(48)-C(47)-C(49)	108.4(6)	C(48)-C(47)-C(50)	109.9(6)
C(49)-C(47)-C(50)	112.5(6)	C(47)-C(48)-H(48A)	109.5
C(47)-C(48)-H(48B)	109.5	C(47)-C(48)-H(48C)	109.5
H(48A)-C(48)-H(48B)	109.5	H(48A)-C(48)-H(48C)	109.5
H(48B)-C(48)-H(48C)	109.5	C(47)-C(49)-H(49A)	109.5
C(47)-C(49)-H(49B)	109.5	C(47)-C(49)-H(49C)	109.5
H(49A)-C(49)-H(49B)	109.5	H(49A)-C(49)-H(49C)	109.5

H(49B)-C(49)-H(49C)	109.5	C(47)-C(50)-H(50A)	110.2
C(47)-C(50)-H(50B)	110.2	C(47)-C(50)-C(55)	107.8(6)
H(50A)-C(50)-H(50B)	108.5	C(55)-C(50)-H(50A)	110.2
C(55)-C(50)-H(50B)	110.2	C(45)-C(51)-C(52B)	108.8(13)
C(45)-C(51)-C(53A)	107.5(8)	C(45)-C(51)-C(53B)	113.7(11)
C(45)-C(51)-C(54)	102.8(6)	C(52A)-C(51)-C(45)	115.0(8)
C(52A)-C(51)-C(53A)	110.4(11)	C(52A)-C(51)-C(54)	116.6(10)
C(53B)-C(51)-C(52B)	106.0(13)	C(54)-C(51)-C(52B)	102.0(12)
C(54)-C(51)-C(53A)	103.5(8)	C(54)-C(51)-C(53B)	122.6(11)
C(51)-C(52A)-H(52A)	109.5	C(51)-C(52A)-H(52B)	109.5
C(51)-C(52A)-H(52C)	109.5	H(52A)-C(52A)-H(52B)	109.5
H(52A)-C(52A)-H(52C)	109.5	H(52B)-C(52A)-H(52C)	109.5
C(51)-C(52B)-H(52D)	109.5	C(51)-C(52B)-H(52E)	109.5
C(51)-C(52B)-H(52F)	109.5	H(52D)-C(52B)-H(52E)	109.5
H(52D)-C(52B)-H(52F)	109.5	H(52E)-C(52B)-H(52F)	109.5
C(51)-C(53A)-H(53A)	109.5	C(51)-C(53A)-H(53B)	109.5
C(51)-C(53A)-H(53C)	109.5	H(53A)-C(53A)-H(53B)	109.5
H(53A)-C(53A)-H(53C)	109.5	H(53B)-C(53A)-H(53C)	109.5
C(51)-C(53B)-H(53D)	109.5	C(51)-C(53B)-H(53E)	109.5
C(51)-C(53B)-H(53F)	109.5	H(53D)-C(53B)-H(53E)	109.5
H(53D)-C(53B)-H(53F)	109.5	H(53E)-C(53B)-H(53F)	109.5
C(51)-C(54)-H(54A)	109.6	C(51)-C(54)-H(54B)	109.6
C(51)-C(54)-C(68)	110.4(6)	H(54A)-C(54)-H(54B)	108.1
C(68)-C(54)-H(54A)	109.6	C(68)-C(54)-H(54B)	109.6
C(42)-C(55)-C(50)	101.4(5)	C(42)-C(55)-C(56)	117.0(6)
C(42)-C(55)-C(67)	115.6(6)	C(56)-C(55)-C(50)	111.6(6)
C(67)-C(55)-C(50)	109.3(5)	C(67)-C(55)-C(56)	102.1(5)
C(57)-C(56)-C(55)	129.3(7)	C(57)-C(56)-C(61)	121.6(7)
C(61)-C(56)-C(55)	109.1(7)	C(56)-C(57)-H(57)	121.2
C(56)-C(57)-C(58)	117.7(8)	C(58)-C(57)-H(57)	121.2
C(57)-C(58)-H(58)	120.0	C(59)-C(58)-C(57)	120.1(9)
C(59)-C(58)-H(58)	120.0	C(58)-C(59)-H(59)	119.1
C(60)-C(59)-C(58)	121.8(8)	C(60)-C(59)-H(59)	119.1
C(59)-C(60)-H(60)	119.9	C(59)-C(60)-C(61)	120.1(8)
C(61)-C(60)-H(60)	119.9	C(56)-C(61)-C(60)	118.7(8)
C(56)-C(61)-C(62)	109.4(7)	C(60)-C(61)-C(62)	131.7(8)

C(63)-C(62)-C(61)	131.0(8)	C(63)-C(62)-C(67)	119.8(8)
C(67)-C(62)-C(61)	109.2(6)	C(62)-C(63)-H(63)	121.2
C(62)-C(63)-C(64)	117.7(9)	C(64)-C(63)-H(63)	121.2
C(63)-C(64)-H(64)	118.8	C(65)-C(64)-C(63)	122.3(9)
C(65)-C(64)-H(64)	118.8	C(64)-C(65)-H(65)	119.9
C(64)-C(65)-C(66)	120.2(10)	C(66)-C(65)-H(65)	119.9
C(65)-C(66)-H(66)	120.8	C(67)-C(66)-C(65)	118.3(8)
C(67)-C(66)-H(66)	120.8	C(62)-C(67)-C(55)	109.4(7)
C(66)-C(67)-C(55)	129.0(7)	C(66)-C(67)-C(62)	121.6(7)
C(46)-C(68)-C(54)	102.3(6)	C(46)-C(68)-C(69)	119.7(6)
C(69)-C(68)-C(54)	110.4(7)	C(80)-C(68)-C(46)	112.5(6)
C(80)-C(68)-C(54)	111.8(7)	C(80)-C(68)-C(69)	100.4(6)
C(70)-C(69)-C(68)	129.2(7)	C(70)-C(69)-C(74)	120.9(7)
C(74)-C(69)-C(68)	109.8(7)	C(69)-C(70)-H(70)	120.9
C(69)-C(70)-C(71)	118.2(7)	C(71)-C(70)-H(70)	120.9
C(70)-C(71)-H(71)	119.4	C(72)-C(71)-C(70)	121.3(8)
C(72)-C(71)-H(71)	119.4	C(71)-C(72)-H(72)	119.6
C(71)-C(72)-C(73)	120.8(7)	C(73)-C(72)-H(72)	119.6
C(72)-C(73)-H(73)	120.9	C(72)-C(73)-C(74)	118.3(7)
C(74)-C(73)-H(73)	120.9	C(69)-C(74)-C(75)	109.3(6)
C(73)-C(74)-C(69)	120.5(7)	C(73)-C(74)-C(75)	130.0(7)
C(76)-C(75)-C(74)	131.5(7)	C(76)-C(75)-C(80)	120.9(7)
C(80)-C(75)-C(74)	107.5(7)	C(75)-C(76)-H(76)	120.4
C(75)-C(76)-C(77)	119.1(8)	C(77)-C(76)-H(76)	120.4
C(76)-C(77)-H(77)	119.5	C(76)-C(77)-C(78)	121.0(8)
C(78)-C(77)-H(77)	119.5	C(77)-C(78)-H(78)	120.1
C(77)-C(78)-C(79)	119.9(8)	C(79)-C(78)-H(78)	120.1
C(78)-C(79)-H(79)	120.3	C(80)-C(79)-C(78)	119.3(8)
C(80)-C(79)-H(79)	120.3	C(75)-C(80)-C(68)	111.9(6)
C(79)-C(80)-C(68)	128.4(7)	C(79)-C(80)-C(75)	119.7(8)

3.3. Single crystal structure analysis of ^{t}Bu-M^{s}Fluind-Br (**S3**) · cyclopentane

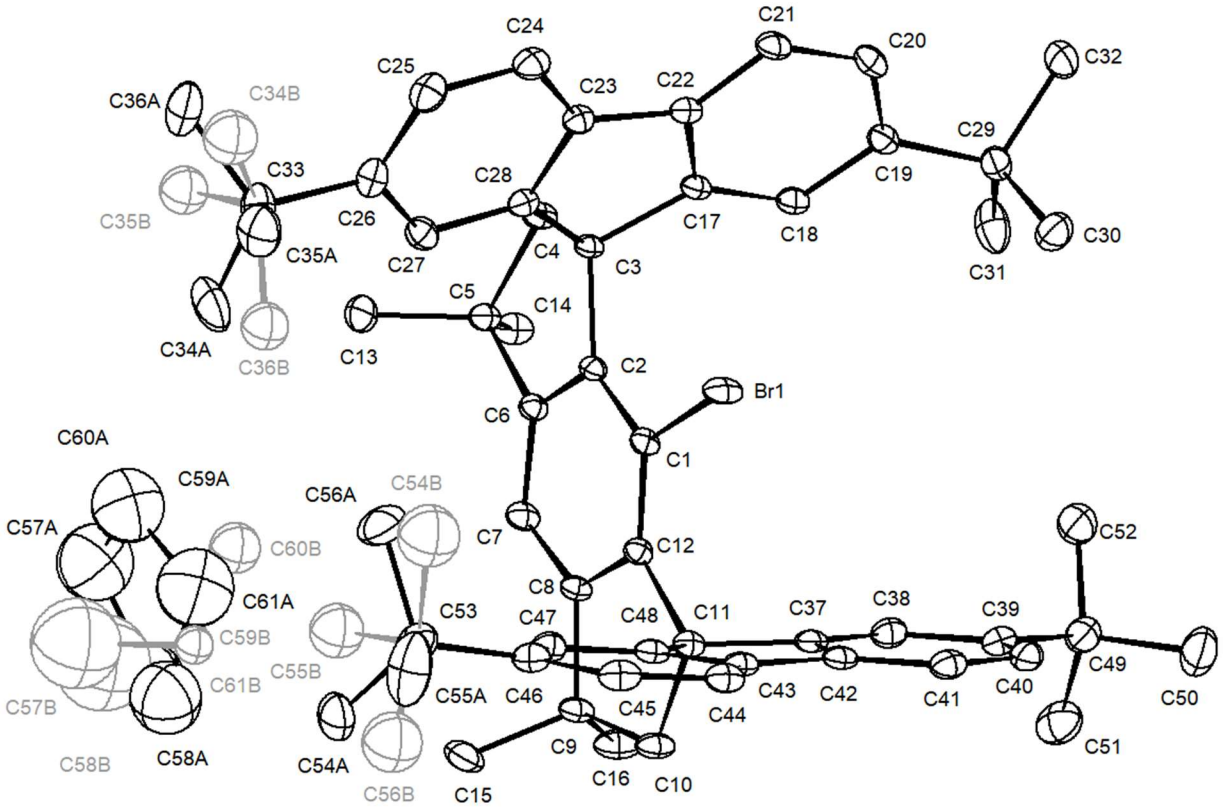

Fig. S37. The molecular structure of ^{t}Bu-M^{s}Fluind-Br (**S3**) · cyclopentane. H atoms have been removed for clarity. Main structure shown in black and disordered parts shown in grey.

X-ray Crystal Structure Analysis of ^{t}Bu-M^{s}Fluind-Br (**S3**) · cyclopentane:

C_{61} H_{75} Br, M_r = 888.12 g mol^{-1}, colorless plate, crystal size 0.124 x 0.105 x 0.021 mm^3, monoclinic, space group $P2_1/c$ [14], a = 15.1714(17) Å, b = 15.8131(18) Å, c = 21.450(2) Å, β = 90.787(2)°, V = 5145.5(10) Å^3, T = 100(2) K, Z = 4, D_{calc} = 1.146 g·cm^3, λ = 0.71073 Å, μ(*Mo-K*$_\alpha$) = 0.836 mm^{-1}, Gaussian absorption correction (T_{min} = 0.92062, T_{max} = 0.98765), Bruker-AXS Kappa Mach3 with APEX-II detector and IμS microfocus Mo-anode X-ray source, 1.342 < θ < 30.508°, 96676 measured reflections, 15713 independent reflections, 11716 reflections with $I > 2\sigma(I)$, R_{int} = 0.0755. The structure was solved by *SHELXT* and refined by full-matrix least-squares (*SHELXL*) against F^2 to R_1 = 0.0431 [$I > 2\sigma(I)$], wR_2 = 0.1103 [all data], 625 parameters and 50 restraints.

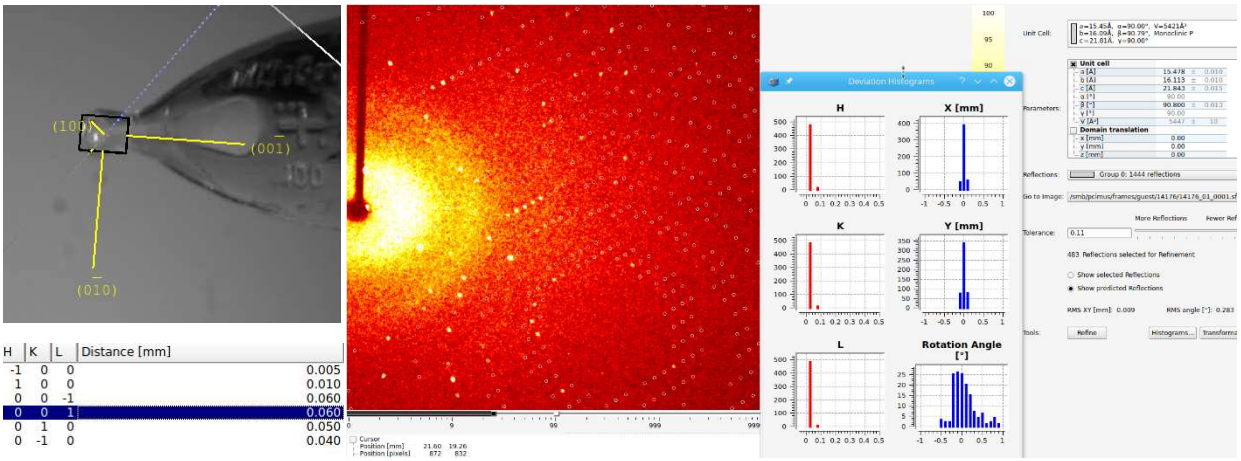

Fig. S38. Crystal faces and unit cell determination/refinement of compound ᵗBu-MˢFluind-Br (**S3**) · cyclopentane.

INTENSITY STATISTICS FOR DATASET

Resolution	#Data	#Theory	%Complete	Redundancy	Mean I	Mean I/s	Rmerge	Rsigma
Inf - 2.85	270	270	100.0	7.74	44.55	42.94	0.0244	0.0194
2.85 - 1.87	632	632	100.0	8.28	19.93	38.48	0.0320	0.0214
1.87 - 1.48	880	880	100.0	8.31	12.54	32.77	0.0386	0.0224
1.48 - 1.29	890	890	100.0	8.25	8.27	27.48	0.0499	0.0266
1.29 - 1.17	888	888	100.0	7.78	7.81	25.35	0.0567	0.0292
1.17 - 1.08	957	957	100.0	7.20	6.79	21.77	0.0662	0.0342
1.08 - 1.01	969	969	100.0	6.70	5.41	17.21	0.0821	0.0435
1.01 - 0.96	899	899	100.0	6.38	4.32	14.07	0.0971	0.0529
0.96 - 0.92	851	851	100.0	6.08	3.27	11.25	0.1166	0.0679
0.92 - 0.88	1003	1003	100.0	5.82	3.38	11.05	0.1213	0.0706
0.88 - 0.85	899	899	100.0	5.55	2.86	9.18	0.1438	0.0859
0.85 - 0.83	659	659	100.0	5.44	2.65	8.58	0.1526	0.0950
0.83 - 0.80	1137	1137	100.0	5.21	2.59	7.93	0.1638	0.1022
0.80 - 0.78	845	845	100.0	5.06	2.18	6.47	0.1911	0.1244
0.78 - 0.76	943	943	100.0	4.90	2.01	5.93	0.2202	0.1408
0.76 - 0.74	1049	1049	100.0	4.71	1.89	5.47	0.2370	0.1555
0.74 - 0.73	566	566	100.0	4.63	1.95	5.47	0.2397	0.1571
0.73 - 0.71	1236	1236	100.0	4.50	1.58	4.44	0.2842	0.1983
0.71 - 0.70	671	671	100.0	4.45	1.43	4.00	0.3195	0.2238
0.70 - 0.69	696	696	100.0	4.27	1.37	3.70	0.3379	0.2437
0.69 - 0.68	864	1101	78.5	2.25	1.26	2.72	0.3491	0.3496
0.78 - 0.68	6025	6262	96.2	4.18	1.65	4.57	0.2691	0.1977
Inf - 0.68	17804	18041	98.7	5.76	5.10	13.39	0.0754	0.0563

Complete .cif-data of ᵗBu-MˢFluind-Br (**S3**) · cyclopentane are available under the CCDC number CCDC-**2225007**.

A resolution cut off (SHEL 999 0.7) was applied to exclude poorly determined reflections at high diffraction angles. Two terminal ᵗBu groups show a rotational disorder over two positions with fixed occupancies of 92:8% and 85:15%. A positional disordered cyclopentane is present in the asymmetric unit and was described with fixed occupancies of 90:10%. The ISOR instruction was used to equalize thermal ellipsoids

of the main part. Isotropic displacement parameters have been used for the description of minor parts. DFIX, SADI, DANG and RIGU have been used to fix the minor part of the disordered solute in shape and position.

Table S7. Crystal data and structure refinement of ^{t}Bu-M^{s}Fluind-Br (**S3**) · cyclopentane.

Identification code	14176	
Empirical formula	$C_{61}H_{75}Br$	
Color	colourless	
Formula weight	888.12 $g \cdot mol^{-1}$	
Temperature	100(2) K	
Wavelength	0.71073 Å	
Crystal system	Monoclinic	
Space group	$P2_1/c$, (no. 14)	
Unit cell dimensions	a = 15.1714(17) Å	α= 90°.
	b = 15.8131(18) Å	β= 90.787(2)°.
	c = 21.450(2) Å	γ = 90°.
Volume	5145.5(10) $Å^3$	
Z	4	
Density (calculated)	1.146 $Mg \cdot m^{-3}$	
Absorption coefficient	0.836 mm^{-1}	
F(000)	1904 e	
Crystal size	0.124 x 0.105 x 0.021 mm^3	
θ range for data collection	1.342 to 30.508°.	
Index ranges	$-21 \le h \le 21$, $-22 \le k \le 21$, $-30 \le l \le 30$	
Reflections collected	96676	
Independent reflections	15713 [R_{int} = 0.0755]	
Reflections with I>2σ(I)	11716	
Completeness to θ = 25.242°	100.0 %	
Absorption correction	Gaussian	
Max. and min. transmission	0.98765 and 0.92062	
Refinement method	Full-matrix least-squares on F^2	
Data / restraints / parameters	15713 / 50 / 625	
Goodness-of-fit on F^2	1.031	
Final R indices [I>2σ(I)]	R_1 = 0.0431	wR^2 = 0.0995
R indices (all data)	R_1 = 0.0697	wR^2 = 0.1103
Extinction coefficient	n/a	
Largest diff. peak and hole	0.738 and –0.617 $e \cdot Å^{-3}$	

Table S8. Bond lengths [Å] and angles [°] of ^{t}Bu-M^{s}Fluind-Br (**S3**) · cyclopentane.

Br(1)-C(1)	1.8936(15)	C(1)-C(2)	1.397(2)
C(1)-C(12)	1.395(2)	C(2)-C(3)	1.519(2)
C(2)-C(6)	1.399(2)	C(3)-C(4)	1.569(2)
C(3)-C(17)	1.528(2)	C(3)-C(28)	1.535(2)
C(4)-H(4A)	0.9900	C(4)-H(4B)	0.9900
C(4)-C(5)	1.553(2)	C(5)-C(6)	1.515(2)
C(5)-C(13)	1.536(2)	C(5)-C(14)	1.534(2)
C(6)-C(7)	1.391(2)	C(7)-H(7)	0.9500
C(7)-C(8)	1.391(2)	C(8)-C(9)	1.515(2)
C(8)-C(12)	1.396(2)	C(9)-C(10)	1.552(2)
C(9)-C(15)	1.529(2)	C(9)-C(16)	1.534(2)
C(10)-H(10A)	0.9900	C(10)-H(10B)	0.9900
C(10)-C(11)	1.576(2)	C(11)-C(12)	1.522(2)
C(11)-C(37)	1.524(2)	C(11)-C(48)	1.525(2)
C(13)-H(13A)	0.9800	C(13)-H(13B)	0.9800
C(13)-H(13C)	0.9800	C(14)-H(14A)	0.9800
C(14)-H(14B)	0.9800	C(14)-H(14C)	0.9800
C(15)-H(15A)	0.9800	C(15)-H(15B)	0.9800
C(15)-H(15C)	0.9800	C(16)-H(16A)	0.9800
C(16)-H(16B)	0.9800	C(16)-H(16C)	0.9800
C(17)-C(18)	1.385(2)	C(17)-C(22)	1.402(2)
C(18)-H(18)	0.9500	C(18)-C(19)	1.403(2)
C(19)-C(20)	1.404(2)	C(19)-C(29)	1.532(2)
C(20)-H(20)	0.9500	C(20)-C(21)	1.388(2)
C(21)-H(21)	0.9500	C(21)-C(22)	1.389(2)
C(22)-C(23)	1.463(2)	C(23)-C(24)	1.393(2)
C(23)-C(28)	1.402(2)	C(24)-H(24)	0.9500
C(24)-C(25)	1.385(3)	C(25)-H(25)	0.9500
C(25)-C(26)	1.402(3)	C(26)-C(27)	1.400(2)
C(26)-C(33)	1.537(3)	C(27)-H(27)	0.9500
C(27)-C(28)	1.384(2)	C(29)-C(30)	1.536(3)
C(29)-C(31)	1.527(3)	C(29)-C(32)	1.540(3)
C(30)-H(30A)	0.9800	C(30)-H(30B)	0.9800

C(30)-H(30C)	0.9800	C(31)-H(31A)	0.9800
C(31)-H(31B)	0.9800	C(31)-H(31C)	0.9800
C(32)-H(32A)	0.9800	C(32)-H(32B)	0.9800
C(32)-H(32C)	0.9800	C(33)-C(34A)	1.527(3)
C(33)-C(34B)	1.55(3)	C(33)-C(35A)	1.540(3)
C(33)-C(35B)	1.54(3)	C(33)-C(36A)	1.541(3)
C(33)-C(36B)	1.55(3)	C(34A)-H(34A)	0.9800
C(34A)-H(34B)	0.9800	C(34A)-H(34C)	0.9800
C(34B)-H(34D)	0.9800	C(34B)-H(34E)	0.9800
C(34B)-H(34F)	0.9800	C(35A)-H(35A)	0.9800
C(35A)-H(35B)	0.9800	C(35A)-H(35C)	0.9800
C(35B)-H(35D)	0.9800	C(35B)-H(35E)	0.9800
C(35B)-H(35F)	0.9800	C(36A)-H(36A)	0.9800
C(36A)-H(36B)	0.9800	C(36A)-H(36C)	0.9800
C(36B)-H(36D)	0.9800	C(36B)-H(36E)	0.9800
C(36B)-H(36F)	0.9800	C(37)-C(38)	1.377(2)
C(37)-C(42)	1.403(2)	C(38)-H(38)	0.9500
C(38)-C(39)	1.406(2)	C(39)-C(40)	1.397(3)
C(39)-C(49)	1.537(3)	C(40)-H(40)	0.9500
C(40)-C(41)	1.397(3)	C(41)-H(41)	0.9500
C(41)-C(42)	1.384(2)	C(42)-C(43)	1.470(2)
C(43)-C(44)	1.389(2)	C(43)-C(48)	1.401(2)
C(44)-H(44)	0.9500	C(44)-C(45)	1.391(3)
C(45)-H(45)	0.9500	C(45)-C(46)	1.404(2)
C(46)-C(47)	1.404(2)	C(46)-C(53)	1.536(3)
C(47)-H(47)	0.9500	C(47)-C(48)	1.382(2)
C(49)-C(50)	1.537(3)	C(49)-C(51)	1.537(3)
C(49)-C(52)	1.532(3)	C(50)-H(50A)	0.9800
C(50)-H(50B)	0.9800	C(50)-H(50C)	0.9800
C(51)-H(51A)	0.9800	C(51)-H(51B)	0.9800
C(51)-H(51C)	0.9800	C(52)-H(52A)	0.9800
C(52)-H(52B)	0.9800	C(52)-H(52C)	0.9800
C(53)-C(54A)	1.549(3)	C(53)-C(54B)	1.60(2)
C(53)-C(55A)	1.513(3)	C(53)-C(55B)	1.378(18)
C(53)-C(56A)	1.538(3)	C(53)-C(56B)	1.61(2)
C(54A)-H(54A)	0.9800	C(54A)-H(54B)	0.9800

C(54A)-H(54C)	0.9800	C(54B)-H(54D)	0.9800
C(54B)-H(54E)	0.9800	C(54B)-H(54F)	0.9800
C(55A)-H(55A)	0.9800	C(55A)-H(55B)	0.9800
C(55A)-H(55C)	0.9800	C(55B)-H(55D)	0.9800
C(55B)-H(55E)	0.9800	C(55B)-H(55F)	0.9800
C(56A)-H(56A)	0.9800	C(56A)-H(56B)	0.9800
C(56A)-H(56C)	0.9800	C(56B)-H(56D)	0.9800
C(56B)-H(56E)	0.9800	C(56B)-H(56F)	0.9800
C(57A)-H(57B)	0.9900	C(57A)-H(57A)	0.9900
C(57A)-C(58A)	1.503(6)	C(57A)-C(61A)	1.532(7)
C(57B)-H(57C)	0.9900	C(57B)-H(57D)	0.9900
C(57B)-C(58B)	1.536(16)	C(57B)-C(61B)	1.552(14)
C(58A)-H(58B)	0.9900	C(58A)-H(58A)	0.9900
C(58A)-C(59A)	1.589(7)	C(58B)-H(58C)	0.9900
C(58B)-H(58D)	0.9900	C(58B)-C(59B)	1.540(16)
C(59A)-H(59A)	0.9900	C(59A)-H(59B)	0.9900
C(59A)-C(60A)	1.491(6)	C(59B)-H(59C)	0.9900
C(59B)-H(59D)	0.9900	C(59B)-C(60B)	1.527(13)
C(60A)-H(60B)	0.9900	C(60A)-H(60A)	0.9900
C(60A)-C(61A)	1.539(7)	C(60B)-H(60D)	0.9900
C(60B)-H(60C)	0.9900	C(60B)-C(61B)	1.556(13)
C(61A)-H(61A)	0.9900	C(61A)-H(61B)	0.9900
C(61B)-H(61D)	0.9900	C(61B)-H(61C)	0.9900

C(2)-C(1)-Br(1)	119.52(12)	C(12)-C(1)-Br(1)	120.15(12)
C(12)-C(1)-C(2)	120.32(14)	C(1)-C(2)-C(3)	129.12(14)
C(1)-C(2)-C(6)	119.19(14)	C(6)-C(2)-C(3)	111.67(13)
C(2)-C(3)-C(4)	101.71(12)	C(2)-C(3)-C(17)	117.27(13)
C(2)-C(3)-C(28)	114.27(13)	C(17)-C(3)-C(4)	110.50(13)
C(17)-C(3)-C(28)	101.22(12)	C(28)-C(3)-C(4)	112.28(13)
C(3)-C(4)-H(4A)	109.9	C(3)-C(4)-H(4B)	109.9
H(4A)-C(4)-H(4B)	108.3	C(5)-C(4)-C(3)	108.81(13)
C(5)-C(4)-H(4A)	109.9	C(5)-C(4)-H(4B)	109.9
C(6)-C(5)-C(4)	102.13(12)	C(6)-C(5)-C(13)	111.66(14)
C(6)-C(5)-C(14)	111.44(14)	C(13)-C(5)-C(4)	112.53(14)
C(14)-C(5)-C(4)	110.38(14)	C(14)-C(5)-C(13)	108.63(14)

C(2)-C(6)-C(5)	112.43(14)	C(7)-C(6)-C(2)	121.08(14)
C(7)-C(6)-C(5)	126.48(14)	C(6)-C(7)-H(7)	120.5
C(6)-C(7)-C(8)	118.93(15)	C(8)-C(7)-H(7)	120.5
C(7)-C(8)-C(9)	126.24(15)	C(7)-C(8)-C(12)	121.04(15)
C(12)-C(8)-C(9)	112.72(14)	C(8)-C(9)-C(10)	103.17(13)
C(8)-C(9)-C(15)	111.21(14)	C(8)-C(9)-C(16)	110.49(14)
C(15)-C(9)-C(10)	111.15(14)	C(15)-C(9)-C(16)	109.55(15)
C(16)-C(9)-C(10)	111.16(15)	C(9)-C(10)-H(10A)	109.9
C(9)-C(10)-H(10B)	109.9	C(9)-C(10)-C(11)	109.09(13)
H(10A)-C(10)-H(10B)	108.3	C(11)-C(10)-H(10A)	109.9
C(11)-C(10)-H(10B)	109.9	C(12)-C(11)-C(10)	102.72(12)
C(12)-C(11)-C(37)	116.47(13)	C(12)-C(11)-C(48)	114.07(13)
C(37)-C(11)-C(10)	109.97(13)	C(37)-C(11)-C(48)	101.33(13)
C(48)-C(11)-C(10)	112.63(13)	C(1)-C(12)-C(8)	119.39(14)
C(1)-C(12)-C(11)	128.72(14)	C(8)-C(12)-C(11)	111.87(14)
C(5)-C(13)-H(13A)	109.5	C(5)-C(13)-H(13B)	109.5
C(5)-C(13)-H(13C)	109.5	H(13A)-C(13)-H(13B)	109.5
H(13A)-C(13)-H(13C)	109.5	H(13B)-C(13)-H(13C)	109.5
C(5)-C(14)-H(14A)	109.5	C(5)-C(14)-H(14B)	109.5
C(5)-C(14)-H(14C)	109.5	H(14A)-C(14)-H(14B)	109.5
H(14A)-C(14)-H(14C)	109.5	H(14B)-C(14)-H(14C)	109.5
C(9)-C(15)-H(15A)	109.5	C(9)-C(15)-H(15B)	109.5
C(9)-C(15)-H(15C)	109.5	H(15A)-C(15)-H(15B)	109.5
H(15A)-C(15)-H(15C)	109.5	H(15B)-C(15)-H(15C)	109.5
C(9)-C(16)-H(16A)	109.5	C(9)-C(16)-H(16B)	109.5
C(9)-C(16)-H(16C)	109.5	H(16A)-C(16)-H(16B)	109.5
H(16A)-C(16)-H(16C)	109.5	H(16B)-C(16)-H(16C)	109.5
C(18)-C(17)-C(3)	128.81(14)	C(18)-C(17)-C(22)	120.72(15)
C(22)-C(17)-C(3)	110.47(14)	C(17)-C(18)-H(18)	120.0
C(17)-C(18)-C(19)	120.10(15)	C(19)-C(18)-H(18)	120.0
C(18)-C(19)-C(20)	118.08(16)	C(18)-C(19)-C(29)	122.02(15)
C(20)-C(19)-C(29)	119.48(15)	C(19)-C(20)-H(20)	118.9
C(21)-C(20)-C(19)	122.22(15)	C(21)-C(20)-H(20)	118.9
C(20)-C(21)-H(21)	120.6	C(20)-C(21)-C(22)	118.76(16)
C(22)-C(21)-H(21)	120.6	C(17)-C(22)-C(23)	108.70(14)
C(21)-C(22)-C(17)	120.04(15)	C(21)-C(22)-C(23)	131.20(15)

C(24)-C(23)-C(22)	131.00(16)	C(24)-C(23)-C(28)	120.05(16)
C(28)-C(23)-C(22)	108.91(14)	C(23)-C(24)-H(24)	120.6
C(25)-C(24)-C(23)	118.89(16)	C(25)-C(24)-H(24)	120.6
C(24)-C(25)-H(25)	119.0	C(24)-C(25)-C(26)	121.95(16)
C(26)-C(25)-H(25)	119.0	C(25)-C(26)-C(33)	119.53(16)
C(27)-C(26)-C(25)	118.32(16)	C(27)-C(26)-C(33)	122.14(17)
C(26)-C(27)-H(27)	119.8	C(28)-C(27)-C(26)	120.35(16)
C(28)-C(27)-H(27)	119.8	C(23)-C(28)-C(3)	110.07(14)
C(27)-C(28)-C(3)	129.57(15)	C(27)-C(28)-C(23)	120.35(15)
C(19)-C(29)-C(30)	106.82(14)	C(19)-C(29)-C(32)	111.72(15)
C(30)-C(29)-C(32)	108.59(15)	C(31)-C(29)-C(19)	112.34(14)
C(31)-C(29)-C(30)	109.12(16)	C(31)-C(29)-C(32)	108.16(16)
C(29)-C(30)-H(30A)	109.5	C(29)-C(30)-H(30B)	109.5
C(29)-C(30)-H(30C)	109.5	H(30A)-C(30)-H(30B)	109.5
H(30A)-C(30)-H(30C)	109.5	H(30B)-C(30)-H(30C)	109.5
C(29)-C(31)-H(31A)	109.5	C(29)-C(31)-H(31B)	109.5
C(29)-C(31)-H(31C)	109.5	H(31A)-C(31)-H(31B)	109.5
H(31A)-C(31)-H(31C)	109.5	H(31B)-C(31)-H(31C)	109.5
C(29)-C(32)-H(32A)	109.5	C(29)-C(32)-H(32B)	109.5
C(29)-C(32)-H(32C)	109.5	H(32A)-C(32)-H(32B)	109.5
H(32A)-C(32)-H(32C)	109.5	H(32B)-C(32)-H(32C)	109.5
C(26)-C(33)-C(34B)	109.7(13)	C(26)-C(33)-C(35A)	110.49(17)
C(26)-C(33)-C(35B)	105.7(11)	C(26)-C(33)-C(36A)	108.29(17)
C(26)-C(33)-C(36B)	105.0(11)	C(34A)-C(33)-C(26)	112.76(17)
C(34A)-C(33)-C(35A)	107.72(19)	C(34A)-C(33)-C(36A)	108.46(19)
C(34B)-C(33)-C(36B)	109.0(18)	C(35A)-C(33)-C(36A)	109.05(18)
C(35B)-C(33)-C(34B)	115.1(18)	C(35B)-C(33)-C(36B)	111.9(16)
C(33)-C(34A)-H(34A)	109.5	C(33)-C(34A)-H(34B)	109.5
C(33)-C(34A)-H(34C)	109.5	H(34A)-C(34A)-H(34B)	109.5
H(34A)-C(34A)-H(34C)	109.5	H(34B)-C(34A)-H(34C)	109.5
C(33)-C(34B)-H(34D)	109.5	C(33)-C(34B)-H(34E)	109.5
C(33)-C(34B)-H(34F)	109.5	H(34D)-C(34B)-H(34E)	109.5
H(34D)-C(34B)-H(34F)	109.5	H(34E)-C(34B)-H(34F)	109.5
C(33)-C(35A)-H(35A)	109.5	C(33)-C(35A)-H(35B)	109.5
C(33)-C(35A)-H(35C)	109.5	H(35A)-C(35A)-H(35B)	109.5
H(35A)-C(35A)-H(35C)	109.5	H(35B)-C(35A)-H(35C)	109.5

C(33)-C(35B)-H(35D)	109.5	C(33)-C(35B)-H(35E)	109.5
C(33)-C(35B)-H(35F)	109.5	H(35D)-C(35B)-H(35E)	109.5
H(35D)-C(35B)-H(35F)	109.5	H(35E)-C(35B)-H(35F)	109.5
C(33)-C(36A)-H(36A)	109.5	C(33)-C(36A)-H(36B)	109.5
C(33)-C(36A)-H(36C)	109.5	H(36A)-C(36A)-H(36B)	109.5
H(36A)-C(36A)-H(36C)	109.5	H(36B)-C(36A)-H(36C)	109.5
C(33)-C(36B)-H(36D)	109.5	C(33)-C(36B)-H(36E)	109.5
C(33)-C(36B)-H(36F)	109.5	H(36D)-C(36B)-H(36E)	109.5
H(36D)-C(36B)-H(36F)	109.5	H(36E)-C(36B)-H(36F)	109.5
C(38)-C(37)-C(11)	128.54(15)	C(38)-C(37)-C(42)	120.59(16)
C(42)-C(37)-C(11)	110.68(15)	C(37)-C(38)-H(38)	119.6
C(37)-C(38)-C(39)	120.84(16)	C(39)-C(38)-H(38)	119.6
C(38)-C(39)-C(49)	119.01(16)	C(40)-C(39)-C(38)	117.74(16)
C(40)-C(39)-C(49)	123.24(16)	C(39)-C(40)-H(40)	119.1
C(41)-C(40)-C(39)	121.83(16)	C(41)-C(40)-H(40)	119.1
C(40)-C(41)-H(41)	120.4	C(42)-C(41)-C(40)	119.29(16)
C(42)-C(41)-H(41)	120.4	C(37)-C(42)-C(43)	108.39(14)
C(41)-C(42)-C(37)	119.70(16)	C(41)-C(42)-C(43)	131.91(16)
C(44)-C(43)-C(42)	131.62(16)	C(44)-C(43)-C(48)	119.82(16)
C(48)-C(43)-C(42)	108.55(14)	C(43)-C(44)-H(44)	120.5
C(43)-C(44)-C(45)	118.95(16)	C(45)-C(44)-H(44)	120.5
C(44)-C(45)-H(45)	119.0	C(44)-C(45)-C(46)	122.01(16)
C(46)-C(45)-H(45)	119.0	C(45)-C(46)-C(53)	121.87(16)
C(47)-C(46)-C(45)	117.99(16)	C(47)-C(46)-C(53)	120.03(16)
C(46)-C(47)-H(47)	119.9	C(48)-C(47)-C(46)	120.22(16)
C(48)-C(47)-H(47)	119.9	C(43)-C(48)-C(11)	110.62(14)
C(47)-C(48)-C(11)	128.49(15)	C(47)-C(48)-C(43)	120.89(15)
C(39)-C(49)-C(50)	112.30(17)	C(39)-C(49)-C(51)	109.27(16)
C(51)-C(49)-C(50)	108.11(17)	C(52)-C(49)-C(39)	109.58(15)
C(52)-C(49)-C(50)	108.27(17)	C(52)-C(49)-C(51)	109.27(17)
C(49)-C(50)-H(50A)	109.5	C(49)-C(50)-H(50B)	109.5
C(49)-C(50)-H(50C)	109.5	H(50A)-C(50)-H(50B)	109.5
H(50A)-C(50)-H(50C)	109.5	H(50B)-C(50)-H(50C)	109.5
C(49)-C(51)-H(51A)	109.5	C(49)-C(51)-H(51B)	109.5
C(49)-C(51)-H(51C)	109.5	H(51A)-C(51)-H(51B)	109.5
H(51A)-C(51)-H(51C)	109.5	H(51B)-C(51)-H(51C)	109.5

C(49)-C(52)-H(52A)	109.5	C(49)-C(52)-H(52B)	109.5
C(49)-C(52)-H(52C)	109.5	H(52A)-C(52)-H(52B)	109.5
H(52A)-C(52)-H(52C)	109.5	H(52B)-C(52)-H(52C)	109.5
C(46)-C(53)-C(54A)	110.34(17)	C(46)-C(53)-C(54B)	102.9(8)
C(46)-C(53)-C(56A)	108.33(17)	C(46)-C(53)-C(56B)	108.2(8)
C(54B)-C(53)-C(56B)	108.4(12)	C(55A)-C(53)-C(46)	113.20(18)
C(55A)-C(53)-C(54A)	107.4(2)	C(55A)-C(53)-C(56A)	110.0(2)
C(55B)-C(53)-C(46)	115.3(8)	C(55B)-C(53)-C(54B)	110.6(12)
C(55B)-C(53)-C(56B)	111.0(12)	C(56A)-C(53)-C(54A)	107.5(2)
C(53)-C(54A)-H(54A)	109.5	C(53)-C(54A)-H(54B)	109.5
C(53)-C(54A)-H(54C)	109.5	H(54A)-C(54A)-H(54B)	109.5
H(54A)-C(54A)-H(54C)	109.5	H(54B)-C(54A)-H(54C)	109.5
C(53)-C(54B)-H(54D)	109.5	C(53)-C(54B)-H(54E)	109.5
C(53)-C(54B)-H(54F)	109.5	H(54D)-C(54B)-H(54E)	109.5
H(54D)-C(54B)-H(54F)	109.5	H(54E)-C(54B)-H(54F)	109.5
C(53)-C(55A)-H(55A)	109.5	C(53)-C(55A)-H(55B)	109.5
C(53)-C(55A)-H(55C)	109.5	H(55A)-C(55A)-H(55B)	109.5
H(55A)-C(55A)-H(55C)	109.5	H(55B)-C(55A)-H(55C)	109.5
C(53)-C(55B)-H(55D)	109.5	C(53)-C(55B)-H(55E)	109.5
C(53)-C(55B)-H(55F)	109.5	H(55D)-C(55B)-H(55E)	109.5
H(55D)-C(55B)-H(55F)	109.5	H(55E)-C(55B)-H(55F)	109.5
C(53)-C(56A)-H(56A)	109.5	C(53)-C(56A)-H(56B)	109.5
C(53)-C(56A)-H(56C)	109.5	H(56A)-C(56A)-H(56B)	109.5
H(56A)-C(56A)-H(56C)	109.5	H(56B)-C(56A)-H(56C)	109.5
C(53)-C(56B)-H(56D)	109.5	C(53)-C(56B)-H(56E)	109.5
C(53)-C(56B)-H(56F)	109.5	H(56D)-C(56B)-H(56E)	109.5
H(56D)-C(56B)-H(56F)	109.5	H(56E)-C(56B)-H(56F)	109.5
H(57B)-C(57A)-H(57A)	108.8	C(58A)-C(57A)-H(57B)	110.6
C(58A)-C(57A)-H(57A)	110.6	C(58A)-C(57A)-C(61A)	105.6(4)
C(61A)-C(57A)-H(57B)	110.6	C(61A)-C(57A)-H(57A)	110.6
H(57C)-C(57B)-H(57D)	110.0	C(58B)-C(57B)-H(57C)	112.5
C(58B)-C(57B)-H(57D)	112.5	C(58B)-C(57B)-C(61B)	96.2(18)
C(61B)-C(57B)-H(57C)	112.5	C(61B)-C(57B)-H(57D)	112.5
C(57A)-C(58A)-H(58B)	111.6	C(57A)-C(58A)-H(58A)	111.6
C(57A)-C(58A)-C(59A)	100.8(4)	H(58B)-C(58A)-H(58A)	109.4
C(59A)-C(58A)-H(58B)	111.6	C(59A)-C(58A)-H(58A)	111.6

C(57B)-C(58B)-H(58C)	111.3	C(57B)-C(58B)-H(58D)	111.3
C(57B)-C(58B)-C(59B)	102(2)	H(58C)-C(58B)-H(58D)	109.2
C(59B)-C(58B)-H(58C)	111.3	C(59B)-C(58B)-H(58D)	111.3
C(58A)-C(59A)-H(59A)	109.9	C(58A)-C(59A)-H(59B)	109.9
H(59A)-C(59A)-H(59B)	108.3	C(60A)-C(59A)-C(58A)	108.8(4)
C(60A)-C(59A)-H(59A)	109.9	C(60A)-C(59A)-H(59B)	109.9
C(58B)-C(59B)-H(59C)	110.4	C(58B)-C(59B)-H(59D)	110.4
H(59C)-C(59B)-H(59D)	108.6	C(60B)-C(59B)-C(58B)	106.4(16)
C(60B)-C(59B)-H(59C)	110.4	C(60B)-C(59B)-H(59D)	110.4
C(59A)-C(60A)-H(60B)	110.6	C(59A)-C(60A)-H(60A)	110.6
C(59A)-C(60A)-C(61A)	105.6(4)	H(60B)-C(60A)-H(60A)	108.8
C(61A)-C(60A)-H(60B)	110.6	C(61A)-C(60A)-H(60A)	110.6
C(59B)-C(60B)-H(60D)	111.9	C(59B)-C(60B)-H(60C)	111.9
C(59B)-C(60B)-C(61B)	99.3(11)	H(60D)-C(60B)-H(60C)	109.6
C(61B)-C(60B)-H(60D)	111.9	C(61B)-C(60B)-H(60C)	111.9
C(57A)-C(61A)-C(60A)	104.9(4)	C(57A)-C(61A)-H(61A)	110.8
C(57A)-C(61A)-H(61B)	110.8	C(60A)-C(61A)-H(61A)	110.8
C(60A)-C(61A)-H(61B)	110.8	H(61A)-C(61A)-H(61B)	108.8
C(57B)-C(61B)-C(60B)	96.9(15)	C(57B)-C(61B)-H(61D)	112.4
C(57B)-C(61B)-H(61C)	112.4	C(60B)-C(61B)-H(61D)	112.4
C(60B)-C(61B)-H(61C)	112.4	H(61D)-C(61B)-H(61C)	109.9

3.4. Single crystal structure analysis of ^{t}Bu-M^{s}Fluind-BiBr$_2$ (**1**) · THF

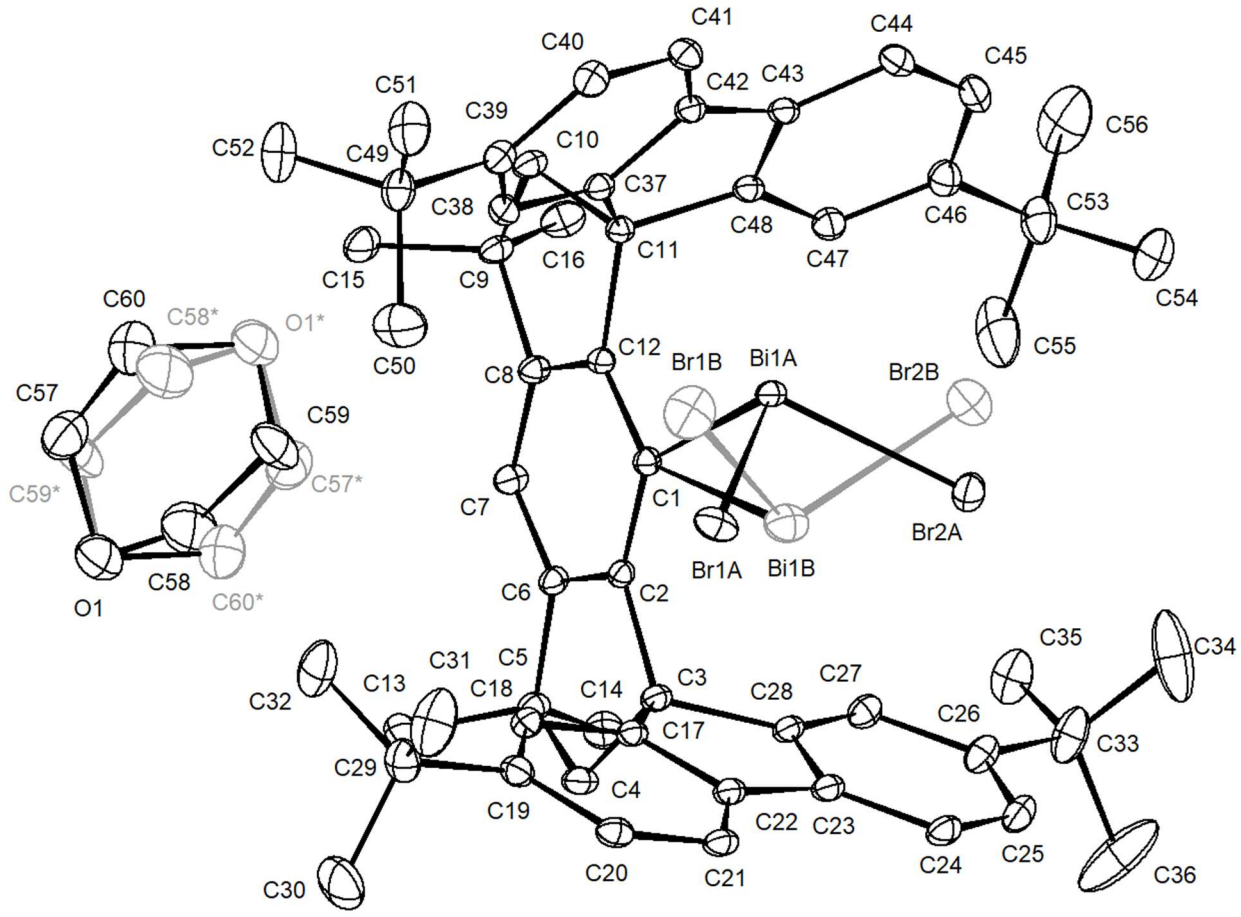

Fig. S39. The molecular structure of ^{t}Bu-M^{s}Fluind-BiBr$_2$ (**1**) · THF. H atoms have been removed for clarity. Main structure shown in black and disordered parts shown in grey.

X-ray Crystal Structure Analysis of ^{t}Bu-M^{s}Fluind-BiBr$_2$ (**1**) · THF:

C_{116} H_{138} Bi_2 Br_4 O, M_r = 2285.86 g mol^{-1}, yellow block, crystal size 0.172 x 0.172 x 0.10 mm^3, triclinic, space group *P*-1 [2], a = 11.428(2) Å, b = 15.181(3) Å, c = 16.499(3) Å, α = 68.190(6)°, β = 76.850(6)°, γ = 78.430(6)°, V = 2566.6(8) Å^3, T = 100(2) K, Z = 1, D_{calc} = 1.479 g·cm^3, λ = 0.71073 Å, μ(*Mo-K*$_\alpha$) = 5.028 mm^{-1}, Gaussian absorption correction (T_{min} = 0.52368, T_{max} = 0.70601), Bruker-AXS Kappa Mach3 with APEX-II detector and IμS microfocus Mo-anode X-ray source, 1.349 < θ < 36.319°, 108673 measured reflections, 24676 independent reflections, 22161 reflections with $I > 2\sigma(I)$, R_{int} = 0.0313. The structure was solved by *SHELXT* and refined by full-matrix least-squares (*SHELXL*) against F^2 to R_1 = 0.0214 [$I > 2\sigma(I)$], wR_2 = 0.0534 [all data], 620 parameters and 75 restraints.

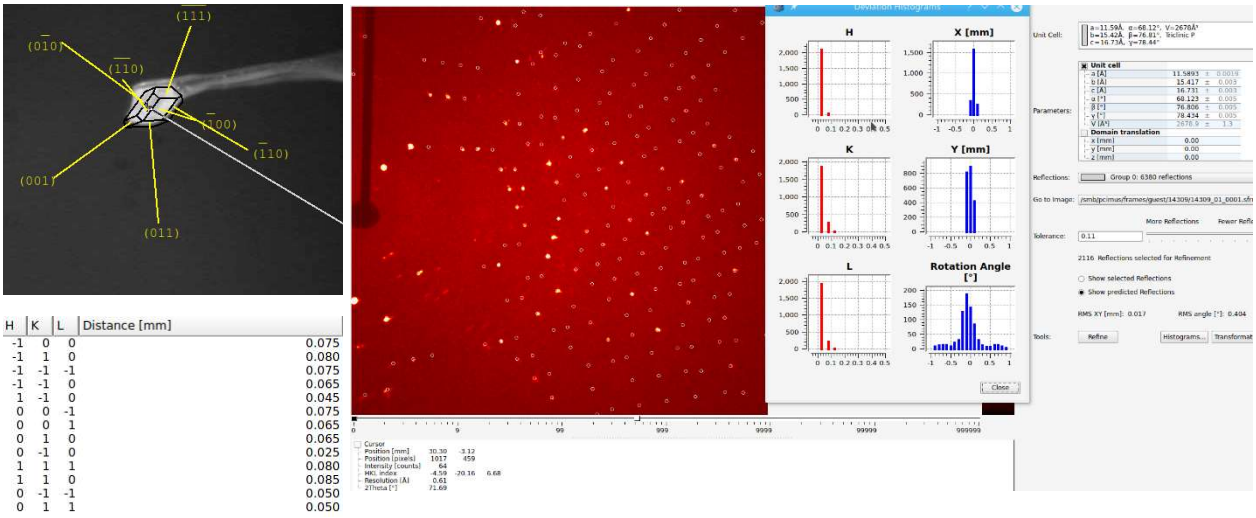

Fig. S40. Crystal faces and unit cell determination/refinement of compound ^{t}Bu-M^{s}Fluind-BiBr$_2$ (**1**) · THF.

INTENSITY STATISTICS FOR DATASET

Resolution	#Data	#Theory	%Complete	Redundancy	Mean I	Mean I/s	Rmerge	Rsigma
Inf - 2.42	385	385	100.0	9.13	138.54	76.80	0.0292	0.0118
2.42 - 1.61	901	901	100.0	9.36	95.61	71.28	0.0243	0.0122
1.61 - 1.28	1272	1272	100.0	9.25	60.79	65.09	0.0260	0.0129
1.28 - 1.12	1268	1268	100.0	8.82	51.14	58.37	0.0271	0.0135
1.12 - 1.02	1253	1253	100.0	6.73	42.92	47.33	0.0292	0.0171
1.02 - 0.94	1393	1393	100.0	5.10	30.87	35.51	0.0321	0.0225
0.94 - 0.88	1415	1415	100.0	4.28	25.44	29.50	0.0349	0.0268
0.88 - 0.84	1190	1190	100.0	3.90	25.01	27.29	0.0344	0.0292
0.84 - 0.80	1410	1410	100.0	3.75	22.72	24.95	0.0356	0.0319
0.80 - 0.77	1267	1267	100.0	3.56	19.67	22.30	0.0405	0.0366
0.77 - 0.75	984	984	100.0	3.42	16.44	19.24	0.0430	0.0421
0.75 - 0.72	1643	1648	99.7	3.27	15.86	18.06	0.0460	0.0456
0.72 - 0.70	1316	1318	99.8	3.14	14.07	16.35	0.0490	0.0513
0.70 - 0.68	1384	1393	99.4	3.03	13.20	15.00	0.0527	0.0559
0.68 - 0.67	765	770	99.4	2.92	11.58	13.31	0.0557	0.0633
0.67 - 0.65	1680	1708	98.4	2.81	10.89	12.45	0.0592	0.0682
0.65 - 0.64	916	929	98.6	2.73	9.96	11.60	0.0657	0.0756
0.64 - 0.62	2045	2100	97.4	2.61	9.13	10.42	0.0747	0.0840
0.62 - 0.61	1017	1057	96.2	2.44	9.09	10.05	0.0791	0.0881
0.61 - 0.60	1174	1237	94.9	2.43	7.62	8.61	0.0946	0.1036
0.60 - 0.59	700	1354	51.7	0.85	6.34	5.76	0.1127	0.1595
0.69 - 0.59	9050	9913	91.3	2.43	9.68	10.91	0.0682	0.0807
Inf - 0.59	25378	26252	96.7	4.18	25.92	26.61	0.0313	0.0298

Complete .cif-data of ^{t}Bu-M^{s}Fluind-BiBr$_2$ (**1**) · THF are available under the CCDC number CCDC-**2225004**. A resolution cut off (SHEL 999 0.6) was applied to exclude poorly determined reflections at high diffraction angles. Two reflections show high ΔI/σ(I) and were excluded before the final refinement cycles. The Bi and Br atoms are found to be disordered over two positions with fixed occupancies of 97:3%. The structure

contains a disordered solute molecule which is located on a crystallographic center of inversion. The occupancy was fixed to be 50:50% and the DSR Tool as an Olex2 plugin was used to model the solute.

Table S9. Crystal data and structure refinement of compound ^{t}Bu-M^{s}Fluind-BiBr$_2$ (**1**) · THF.

Identification code	14309	
Empirical formula	$C_{116}\,H_{138}\,Bi_2\,Br_4\,O$	
Color	yellow	
Formula weight	2285.86 g·mol^{-1}	
Temperature	100(2) K	
Wavelength	0.71073 Å	
Crystal system	Triclinic	
Space group	*P*-1, (no. 2)	
Unit cell dimensions	a = 11.428(2) Å	α= 68.190(6)°.
	b = 15.181(3) Å	β= 76.850(6)°.
	c = 16.499(3) Å	γ = 78.430(6)°.
Volume	2566.6(8) Å^3	
Z	1	
Density (calculated)	1.479 Mg·m^{-3}	
Absorption coefficient	5.028 mm^{-1}	
F(000)	1148 e	
Crystal size	0.172 x 0.172 x 0.10 mm^3	
θ range for data collection	1.349 to 36.319°.	
Index ranges	$-18 \le h \le 19$, $-25 \le k \le 25$, $-27 \le l \le 27$	
Reflections collected	108673	
Independent reflections	24676 [R_{int} = 0.0313]	
Reflections with I>2σ(I)	22161	
Completeness to θ = 25.242°	100.0 %	
Absorption correction	Gaussian	
Max. and min. transmission	0.70601 and 0.52368	
Refinement method	Full-matrix least-squares on F^2	
Data / restraints / parameters	24676 / 75 / 620	
Goodness-of-fit on F^2	1.040	
Final R indices [I>2σ(I)]	R_1 = 0.0214	wR^2 = 0.0522
R indices (all data)	R_1 = 0.0265	wR^2 = 0.0534
Extinction coefficient	n/a	
Largest diff. peak and hole	1.526 and –1.623 e·Å^{-3}	

Table S10. Bond lengths [Å] and angles [°] of ^{t}Bu-M^{s}Fluind-BiBr$_2$ (**1**) · THF.

Bi(1A)-Br(1A)	2.6222(4)	Bi(1A)-Br(2A)	2.6111(4)
Bi(1A)-C(1)	2.2945(12)	Bi(1B)-Br(1B)	2.589(5)
Bi(1B)-Br(2B)	2.613(6)	Bi(1B)-C(1)	2.351(2)
C(1)-C(2)	1.4139(16)	C(1)-C(12)	1.4043(17)
C(2)-C(3)	1.5311(17)	C(2)-C(6)	1.4052(16)
C(3)-C(4)	1.5727(17)	C(3)-C(17)	1.5195(17)
C(3)-C(28)	1.5267(17)	C(4)-H(4A)	0.9900
C(4)-H(4B)	0.9900	C(4)-C(5)	1.5439(18)
C(5)-C(6)	1.5166(16)	C(5)-C(13)	1.5336(18)
C(5)-C(14)	1.5336(17)	C(6)-C(7)	1.3893(18)
C(7)-H(7)	0.9500	C(7)-C(8)	1.3837(16)
C(8)-C(9)	1.5150(18)	C(8)-C(12)	1.3998(16)
C(9)-C(10)	1.5424(16)	C(9)-C(15)	1.5333(18)
C(9)-C(16)	1.5311(18)	C(10)-H(10A)	0.9900
C(10)-H(10B)	0.9900	C(10)-C(11)	1.5644(18)
C(11)-C(12)	1.5322(16)	C(11)-C(37)	1.5293(16)
C(11)-C(48)	1.5322(16)	C(13)-H(13A)	0.9800
C(13)-H(13B)	0.9800	C(13)-H(13C)	0.9800
C(14)-H(14A)	0.9800	C(14)-H(14B)	0.9800
C(14)-H(14C)	0.9800	C(15)-H(15A)	0.9800
C(15)-H(15B)	0.9800	C(15)-H(15C)	0.9800
C(16)-H(16A)	0.9800	C(16)-H(16B)	0.9800
C(16)-H(16C)	0.9800	C(17)-C(18)	1.3848(17)
C(17)-C(22)	1.3931(18)	C(18)-H(18)	0.9500
C(18)-C(19)	1.3990(18)	C(19)-C(20)	1.3984(19)
C(19)-C(29)	1.5305(18)	C(20)-H(20)	0.9500
C(20)-C(21)	1.3857(18)	C(21)-H(21)	0.9500
C(21)-C(22)	1.3884(17)	C(22)-C(23)	1.4671(17)
C(23)-C(24)	1.3889(18)	C(23)-C(28)	1.4012(17)
C(24)-H(24)	0.9500	C(24)-C(25)	1.3866(18)
C(25)-H(25)	0.9500	C(25)-C(26)	1.4003(19)
C(26)-C(27)	1.3972(18)	C(26)-C(33)	1.5363(19)
C(27)-H(27)	0.9500	C(27)-C(28)	1.3835(17)

C(29)-C(30)	1.535(2)	C(29)-C(31)	1.536(2)
C(29)-C(32)	1.520(2)	C(30)-H(30A)	0.9800
C(30)-H(30B)	0.9800	C(30)-H(30C)	0.9800
C(31)-H(31A)	0.9800	C(31)-H(31B)	0.9800
C(31)-H(31C)	0.9800	C(32)-H(32A)	0.9800
C(32)-H(32B)	0.9800	C(32)-H(32C)	0.9800
C(33)-C(34)	1.533(3)	C(33)-C(35)	1.522(2)
C(33)-C(36)	1.526(3)	C(34)-H(34A)	0.9800
C(34)-H(34B)	0.9800	C(34)-H(34C)	0.9800
C(35)-H(35A)	0.9800	C(35)-H(35B)	0.9800
C(35)-H(35C)	0.9800	C(36)-H(36A)	0.9800
C(36)-H(36B)	0.9800	C(36)-H(36C)	0.9800
C(37)-C(38)	1.3827(16)	C(37)-C(42)	1.4070(16)
C(38)-H(38)	0.9500	C(38)-C(39)	1.4098(16)
C(39)-C(40)	1.3991(17)	C(39)-C(49)	1.5284(17)
C(40)-H(40)	0.9500	C(40)-C(41)	1.3869(18)
C(41)-H(41)	0.9500	C(41)-C(42)	1.3890(16)
C(42)-C(43)	1.4589(17)	C(43)-C(44)	1.3922(17)
C(43)-C(48)	1.4028(16)	C(44)-H(44)	0.9500
C(44)-C(45)	1.3859(18)	C(45)-H(45)	0.9500
C(45)-C(46)	1.4010(18)	C(46)-C(47)	1.3958(18)
C(46)-C(53)	1.5301(18)	C(47)-H(47)	0.9500
C(47)-C(48)	1.3849(16)	C(49)-C(50)	1.533(2)
C(49)-C(51)	1.5293(19)	C(49)-C(52)	1.533(2)
C(50)-H(50A)	0.9800	C(50)-H(50B)	0.9800
C(50)-H(50C)	0.9800	C(51)-H(51A)	0.9800
C(51)-H(51B)	0.9800	C(51)-H(51C)	0.9800
C(52)-H(52A)	0.9800	C(52)-H(52B)	0.9800
C(52)-H(52C)	0.9800	C(53)-C(54)	1.537(2)
C(53)-C(55)	1.528(2)	C(53)-C(56)	1.527(2)
C(54)-H(54A)	0.9800	C(54)-H(54B)	0.9800
C(54)-H(54C)	0.9800	C(55)-H(55A)	0.9800
C(55)-H(55B)	0.9800	C(55)-H(55C)	0.9800
C(56)-H(56A)	0.9800	C(56)-H(56B)	0.9800
C(56)-H(56C)	0.9800	O(1)-C(57)	1.432(8)
O(1)-C(60)	1.419(6)	C(57)-H(57A)	0.9900

C(57)-H(57B)	0.9900	C(57)-C(58)	1.499(8)
C(58)-H(58A)	0.9900	C(58)-H(58B)	0.9900
C(58)-C(59)	1.538(8)	C(59)-H(59A)	0.9900
C(59)-H(59B)	0.9900	C(59)-C(60)	1.520(7)
C(60)-H(60A)	0.9900	C(60)-H(60B)	0.9900

Br(2A)-Bi(1A)-Br(1A)	101.894(14)	C(1)-Bi(1A)-Br(1A)	104.05(3)
C(1)-Bi(1A)-Br(2A)	98.49(3)	Br(1B)-Bi(1B)-Br(2B)	109.11(19)
C(1)-Bi(1B)-Br(1B)	95.99(15)	C(1)-Bi(1B)-Br(2B)	98.13(15)
C(2)-C(1)-Bi(1A)	135.21(9)	C(2)-C(1)-Bi(1B)	98.22(9)
C(12)-C(1)-Bi(1A)	106.75(7)	C(12)-C(1)-Bi(1B)	143.35(9)
C(12)-C(1)-C(2)	117.64(10)	C(1)-C(2)-C(3)	130.42(10)
C(6)-C(2)-C(1)	119.58(11)	C(6)-C(2)-C(3)	109.99(9)
C(2)-C(3)-C(4)	102.60(9)	C(17)-C(3)-C(2)	118.32(9)
C(17)-C(3)-C(4)	107.93(9)	C(17)-C(3)-C(28)	101.18(10)
C(28)-C(3)-C(2)	115.97(10)	C(28)-C(3)-C(4)	110.79(9)
C(3)-C(4)-H(4A)	109.9	C(3)-C(4)-H(4B)	109.9
H(4A)-C(4)-H(4B)	108.3	C(5)-C(4)-C(3)	108.92(10)
C(5)-C(4)-H(4A)	109.9	C(5)-C(4)-H(4B)	109.9
C(6)-C(5)-C(4)	101.96(9)	C(6)-C(5)-C(13)	111.68(10)
C(6)-C(5)-C(14)	111.18(10)	C(13)-C(5)-C(4)	111.13(10)
C(14)-C(5)-C(4)	112.94(11)	C(14)-C(5)-C(13)	107.95(10)
C(2)-C(6)-C(5)	113.59(10)	C(7)-C(6)-C(2)	121.81(10)
C(7)-C(6)-C(5)	124.59(10)	C(6)-C(7)-H(7)	120.5
C(8)-C(7)-C(6)	118.91(11)	C(8)-C(7)-H(7)	120.5
C(7)-C(8)-C(9)	126.67(11)	C(7)-C(8)-C(12)	120.20(11)
C(12)-C(8)-C(9)	113.12(10)	C(8)-C(9)-C(10)	102.19(9)
C(8)-C(9)-C(15)	112.07(10)	C(8)-C(9)-C(16)	111.46(10)
C(15)-C(9)-C(10)	110.52(10)	C(16)-C(9)-C(10)	111.84(10)
C(16)-C(9)-C(15)	108.69(11)	C(9)-C(10)-H(10A)	110.0
C(9)-C(10)-H(10B)	110.0	C(9)-C(10)-C(11)	108.49(9)
H(10A)-C(10)-H(10B)	108.4	C(11)-C(10)-H(10A)	110.0
C(11)-C(10)-H(10B)	110.0	C(12)-C(11)-C(10)	102.36(9)
C(37)-C(11)-C(10)	108.32(9)	C(37)-C(11)-C(12)	120.00(10)
C(37)-C(11)-C(48)	100.41(9)	C(48)-C(11)-C(10)	113.26(10)
C(48)-C(11)-C(12)	112.88(9)	C(1)-C(12)-C(11)	127.95(10)

C(8)-C(12)-C(1)	121.81(10)	C(8)-C(12)-C(11)	110.06(10)
C(5)-C(13)-H(13A)	109.5	C(5)-C(13)-H(13B)	109.5
C(5)-C(13)-H(13C)	109.5	H(13A)-C(13)-H(13B)	109.5
H(13A)-C(13)-H(13C)	109.5	H(13B)-C(13)-H(13C)	109.5
C(5)-C(14)-H(14A)	109.5	C(5)-C(14)-H(14B)	109.5
C(5)-C(14)-H(14C)	109.5	H(14A)-C(14)-H(14B)	109.5
H(14A)-C(14)-H(14C)	109.5	H(14B)-C(14)-H(14C)	109.5
C(9)-C(15)-H(15A)	109.5	C(9)-C(15)-H(15B)	109.5
C(9)-C(15)-H(15C)	109.5	H(15A)-C(15)-H(15B)	109.5
H(15A)-C(15)-H(15C)	109.5	H(15B)-C(15)-H(15C)	109.5
C(9)-C(16)-H(16A)	109.5	C(9)-C(16)-H(16B)	109.5
C(9)-C(16)-H(16C)	109.5	H(16A)-C(16)-H(16B)	109.5
H(16A)-C(16)-H(16C)	109.5	H(16B)-C(16)-H(16C)	109.5
C(18)-C(17)-C(3)	127.95(11)	C(18)-C(17)-C(22)	120.89(11)
C(22)-C(17)-C(3)	110.91(10)	C(17)-C(18)-H(18)	120.0
C(17)-C(18)-C(19)	119.94(12)	C(19)-C(18)-H(18)	120.0
C(18)-C(19)-C(29)	122.14(12)	C(20)-C(19)-C(18)	118.21(11)
C(20)-C(19)-C(29)	119.65(11)	C(19)-C(20)-H(20)	118.9
C(21)-C(20)-C(19)	122.17(12)	C(21)-C(20)-H(20)	118.9
C(20)-C(21)-H(21)	120.6	C(20)-C(21)-C(22)	118.75(12)
C(22)-C(21)-H(21)	120.6	C(17)-C(22)-C(23)	108.47(10)
C(21)-C(22)-C(17)	120.00(11)	C(21)-C(22)-C(23)	131.51(12)
C(24)-C(23)-C(22)	131.43(12)	C(24)-C(23)-C(28)	120.06(11)
C(28)-C(23)-C(22)	108.51(11)	C(23)-C(24)-H(24)	120.6
C(25)-C(24)-C(23)	118.77(12)	C(25)-C(24)-H(24)	120.6
C(24)-C(25)-H(25)	118.9	C(24)-C(25)-C(26)	122.13(12)
C(26)-C(25)-H(25)	118.9	C(25)-C(26)-C(33)	119.66(12)
C(27)-C(26)-C(25)	118.21(12)	C(27)-C(26)-C(33)	122.12(12)
C(26)-C(27)-H(27)	119.8	C(28)-C(27)-C(26)	120.34(12)
C(28)-C(27)-H(27)	119.8	C(23)-C(28)-C(3)	110.35(10)
C(27)-C(28)-C(3)	129.10(11)	C(27)-C(28)-C(23)	120.48(11)
C(19)-C(29)-C(30)	108.62(13)	C(19)-C(29)-C(31)	109.64(12)
C(30)-C(29)-C(31)	109.50(14)	C(32)-C(29)-C(19)	112.33(11)
C(32)-C(29)-C(30)	108.99(14)	C(32)-C(29)-C(31)	107.73(14)
C(29)-C(30)-H(30A)	109.5	C(29)-C(30)-H(30B)	109.5
C(29)-C(30)-H(30C)	109.5	H(30A)-C(30)-H(30B)	109.5

H(30A)-C(30)-H(30C)	109.5	H(30B)-C(30)-H(30C)	109.5
C(29)-C(31)-H(31A)	109.5	C(29)-C(31)-H(31B)	109.5
C(29)-C(31)-H(31C)	109.5	H(31A)-C(31)-H(31B)	109.5
H(31A)-C(31)-H(31C)	109.5	H(31B)-C(31)-H(31C)	109.5
C(29)-C(32)-H(32A)	109.5	C(29)-C(32)-H(32B)	109.5
C(29)-C(32)-H(32C)	109.5	H(32A)-C(32)-H(32B)	109.5
H(32A)-C(32)-H(32C)	109.5	H(32B)-C(32)-H(32C)	109.5
C(34)-C(33)-C(26)	109.23(12)	C(35)-C(33)-C(26)	112.36(12)
C(35)-C(33)-C(34)	108.96(16)	C(35)-C(33)-C(36)	106.70(14)
C(36)-C(33)-C(26)	109.53(15)	C(36)-C(33)-C(34)	110.04(18)
C(33)-C(34)-H(34A)	109.5	C(33)-C(34)-H(34B)	109.5
C(33)-C(34)-H(34C)	109.5	H(34A)-C(34)-H(34B)	109.5
H(34A)-C(34)-H(34C)	109.5	H(34B)-C(34)-H(34C)	109.5
C(33)-C(35)-H(35A)	109.5	C(33)-C(35)-H(35B)	109.5
C(33)-C(35)-H(35C)	109.5	H(35A)-C(35)-H(35B)	109.5
H(35A)-C(35)-H(35C)	109.5	H(35B)-C(35)-H(35C)	109.5
C(33)-C(36)-H(36A)	109.5	C(33)-C(36)-H(36B)	109.5
C(33)-C(36)-H(36C)	109.5	H(36A)-C(36)-H(36B)	109.5
H(36A)-C(36)-H(36C)	109.5	H(36B)-C(36)-H(36C)	109.5
C(38)-C(37)-C(11)	128.94(10)	C(38)-C(37)-C(42)	120.61(10)
C(42)-C(37)-C(11)	110.36(10)	C(37)-C(38)-H(38)	120.0
C(37)-C(38)-C(39)	119.94(11)	C(39)-C(38)-H(38)	120.0
C(38)-C(39)-C(49)	119.39(11)	C(40)-C(39)-C(38)	118.32(11)
C(40)-C(39)-C(49)	122.26(11)	C(39)-C(40)-H(40)	118.9
C(41)-C(40)-C(39)	122.14(11)	C(41)-C(40)-H(40)	118.9
C(40)-C(41)-H(41)	120.5	C(40)-C(41)-C(42)	118.91(11)
C(42)-C(41)-H(41)	120.5	C(37)-C(42)-C(43)	108.48(10)
C(41)-C(42)-C(37)	120.05(11)	C(41)-C(42)-C(43)	131.20(11)
C(44)-C(43)-C(42)	131.21(11)	C(44)-C(43)-C(48)	119.86(11)
C(48)-C(43)-C(42)	108.59(10)	C(43)-C(44)-H(44)	120.8
C(45)-C(44)-C(43)	118.43(11)	C(45)-C(44)-H(44)	120.8
C(44)-C(45)-H(45)	118.8	C(44)-C(45)-C(46)	122.44(11)
C(46)-C(45)-H(45)	118.8	C(45)-C(46)-C(53)	119.78(11)
C(47)-C(46)-C(45)	118.22(11)	C(47)-C(46)-C(53)	121.98(11)
C(46)-C(47)-H(47)	120.0	C(48)-C(47)-C(46)	119.99(11)
C(48)-C(47)-H(47)	120.0	C(43)-C(48)-C(11)	110.44(10)

C(47)-C(48)-C(11)	128.69(10)	C(47)-C(48)-C(43)	120.78(11)
C(39)-C(49)-C(50)	108.64(11)	C(39)-C(49)-C(51)	112.62(11)
C(39)-C(49)-C(52)	109.45(11)	C(51)-C(49)-C(50)	108.32(13)
C(51)-C(49)-C(52)	107.85(12)	C(52)-C(49)-C(50)	109.93(13)
C(49)-C(50)-H(50A)	109.5	C(49)-C(50)-H(50B)	109.5
C(49)-C(50)-H(50C)	109.5	H(50A)-C(50)-H(50B)	109.5
H(50A)-C(50)-H(50C)	109.5	H(50B)-C(50)-H(50C)	109.5
C(49)-C(51)-H(51A)	109.5	C(49)-C(51)-H(51B)	109.5
C(49)-C(51)-H(51C)	109.5	H(51A)-C(51)-H(51B)	109.5
H(51A)-C(51)-H(51C)	109.5	H(51B)-C(51)-H(51C)	109.5
C(49)-C(52)-H(52A)	109.5	C(49)-C(52)-H(52B)	109.5
C(49)-C(52)-H(52C)	109.5	H(52A)-C(52)-H(52B)	109.5
H(52A)-C(52)-H(52C)	109.5	H(52B)-C(52)-H(52C)	109.5
C(46)-C(53)-C(54)	109.77(12)	C(55)-C(53)-C(46)	111.50(12)
C(55)-C(53)-C(54)	106.66(15)	C(56)-C(53)-C(46)	109.02(13)
C(56)-C(53)-C(54)	109.82(14)	C(56)-C(53)-C(55)	110.04(16)
C(53)-C(54)-H(54A)	109.5	C(53)-C(54)-H(54B)	109.5
C(53)-C(54)-H(54C)	109.5	H(54A)-C(54)-H(54B)	109.5
H(54A)-C(54)-H(54C)	109.5	H(54B)-C(54)-H(54C)	109.5
C(53)-C(55)-H(55A)	109.5	C(53)-C(55)-H(55B)	109.5
C(53)-C(55)-H(55C)	109.5	H(55A)-C(55)-H(55B)	109.5
H(55A)-C(55)-H(55C)	109.5	H(55B)-C(55)-H(55C)	109.5
C(53)-C(56)-H(56A)	109.5	C(53)-C(56)-H(56B)	109.5
C(53)-C(56)-H(56C)	109.5	H(56A)-C(56)-H(56B)	109.5
H(56A)-C(56)-H(56C)	109.5	H(56B)-C(56)-H(56C)	109.5
C(60)-O(1)-C(57)	103.3(6)	O(1)-C(57)-H(57A)	110.5
O(1)-C(57)-H(57B)	110.5	O(1)-C(57)-C(58)	106.3(6)
H(57A)-C(57)-H(57B)	108.7	C(58)-C(57)-H(57A)	110.5
C(58)-C(57)-H(57B)	110.5	C(57)-C(58)-H(58A)	111.1
C(57)-C(58)-H(58B)	111.1	C(57)-C(58)-C(59)	103.3(5)
H(58A)-C(58)-H(58B)	109.1	C(59)-C(58)-H(58A)	111.1
C(59)-C(58)-H(58B)	111.1	C(58)-C(59)-H(59A)	111.1
C(58)-C(59)-H(59B)	111.1	H(59A)-C(59)-H(59B)	109.1
C(60)-C(59)-C(58)	103.2(4)	C(60)-C(59)-H(59A)	111.1
C(60)-C(59)-H(59B)	111.1	O(1)-C(60)-C(59)	107.5(5)
O(1)-C(60)-H(60A)	110.2	O(1)-C(60)-H(60B)	110.2

C(59)-C(60)-H(60A)	110.2	C(59)-C(60)-H(60B)	110.2
H(60A)-C(60)-H(60B)	108.5		

3.5. Single crystal structure analysis of ^{t}Bu-M^{s}Fluind-Bi(I) (**2**)

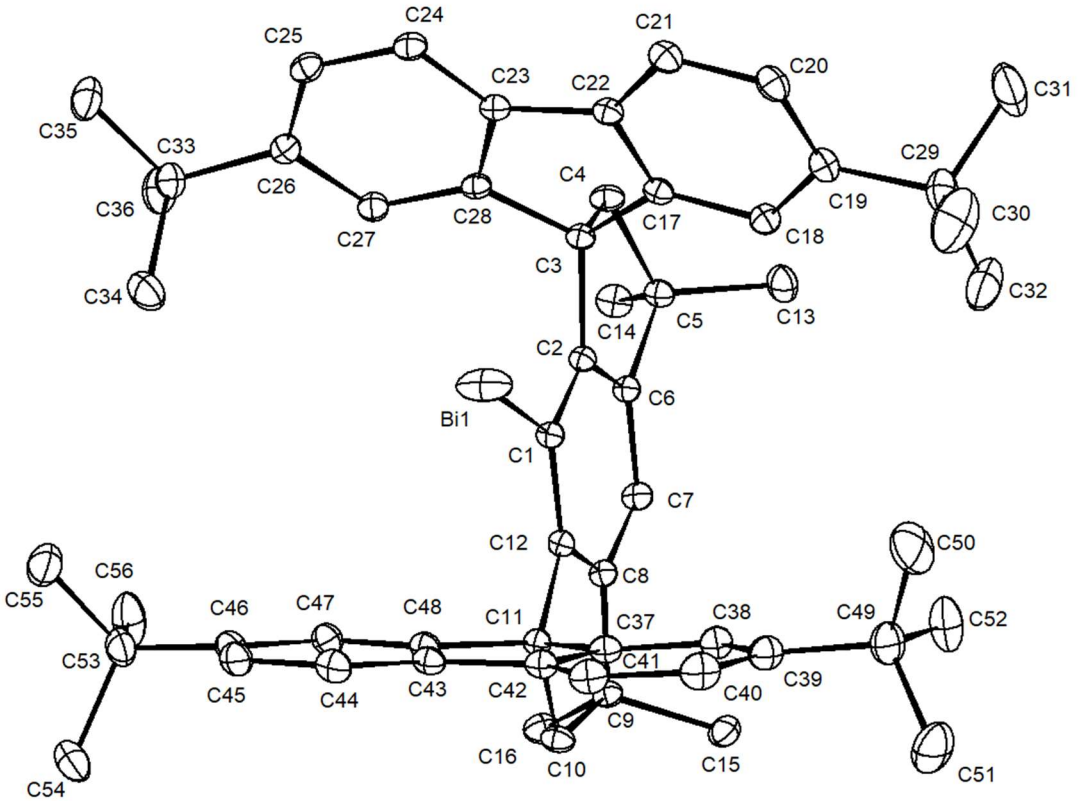

Fig. S41. The molecular structure of ^{t}Bu-M^{s}Fluind-Bi(I) (**2**). H atoms have been removed for clarity.

X-ray Crystal Structure Analysis of ^{t}Bu-M^{s}Fluind-Bi(I) (**2**):

C_{56} H_{65} Bi, M_r = 947.121 g mol^{-1}, yellow plate, crystal size 0.256 x 0.253 x 0.1 mm^3, triclinic, space group *P*-1 [2], a = 12.6987(3) Å, b = 14.3359(3) Å, c = 15.3368(4), α = 108.811(1)°, β = 102.403(1)°, γ = 106.274(1)°, V = 2389.67(10) Å^3, T = 100(2) K, Z = 2, D_{calc} = 1.316 g·cm^3, λ = 0.71073 Å, μ(*Mo-K*$_\alpha$) = 3.723 mm^{-1}, Gaussian absorption correction (T_{min} = 0.5024, T_{max} = 0.9972), Bruker-AXS D8 Venture with Photon III detector and IμS Diamond microfocus Mo-anode X-ray source, 1.90 < θ < 34.97°, 553798 measured reflections, 20990 independent reflections, 18820 reflections with $I > 2\sigma(I)$, R_{int} = 0.0487. The structure was solved by *SHELXT* and refined by full-matrix least-squares (*SHELXL*) against F^2 to R_1 = 0.0209 [$I > 2\sigma(I)$], wR_2 = 0.0500 [all data], 555 parameters and 0 restraints.

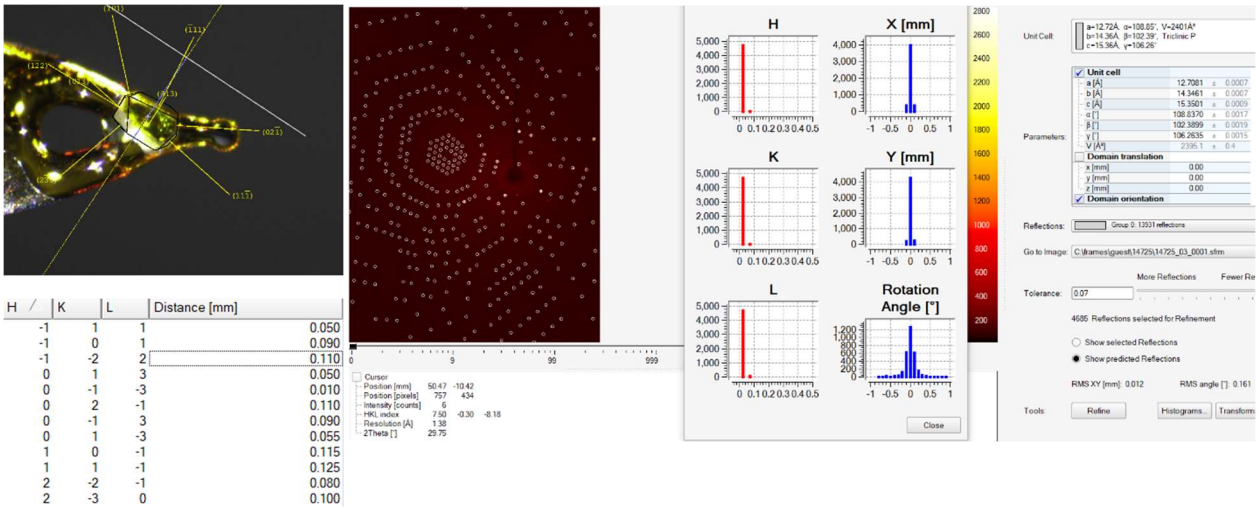

H	K	L	Distance [mm]
-1	1	1	0.050
-1	0	1	0.090
-1	-2	2	0.110
0	1	3	0.050
0	-1	-3	0.010
0	2	-1	0.110
0	-1	3	0.090
0	1	-3	0.055
1	0	-1	0.115
1	1	-1	0.125
2	-2	-1	0.080
2	-3	0	0.100

Fig. S42. Crystal faces and unit cell determination/refinement of compound ^{t}Bu-M^{s}Fluind-Bi(I) (**2**).

INTENSITY STATISTICS FOR DATASET

Resolution	#Data	#Theory	%Complete	Redundancy	Mean I	Mean I/s	Rmerge	Rsigma
Inf - 2.34	386	390	99.0	42.19	111.01	187.13	0.0208	0.0058
2.34 - 1.57	897	897	100.0	44.29	66.07	170.31	0.0215	0.0048
1.57 - 1.25	1276	1276	100.0	38.36	41.49	133.26	0.0272	0.0060
1.25 - 1.09	1295	1295	100.0	28.98	28.90	93.11	0.0345	0.0082
1.09 - 0.99	1303	1303	100.0	26.11	23.89	79.11	0.0425	0.0099
0.99 - 0.92	1263	1263	100.0	24.76	16.44	61.36	0.0530	0.0127
0.92 - 0.86	1453	1453	100.0	24.02	13.91	52.06	0.0616	0.0150
0.86 - 0.82	1209	1209	100.0	22.52	12.84	45.02	0.0689	0.0172
0.82 - 0.78	1483	1483	100.0	20.98	10.33	35.79	0.0818	0.0217
0.78 - 0.75	1270	1270	100.0	19.75	8.14	28.02	0.0977	0.0278
0.75 - 0.73	1029	1029	100.0	18.57	8.28	26.34	0.1040	0.0295
0.73 - 0.70	1725	1725	100.0	18.50	7.31	22.83	0.1136	0.0338
0.70 - 0.68	1328	1328	100.0	18.16	6.72	20.34	0.1247	0.0380
0.68 - 0.67	724	724	100.0	17.56	5.26	16.13	0.1522	0.0478
0.67 - 0.65	1573	1573	100.0	17.54	5.00	15.46	0.1585	0.0513
0.65 - 0.63	1810	1810	100.0	16.78	4.27	12.81	0.1864	0.0621
0.63 - 0.62	967	967	100.0	16.52	4.11	12.11	0.1991	0.0669
0.62 - 0.61	1040	1040	100.0	14.74	4.24	10.98	0.2207	0.0735
0.61 - 0.60	1140	1140	100.0	14.93	3.62	9.47	0.2477	0.0852
0.60 - 0.59	1187	1187	100.0	14.69	3.32	8.70	0.2703	0.0949
0.59 - 0.58	1211	1294	93.6	12.32	2.83	6.98	0.3008	0.1308
0.68 - 0.58	9652	9735	99.1	15.65	4.07	11.59	0.2037	0.0720
Inf - 0.58	25569	25656	99.7	21.59	14.67	43.81	0.0472	0.0180

Complete .cif-data of the **2** are available under the CCDC number CCDC-**2225002**.

A resolution cut off (SHEL 999 0.62) was applied to exclude poorly determined intensities at high diffraction angles. One reflection (OMIT -1 0 1) with high I/σ(I) was excluded before the final refinement cycles. For final refinement, the anis -a (anharmonic motion refinement) instruction in Olex2 refinement was applied to the Bi central atom. This applies higher Gram-Charlier coefficients to the refinement, taking the anharmonic motion of the central atom into account.

High residual density peaks (Q1 = 4.05 e/Å^3) can be found in the vicinity of the heavy Bi central atom (0.658 Å away from Bi1). It appears as a shashlik-like distribution, which indicates that anharmonic motion could presumably cause this observation. To take this into account, higher order Gram-Charlier coefficients have been applied before final refinement cycles. This does not influence the reflection-to-parameter ratio significantly.

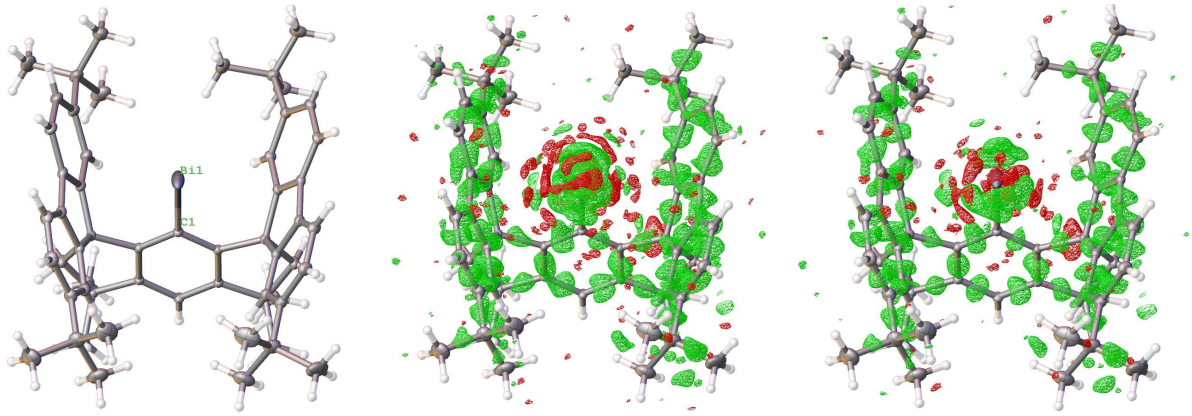

Fig. S43. Structure (left) and difference density distribution (middle, right) of compound ^{t}Bu-M^{s}Fluind-Bi(I) (**2**) before and after applying the Gramm-Charlier anharmonic displacement correction to the Bi atom (source: Olex2, diff-map, level 0.25 e/Å^3, 0.1 Å resolution), showing the otherwise well resolved bonding electron density in the C-C bonds.

The application of Gramm-Charlier coefficients reduce the residual density (Q1 = 1.73 e/Å^3; 0.9 Å away from Bi1) in the heavy atom regimen to an acceptable value. Additionally, the absence of H atoms attached to the Bi central atom was confirmed by IR, XAS and ^{1}H NMR.

Table S11. Crystal data and structure refinement of compound ^{t}Bu-M^{s}Fluind-Bi(I) (**2**).

Identification code	14725	
Empirical formula	$C_{56}H_{65}Bi$	
Color	yellow	
Formula weight	947.121 $g \cdot mol^{-1}$	
Temperature	100(2) K	
Wavelength	0.71073 Å	
Crystal system	Triclinic	
Space group	*P*-1, (no. 2)	
Unit cell dimensions	a = 12.6987(3) Å	α= 108.811(1)°.
	b = 14.3359(3) Å	β= 102.403(1)°.
	c = 15.3368(4) Å	γ = 106.274(1)°.
Volume	2389.67(10) $Å^3$	
Z	2	
Density (calculated)	1.316 $Mg \cdot m^{-3}$	
Absorption coefficient	3.723 mm^{-1}	
F(000)	961.645 e	
Crystal size	0.256 x 0.253 x 0.1 mm^3	
θ range for data collection	1.90 to 34.97°.	
Index ranges	$-21 \le h \le 21$, $-24 \le k \le 24$, $-26 \le l \le 26$	
Reflections collected	553798	
Independent reflections	20990 [R_{int} = 0.0487]	
Reflections with I>2σ(I)	18820	
Completeness to θ = 25.2417°	99.94 %	
Absorption correction	Gaussian	
Max. and min. transmission	0.9972 and 0.5024	
Refinement method	Full-matrix least-squares on F^2	
Data / restraints / parameters	20990 / 0 / 555	
Goodness-of-fit on F^2	1.0261	
Final R indices [I>2σ(I)]	R_1 = 0.0209	wR^2 = 0.0483
R indices (all data)	R_1 = 0.0257	wR^2 = 0.0500
Largest diff. peak and hole	1.7335 and –1.3358 $e \cdot Å^{-3}$	

Table S12. Bond lengths [Å] and angles [°] of compound ^{t}Bu-M^{s}Fluind-Bi(I) (**2**).

Bi(1)-C(1)	2.2783(10)	C(1)-C(2)	1.4048(14)
C(1)-C(12)	1.4029(14)	C(2)-C(3)	1.5224(14)
C(2)-C(6)	1.4011(14)	C(3)-C(4)	1.5692(15)
C(3)-C(17)	1.5303(15)	C(3)-C(28)	1.5239(15)
C(4)-H(4a)	0.9900	C(4)-H(4b)	0.9900
C(4)-C(5)	1.5499(15)	C(5)-C(6)	1.5171(14)
C(5)-C(13)	1.5378(16)	C(5)-C(14)	1.5337(15)
C(6)-C(7)	1.3900(14)	C(7)-H(7)	0.9500
C(7)-C(8)	1.3911(14)	C(8)-C(9)	1.5123(14)
C(8)-C(12)	1.3970(14)	C(9)-C(10)	1.5533(15)
C(9)-C(15)	1.5330(16)	C(9)-C(16)	1.5339(15)
C(10)-H(10a)	0.9900	C(10)-H(10b)	0.9900
C(10)-C(11)	1.5703(15)	C(11)-C(12)	1.5276(14)
C(11)-C(37)	1.5256(15)	C(11)-C(48)	1.5230(15)
C(13)-H(13a)	0.9800	C(13)-H(13b)	0.9800
C(13)-H(13c)	0.9800	C(14)-H(14a)	0.9800
C(14)-H(14b)	0.9800	C(14)-H(14c)	0.9800
C(15)-H(15a)	0.9800	C(15)-H(15b)	0.9800
C(15)-H(15c)	0.9800	C(16)-H(16a)	0.9800
C(16)-H(16b)	0.9800	C(16)-H(16c)	0.9800
C(17)-C(18)	1.3897(16)	C(17)-C(22)	1.4004(15)
C(18)-H(18)	0.9500	C(18)-C(19)	1.4006(16)
C(19)-C(20)	1.4052(17)	C(19)-C(29)	1.5288(17)
C(20)-H(20)	0.9500	C(20)-C(21)	1.3889(17)
C(21)-H(21)	0.9500	C(21)-C(22)	1.3916(15)
C(22)-C(23)	1.4646(15)	C(23)-C(24)	1.3885(15)
C(23)-C(28)	1.4037(14)	C(24)-H(24)	0.9500
C(24)-C(25)	1.3929(16)	C(25)-H(25)	0.9500
C(25)-C(26)	1.4024(16)	C(26)-C(27)	1.4084(15)
C(26)-C(33)	1.5324(16)	C(27)-H(27)	0.9500
C(27)-C(28)	1.3834(15)	C(29)-C(30)	1.533(2)
C(29)-C(31)	1.541(2)	C(29)-C(32)	1.529(2)
C(30)-H(30a)	0.9800	C(30)-H(30b)	0.9800

C(30)-H(30c)	0.9800	C(31)-H(31a)	0.9800
C(31)-H(31b)	0.9800	C(31)-H(31c)	0.9800
C(32)-H(32a)	0.9800	C(32)-H(32b)	0.9800
C(32)-H(32c)	0.9800	C(33)-C(34)	1.5386(18)
C(33)-C(35)	1.5340(18)	C(33)-C(36)	1.5343(18)
C(34)-H(34a)	0.9800	C(34)-H(34b)	0.9800
C(34)-H(34c)	0.9800	C(35)-H(35a)	0.9800
C(35)-H(35b)	0.9800	C(35)-H(35c)	0.9800
C(36)-H(36a)	0.9800	C(36)-H(36b)	0.9800
C(36)-H(36c)	0.9800	C(37)-C(38)	1.3856(16)
C(37)-C(42)	1.4018(15)	C(38)-H(38)	0.9500
C(38)-C(39)	1.4034(16)	C(39)-C(40)	1.4035(18)
C(39)-C(49)	1.5322(18)	C(40)-H(40)	0.9500
C(40)-C(41)	1.3900(19)	C(41)-H(41)	0.9500
C(41)-C(42)	1.3928(16)	C(42)-C(43)	1.4654(16)
C(43)-C(44)	1.3964(16)	C(43)-C(48)	1.4015(15)
C(44)-H(44)	0.9500	C(44)-C(45)	1.3902(18)
C(45)-H(45)	0.9500	C(45)-C(46)	1.4082(17)
C(46)-C(47)	1.4026(16)	C(46)-C(53)	1.5321(18)
C(47)-H(47)	0.9500	C(47)-C(48)	1.3879(16)
C(49)-C(50)	1.535(2)	C(49)-C(51)	1.539(2)
C(49)-C(52)	1.531(2)	C(50)-H(50a)	0.9800
C(50)-H(50b)	0.9800	C(50)-H(50c)	0.9800
C(51)-H(51a)	0.9800	C(51)-H(51b)	0.9800
C(51)-H(51c)	0.9800	C(52)-H(52a)	0.9800
C(52)-H(52b)	0.9800	C(52)-H(52c)	0.9800
C(53)-C(54)	1.5416(19)	C(53)-C(55)	1.539(2)
C(53)-C(56)	1.531(2)	C(54)-H(54a)	0.9800
C(54)-H(54b)	0.9800	C(54)-H(54c)	0.9800
C(55)-H(55a)	0.9800	C(55)-H(55b)	0.9800
C(55)-H(55c)	0.9800	C(56)-H(56a)	0.9800
C(56)-H(56b)	0.9800	C(56)-H(56c)	0.9800

C(2)-C(1)-Bi(1)	121.41(7)	C(12)-C(1)-Bi(1)	122.22(7)
C(12)-C(1)-C(2)	116.37(9)	C(3)-C(2)-C(1)	127.45(9)
C(6)-C(2)-C(1)	121.91(9)	C(6)-C(2)-C(3)	110.61(8)

C(4)-C(3)-C(2)	102.48(8)	C(17)-C(3)-C(2)	114.68(9)
C(17)-C(3)-C(4)	112.62(8)	C(28)-C(3)-C(2)	116.89(8)
C(28)-C(3)-C(4)	109.81(8)	C(28)-C(3)-C(17)	100.72(8)
H(4a)-C(4)-C(3)	110.01(6)	H(4b)-C(4)-C(3)	110.01(5)
H(4b)-C(4)-H(4a)	108.4	C(5)-C(4)-C(3)	108.45(8)
C(5)-C(4)-H(4a)	110.01(6)	C(5)-C(4)-H(4b)	110.01(6)
C(6)-C(5)-C(4)	101.90(8)	C(13)-C(5)-C(4)	112.50(9)
C(13)-C(5)-C(6)	111.00(9)	C(14)-C(5)-C(4)	110.90(9)
C(14)-C(5)-C(6)	112.15(9)	C(14)-C(5)-C(13)	108.35(9)
C(5)-C(6)-C(2)	113.02(8)	C(7)-C(6)-C(2)	120.62(9)
C(7)-C(6)-C(5)	126.36(9)	H(7)-C(7)-C(6)	120.83(6)
C(8)-C(7)-C(6)	118.34(9)	C(8)-C(7)-H(7)	120.83(6)
C(9)-C(8)-C(7)	125.90(9)	C(12)-C(8)-C(7)	120.93(9)
C(12)-C(8)-C(9)	113.17(9)	C(10)-C(9)-C(8)	103.42(8)
C(15)-C(9)-C(8)	110.25(9)	C(15)-C(9)-C(10)	112.12(9)
C(16)-C(9)-C(8)	110.88(9)	C(16)-C(9)-C(10)	110.51(9)
C(16)-C(9)-C(15)	109.56(9)	H(10a)-C(10)-C(9)	109.99(6)
H(10b)-C(10)-C(9)	109.99(6)	H(10b)-C(10)-H(10a)	108.4
C(11)-C(10)-C(9)	108.53(8)	C(11)-C(10)-H(10a)	109.99(6)
C(11)-C(10)-H(10b)	109.99(6)	C(12)-C(11)-C(10)	103.53(8)
C(37)-C(11)-C(10)	112.40(9)	C(37)-C(11)-C(12)	113.11(8)
C(48)-C(11)-C(10)	111.85(8)	C(48)-C(11)-C(12)	115.21(9)
C(48)-C(11)-C(37)	101.12(8)	C(8)-C(12)-C(1)	121.81(9)
C(11)-C(12)-C(1)	127.35(9)	C(11)-C(12)-C(8)	110.80(8)
H(13a)-C(13)-C(5)	109.5	H(13b)-C(13)-C(5)	109.5
H(13b)-C(13)-H(13a)	109.5	H(13c)-C(13)-C(5)	109.5
H(13c)-C(13)-H(13a)	109.5	H(13c)-C(13)-H(13b)	109.5
H(14a)-C(14)-C(5)	109.5	H(14b)-C(14)-C(5)	109.5
H(14b)-C(14)-H(14a)	109.5	H(14c)-C(14)-C(5)	109.5
H(14c)-C(14)-H(14a)	109.5	H(14c)-C(14)-H(14b)	109.5
H(15a)-C(15)-C(9)	109.5	H(15b)-C(15)-C(9)	109.5
H(15b)-C(15)-H(15a)	109.5	H(15c)-C(15)-C(9)	109.5
H(15c)-C(15)-H(15a)	109.5	H(15c)-C(15)-H(15b)	109.5
H(16a)-C(16)-C(9)	109.5	H(16b)-C(16)-C(9)	109.5
H(16b)-C(16)-H(16a)	109.5	H(16c)-C(16)-C(9)	109.5
H(16c)-C(16)-H(16a)	109.5	H(16c)-C(16)-H(16b)	109.5

C(18)-C(17)-C(3)	128.97(9)	C(22)-C(17)-C(3)	110.42(9)
C(22)-C(17)-C(18)	120.60(10)	H(18)-C(18)-C(17)	119.94(6)
C(19)-C(18)-C(17)	120.12(10)	C(19)-C(18)-H(18)	119.94(7)
C(20)-C(19)-C(18)	118.37(10)	C(29)-C(19)-C(18)	122.43(10)
C(29)-C(19)-C(20)	119.19(10)	H(20)-C(20)-C(19)	119.09(7)
C(21)-C(20)-C(19)	121.82(10)	C(21)-C(20)-H(20)	119.09(6)
H(21)-C(21)-C(20)	120.47(6)	C(22)-C(21)-C(20)	119.06(10)
C(22)-C(21)-H(21)	120.47(7)	C(21)-C(22)-C(17)	119.98(10)
C(23)-C(22)-C(17)	108.82(9)	C(23)-C(22)-C(21)	131.05(10)
C(24)-C(23)-C(22)	131.82(10)	C(28)-C(23)-C(22)	108.08(9)
C(28)-C(23)-C(24)	120.03(10)	H(24)-C(24)-C(23)	120.55(6)
C(25)-C(24)-C(23)	118.91(10)	C(25)-C(24)-H(24)	120.55(6)
H(25)-C(25)-C(24)	118.99(6)	C(26)-C(25)-C(24)	122.02(10)
C(26)-C(25)-H(25)	118.99(7)	C(27)-C(26)-C(25)	118.05(10)
C(33)-C(26)-C(25)	121.94(10)	C(33)-C(26)-C(27)	119.89(10)
H(27)-C(27)-C(26)	119.89(6)	C(28)-C(27)-C(26)	120.22(10)
C(28)-C(27)-H(27)	119.89(6)	C(23)-C(28)-C(3)	110.87(9)
C(27)-C(28)-C(3)	128.45(9)	C(27)-C(28)-C(23)	120.65(10)
C(30)-C(29)-C(19)	109.32(12)	C(31)-C(29)-C(19)	108.36(12)
C(31)-C(29)-C(30)	109.69(15)	C(32)-C(29)-C(19)	112.55(11)
C(32)-C(29)-C(30)	108.51(14)	C(32)-C(29)-C(31)	108.38(13)
H(30a)-C(30)-C(29)	109.5	H(30b)-C(30)-C(29)	109.5
H(30b)-C(30)-H(30a)	109.5	H(30c)-C(30)-C(29)	109.5
H(30c)-C(30)-H(30a)	109.5	H(30c)-C(30)-H(30b)	109.5
H(31a)-C(31)-C(29)	109.5	H(31b)-C(31)-C(29)	109.5
H(31b)-C(31)-H(31a)	109.5	H(31c)-C(31)-C(29)	109.5
H(31c)-C(31)-H(31a)	109.5	H(31c)-C(31)-H(31b)	109.5
H(32a)-C(32)-C(29)	109.5	H(32b)-C(32)-C(29)	109.5
H(32b)-C(32)-H(32a)	109.5	H(32c)-C(32)-C(29)	109.5
H(32c)-C(32)-H(32a)	109.5	H(32c)-C(32)-H(32b)	109.5
C(34)-C(33)-C(26)	107.84(10)	C(35)-C(33)-C(26)	112.55(10)
C(35)-C(33)-C(34)	108.97(11)	C(36)-C(33)-C(26)	110.79(10)
C(36)-C(33)-C(34)	108.63(11)	C(36)-C(33)-C(35)	107.98(11)
H(34a)-C(34)-C(33)	109.5	H(34b)-C(34)-C(33)	109.5
H(34b)-C(34)-H(34a)	109.5	H(34c)-C(34)-C(33)	109.5
H(34c)-C(34)-H(34a)	109.5	H(34c)-C(34)-H(34b)	109.5

H(35a)-C(35)-C(33)	109.5	H(35b)-C(35)-C(33)	109.5
H(35b)-C(35)-H(35a)	109.5	H(35c)-C(35)-C(33)	109.5
H(35c)-C(35)-H(35a)	109.5	H(35c)-C(35)-H(35b)	109.5
H(36a)-C(36)-C(33)	109.5	H(36b)-C(36)-C(33)	109.5
H(36b)-C(36)-H(36a)	109.5	H(36c)-C(36)-C(33)	109.5
H(36c)-C(36)-H(36a)	109.5	H(36c)-C(36)-H(36b)	109.5
C(38)-C(37)-C(11)	128.19(10)	C(42)-C(37)-C(11)	110.73(9)
C(42)-C(37)-C(38)	121.08(10)	H(38)-C(38)-C(37)	120.02(6)
C(39)-C(38)-C(37)	119.97(11)	C(39)-C(38)-H(38)	120.02(7)
C(40)-C(39)-C(38)	118.10(11)	C(49)-C(39)-C(38)	122.28(11)
C(49)-C(39)-C(40)	119.61(11)	H(40)-C(40)-C(39)	118.84(7)
C(41)-C(40)-C(39)	122.31(11)	C(41)-C(40)-H(40)	118.84(7)
H(41)-C(41)-C(40)	120.63(7)	C(42)-C(41)-C(40)	118.75(11)
C(42)-C(41)-H(41)	120.63(7)	C(41)-C(42)-C(37)	119.74(11)
C(43)-C(42)-C(37)	108.58(9)	C(43)-C(42)-C(41)	131.67(10)
C(44)-C(43)-C(42)	131.75(10)	C(48)-C(43)-C(42)	108.39(9)
C(48)-C(43)-C(44)	119.83(11)	H(44)-C(44)-C(43)	120.67(7)
C(45)-C(44)-C(43)	118.67(10)	C(45)-C(44)-H(44)	120.67(7)
H(45)-C(45)-C(44)	118.85(7)	C(46)-C(45)-C(44)	122.30(11)
C(46)-C(45)-H(45)	118.85(7)	C(47)-C(46)-C(45)	118.10(11)
C(53)-C(46)-C(45)	119.37(10)	C(53)-C(46)-C(47)	122.47(11)
H(47)-C(47)-C(46)	119.99(7)	C(48)-C(47)-C(46)	120.01(11)
C(48)-C(47)-H(47)	119.99(6)	C(43)-C(48)-C(11)	110.98(9)
C(47)-C(48)-C(11)	127.94(10)	C(47)-C(48)-C(43)	121.06(10)
C(50)-C(49)-C(39)	109.23(12)	C(51)-C(49)-C(39)	109.79(12)
C(51)-C(49)-C(50)	109.24(13)	C(52)-C(49)-C(39)	112.30(11)
C(52)-C(49)-C(50)	108.60(14)	C(52)-C(49)-C(51)	107.62(13)
H(50a)-C(50)-C(49)	109.5	H(50b)-C(50)-C(49)	109.5
H(50b)-C(50)-H(50a)	109.5	H(50c)-C(50)-C(49)	109.5
H(50c)-C(50)-H(50a)	109.5	H(50c)-C(50)-H(50b)	109.5
H(51a)-C(51)-C(49)	109.5	H(51b)-C(51)-C(49)	109.5
H(51b)-C(51)-H(51a)	109.5	H(51c)-C(51)-C(49)	109.5
H(51c)-C(51)-H(51a)	109.5	H(51c)-C(51)-H(51b)	109.5
H(52a)-C(52)-C(49)	109.5	H(52b)-C(52)-C(49)	109.5
H(52b)-C(52)-H(52a)	109.5	H(52c)-C(52)-C(49)	109.5
H(52c)-C(52)-H(52a)	109.5	H(52c)-C(52)-H(52b)	109.5

C(54)-C(53)-C(46)	108.15(11)	C(55)-C(53)-C(46)	110.63(12)
C(55)-C(53)-C(54)	109.28(11)	C(56)-C(53)-C(46)	112.18(10)
C(56)-C(53)-C(54)	108.36(13)	C(56)-C(53)-C(55)	108.18(12)
H(54a)-C(54)-C(53)	109.5	H(54b)-C(54)-C(53)	109.5
H(54b)-C(54)-H(54a)	109.5	H(54c)-C(54)-C(53)	109.5
H(54c)-C(54)-H(54a)	109.5	H(54c)-C(54)-H(54b)	109.5
H(55a)-C(55)-C(53)	109.5	H(55b)-C(55)-C(53)	109.5
H(55b)-C(55)-H(55a)	109.5	H(55c)-C(55)-C(53)	109.5
H(55c)-C(55)-H(55a)	109.5	H(55c)-C(55)-H(55b)	109.5
H(56a)-C(56)-C(53)	109.5	H(56b)-C(56)-C(53)	109.5
H(56b)-C(56)-H(56a)	109.5	H(56c)-C(56)-C(53)	109.5
H(56c)-C(56)-H(56a)	109.5	H(56c)-C(56)-H(56b)	109.5

3.6. Single crystal structure analysis of ^{t}Bu-M^{s}Fluind- Bi(Me)I (**3**).

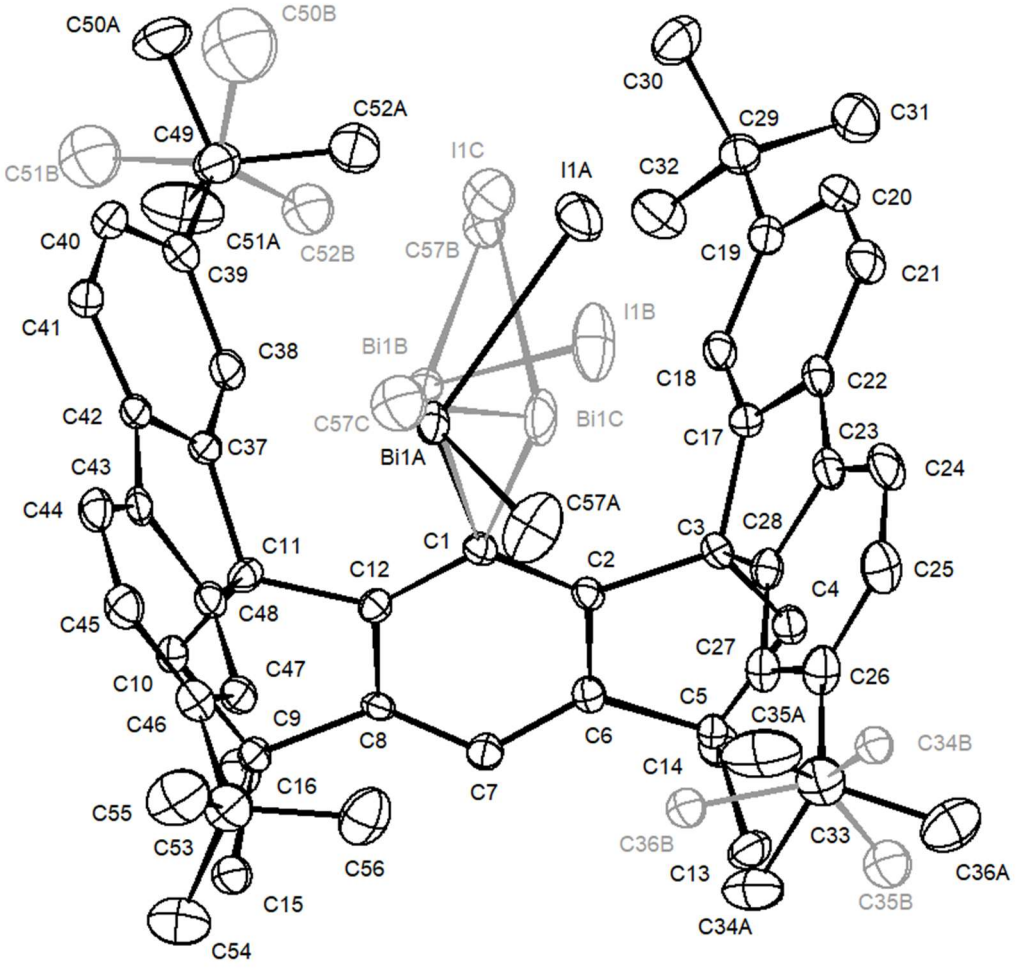

Fig. S44. The molecular structure of ^{t}Bu-M^{s}Fluind-Bi(Me)I (**3**). H atoms have been removed for clarity. Main structure shown in black and disordered parts shown in grey.

X-ray Crystal Structure Analysis of ^{t}Bu-M^{s}Fluind- Bi(Me)I (**3**):

C_{57} H_{68} Bi I, M_r = 1088.99 g mol^{-1}, yellow prism, crystal size 0.13 x 0.04 x 0.04 mm^3, monoclinic, space group $P2_1/c$ [14], a = 12.1803(10) Å, b = 21.751(3) Å, c = 18.548(3) Å, β = 92.942(11)°, V = 4907.7(11) Å^3, T = 100(2) K, Z = 4, D_{calc} = 1.474 g·cm^3, λ = 0.71073 Å, μ(*Mo-K*$_\alpha$) = 4.257 mm^{-1}, Gaussian absorption correction (T_{min} = 0.67015, T_{max} = 0.85559), Bruker-AXS Kappa Mach3 with KappaCCD detector and FR591 rotating Mo anode X-ray source, 2.695 < θ < 29.130°, 70463 measured reflections, 13192 independent reflections, 9598 reflections with $I > 2\sigma(I)$, R_{int} = 0.0757. The structure was solved by *SHELXT* and refined by full-matrix least-squares (*SHELXL*) against F^2 to R_1 = 0.0414 [$I > 2\sigma(I)$], wR_2 = 0.0835 [all data], 625 parameters and 12 restraints.

	h	k	l	distance (mm)
1.	0	-1	0	0.015
2.	0	1	0	0.025
3.	1	0	0	0.065
4.	-1	0	0	0.065
5.	0	0	1	0.02
6.	0	0	-1	0.02

Fig. S45. Crystal faces and unit cell determination/refinement of compound ^{t}Bu-M^{s}Fluind-Bi(Me)I (**3**).

INTENSITY STATISTICS FOR DATASET

Resolution	#Data	#Theory	%Complete	Redundancy	Mean I	Mean I/s	Rmerge	Rsigma
Inf - 2.65	290	304	95.4	9.93	98.24	48.79	0.0471	0.0168
2.65 - 1.78	670	670	100.0	7.47	63.38	36.21	0.0428	0.0206
1.78 - 1.41	960	960	100.0	6.77	36.16	27.60	0.0477	0.0261
1.41 - 1.22	1022	1022	100.0	6.40	29.11	22.86	0.0501	0.0306
1.22 - 1.11	955	955	100.0	5.94	22.41	18.75	0.0592	0.0373
1.11 - 1.03	954	954	100.0	5.68	18.08	15.63	0.0710	0.0447
1.03 - 0.97	978	978	100.0	5.35	14.01	12.36	0.0883	0.0566
0.97 - 0.92	974	974	100.0	5.13	12.19	11.08	0.1020	0.0668
0.92 - 0.88	964	964	100.0	4.85	10.14	9.21	0.1201	0.0831
0.88 - 0.84	1146	1146	100.0	4.63	9.54	8.31	0.1320	0.0958
0.84 - 0.81	1016	1017	99.9	4.40	8.03	6.74	0.1583	0.1225
0.81 - 0.79	788	789	99.9	4.29	6.73	5.59	0.1902	0.1549
0.79 - 0.77	837	838	99.9	4.12	6.07	4.81	0.2168	0.1881
0.77 - 0.75	934	936	99.8	3.99	5.61	4.10	0.2445	0.2283
0.75 - 0.73	1043	1046	99.7	3.87	4.74	3.27	0.2927	0.2996
0.73 - 0.71	1157	1164	99.4	3.77	4.54	2.86	0.3141	0.3561
0.71 - 0.69	1322	1332	99.2	3.62	3.61	1.94	0.4098	0.5369
0.69 - 0.68	679	683	99.4	3.48	3.37	1.60	0.4418	0.6553
0.68 - 0.67	751	761	98.7	3.44	2.87	1.27	0.4854	0.8717
0.67 - 0.66	812	824	98.5	3.33	3.15	1.25	0.4700	0.8538
0.66 - 0.65	934	966	96.7	3.22	2.30	0.83	0.5928	1.3082
0.75 - 0.65	6698	6776	98.8	3.56	3.60	1.96	0.3992	0.5923
Inf - 0.65	19186	19283	99.5	4.75	13.98	10.14	0.0903	0.0985

Complete .cif-data of **3** are available under the CCDC number CCDC-**2225006**.

A resolution cut off (SHEL 999 0.73) was applied to exclude poorly determined reflections at high diffraction angles. One reflection (OMIT 4 0 2) showed high $\Delta I/\sigma(I)$ and was omitted from the data set

before final refinement cycles. The central H_3C-Bi-I unit is disordered over three positions with fixed occupancies of 85:12:3% respectively. Two terminal *tert*-butyl groups have a rotational disorder and were both refined with fixed occupancies of 80:20%. Minor parts are partially described using isotropic displacement parameters.

Table S13. Crystal data and structure refinement of compound ^{t}Bu-M^{s}Fluind-Bi(Me)I (**3**).

Identification code	14524	
Empirical formula	$C_{57}H_{68}BiI$	
Color	yellow	
Formula weight	1088.99 $g \cdot mol^{-1}$	
Temperature	100(2) K	
Wavelength	0.71073 Å	
Crystal system	Monoclinic	
Space group	$P2_1/c$, (no. 14)	
Unit cell dimensions	a = 12.1803(10) Å	α= 90°.
	b = 21.751(3) Å	β= 92.942(11)°.
	c = 18.548(3) Å	γ = 90°.
Volume	4907.7(11) $Å^3$	
Z	4	
Density (calculated)	1.474 $Mg \cdot m^{-3}$	
Absorption coefficient	4.257 mm^{-1}	
F(000)	2184 e	
Crystal size	0.13 x 0.04 x 0.04 mm^3	
θ range for data collection	2.695 to 29.130°.	
Index ranges	$-16 \le h \le 16$, $-29 \le k \le 29$, $-25 \le l \le 25$	
Reflections collected	70463	
Independent reflections	13192 [R_{int} = 0.0757]	
Reflections with I>2σ(I)	9598	
Completeness to θ = 25.242°	99.9 %	
Absorption correction	Gaussian	
Max. and min. transmission	0.85559 and 0.67015	
Refinement method	Full-matrix least-squares on F^2	
Data / restraints / parameters	13192 / 12 / 625	
Goodness-of-fit on F^2	1.035	
Final R indices [I>2σ(I)]	R_1 = 0.0414	wR^2 = 0.0729
R indices (all data)	R_1 = 0.0746	wR^2 = 0.0835
Extinction coefficient	n/a	
Largest diff. peak and hole	1.003 and –1.742 $e \cdot Å^{-3}$	

Table S14. Bond lengths [Å] and angles [°] of compound ^{t}Bu-M^{s}Fluind-Bi(Me)I (**3**).

Bi(1A)-I(1A)	2.8429(5)	Bi(1A)-C(1)	2.304(3)
Bi(1A)-C(57A)	2.251(6)	Bi(1B)-I(1B)	2.820(3)
Bi(1B)-C(1)	2.324(4)	Bi(1B)-C(57B)	2.29(3)
Bi(1C)-I(1C)	2.793(13)	Bi(1C)-C(1)	2.349(7)
Bi(1C)-C(57C)	2.29(16)	C(1)-C(2)	1.413(5)
C(1)-C(12)	1.414(5)	C(2)-C(3)	1.546(4)
C(2)-C(6)	1.401(5)	C(3)-C(4)	1.574(5)
C(3)-C(17)	1.528(5)	C(3)-C(28)	1.526(5)
C(4)-H(4A)	0.9900	C(4)-H(4B)	0.9900
C(4)-C(5)	1.546(5)	C(5)-C(6)	1.517(5)
C(5)-C(13)	1.539(5)	C(5)-C(14)	1.539(5)
C(6)-C(7)	1.388(5)	C(7)-H(7)	0.9500
C(7)-C(8)	1.380(5)	C(8)-C(9)	1.527(5)
C(8)-C(12)	1.402(5)	C(9)-C(10)	1.548(5)
C(9)-C(15)	1.537(5)	C(9)-C(16)	1.541(5)
C(10)-H(10A)	0.9900	C(10)-H(10B)	0.9900
C(10)-C(11)	1.575(5)	C(11)-C(12)	1.540(5)
C(11)-C(37)	1.524(5)	C(11)-C(48)	1.533(5)
C(13)-H(13A)	0.9800	C(13)-H(13B)	0.9800
C(13)-H(13C)	0.9800	C(14)-H(14A)	0.9800
C(14)-H(14B)	0.9800	C(14)-H(14C)	0.9800
C(15)-H(15A)	0.9800	C(15)-H(15B)	0.9800
C(15)-H(15C)	0.9800	C(16)-H(16A)	0.9800
C(16)-H(16B)	0.9800	C(16)-H(16C)	0.9800
C(17)-C(18)	1.385(5)	C(17)-C(22)	1.397(5)
C(18)-H(18)	0.9500	C(18)-C(19)	1.401(5)
C(19)-C(20)	1.407(5)	C(19)-C(29)	1.534(5)
C(20)-H(20)	0.9500	C(20)-C(21)	1.381(6)
C(21)-H(21)	0.9500	C(21)-C(22)	1.392(5)
C(22)-C(23)	1.468(5)	C(23)-C(24)	1.396(5)
C(23)-C(28)	1.398(5)	C(24)-H(24)	0.9500
C(24)-C(25)	1.390(6)	C(25)-H(25)	0.9500
C(25)-C(26)	1.395(6)	C(26)-C(27)	1.400(5)

C(26)-C(33)	1.538(6)	C(27)-H(27)	0.9500
C(27)-C(28)	1.387(5)	C(29)-C(30)	1.542(6)
C(29)-C(31)	1.528(5)	C(29)-C(32)	1.527(6)
C(30)-H(30A)	0.9800	C(30)-H(30B)	0.9800
C(30)-H(30C)	0.9800	C(31)-H(31A)	0.9800
C(31)-H(31B)	0.9800	C(31)-H(31C)	0.9800
C(32)-H(32A)	0.9800	C(32)-H(32B)	0.9800
C(32)-H(32C)	0.9800	C(33)-C(34A)	1.569(7)
C(33)-C(34B)	1.615(18)	C(33)-C(35A)	1.505(7)
C(33)-C(35B)	1.37(2)	C(33)-C(36A)	1.554(7)
C(33)-C(36B)	1.566(19)	C(34A)-H(34D)	0.9800
C(34A)-H(34E)	0.9800	C(34A)-H(34F)	0.9800
C(34B)-H(34A)	0.9800	C(34B)-H(34B)	0.9800
C(34B)-H(34C)	0.9800	C(35A)-H(35A)	0.9800
C(35A)-H(35B)	0.9800	C(35A)-H(35C)	0.9800
C(35B)-H(35D)	0.9800	C(35B)-H(35E)	0.9800
C(35B)-H(35F)	0.9800	C(36A)-H(36D)	0.9800
C(36A)-H(36E)	0.9800	C(36A)-H(36F)	0.9800
C(36B)-H(36A)	0.9800	C(36B)-H(36B)	0.9800
C(36B)-H(36C)	0.9800	C(37)-C(38)	1.385(5)
C(37)-C(42)	1.403(5)	C(38)-H(38)	0.9500
C(38)-C(39)	1.410(5)	C(39)-C(40)	1.398(5)
C(39)-C(49)	1.534(6)	C(40)-H(40)	0.9500
C(40)-C(41)	1.385(6)	C(41)-H(41)	0.9500
C(41)-C(42)	1.386(5)	C(42)-C(43)	1.471(5)
C(43)-C(44)	1.387(5)	C(43)-C(48)	1.419(5)
C(44)-H(44)	0.9500	C(44)-C(45)	1.392(6)
C(45)-H(45)	0.9500	C(45)-C(46)	1.405(5)
C(46)-C(47)	1.401(5)	C(46)-C(53)	1.536(6)
C(47)-H(47)	0.9500	C(47)-C(48)	1.383(5)
C(49)-C(50A)	1.542(7)	C(49)-C(50B)	1.38(4)
C(49)-C(51A)	1.482(8)	C(49)-C(51B)	1.83(3)
C(49)-C(52A)	1.553(7)	C(49)-C(52B)	1.59(2)
C(50A)-H(50A)	0.9800	C(50A)-H(50B)	0.9800
C(50A)-H(50C)	0.9800	C(50B)-H(50D)	0.9800
C(50B)-H(50E)	0.9800	C(50B)-H(50F)	0.9800

C(51A)-H(51A)	0.9800	C(51A)-H(51B)	0.9800
C(51A)-H(51C)	0.9800	C(51B)-H(51D)	0.9800
C(51B)-H(51E)	0.9800	C(51B)-H(51F)	0.9800
C(52A)-H(52A)	0.9800	C(52A)-H(52B)	0.9800
C(52A)-H(52C)	0.9800	C(52B)-H(52D)	0.9800
C(52B)-H(52E)	0.9800	C(52B)-H(52F)	0.9800
C(53)-C(54)	1.532(6)	C(53)-C(55)	1.534(6)
C(53)-C(56)	1.536(6)	C(54)-H(54A)	0.9800
C(54)-H(54B)	0.9800	C(54)-H(54C)	0.9800
C(55)-H(55A)	0.9800	C(55)-H(55B)	0.9800
C(55)-H(55C)	0.9800	C(56)-H(56A)	0.9800
C(56)-H(56B)	0.9800	C(56)-H(56C)	0.9800
C(57A)-H(57A)	0.9800	C(57A)-H(57B)	0.9800
C(57A)-H(57C)	0.9800	C(57B)-H(57D)	0.9800
C(57B)-H(57E)	0.9800	C(57B)-H(57F)	0.9800
C(57C)-H(57G)	0.9800	C(57C)-H(57H)	0.9800
C(57C)-H(57I)	0.9800		

C(1)-Bi(1A)-I(1A)	113.41(9)	C(57A)-Bi(1A)-I(1A)	96.24(18)
C(57A)-Bi(1A)-C(1)	94.38(17)	C(1)-Bi(1B)-I(1B)	110.35(12)
C(57B)-Bi(1B)-I(1B)	93.9(9)	C(57B)-Bi(1B)-C(1)	103.5(9)
C(1)-Bi(1C)-I(1C)	102.6(4)	C(57C)-Bi(1C)-I(1C)	94(4)
C(57C)-Bi(1C)-C(1)	110(4)	C(2)-C(1)-Bi(1A)	133.7(2)
C(2)-C(1)-Bi(1B)	135.3(3)	C(2)-C(1)-Bi(1C)	103.5(3)
C(2)-C(1)-C(12)	116.7(3)	C(12)-C(1)-Bi(1A)	108.4(2)
C(12)-C(1)-Bi(1B)	107.5(2)	C(12)-C(1)-Bi(1C)	138.7(3)
C(1)-C(2)-C(3)	129.9(3)	C(6)-C(2)-C(1)	120.4(3)
C(6)-C(2)-C(3)	109.6(3)	C(2)-C(3)-C(4)	102.4(3)
C(17)-C(3)-C(2)	118.5(3)	C(17)-C(3)-C(4)	107.4(3)
C(28)-C(3)-C(2)	116.0(3)	C(28)-C(3)-C(4)	111.2(3)
C(28)-C(3)-C(17)	101.3(3)	C(3)-C(4)-H(4A)	109.9
C(3)-C(4)-H(4B)	109.9	H(4A)-C(4)-H(4B)	108.3
C(5)-C(4)-C(3)	108.9(3)	C(5)-C(4)-H(4A)	109.9
C(5)-C(4)-H(4B)	109.9	C(6)-C(5)-C(4)	102.0(3)
C(6)-C(5)-C(13)	110.9(3)	C(6)-C(5)-C(14)	112.1(3)
C(13)-C(5)-C(4)	112.9(3)	C(13)-C(5)-C(14)	108.4(3)

C(14)-C(5)-C(4)	110.6(3)	C(2)-C(6)-C(5)	114.0(3)
C(7)-C(6)-C(2)	121.7(3)	C(7)-C(6)-C(5)	124.3(3)
C(6)-C(7)-H(7)	120.6	C(8)-C(7)-C(6)	118.7(3)
C(8)-C(7)-H(7)	120.6	C(7)-C(8)-C(9)	126.0(3)
C(7)-C(8)-C(12)	120.6(3)	C(12)-C(8)-C(9)	113.4(3)
C(8)-C(9)-C(10)	101.9(3)	C(8)-C(9)-C(15)	111.3(3)
C(8)-C(9)-C(16)	111.4(3)	C(15)-C(9)-C(10)	112.8(3)
C(15)-C(9)-C(16)	108.6(3)	C(16)-C(9)-C(10)	110.7(3)
C(9)-C(10)-H(10A)	110.0	C(9)-C(10)-H(10B)	110.0
C(9)-C(10)-C(11)	108.4(3)	H(10A)-C(10)-H(10B)	108.4
C(11)-C(10)-H(10A)	110.0	C(11)-C(10)-H(10B)	110.0
C(12)-C(11)-C(10)	102.5(3)	C(37)-C(11)-C(10)	108.5(3)
C(37)-C(11)-C(12)	117.7(3)	C(37)-C(11)-C(48)	101.0(3)
C(48)-C(11)-C(10)	112.5(3)	C(48)-C(11)-C(12)	114.8(3)
C(1)-C(12)-C(11)	128.4(3)	C(8)-C(12)-C(1)	121.7(3)
C(8)-C(12)-C(11)	109.8(3)	C(5)-C(13)-H(13A)	109.5
C(5)-C(13)-H(13B)	109.5	C(5)-C(13)-H(13C)	109.5
H(13A)-C(13)-H(13B)	109.5	H(13A)-C(13)-H(13C)	109.5
H(13B)-C(13)-H(13C)	109.5	C(5)-C(14)-H(14A)	109.5
C(5)-C(14)-H(14B)	109.5	C(5)-C(14)-H(14C)	109.5
H(14A)-C(14)-H(14B)	109.5	H(14A)-C(14)-H(14C)	109.5
H(14B)-C(14)-H(14C)	109.5	C(9)-C(15)-H(15A)	109.5
C(9)-C(15)-H(15B)	109.5	C(9)-C(15)-H(15C)	109.5
H(15A)-C(15)-H(15B)	109.5	H(15A)-C(15)-H(15C)	109.5
H(15B)-C(15)-H(15C)	109.5	C(9)-C(16)-H(16A)	109.5
C(9)-C(16)-H(16B)	109.5	C(9)-C(16)-H(16C)	109.5
H(16A)-C(16)-H(16B)	109.5	H(16A)-C(16)-H(16C)	109.5
H(16B)-C(16)-H(16C)	109.5	C(18)-C(17)-C(3)	128.3(3)
C(18)-C(17)-C(22)	120.8(3)	C(22)-C(17)-C(3)	110.5(3)
C(17)-C(18)-H(18)	120.0	C(17)-C(18)-C(19)	119.9(3)
C(19)-C(18)-H(18)	120.0	C(18)-C(19)-C(20)	118.1(3)
C(18)-C(19)-C(29)	122.4(3)	C(20)-C(19)-C(29)	119.5(3)
C(19)-C(20)-H(20)	118.8	C(21)-C(20)-C(19)	122.3(4)
C(21)-C(20)-H(20)	118.8	C(20)-C(21)-H(21)	120.7
C(20)-C(21)-C(22)	118.6(3)	C(22)-C(21)-H(21)	120.7
C(17)-C(22)-C(23)	108.3(3)	C(21)-C(22)-C(17)	120.2(3)

C(21)-C(22)-C(23)	131.5(3)	C(24)-C(23)-C(22)	130.7(3)
C(24)-C(23)-C(28)	120.3(4)	C(28)-C(23)-C(22)	109.0(3)
C(23)-C(24)-H(24)	120.7	C(25)-C(24)-C(23)	118.5(4)
C(25)-C(24)-H(24)	120.7	C(24)-C(25)-H(25)	118.9
C(24)-C(25)-C(26)	122.2(4)	C(26)-C(25)-H(25)	118.9
C(25)-C(26)-C(27)	118.4(4)	C(25)-C(26)-C(33)	120.0(4)
C(27)-C(26)-C(33)	121.6(4)	C(26)-C(27)-H(27)	119.8
C(28)-C(27)-C(26)	120.4(4)	C(28)-C(27)-H(27)	119.8
C(23)-C(28)-C(3)	110.2(3)	C(27)-C(28)-C(3)	129.4(3)
C(27)-C(28)-C(23)	120.3(3)	C(19)-C(29)-C(30)	108.7(3)
C(31)-C(29)-C(19)	110.0(3)	C(31)-C(29)-C(30)	108.8(3)
C(32)-C(29)-C(19)	112.3(3)	C(32)-C(29)-C(30)	108.2(3)
C(32)-C(29)-C(31)	108.7(4)	C(29)-C(30)-H(30A)	109.5
C(29)-C(30)-H(30B)	109.5	C(29)-C(30)-H(30C)	109.5
H(30A)-C(30)-H(30B)	109.5	H(30A)-C(30)-H(30C)	109.5
H(30B)-C(30)-H(30C)	109.5	C(29)-C(31)-H(31A)	109.5
C(29)-C(31)-H(31B)	109.5	C(29)-C(31)-H(31C)	109.5
H(31A)-C(31)-H(31B)	109.5	H(31A)-C(31)-H(31C)	109.5
H(31B)-C(31)-H(31C)	109.5	C(29)-C(32)-H(32A)	109.5
C(29)-C(32)-H(32B)	109.5	C(29)-C(32)-H(32C)	109.5
H(32A)-C(32)-H(32B)	109.5	H(32A)-C(32)-H(32C)	109.5
H(32B)-C(32)-H(32C)	109.5	C(26)-C(33)-C(34A)	113.0(4)
C(26)-C(33)-C(34B)	109.0(7)	C(26)-C(33)-C(36A)	109.8(4)
C(26)-C(33)-C(36B)	105.2(8)	C(35A)-C(33)-C(26)	110.6(4)
C(35A)-C(33)-C(34A)	107.3(4)	C(35A)-C(33)-C(36A)	110.6(5)
C(35B)-C(33)-C(26)	104.9(10)	C(35B)-C(33)-C(34B)	114.1(12)
C(35B)-C(33)-C(36B)	118.6(12)	C(36A)-C(33)-C(34A)	105.4(4)
C(36B)-C(33)-C(34B)	104.5(10)	C(33)-C(34A)-H(34D)	109.5
C(33)-C(34A)-H(34E)	109.5	C(33)-C(34A)-H(34F)	109.5
H(34D)-C(34A)-H(34E)	109.5	H(34D)-C(34A)-H(34F)	109.5
H(34E)-C(34A)-H(34F)	109.5	C(33)-C(34B)-H(34A)	109.5
C(33)-C(34B)-H(34B)	109.5	C(33)-C(34B)-H(34C)	109.5
H(34A)-C(34B)-H(34B)	109.5	H(34A)-C(34B)-H(34C)	109.5
H(34B)-C(34B)-H(34C)	109.5	C(33)-C(35A)-H(35A)	109.5
C(33)-C(35A)-H(35B)	109.5	C(33)-C(35A)-H(35C)	109.5
H(35A)-C(35A)-H(35B)	109.5	H(35A)-C(35A)-H(35C)	109.5

H(35B)-C(35A)-H(35C)	109.5	C(33)-C(35B)-H(35D)	109.5
C(33)-C(35B)-H(35E)	109.5	C(33)-C(35B)-H(35F)	109.5
H(35D)-C(35B)-H(35E)	109.5	H(35D)-C(35B)-H(35F)	109.5
H(35E)-C(35B)-H(35F)	109.5	C(33)-C(36A)-H(36D)	109.5
C(33)-C(36A)-H(36E)	109.5	C(33)-C(36A)-H(36F)	109.5
H(36D)-C(36A)-H(36E)	109.5	H(36D)-C(36A)-H(36F)	109.5
H(36E)-C(36A)-H(36F)	109.5	C(33)-C(36B)-H(36A)	109.5
C(33)-C(36B)-H(36B)	109.5	C(33)-C(36B)-H(36C)	109.5
H(36A)-C(36B)-H(36B)	109.5	H(36A)-C(36B)-H(36C)	109.5
H(36B)-C(36B)-H(36C)	109.5	C(38)-C(37)-C(11)	128.5(3)
C(38)-C(37)-C(42)	120.5(3)	C(42)-C(37)-C(11)	111.0(3)
C(37)-C(38)-H(38)	120.0	C(37)-C(38)-C(39)	120.0(4)
C(39)-C(38)-H(38)	120.0	C(38)-C(39)-C(49)	119.6(3)
C(40)-C(39)-C(38)	118.3(4)	C(40)-C(39)-C(49)	122.0(3)
C(39)-C(40)-H(40)	119.1	C(41)-C(40)-C(39)	121.8(4)
C(41)-C(40)-H(40)	119.1	C(40)-C(41)-H(41)	120.3
C(40)-C(41)-C(42)	119.4(4)	C(42)-C(41)-H(41)	120.3
C(37)-C(42)-C(43)	108.4(3)	C(41)-C(42)-C(37)	119.9(4)
C(41)-C(42)-C(43)	131.5(3)	C(44)-C(43)-C(42)	131.4(3)
C(44)-C(43)-C(48)	120.0(4)	C(48)-C(43)-C(42)	108.2(3)
C(43)-C(44)-H(44)	120.3	C(43)-C(44)-C(45)	119.4(4)
C(45)-C(44)-H(44)	120.3	C(44)-C(45)-H(45)	119.2
C(44)-C(45)-C(46)	121.5(4)	C(46)-C(45)-H(45)	119.2
C(45)-C(46)-C(53)	122.1(4)	C(47)-C(46)-C(45)	118.2(4)
C(47)-C(46)-C(53)	119.6(3)	C(46)-C(47)-H(47)	119.4
C(48)-C(47)-C(46)	121.2(3)	C(48)-C(47)-H(47)	119.4
C(43)-C(48)-C(11)	110.1(3)	C(47)-C(48)-C(11)	130.3(3)
C(47)-C(48)-C(43)	119.6(3)	C(39)-C(49)-C(50A)	112.7(4)
C(39)-C(49)-C(51B)	105.3(9)	C(39)-C(49)-C(52A)	106.6(4)
C(39)-C(49)-C(52B)	116.6(9)	C(50A)-C(49)-C(52A)	106.8(4)
C(50B)-C(49)-C(39)	119.9(16)	C(50B)-C(49)-C(51B)	105.2(19)
C(50B)-C(49)-C(52B)	111.2(18)	C(51A)-C(49)-C(39)	110.6(4)
C(51A)-C(49)-C(50A)	109.4(5)	C(51A)-C(49)-C(52A)	110.6(5)
C(52B)-C(49)-C(51B)	94.3(13)	C(49)-C(50A)-H(50A)	109.5
C(49)-C(50A)-H(50B)	109.5	C(49)-C(50A)-H(50C)	109.5
H(50A)-C(50A)-H(50B)	109.5	H(50A)-C(50A)-H(50C)	109.5

H(50B)-C(50A)-H(50C)	109.5	C(49)-C(50B)-H(50D)	109.5
C(49)-C(50B)-H(50E)	109.5	C(49)-C(50B)-H(50F)	109.5
H(50D)-C(50B)-H(50E)	109.5	H(50D)-C(50B)-H(50F)	109.5
H(50E)-C(50B)-H(50F)	109.5	C(49)-C(51A)-H(51A)	109.5
C(49)-C(51A)-H(51B)	109.5	C(49)-C(51A)-H(51C)	109.5
H(51A)-C(51A)-H(51B)	109.5	H(51A)-C(51A)-H(51C)	109.5
H(51B)-C(51A)-H(51C)	109.5	C(49)-C(51B)-H(51D)	109.5
C(49)-C(51B)-H(51E)	109.5	C(49)-C(51B)-H(51F)	109.5
H(51D)-C(51B)-H(51E)	109.5	H(51D)-C(51B)-H(51F)	109.5
H(51E)-C(51B)-H(51F)	109.5	C(49)-C(52A)-H(52A)	109.5
C(49)-C(52A)-H(52B)	109.5	C(49)-C(52A)-H(52C)	109.5
H(52A)-C(52A)-H(52B)	109.5	H(52A)-C(52A)-H(52C)	109.5
H(52B)-C(52A)-H(52C)	109.5	C(49)-C(52B)-H(52D)	109.5
C(49)-C(52B)-H(52E)	109.5	C(49)-C(52B)-H(52F)	109.5
H(52D)-C(52B)-H(52E)	109.5	H(52D)-C(52B)-H(52F)	109.5
H(52E)-C(52B)-H(52F)	109.5	C(46)-C(53)-C(56)	109.1(3)
C(54)-C(53)-C(46)	108.9(4)	C(54)-C(53)-C(55)	108.8(4)
C(54)-C(53)-C(56)	109.6(4)	C(55)-C(53)-C(46)	112.9(4)
C(55)-C(53)-C(56)	107.5(4)	C(53)-C(54)-H(54A)	109.5
C(53)-C(54)-H(54B)	109.5	C(53)-C(54)-H(54C)	109.5
H(54A)-C(54)-H(54B)	109.5	H(54A)-C(54)-H(54C)	109.5
H(54B)-C(54)-H(54C)	109.5	C(53)-C(55)-H(55A)	109.5
C(53)-C(55)-H(55B)	109.5	C(53)-C(55)-H(55C)	109.5
H(55A)-C(55)-H(55B)	109.5	H(55A)-C(55)-H(55C)	109.5
H(55B)-C(55)-H(55C)	109.5	C(53)-C(56)-H(56A)	109.5
C(53)-C(56)-H(56B)	109.5	C(53)-C(56)-H(56C)	109.5
H(56A)-C(56)-H(56B)	109.5	H(56A)-C(56)-H(56C)	109.5
H(56B)-C(56)-H(56C)	109.5	Bi(1A)-C(57A)-H(57A)	109.5
Bi(1A)-C(57A)-H(57B)	109.5	Bi(1A)-C(57A)-H(57C)	109.5
H(57A)-C(57A)-H(57B)	109.5	H(57A)-C(57A)-H(57C)	109.5
H(57B)-C(57A)-H(57C)	109.5	Bi(1B)-C(57B)-H(57D)	109.5
Bi(1B)-C(57B)-H(57E)	109.5	Bi(1B)-C(57B)-H(57F)	109.5
H(57D)-C(57B)-H(57E)	109.5	H(57D)-C(57B)-H(57F)	109.5
H(57E)-C(57B)-H(57F)	109.5	Bi(1C)-C(57C)-H(57G)	109.5
Bi(1C)-C(57C)-H(57H)	109.5	Bi(1C)-C(57C)-H(57I)	109.5
H(57G)-C(57C)-H(57H)	109.5	H(57G)-C(57C)-H(57I)	109.5

H(57H)-C(57C)-H(57I)	109.5

3.7. Structure search in the Cambridge Structural Database (CSD)

A database (WebCSD Version 1.9.32; https://www.ccdc.cam.ac.uk/structures/WebCSD/StructureSearch) survey was performed on 7 December 2022 to search for related structural motifs. The following search motif was used in the web interface structure search with 'substructure' match conditions:

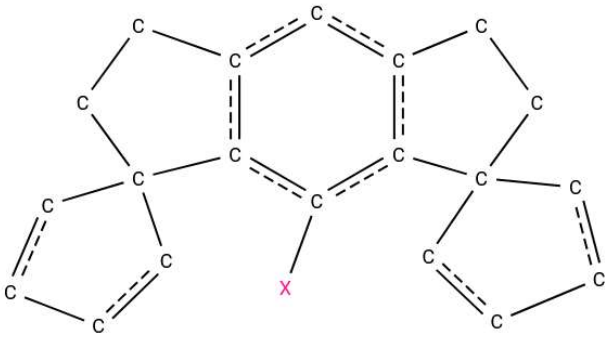

Fig. S46. Search motif for data survey on shown ligand scaffold.

The initial search found 23 structures containing the predefined ligand scaffold. All entries are listed in the following table. Herein X can be Li, P, As, Br, Ge or Cu in various oxidation states.

Table S15. Overview of search results for M^{s}Fluind scaffold.

Database identifier	**Deposition number**	**Distance C-X (Å)**	**Database identifier**	**Deposition number**	**Distance C-X (Å)**
ABANEA	2069464	C-Li 2.112	JAZQAG	2133471	C-P 1.826
ABANIE	2069465	C-P 1.865	JAZQEK	2133472	C-As 1.968
ABANOK	2069466	C-As 1.984	JAZQIO	2133473	C-Ge 2.043
ABANUQ	2069467	C-P 1.828	LUTMAP	780796	C-Cu 1.915
ABAPAY	2069468	C-P 1.827	LUTMIX	780798	C-Br 1.892
ABAPEC	2069469	C-As 1.960	VEQDEE	2166315	C-Ge 2.000
JAZNUX	2133465	C-Br 1.899	VEQMAJ	2125008	C-Ge 2.039
JAZPAF	2133466	C-Li 2.105	VEQMEN	2125009	C-Ge 1.985
JAZPEJ	2133467	C-Ge 2.007	VEQMIR	2125010	C-Ge 2.021
JAZPIN	2133468	C-Ge 2.016	VEQMOX	2125011	C-Ge 1.980
JAZPOT	2133469	C-Ge 2.038	VEQZIE	2125007	C-Br 1.891
JAZPUZ	2133470	C-P 1.804			

3.8. Geometry comparison of **2**: between X-ray crystal structure and DFT calculations

Comparison of the experimental geometry (crystal structure of **2** at 100K) and the theoretically calculated structures of different spin systems was undertaken. The comparisons were carried out using the program Mercury version 2021.2.0. The superposition of the molecules was carried out by the routine *molecular overlay*. All observations are listed in Table S16 at the end of this section.

3.8.1. X-ray crystal structure of **2** versus DFT calculations on the Bi closed-shell system

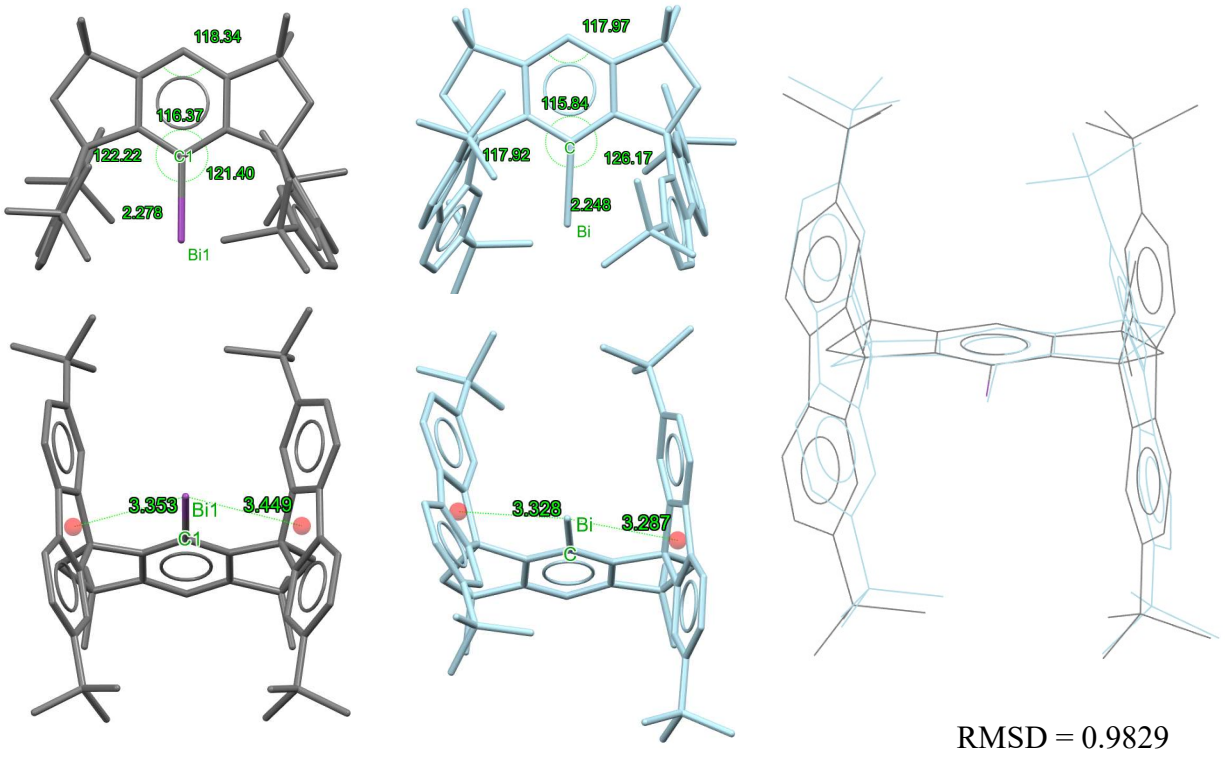

Fig. S47. Geometrical comparison of the X-ray crystal structure of **2** (colored by elements) and closed shell system (light blue). Selected bond length and angles (top left), Bi···ligand centroid distance (bottom left) and molecular superposition (right).

3.8.2. X-ray crystal structure of **2** versus DFT calculations on the Bi open-shell singlet

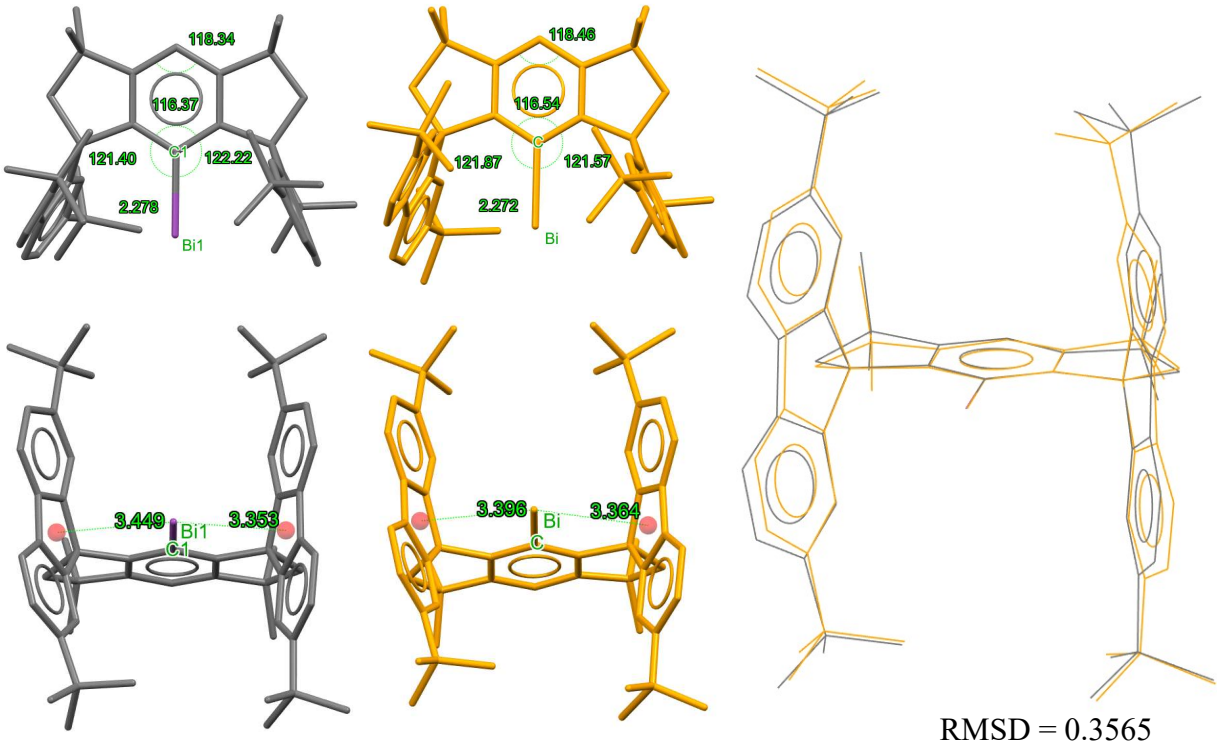

Fig. S48. Geometrical comparison of the X-ray crystal structure of **2** (colored by elements) and open shell system (orange). Selected bond length and angles (top left), Bi···ligand centroid distance (bottom left) and molecular super positioning (right).

3.8.3. X-ray crystal structure of **2** versus DFT calculations on the Bi-triplet

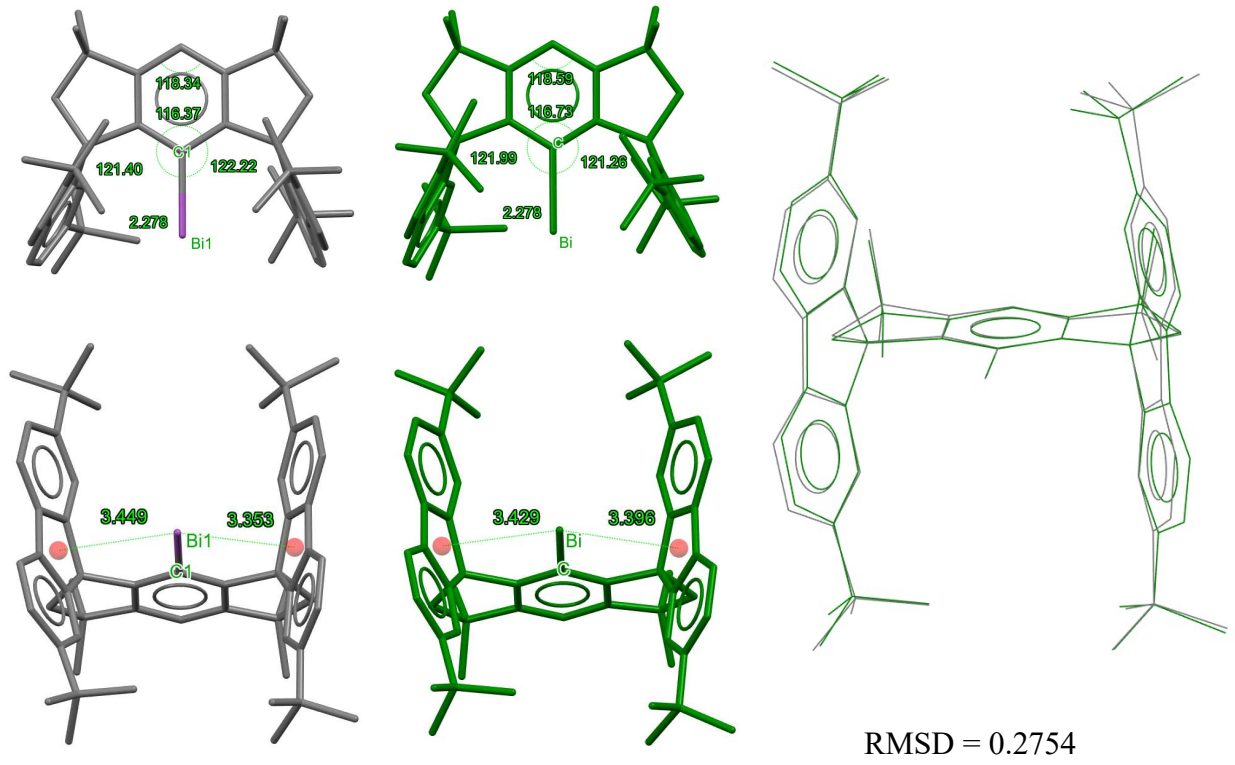

Fig. S49. Geometrical comparison of the X-ray crystal structure of **2** (colored by elements) and triplet system (green). Selected bond length and angles (top left), Bi···ligand centroid distances (bottom left) and molecular super position (right).

Table S16. Overview of selected geometrical differences between experimental X-ray crystal structure and theoretically calculated structure models.

Type	Bi-C bond length / Å	C-C(ipso)-C angle /°	C-C-C angle /°	centroid 1···Bi distance / Å	centroid 2···Bi distance / Å
X-ray	2.278(1)	116.37(9)	118.34(9)	3.353	3.449
closed-shell singlet	2.248	115.84	117.97	3.328	3.287
open-shell singlet	2.272	116.54	118.46	3.396	3.364
triplet	2.278	116.73	118.59	3.429	3.396

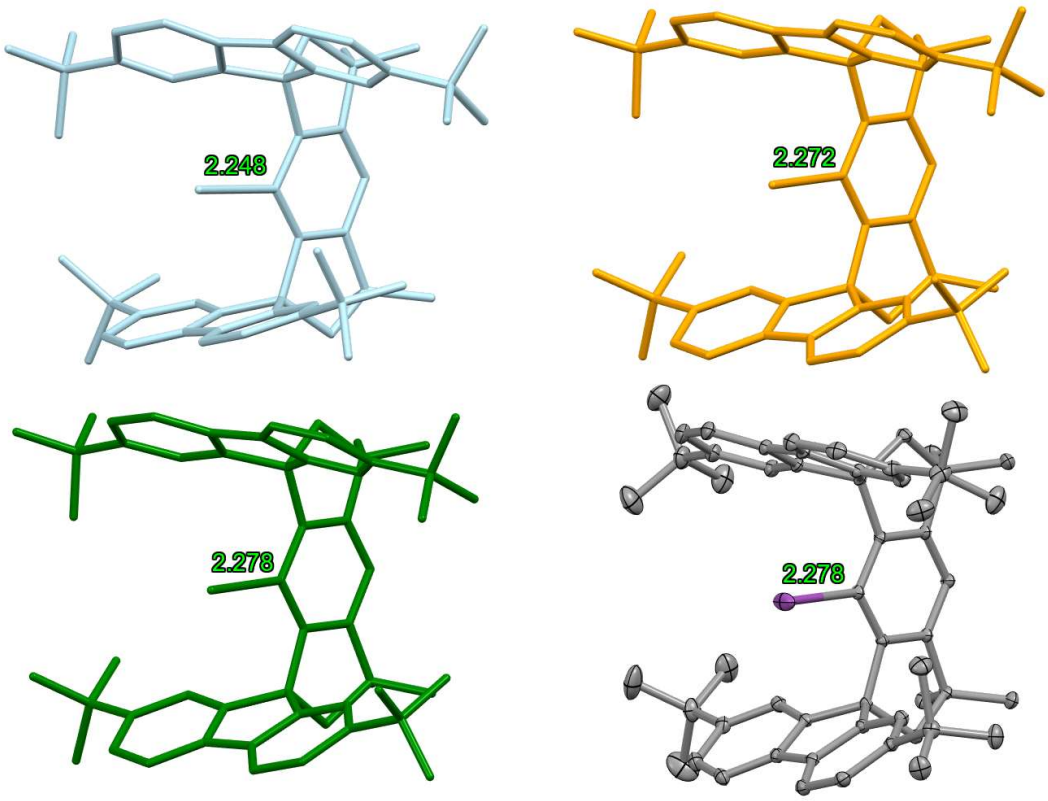

3.9. XRD comparison of **2** with **S2** and **S3**

In addition to the theoretical structures, a comparison of **2** with other structurally analogous compounds can also be made. The dimer **S2** and the Br compound **S3** are particularly suitable for this purpose.

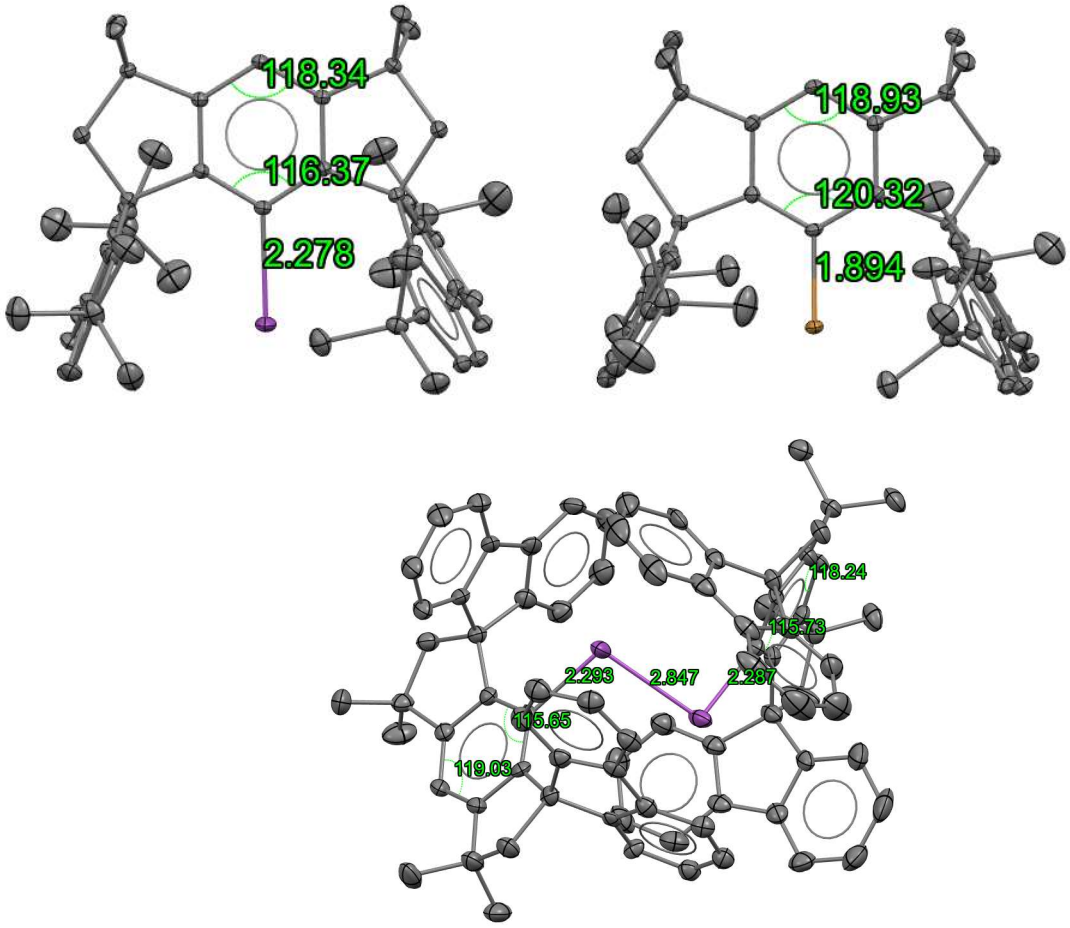

Fig. S50. ORTEP plot and selected bond lengths/angles of structurally similar compounds: **2** (top left), **S3** (top right), and dimer **S2** (bottom).

The selected bond lengths and angles are in accordance with the expected values. Further, small differences can be found in the C-C(ipso)-C angles. Remarkable is the comparison between Bi–C bond lengths of the monomeric **2** and the dimeric **S2** compound. Caused by the lower steric hindrance of the ligand backbone, a Bi=Bi double bond can be formed in **S2**. The different bonding situation also influences the Bi–C distance significantly. In the dimer **S2**, a slightly elongated Bi–C (2.293 and 2.287 Å) bond can be observed.

3.9.1. Intramolecular interactions

The experimental structures have been inspected for inter- and intramolecular interactions as well. The *short contact* function in the program Mercury (version 2021.2.0) was used for the inspections. The search was set up for distances smaller than the sum of the van der Waals radii of the involved atoms. Furthermore, it was defined that intramolecular distances are only shown for atoms that are separated by at least three bonds.

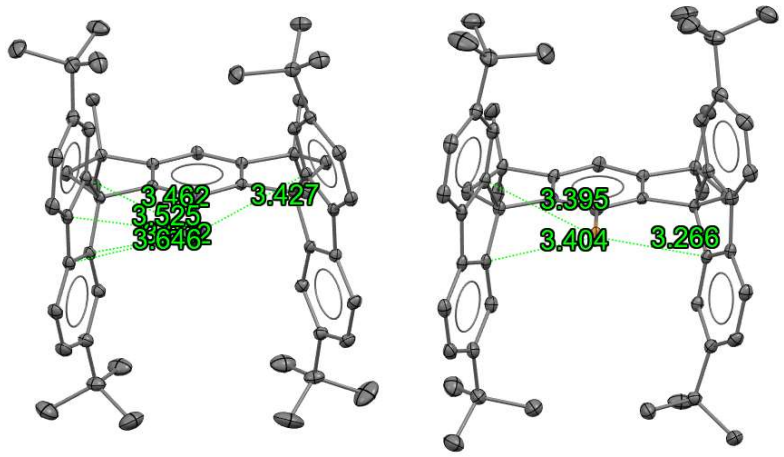

Fig. S51. Intramolecular short contacts in three different structures (**2** left and **S3** right).

Table S17. Summary of found intramolecular short contacts.

Contact No.	M^{s}Flunid-Bi **2**			M^{s}Flunid-Br **S3**		
	Atom 1	Atom 2	d / Å	Atom 1	Atom 2	d / Å
1	C48	Bi1	3.462	C37	Br1	3.395
2	C43	Bi1	3.525	C48	Br1	3.404
3	C42	Bi1	3.646	C17	Br1	3.266
4	C37	Bi1	3.632			
5	C28	Bi1	3.427			

3.9.2. Intermolecular interactions

Furthermore, the structures were examined for possible intermolecular interactions. This was done using the parameters defined above.

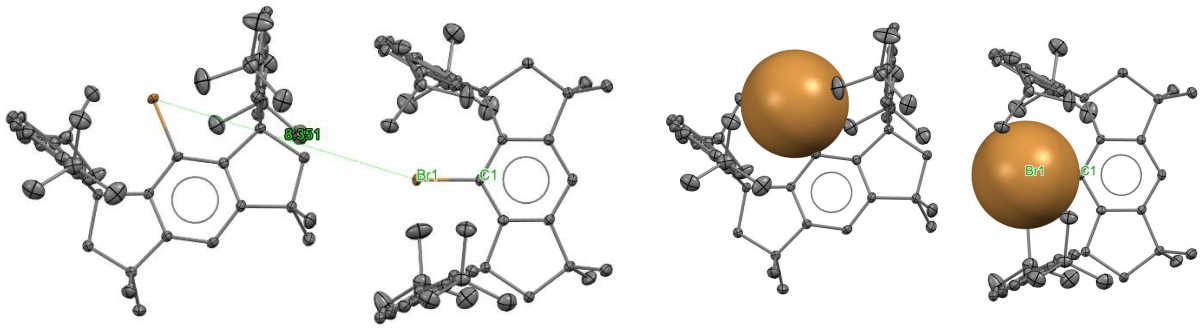

Fig. S52. Central atom distances and molecular orientations in **S3**. The shortest Br–Br distance is 8.351 Å.

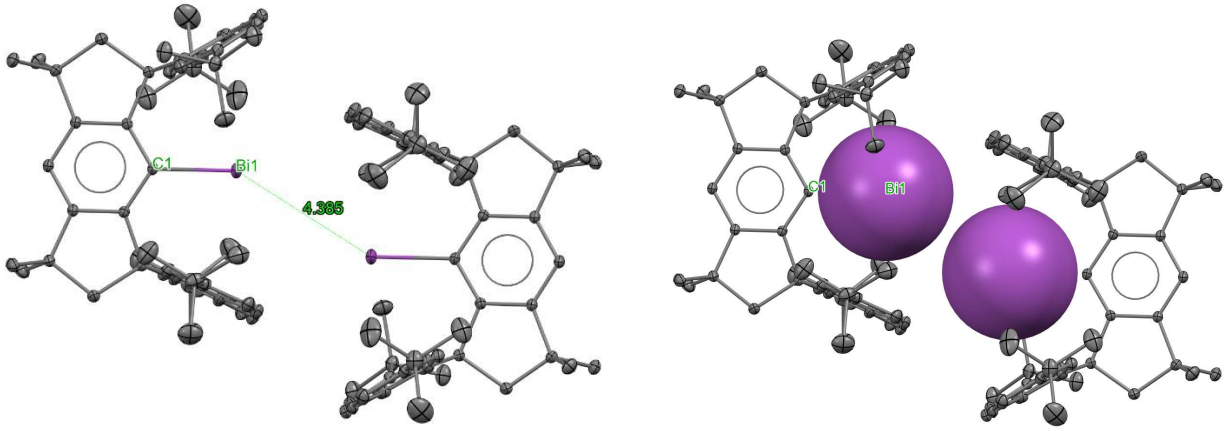

Fig. S53. Central atom distances and molecular orientations in **2**. The shortest Bi–Bi distance is 4.385 Å.

The compared structures show significant differences; it is noticeable that the Bi structure has a face-to-face orientation (central atoms are pointing towards each other), while in the Br structure, **S3**, the central Br atoms of the two neighboring molecules do not point towards each other and are more or less randomly orientated. *This finding supports that the supposition that the **2** has a strong tendency to form dimers, which is prevented in this case by the steric bulk of the ligand.*

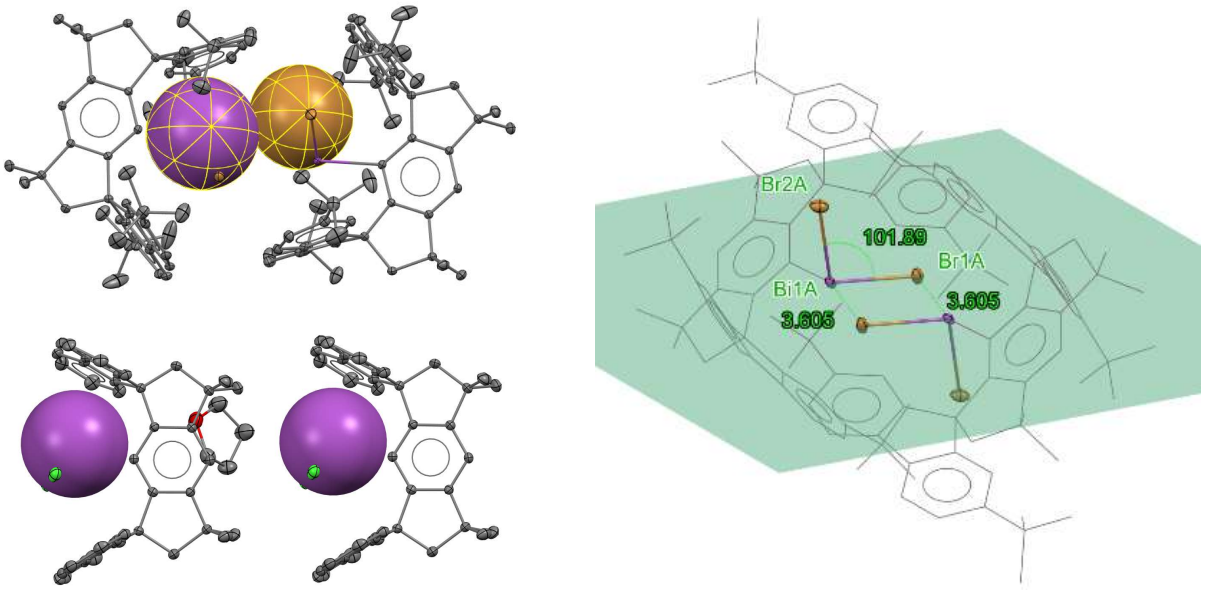

Fig. S54. Comparison of the intermolecular interactions in the structures **1** and **S1**.

Another interesting observation can be made with respect to the intermolecular interactions of the Bi(+III) halogen precursors **1** and **S1**. Despite the large steric hindrance of the *tert*-butyl substituted ligand, the L–$BiBr_2$ compound exhibits a face-to-face orientation in the crystal, whereby two Br atoms and two Bi atoms are coplanar. The resulting Br···Bi intermolecular distances are shorter than the sum of the van der Waals radii. This indicates the formation of a weak halogen-bridged dimer. The remaining two Br atoms lie at an angle of 101.89°, almost perpendicular to the plane and do not show any further interactions.

In contrast, the $BiCl_2$ compound **S1** shows a clearly different packing behavior. In this case, the central $BiCl_2$ units do not point towards one another, as in the dibromide. This means that no bridging intermolecular Bi···halogen interaction can be found in the case of Cl. This observation is particularly surprising, since the ligand of the $BiCl_2$ compound **S1** (due to the missing *tert*-butyl groups) is less sterically demanding than that in the Br compound **1**. This observation indicates that the formation of the intermolecular interactions may have an electronic origin.

3.9.3. Analysis of voids

The investigation of the voids was also carried out using the Mercury program. A sample radius of 1.2 Å and an approx. grid spacing of 0.7 Å were used for the display.

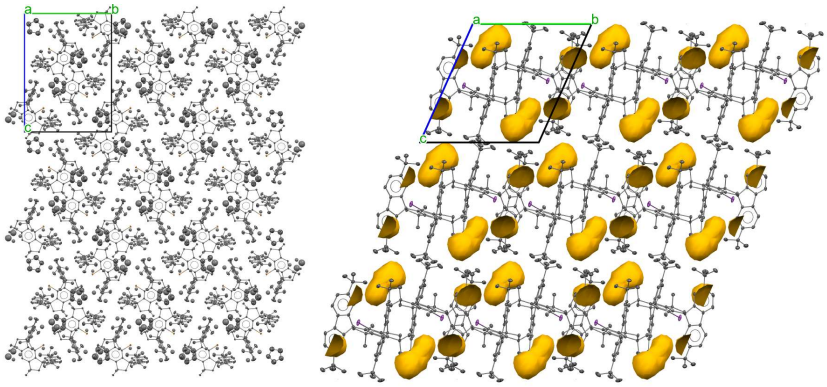

Fig. S55. Packing of three analogues structural models (left –Br **S1**, right –Bi **2**) viewed along crystallographic *a* axis. Voids are represented by yellow surface.

It turns out that the Br compound **S3** does not contain any voids. The -Bi compound **2** shows voids with a total volume of 86.03 Å^3, which corresponds to 3.6% of the volume of the unit cell. The KPI (Kitaigorodskii packing index) was estimated to be 64.2% (after removing disordered parts; using the program: Platon v1.19). Such a small void size is not unusual and may be caused by the low packing density due to the *tert*-butyl groups. *Furthermore, the presence of an incorporated solvent can be excluded due to low residual electron density in the final difference Fourier synthesis.*

4. X-ray absorption spectroscopy (XAS)

4.1. XAS Data Collection

The Bi L_1-edge XAS studies were carried out at the P65 beamline of PETRA III (Germany) (*44*). The PETRA III storage ring was operated at 6 GeV in top-up mode (480 bunches) with a ring current of 120 mA. At the P65 beamline, the X-ray beam was generated using the 5th order harmonic radiation from an 11-periods undulator (period length of 32.9 mm) and then monochromatized by a water-cooled fixed exit Si(311) double crystal monochromator (DCM) operated in QEXAFS mode with an energy resolving power of $\Delta E/E = 6.0 \times 10^{-5}$. The X-ray beam was focused by Rh coated focusing mirrors and collimated at the sample position to a spot size of approx. 1.0 mm × 0.5 mm (H × V). XAS spectra between 16250 eV and 16860 eV were collected in transmission mode. The energy of the incident beam was calibrated by simultaneous measurement of a Bi foil and assigning the energy of the first inflection in the first derivative XAS of Bi foil to 16388 eV. The intensity of incident beam (I_0) and the transmitted beam (I_t) was monitored by two ionization chambers (length of 5.0 cm and 14.0 cm and filled with 220 mbar N_2 + 800 mbar Ar and 870 mbar N_2 + 150 mbar Kr, respectively). The Bi samples were prepared in Kapton sealed powder cells by mixing with α-BN (graphitic boron nitride) based on the Bi concentration to get the optimal X-ray absorption. The Bi samples were transferred to the beamline anaerobically and measured in a liquid He cryostat at 10~15 K. Prior to the full XAS spectra collection, each Bi sample was checked for signs of radiation damage under the full flux of the beam by performing consecutive 1-minute scans of the absorption edge (between 16320 eV and 16460 eV) on the same sample spot 10 times (in total of 10 minutes exposure). The radiation damage tests showed these Bi samples were stable for over 10 minutes. To prevent any impact from the potential radiation damage, each XAS scan was completed within 10 minutes, and the incident beam was further attenuated by glassy carbon filters (5.0 mm thickness). For each sample, five repetitions of XAS scans at five different spots were collected and merged to improve the signal to noise ratio.

The Bi L_1-edge XAS measurements were repeated at the I20-scanning beamline of the Diamond Light Source (DLS, UK) (*45*). The DLS storage ring was operated at 3 GeV in top-up mode (900 bunches) with a ring current of 300 mA. The I20-scanning beamline was equipped with a wiggler (20 mm gap) to generate X-ray radiation and an in-house designed liquid N_2 cooled four-bounce Si(111) monochromator (QCM) to produce a monochromatic beam with high stability and reproducibility (*46*). The QCM was operated in conventional scanning XAS mode, and the energy resolution was $\Delta E/E = 1.3 \times 10^{-4}$. The X-ray beam was focused by Rh coated focusing mirrors and collimated at the sample position to a spot size of approx. 0.4 mm × 0.3 mm (H × V). XAS spectra between 16238 eV and 16588 eV were collected in transmission mode at room temperature. The energy of the incident beam was calibrated by a measurement of a Bi foil and assigning the energy of the first inflection in the first derivative XAS of Bi foil to 16388 eV. The intensity of the incident beam (I_0) and the transmitted beam (I_t) was monitored by two ionization chambers (length of 15.0 cm and 30.0 cm and filled with 1400 mbar He + 400 mbar Ar and 1800 mbar Ar, respectively). The incident beam was attenuated by a combination of filters (0.7 mm aluminum + 2.0 mm glassy carbon) to ensure the linear response of the ionization chambers to the beam intensity. The samples were prepared differently compared to the P65 beam time experiment. Mixtures of Bi compounds and α-BN power were filled into 1.0 mm diameter borosilicate capillaries (0.01 mm thickness). The capillaries were then sealed at the top using vacuum grease in the glovebox and flame sealed at the middle of the capillaries immediately after being taken out from the transfer chamber of the glovebox. Next, additional melted wax was applied to the flame sealed part to protect the fragile end of the capillaries from damage. The Bi samples prepared by this method can be stored at room temperature outside of glovebox for months without decomposition/oxidation. For the XAS experiment, the borosilicate capillaries were mounted horizontally on an in-house designed capillary holder and vertically scanned across the X-ray beam to find the highest

absorption spot (middle positions of the capillaries). For each sample, five repetitions of XAS scans at five different spots (at the same vertical position but different horizontal positions) were collected and merged to improve the signal to noise ratio. Due to the limited rotation speed of QCM, each XAS scan took approx. seven minutes to complete, and no radiation damage test was performed. No noticeable difference could be found between the XAS spectra collected at the I20-scanning and XAS spectra from the P65 beamlines for each Bi compound.

4.2. XAS Data Processing

The Bi L_1-edge XAS spectra were analyzed using the Larch software package (version 0.9.65) (*47*). Pre-edge background subtraction and post-edge normalization of the XAS data were performed using the built-in pre_edge and autobk functions in Larch. A linear regression background (16260-16320eV) was determined, and a quadratic polynomial regression for post-edge normalization (16480-16850eV) was applied. The spectra were splined from k=0 $Å^{-1}$ to k=11 $Å^{-1}$ with rbkg of 1.0 and k-weight of 2. The peak curve fitting of flattened XAS spectra was performed by the LMFIT program (version 1.1.0) using a non-linear least-squares minimization method (*48*). A pseudo Voigt peak and an error function background were included in the fitting model to reproduce the experimental XAS spectra between 16370 eV and 16405 eV. The fitting results are listed in Table S19.

TD-DFT calculations (100 roots in total) were performed based on the DFT optimized geometries using the same B3LYP functional and ZORA-def2-TZVP basis set (*vide infra*). The calculated absorption intensities include contributions from electric dipole, magnetic dipole, and electric quadrupole transitions.

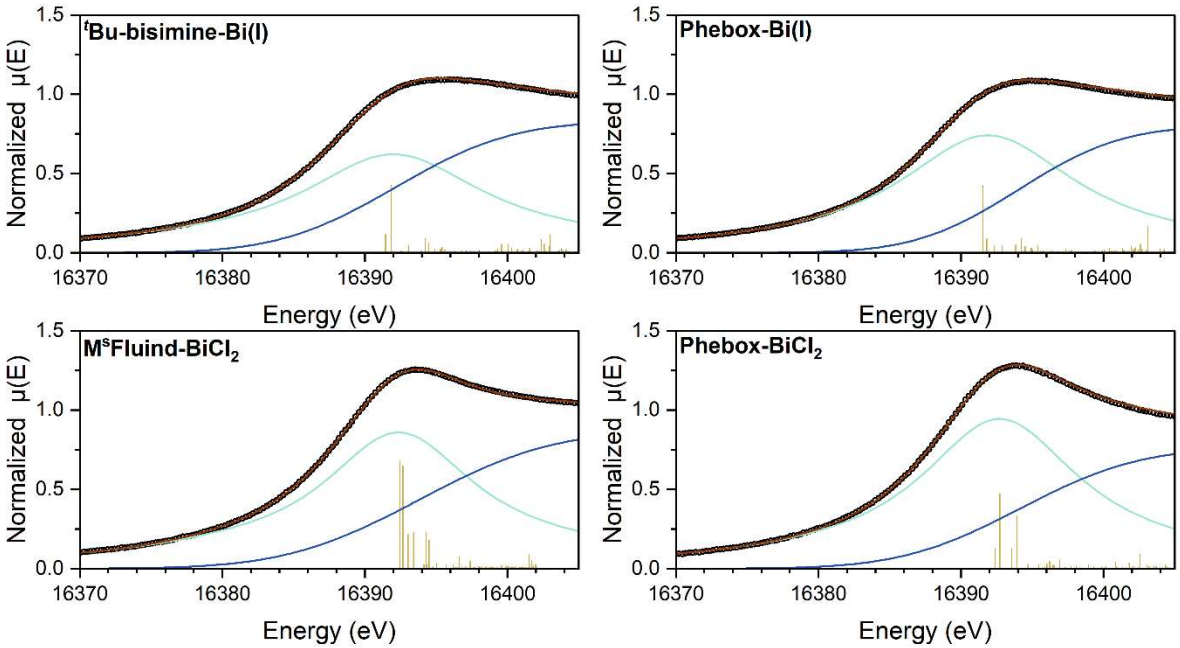

Fig. S56. Experimental Bi L_1-edge XAS spectra (black circles) with peak fitting results (dark red curve) and TD-DFT calculated transitions of (a) ^{t}Bu-bisimine-Bi(I), (b) Phebox-Bi(I), (c) M^{s}Fluind-$BiCl_2$ and (d) Phebox-$BiCl_2$. For each sample, the absorption edge is modeled using a pseudo Voigt peak (cyan curve) and an error function background (blue curve) to reproduce the experimental XAS spectra between 16370 eV and 16405 eV. The detailed peak fitting parameters are listed in Table S19. The TD-DFT calculated absorption transitions (plotted as yellow vertical stick spectra) are shifted by a constant value of +312.4 eV based on the calibration established by XAS of Bi(I)/Bi(III) reference complexes and their corresponding TD-DFT calculated energies (Table S18).

Table S18. Comparison between TD-DFT calculation and experimental XAS of ^{t}Bu-M^{s}Fluind-Bi(I) (**2**) and Bi(I)/Bi(III) reference compounds.

Compounds	Valence states	$E_{calc.}$ (eV) [a]	$E_{exp.}$ (eV) [b]	$E_{calc.} - E_{exp.}$(eV)
2	+1	16702.2 (triplet)	16390.0	312.2
		16702.2 (closedshell)		
		16702.0 (BS)		
$BiPh_3$	+3	16704.7	16392.3	312.4
M^{s}Fluind-$BiCl_2$ (**S1**)	+3	16705.0	16392.4	312.6
^{t}Bu-bisimine-Bi(I)	+1	16704.2	16392.0	312.2
Phebox-Bi(I)	+1	16704.0	16391.9	312.1
Phebox-$BiCl_2$	+3	16705.1	16392.7	312.4

[a] The energy positions of TD-DFT calculated XAS are estimated by the mass center of the first two transition lines.
[b] The energy positions of experimental XAS are determined by the peak fitting results.

Table S19. Peak fitting results of experimental XAS data.

Compounds	Peak (Pseudo Voigt)		Background (Error Function)		R-factor ($\times 10^{-6}$)
	Peak center (eV)	FWHM (eV)	Center (eV)	Width (eV)	
2	16390.0 ± 0.2	15.7 ± 0.1	16393.9 ± 0.1	7.3 ± 0.1	2.4
$BiPh_3$	16392.3 ± 0.2	14.4 ± 0.1	16395.2 ± 0.2	5.6 ± 0.1	5.2
M^{s}Fluind-$BiCl_2$ (**S1**)	16392.4 ± 0.4	14.2 ± 0.1	16393.8 ± 0.6	10.4 ± 0.1	16.4
^{t}Bu-bisimine-Bi(I)	16392.0 ± 0.4	16.6 ± 0.2	16392.2 ± 0.3	9.1 ± 0.3	27.1
Phebox-Bi(I)	16391.9 ± 0.2	15.6 ± 0.2	16394.1 ± 0.3	8.1 ± 0.3	13.1
Phebox-$BiCl_2$	16392.7 ± 0.3	14.2 ± 0.2	16394.2 ± 0.7	9.3 ± 0.2	11.2

5. Computational Studies of 2

5.1. Computational methods

All calculations were carried out with a development version of ORCA based on ORCA 5.0 (*38, 39*). Geometries were optimized using scalar relativistic density functional theory (DFT) in conjunction with the ZORA Hamiltonian (*49*) in the variant proposed by Van Wüllen (*50*). We used the B3LYP functional (*51,52*) in conjunction with the def2-TZVPP basis set (Exponents from def2-TZVP (*53*), recontracted for ZORA by D. A. Pantazis. The Bi center used the SARC basis set Tl-Rn: (*54*)) Dispersion effects were considered at the D3(BJ) level (*55*). Vibrational frequencies were calculated analytically (*56*) and revealed that all structures are true minima without any negative frequency.

Complete active space self-consistent field (CASSCF) and N-electron valence 2nd-order perturbation theory (NEVPT2; (*57*)) calculations were carried out at the DFT optimized geometries using all electron calculations using the X2C scalar relativistic Hamiltonian (The generic acronym "X2C" for exact two-component Hamiltonians resulted from intensive discussions among H. J. Aa. Jensen, W. Kutzelnigg, W. Liu, T. Saue and L. Visscher during the Twelfth International Conference on the Applications of Density Functional Theory DFT-2007, Amsterdam, 26-30 August 2007; (*58*)) as implemented into a development version of ORCA (unpublished work of G. Stoychev, C. Riplinger, F. Neese) and the X2C-TZVPPall basis set (*59, 60*). Spin-orbit coupling (SOC) was treated using the mean-field SOC Hamiltonian (*61, 62*) including picture change effects.

5.2. Computational details

The way that these calculations are performed is well-documented in the literature (*61*, *63-67*). However, in order for this paper to be self-contained, we provide a description here. We have initially experimented with the active space and landed on a choice that matches widely followed recommendation for CASSCF calculations. Hence, the active space includes the three Bismuth 6p orbitals as well as the σ-bonding orbital formed between the Bismuth-center and the central aryl ring (as shown in Figure 5 of the paper). After initial tests, the orbital optimization proceeded by averaging over six singlet and five triplet states. This covers the non-relativistic spectrum up to about 50,000 cm^{-1} which was deemed appropriate to cover all important SOC effects in the subsequent quasi-degenerate perturbation (QDPT) calculation. In this step, the following matrix is diagonalized:

$$\langle \Psi_I^{SM}|H_{BO}+H_{SOC}|\Psi_J^{S'M'}\rangle = \delta_{IJ}\delta_{SS'}\delta_{MM'}E_I + \sum_{m=0,\pm1}(-1)^m \begin{pmatrix} S & 1 & S' \\ M & m & M' \end{pmatrix} \langle \Psi_I^{SS}||\sum_i h_m^{SOC}(\boldsymbol{r}_i)\hat{s}_{i;-m}||\Psi_J^{S'S'}\rangle \tag{1}$$

In this equation $|\Psi_I^{SM}\rangle$ is a CASSCF state with total spin S and spin-projection quantum number M:

$$|\Psi_I^{SM}\rangle = \sum_K C_{KI}|\Phi_K^{SM}\rangle \tag{2}$$

In the calculations based directly on CASSCF E_I would be the CASSCF energy of state I (with spin S). However, since we are basing our calculation on NEVPT2, this energy contains the NEVPT2 correction calculated for the scalar relativistic CASSCF states.

In eq(2) C_{KI} are the CASSCF expansion coefficients and $|\Phi_K^{SM}\rangle$ are the configuration state functions that are constructed by distributing the active electrons over all active orbitals and spin coupling them to a given total spin S. Of course, all inactive orbitals remain doubly occupied in each reference CSF. In practice, it is only necessary to treat the principle component M=S in the CASSCF step, while all magnetic sublevels M=S,S-1,…,-S must be treated in the subsequent QDPT step. This is accomplished in eq (1) by using the Wigner Eckart theorem. Here, $\begin{pmatrix} S & 1 & S' \\ M & m & M' \end{pmatrix}$ is a Clebsch-Gordon coupling coefficient and $\langle \Psi_I^{SS}||\sum_i h_m^{SOC}(\boldsymbol{r}_i)\hat{s}_{i;-m}||\Psi_J^{S'S'}\rangle$ is a reduced matrix element. The summation m= $0,\pm1$ is over the components of the standard vector operator components of the reduced SOC operator $h_m^{SOC}(\boldsymbol{r}_i)$ and the spin-operator $\hat{\boldsymbol{s}}_i$ for the i'th electron ($\boldsymbol{r}_i$ is the position operator for the I'th electron). Explicit expressions for the reduced matrix elements over the principle components of any scalar-relativistic or non-relativistic many particle wavefunction of a given total spin are given in reference 63. For the SOC operator, we use the widely used and widely successful spin-orbit mean field (SOMF) operator (*61*). In the extension developed in reference 62 it can be written as:

$$\langle p|\hat{H}_{SOMF}|q\rangle = \frac{1}{2}\alpha^2\sum_i \hat{\boldsymbol{s}}_i\left\{\sum_A Z_A\langle p|r_A^{-3}\boldsymbol{l}_i^{(A)}|q\rangle - \sum_{rs}P_{rs}\left[\left(pq|r_{ij}^{-3}(\boldsymbol{l}_1^{(2)}+2\boldsymbol{l}_2^{(1)})|rs\right)-\left(pr|r_{ij}^{-3}(\boldsymbol{l}_1^{(2)}+2\boldsymbol{l}_2^{(1)})|qs\right)\right]\right\} \tag{3}$$

Here p,q are arbitrary basis functions or molecular orbitals, α is the fine-structure constant, Z_A the nuclear charge, r_A^{-3} is the inverse third power of the distance of an electron from nucleus A, $\boldsymbol{l}_i^{(A)}$ the angular momentum w.r.t nucleus A, $\boldsymbol{l}_i^{(j)}$ the angular momentum of electron i relative to electron j. P_{rs} is an electron density, in our case, the scalar relativistic, state average CASSCF density. In the actual calculations, the one-electron part (first term of the right-hand side of equation (3), first line) is subjected to a picture change transformation in the X2C framework. Equation (3) has been evaluated in a way where the one-electron terms have been calculated exactly as written, for the two-electron Coulomb term (first term, second row of equation (3), the density fitting approximation has been used as described in reference 62 and the exchange term (second term, second line of equation (3)) has been approximated using only one-center terms. This is a widely tested approximation that delivers sufficiently accurate results. In particular for heavy elements, it is well-known that the one-electron contribution to the SOC dominates and consequently, the additional approximation on the two-electron part of the SOMF operator are of very limited consequence for the accuracy of the results.

Finally, we remark that the Zero-Field splitting (ZFS) itself was calculated using the formalism in reference 64, but no special treatment is necessary here since for an axial triplet state, the D-parameter follows directly from the splitting of the M=0 and M=+/-1 magnetic sublevels. No calculated D-value was used anywhere in the manuscript.

Since the methodology we use was called into question by a referee to this paper, we document the results that we obtain for all group fifteen elements including the mono-positive ion of Bismuth. Experimental data were taken from the NIST tables (https://physics.nist.gov/PhysRefData/ASD/levels_form.html; access date, March 5th, 2023). The results of the CASSCF-NEVPT2-X2C calculations in Tables S20-S25 demonstrate that the chosen methodology faithfully reproduces the level structure of all group fifteen elements including Bismuth. The quantitative accuracy varies from a few hundred wavenumbers to about 2000-2500 cm^{-1}. Interestingly, the accuracy obtained for Bismuth is not lower than what is observed for the lighter elements. We conclude from this data that our results reported in the main body of the paper are not compromised by an insufficient treatment of relativity. Rather, the errors are uniform and reflect the intrinsic accuracy of the CASSCF/NEVPT2 methodology in conjunction with minimal active spaces. Nevertheless, we believe that the achieved accuracy is high enough in order to draw the conclusions that we have drawn in the main body of the paper.

While we have no interested in re-litigating the century old debate of LS vs jj coupling, we will add a few remarks here: It appears to be conventional wisdom that a jj coupling approach, in which the orbitals become complex valued, is preferred for very heavy elements such as bismuth. We do not disagree with that notion but it is our contention that LS type approaches, such as used here, are still useful. Hence, jj coupling might be *preferred* (on numerical grounds), but it is not *strictly required*. In fact, we do strongly argue, that the results delivered by our approach are accurate enough for the purpose at hand. It is undisputable that the LS-based approach taken here misses certain SOC effects, in particular the different radial shapes of the $p_{1/2}$ and $p_{3/2}$ orbitals. However, as borne out by our results (including the atomic ones collected below), this effect is not large enough in order to compromise the results of this study. Our preference for LS over jj approaches stems from the fact that, in our opinion, the results are much more amenable to chemical interpretation in terms of orbitals, states and configurations – a language that is far more accessible to chemists than complex valued spinors and many particle wavefunctions built from them. In addition to these considerations, we are not aware of a correlated, multiconfigurational two- or four-component program that would have enabled us to study a system of the size that we have studied here (122 atoms, 2500+ basis functions) while such calculations are readily doable using our approach.

Table S20 Results for N(I)

Configuration	Term	J	Energy (NIST) /cm^{-1}	Energy (calc) /cm^{-1}
$2p^3$	^4S	3/2	0	0
$2p^3$	^2D	5/2	19224	20902
		3/2	19233	20907
$2p^3$	^2P	1/2	28838	31201
		3/2	28839	31203

Table S21 Results for P(I)

Configuration	Term	J	Energy (NIST) /cm^{-1}	Energy (calc) /cm^{-1}
$3p^3$	^4S	3/2	0	0
$3p^3$	^2D	5/2	11361	13444
		3/2	11376	13479
$3p^3$	^2P	1/2	18722	21932
		3/2	18748	21932

Table S22 Results for As(I)

Configuration	Term	J	Energy (NIST) /cm^{-1}	Energy (calc) /cm^{-1}
$4p^3$	^4S	3/2	0	0
$4p^3$	^2D	5/2	10592	12626
		3/2	10914	12868
$4p^3$	^2P	1/2	18186	21297
		3/2	18647	21565

Table S23 Results for Sb(I)

Configuration	Term	J	Energy (NIST) /cm^{-1}	Energy (calc) /cm^{-1}
$5p^3$	^4S	3/2	0	0
$5p^3$	^2D	5/2	8512	10973
		3/2	9854	11910
$5p^3$	^2P	1/2	16395	20666
		3/2	18464	21894

Table S24 Results for Bi(I)

Configuration	Term	J	Energy (NIST) /cm^{-1}	Energy (calc) /cm^{-1}
$6p^3$	^4S	3/2	0	0
$6p^3$	^2D	3/2	11419	11295
		5/2	15437	15338
$6p^3$	^2P	1/2	21660	24157
		3/2	33164	32341

Table S25 Results for Bi(II)

Configuration	Term	J	Energy (NIST) /cm^{-1}	Energy (calc) /cm^{-1}
$6p^2$	(1/2,1/2)	0	0	0
$6p^2$	(3/2,1/2)	1	13325	10898
		2	17031	15098
$6p^2$	(3/2,3/2)	2	33938	29875

An ORCA input file for the Bi-mono cation is shown below. The exact same keywords have been used to generate the results of the target complex **2** in the paper.

```
# Bi mono cation
! X2C-TZVPPall RIJCOSX SARC/J X2C TightSCF
%maxcore 12000
%rel    picturechange true
        end
%basis  AuxC = "SARC/J"
        end
%casscf nel    4
        norb   4
        mult   5,3,1
        nroots 1,15,20
        trafostep RI
        PTMethod  SC_NEVPT2
        Rel       DoSOC true end
        end
* xyz 1 3
Bi 0 0 0
*
```

5.3. Methods for X-ray absorption calculations

The X-ray absorption calculations were done following standard protocols using the B3LYP functional, the scalar relativistic ZORA approximation and the corresponding SARC basis sets. The calculations are based on time-dependent density functional theory by allowing only excitations out of the core orbitals into all virtual orbitals. Since we are doing K-edge calculations here, SOC effects are very limited and they have, in fact, been neglected. This will compromise the absolute accuracy of the results to some extent but for the qualitative considerations that we have used these calculations for, the results are, in our opinion, sufficient.

An ORCA input file is replicated below

```
# XAS calculations
! B3LYP D3BJ ZORA-def2-TZVP SARC/J ZORA TightSCF
%maxcore 64000
%pal    nprocs 4
        end
%basis  newgto bi "SARC-ZORA-TZVP" end
        end
%geom   optimizehydrogens true
        end
%tddft  orbwin[0] = 1,1,-1,-1
        orbwin[1] = 1,1,-1,-1
        doquad true
        nroots 100
        maxdim 10
        end
* xyzfile 0 3 BiL.xyz
```

5.4. Computational insights into the interaction between the Bi(I) center and the ligand in **2**

We finally addressed the interaction of the bismuth center with the supporting ligand framework and specifically whether there is a sizable interaction between the bismuth and the fluorenyl groups. We thank one of the referees for this insightful comment. The three main active orbitals shown in Figure 5 of the original manuscript have 42.6%, 87.6% and 82.5% bismuth character (Löwdin analysis; see Table S26) The first active orbital therefore represents a very covalent sigma-bond between the bismuth and aryl group, whereas the remaining two (singly occupied) orbitals represent bismuth 6p lone-pair orbitals.

We have provided a breakdown of the scalar relativistic CASSCF active molecular orbitals in Table S26.

Table S26 Composition of the active molecular orbitals from the CASSCF calculations reported in this study (Fragment 1: the bismuth center, Fragment 2: the Central Ring, Fragment 3: the "left hand side Fluorenyl, Fragment 4: the "Right hand side", Fragment 5: all remaining substituent atoms).

	Bismuth	**Aryl**	**Fluorenyl-1**	**Fluorenyl-2**	**Rest**
MO #240(σ-bond)	42.6	55.3	0.8	0.7	0.7
MO #241(6p-SOMO)	87.6	7.3	2.2	2.3	0.6
MO #242(6p-SOMO)	82.5	3.9	7.0	6.3	0.3

Based on this data, the single bond between the bismuth and the aryl ring is readily apparent.

Furthermore, we have looked at the fragment-based Löwdin bond-order analysis in Table S27.

Table S27 Fragment based Löwdin bond orders based on the CASSCF calculations reported in this study.

	Bismuth	**Aryl**	**Fluorenyl-1**	**Fluorenyl-2**	**Rest**
Bismuth	-	1.05	0.20	0.19	0.01
Aryl		-	1.74	1.74	4.17
Fluorenyl-1			-	0.00	5.87
Fluorenyl-2				-	5.86
Rest					-

Based on this analysis and the fluorenyl character in the two SOMOs is, there is a sizeable interaction between the fluorenyl group and the central bismuth. This points to a role of these ligand in stabilizing the unusual bonding situation.

Below we present the AIM analysis that a referee to this paper has suggested. Results for B3LYP, CASSCF, CASSCF/NEVPT2 and CASSCF/NEVPT2 with SOC have been obtained. Interestingly, all calculations find bond critical points between the bismuth center and the fluorenyl groups in addition to the obvious bond critical point present between the bismuth center and the aryl ring. This supports the notion of a sizeable interaction between the bismuth center and the supporting ligand framework and also borne out by the orbital analysis. Since all plots looks similar, we only show the results for the highest level of theory used here: the relativistic density obtained from the CASSCF/NEVPT2-X2C + SOC(QDPT) calculations (Fig. S57).

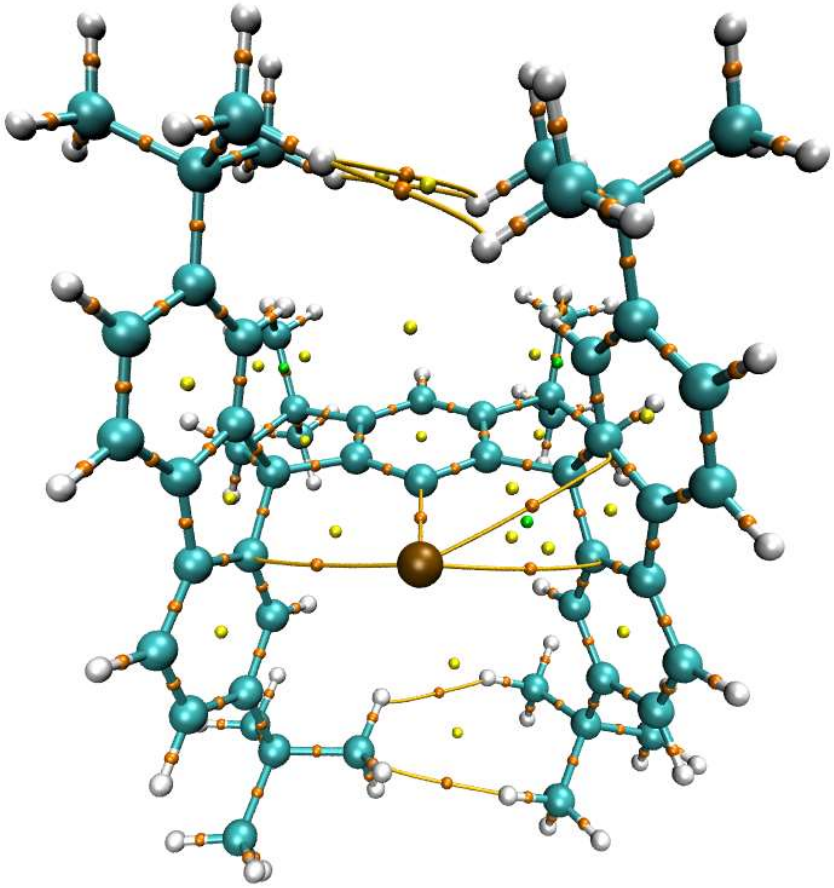

Fig. S57 AIM Analysis of the ground state relativistic density obtained from the CASSCF/NEVPT2-X2C + SOC(QDPT) calculations. Bond critical points are shown in orange, ring critical points in yellow and cage critical points in green.

5.5. Coordinates of the optimized structures of **2**

5.5.1. Coordinates of the optimized closed-shell singlet structure of **2**

Bi	-0.75360726935105	-1.01552426704245	6.99578083012492
C	0.95376274366395	0.17815291862639	7.84074549225544
C	0.70520689156255	1.49570854925905	8.21647781990667
C	2.27390164038375	-0.25395981149246	7.97526517931319
C	1.34731111451737	-3.53685295533050	7.23297069942642
C	1.71762062875525	2.37811274225337	8.58412788597873
C	3.02525313885205	1.92171440092984	8.72576011664455
H	3.81896554927687	2.58720639688612	9.04512938986059
C	0.41366285108798	-4.52015807971076	7.56240105234258
H	-0.00082720698356	-5.16959071055727	6.80110953691159
C	-0.65595098543306	2.13526128438471	8.30888786916588
C	-1.45100271950515	1.77335879763401	9.56665162886760
C	1.91697541022976	-3.10592618539781	5.95029407618568
C	-3.82114743128607	1.33247775969003	5.57140021645364
H	-4.68282713437663	1.17491947336512	4.93951222680744
C	1.85827544072180	-2.70970297192723	8.24436451537008
C	-2.80078015464414	1.56694008935148	9.24933288860141
C	-1.65560587058982	1.75104220115113	7.23333200754292
C	-2.94607217219330	1.57108507319675	7.79484710919961
C	-2.56489528079264	1.46646589678837	4.99532384737299
C	3.28333107027840	0.57934258813475	8.44829868672157
C	1.95857840418281	4.76576303587414	7.83880559654883
H	1.95216343636222	4.41623922494623	6.80499303664909
H	2.99930167467378	4.86019611736726	8.15610012702614
H	1.50692130086861	5.76073409324392	7.86950159115317
C	-4.02607962451463	1.38192680076460	6.96115421371539
H	-5.02379552983437	1.24915196714806	7.36028048176121
C	1.19089079920688	3.79602605571518	8.74775779062241
C	-3.25635670800982	1.17822310677746	11.56596408127511
H	-3.97217018082966	0.95112018640179	12.34475875242561
C	2.78474068922197	-1.65046497963021	7.66755905127033
C	1.43873241202380	-2.84429981559194	9.55660162328792
H	1.81980505631170	-2.15795985989969	10.29871421724500
C	0.00528224806283	-4.64576333840637	8.88302744713164
H	-0.73779096639027	-5.39439343458950	9.12271539731511
C	-1.45951205586703	1.67518803462079	5.85655603482533
H	-0.47312959980707	1.85584522826349	5.45147410704707
C	-0.28708434838667	3.65903420839220	8.26831046859315
H	-0.36082986829134	3.99557368580287	7.23342794089729
H	-0.97684199499614	4.25836116266936	8.86187233686673
C	2.28119305559283	-2.86404461164765	3.59924471863540
H	2.10219327273887	-3.21473764600035	2.59128447694181
C	2.72549722443657	-1.98496546280124	6.17732664395862
C	3.05069031802002	-1.71001321848666	3.80172607508265
C	4.60610199330198	-0.15353316478979	8.58723627691619
C	3.27008322324452	-1.28687198794499	5.11548227711461
H	3.83556225280651	-0.38883154791475	5.30915020344618
C	-1.00270003467434	1.62596948235900	10.86547651387224
H	0.05329232427412	1.71199025675492	11.06850269604949

C	-3.71159841144947	1.28401444755764	10.25881231296282
H	-4.75802292150863	1.11779956812363	10.03367466169219
C	1.70971969985839	-3.56050062207396	4.65416045496111
H	1.08635778713023	-4.42475036407918	4.46008117340232
C	5.65036626096680	0.37954313109814	7.59560301828235
H	5.31226526470461	0.27696978314862	6.56518459777929
H	6.59173362335787	-0.16588109096711	7.69893222197220
H	5.85039279057114	1.43749013857708	7.77713705057612
C	4.21809809974682	-1.63408874862490	8.28241722324348
C	-1.90132816326360	1.32245379010730	11.89332645492630
C	0.49428391318567	-3.81191210592285	9.90032553518296
C	-2.32790157102308	1.42541473857471	3.48383799284959
C	1.28927867250100	4.29703053538457	10.19587309989327
H	2.32578184302649	4.27552012618346	10.53881304496801
H	0.69537942775267	3.68935940681400	10.87511652296808
H	0.93216438539381	5.32740731031120	10.26814081950680
C	-1.29826427996769	0.33279341472704	3.14577477281440
H	-0.35058074205269	0.49157975266017	3.65832515689762
H	-1.10628249408959	0.32079883866470	2.07041284833899
H	-1.65880702394665	-0.65259145304698	3.44379058363446
C	-3.61236407814514	1.13574131745743	2.70034090047772
H	-4.03972611339498	0.16935894283360	2.97411236698278
H	-3.38848437357724	1.10943552528109	1.63252610496121
H	-4.37004872070442	1.90540493809176	2.85961721250159
C	5.16210544095911	-0.02477877344082	10.01190941793658
H	5.42559429777465	1.01011803924694	10.23983437476962
H	6.06166016624619	-0.63429291134434	10.12979478365464
H	4.42513404511249	-0.35398738995087	10.74664135729359
C	-1.78176503120392	2.79341246411925	3.02912040477601
H	-2.49198667269377	3.59071309946008	3.25695017396724
H	-1.60438228569770	2.78900282357034	1.95123257338660
H	-0.83822057157100	3.03234003906621	3.52137686364735
C	-0.07947746761832	-3.92210266919653	11.31445210229228
C	-1.45043611533534	1.15398045307105	13.34666288510907
C	3.59634572692601	-0.94388837922476	2.59393840344966
C	4.53344650407922	-1.85803577600172	1.78338953560251
H	5.38138187577554	-2.17940584661216	2.39128326021600
H	4.91949221594859	-1.32679550795392	0.91008336655226
H	4.01644153164918	-2.75129284889418	1.43175099145732
C	0.06681100963713	-5.36290483590502	11.83454120749560
H	-0.46225208884489	-6.07886302853433	11.20507313905867
H	-0.34260375297644	-5.44283274490286	12.84419458120098
H	1.11760373199045	-5.65756007119291	11.86797518117947
C	0.62736251009761	-2.98428761010891	12.30004345221996
H	1.69459059605405	-3.20359327266479	12.37204539266705
H	0.19408394526105	-3.10533205927839	13.29417061924332
H	0.51003565514261	-1.93793190041903	12.01541513918848
C	2.42166904886443	-0.49709524990713	1.70275475936814
H	1.84824407841787	-1.34784970907658	1.33363904427280
H	2.79349516233195	0.05863514908204	0.83851018568174
H	1.73965755726534	0.14759124540518	2.25894088277979
C	0.07487065986189	1.21795525973171	13.49175968455133
H	0.56935381759706	0.44543352287405	12.90042425187302
H	0.34893110178228	1.06421990137842	14.53698050879755

H	0.47199347472637	2.18748321344630	13.18651820436866
C	4.38102885802488	0.30818006675149	3.00321867508478
H	3.75632074461635	1.01249200985310	3.55562608062420
H	4.74502305133696	0.81821802330465	2.10944109951513
H	5.24766177662343	0.06261901221505	3.61988330194685
C	-1.57030281328277	-3.53414499678328	11.26484206561391
H	-1.69391784882449	-2.52179942956097	10.87606602794029
H	-2.00810939914374	-3.57748372260376	12.26517925801569
H	-2.13570102436174	-4.20806546295884	10.62002290733338
C	-2.06523675444032	2.28238936626059	14.19562462993444
H	-1.73523904473181	3.25892673477529	13.83609719738594
H	-1.76167651088325	2.18123354571928	15.24060533069836
H	-3.15502404451628	2.26193172975250	14.15685194553090
C	-1.92446679690573	-0.20804012298897	13.88633446774852
H	-3.01142178282407	-0.29019554889442	13.88327455840260
H	-1.58300806862606	-0.34515264007994	14.91511461586271
H	-1.52602720418155	-1.02327319074162	13.28221998322980
H	4.93703652576108	-2.11483404014099	7.61974685263178
H	4.20606626582369	-2.20412105019343	9.21147288993518

5.5.2. Coordinates of the optimized open-shell singlet structure of **2**

Bi	-0.85226768355033	-1.05275619553701	7.11365387150198
C	0.87101650803659	0.24567960066609	7.82477294346994
C	0.68009509635242	1.57432798395795	8.22391285052023
C	2.17812885239482	-0.25334087588326	7.91334183949264
C	1.51958416780074	-3.78163891193372	7.53979370583974
C	1.73803885304913	2.36932605546351	8.66819182580962
C	3.01746974661758	1.84295311363727	8.78452744946364
H	3.83596692477015	2.45041801675982	9.15311994595600
C	0.87255697453074	-4.88022778777568	8.09233921540382
H	0.51563483626134	-5.68957891731924	7.46707152492359
C	-0.63556867478873	2.33475285696038	8.30198775442705
C	-1.55943084693710	1.83541809640821	9.41325805436369
C	1.77816621650794	-3.39826450039629	6.14934050431502
C	-3.50254604825396	1.93258296351874	5.17013682468838
H	-4.27780321681895	1.80959434222628	4.42824017282727
C	1.96829646284590	-2.75050783191621	8.37644991140297
C	-2.85571877125315	1.63209996251008	8.92287605587079
C	-1.54667082340139	2.22077306748479	7.09110134461201
C	-2.85099462196500	1.86622839915534	7.47698034500607
C	-2.20590100948725	2.26559312878624	4.76962800578538
C	3.22515638903310	0.52030497199969	8.41451279098110
C	2.14337306980140	4.80145518030306	8.17425248212705
H	2.09461889089689	4.57777420281152	7.10711399663379
H	3.19282794978196	4.78112944864737	8.47548522979444
H	1.76937732415544	5.81647104917257	8.33033060156759
C	-3.83485646346895	1.73338137900029	6.50934603495217
H	-4.84775139628958	1.45933865047794	6.77790330707668
C	1.31521101586538	3.79178634737010	8.98152130349716
C	-3.54775600366484	0.97440547753354	11.11852735824259
H	-4.33567532111586	0.64065941474965	11.78089751296597
C	2.65041971570125	-1.65632211853033	7.56293515617993
C	1.73290455595445	-2.78723557344394	9.73843974651109
H	2.04118868655435	-1.94974012862099	10.34601745097744
C	0.65600656855226	-4.91420660621927	9.46343042144027
H	0.13744975971513	-5.76697465164257	9.88151930022220
C	-1.22999186424802	2.41971983053570	5.76384952013873
H	-0.20930719144399	2.66224459491373	5.49574904824854
C	-0.16859863272702	3.81305915051597	8.52264452199936
H	-0.24527652650908	4.34051923723558	7.57238973611810
H	-0.81470377709000	4.32816939064752	9.23247398336791
C	1.79852174342537	-3.37744420925876	3.75652554342836
H	1.57732041797219	-3.87928339190250	2.82395401514932
C	2.36469237621161	-2.12667021849050	6.14180645876768
C	2.37217277036919	-2.09797525583730	3.73076633403551
C	4.52392296828496	-0.25176978102087	8.52959702085658
C	2.65592287240145	-1.48190973838627	4.95320338174265
H	3.09219916789556	-0.49341927486786	4.98519108754093
C	-1.25638782135218	1.57743492383416	10.73780819636602
H	-0.23773751825468	1.68885858998914	11.07518865644901
C	-3.85726234196167	1.20146573201363	9.78437571021906
H	-4.86466645744552	1.03024616971211	9.42484557716448

C	1.49733085038506	-4.03020874089638	4.94439128988247
H	1.04373379675065	-5.01361641184219	4.92243001134081
C	5.68766264638755	0.47514127900059	7.84553735030298
H	5.45090317319462	0.68795042126884	6.80145560588871
H	6.59305269272890	-0.13616584281163	7.87403724749231
H	5.90949001395715	1.42254171361698	8.34138333149474
C	4.20005606099841	-1.58429696932101	7.80368850713877
C	-2.25089907589395	1.14834423705274	11.62160596507826
C	1.05909707564391	-3.87069593330996	10.30833892986663
C	-1.80449300837577	2.41931038072788	3.30119675960213
C	1.46381494953112	4.11219285569755	10.47622963473040
H	2.50419357716057	4.01060733398475	10.79178725328983
H	0.85980042731418	3.44748891488569	11.09159429050090
H	1.14763414318752	5.13843490223401	10.67834295046596
C	-0.74486236267913	1.35247753537307	2.96806478369054
H	0.14281522817127	1.46083865696335	3.59145312628180
H	-0.43669942398553	1.43419111509233	1.92324538300217
H	-1.14151014295729	0.34966139708032	3.13505400636247
C	-2.98846569766593	2.23577590858294	2.34585464613764
H	-3.42620765013618	1.23959690519621	2.43130329950058
H	-2.64872635190506	2.35958512872267	1.31593229653041
H	-3.77331490835147	2.97262536178703	2.52736633616460
C	4.87147221009634	-0.49093596896454	10.00763936304158
H	5.02255184025522	0.45538097125891	10.53115219491999
H	5.78897138626006	-1.07825588400954	10.09438052533903
H	4.07349893421660	-1.03237328298630	10.51650637531118
C	-1.20919662598571	3.82048314594615	3.07005267312658
H	-1.94046799339783	4.59563515554222	3.30704438406541
H	-0.91140113947793	3.93792787554176	2.02543648864781
H	-0.32826214249619	3.99056394171373	3.68946217341286
C	0.72992950025310	-3.93380610505631	11.80161824721639
C	-1.96839091777430	0.87346410896037	13.10164763619159
C	2.69716657570913	-1.44043035145591	2.38629942779882
C	3.82661032829970	-2.23537020247811	1.70356068124589
H	4.72614988206160	-2.23915899123727	2.32212019462861
H	4.07577132354065	-1.78880910003017	0.73773513037637
H	3.53437543401897	-3.27213638357722	1.53142653285434
C	1.44562587488657	-5.14086376674294	12.43465630916965
H	1.13628756172603	-6.07783348142141	11.97001829742991
H	1.21722656073282	-5.20256789846881	13.50150107353097
H	2.52772827249848	-5.05163802925941	12.32079481144652
C	1.16991704649707	-2.66613326182642	12.54313486602399
H	2.25114964804890	-2.52355166034546	12.49659200014521
H	0.88966820211276	-2.74032791080866	13.59521606291186
H	0.69018893956991	-1.77623970575477	12.13360878289151
C	1.45423500488874	-1.44766156159324	1.47824590312187
H	1.12072776404159	-2.46084267867448	1.25378735219448
H	1.68076917807938	-0.95585148321782	0.52934994635209
H	0.62630611780777	-0.91779772107439	1.94876832181259
C	-0.49722506432082	1.10676534611827	13.46609282728726
H	0.17071642884538	0.45453494906909	12.90160780544716
H	-0.34669943376213	0.89530424497864	14.52622388638176
H	-0.19589295415115	2.14081220391028	13.28865122086819
C	3.15875272842844	0.01296340532382	2.54885943620877

H	2.39872255464966	0.62244044734265	3.04013888315548
H	3.35200842421868	0.44682712075072	1.56608805235091
H	4.08201798867779	0.08359486625502	3.12624481643577
C	-0.79213049578925	-4.08852517264404	11.98059548008166
H	-1.32271831903324	-3.26124443843696	11.50649669619285
H	-1.05044786832026	-4.09982193567460	13.04206458742081
H	-1.15798007201493	-5.01531324909609	11.53830888612119
C	-2.83024789167497	1.81379162857058	13.96544442937862
H	-2.60104794431221	2.85828521029646	13.74582898626584
H	-2.63773347303468	1.63612587264260	15.02623799510175
H	-3.89497083374413	1.66024563795458	13.78723254905312
C	-2.32031686827052	-0.58805834585729	13.43229777995109
H	-3.37283860123779	-0.80147086008092	13.24419743332020
H	-2.11836741711009	-0.79758105570525	14.48551527980492
H	-1.72710783929856	-1.27455054360585	12.82856118917684
H	4.70292023192195	-1.60564992896441	6.83819231918472
H	4.54709506969054	-2.45017068222845	8.36612307041514

5.5.3. Coordinates of the optimized triplet structure of **2**

Bi	-0.86468034805969	-1.06810925161918	7.14002189034142
C	0.86319578503890	0.24786509923446	7.82687523403225
C	0.67204419735460	1.58004017968308	8.21709168679167
C	2.16932531661724	-0.25469342430715	7.91736057611346
C	1.58185751477825	-3.81715974369430	7.60175318055309
C	1.73034928373219	2.37019766070597	8.67115033041754
C	3.00854610121645	1.84207575854707	8.78679163848699
H	3.82650399432634	2.44827971128405	9.15878942547738
C	0.98242750586246	-4.92859537738683	8.18046591015217
H	0.64684861994465	-5.76038078438283	7.57302958043595
C	-0.63971838652618	2.35097867352520	8.28386475189610
C	-1.58549853376469	1.84682507362729	9.37304459054012
C	1.80172530707470	-3.44579529114781	6.20253261820407
C	-3.47869751729725	2.07488383020440	5.11357755500393
H	-4.24883016425754	1.98562994544933	4.36162530564990
C	2.00342052021201	-2.75681636692753	8.41538755183895
C	-2.88111354259373	1.68754303299457	8.86441222043606
C	-1.53768352667509	2.27802291468090	7.05964973843511
C	-2.85510914615802	1.95637382092525	7.42530984685583
C	-2.16838883239784	2.37538025339171	4.73295929617343
C	3.21806905073647	0.52160056505669	8.41283409814276
C	2.15217533937898	4.81114456335383	8.22732548605977
H	2.11439590501223	4.60995166876916	7.15526396673516
H	3.19817636849776	4.78136975595671	8.53974244847018
H	1.78002986206563	5.82408263234694	8.40012895778413
C	-3.83152692043500	1.86697895217796	6.44626307794887
H	-4.85465733090184	1.61756537104245	6.69983034322954
C	1.31151078369607	3.78861963139914	9.00443900176689
C	-3.60953805590289	0.99178322842388	11.03706772050664
H	-4.41125980780555	0.65824496390504	11.68287969601150
C	2.64623492171401	-1.65923411797255	7.57420572906298
C	1.78643320337186	-2.77914562235091	9.78047223735069
H	2.07157357806581	-1.92158267089188	10.37100631412756
C	0.78554517595222	-4.94874009646642	9.55510429715061
H	0.30535919948585	-5.81365923839285	9.99369637283973
C	-1.19979245507190	2.48868486329570	5.74045419981426
H	-0.16985166175744	2.70731990354676	5.48708484861961
C	-0.16611715269730	3.82418927047781	8.53232351515375
H	-0.23101781013184	4.36616834794275	7.58959831331989
H	-0.81718287202694	4.33148527532808	9.24321495440587
C	1.77444533208903	-3.45640707528432	3.80920235811193
H	1.54908590232714	-3.97682584260985	2.88766321691526
C	2.34485361481601	-2.15562165043840	6.16604147878365
C	2.31057064817233	-2.16160285936928	3.75507930566578
C	4.52169854712045	-0.24317531393690	8.51767965927059
C	2.59586460839626	-1.51927572238907	4.96359607179886
H	3.00383674721534	-0.51831794785469	4.97459011257672
C	-1.30172558828031	1.55224544954247	10.69437274086859
H	-0.28419365873698	1.63498681637979	11.04348108532061
C	-3.90045673403098	1.25837774561831	9.70592946991251
H	-4.90789788938853	1.11885843854065	9.33304339820217

C	1.51660468059796	-4.10177855714070	5.01136577254982
H	1.09354243668337	-5.09896101328517	5.01105759331346
C	5.67782587549229	0.49537169470458	7.83305817993308
H	5.43329411474279	0.71811840713879	6.79285725570374
H	6.58540333075993	-0.11310124044713	7.84908624253116
H	5.90021088728271	1.43828238192755	8.33720790060647
C	4.20053164815953	-1.56980088658490	7.78241077071946
C	-2.31487375671648	1.12584864042355	11.55800534426860
C	1.16080585696935	-3.87749407520878	10.37731266662375
C	-1.74634681301397	2.53710058369809	3.27111088316810
C	1.44456676669042	4.07669326311465	10.50746263736629
H	2.48053502535731	3.96270441433738	10.83315037083337
H	0.82927693318179	3.40240547250584	11.10094369288761
H	1.13106505183905	5.10009540115820	10.72729082928245
C	-0.72299455126461	1.43714192086618	2.93309834366195
H	0.15844355346129	1.50118523338674	3.57129921739693
H	-0.39554519675653	1.52309549771787	1.89445904333726
H	-1.16109177684679	0.44783166639027	3.07586531814453
C	-2.92557332832784	2.41023215330999	2.30084081702975
H	-3.40044267247829	1.42982510478961	2.36817187268006
H	-2.57041185052113	2.53529331639689	1.27626708519209
H	-3.68489059735260	3.17271655390328	2.48487863577748
C	4.87938836097825	-0.49040369682225	9.99198766967494
H	5.02467431073476	0.45352672686633	10.52151841444022
H	5.80312305473783	-1.06917655168140	10.06895557734227
H	4.09036652850526	-1.04350506532697	10.50159084983577
C	-1.09826498945129	3.91877790231651	3.06595485220919
H	-1.80406585983875	4.71635656235667	3.30562051585097
H	-0.78461318497688	4.03958289859366	2.02636989672784
H	-0.21912015908883	4.04864516687557	3.69734019707843
C	0.85635252061033	-3.92891375945829	11.87643584358034
C	-2.05367672816631	0.80569272980174	13.03268735577713
C	2.58860677053423	-1.51381001932431	2.39556247367337
C	3.68868161422868	-2.31573481356189	1.67450813748353
H	4.60969283397154	-2.32219562475398	2.26059737120537
H	3.90537042814875	-1.87187385043577	0.69966386285176
H	3.38692161625802	-3.35147082509506	1.51394203426941
C	1.62858483165466	-5.09609876196895	12.51791528604253
H	1.35046151764804	-6.05214149485834	12.07287333473654
H	1.41820694074025	-5.14913439476123	13.58894833389029
H	2.70449561064969	-4.96587776781755	12.38635872852438
C	1.25624608089592	-2.63292976322316	12.59127474755287
H	2.33071862417951	-2.45058352620595	12.52959114442055
H	0.99102608855312	-2.69942677055738	13.64778064485362
H	0.73894233663765	-1.76864675113843	12.17288214694612
C	1.31023816600908	-1.52323597531770	1.53804263906755
H	0.96293828233709	-2.53760901704456	1.34125345804125
H	1.50016591334000	-1.04351706247043	0.57498991073516
H	0.50542220037432	-0.98304489445184	2.03621008294778
C	-0.58735755340894	1.02542689190004	13.42398419835225
H	0.08721781589202	0.38696460265260	12.85214149802775
H	-0.45154725186801	0.78568199884173	14.48009611881317
H	-0.28241954231336	2.06324537398813	13.27716147783940
C	3.06266501340343	-0.06186371080664	2.53133415609453

H	2.32146440451804	0.55725998658938	3.03861400356100
H	3.22935468600532	0.36225938901068	1.53952119030877
H	4.00267667308328	0.00709526444964	3.08143996110561
C	-0.65537152546196	-4.14113546429160	12.08141504219182
H	-1.22545847624902	-3.34495749917093	11.60011469821443
H	-0.89833345753406	-4.14183121810871	13.14656671508823
H	-0.98989188295068	-5.08999660330074	11.66180915718872
C	-2.92484787557698	1.71954619771552	13.91515112674694
H	-2.69370954947337	2.77015916045754	13.72939962787486
H	-2.74273638659620	1.51018147654937	14.97196288044069
H	-3.98775722268491	1.57149244259290	13.72257043368849
C	-2.41346345993416	-0.66515094247082	13.30936212527049
H	-3.46347241079239	-0.86795593959446	13.09679071964693
H	-2.22859536405198	-0.91213901360231	14.35764813994447
H	-1.81267376571950	-1.33252330740115	12.69154198219012
H	4.68210373560532	-1.57084276113960	6.80572664525072
H	4.57106006858962	-2.43872885843304	8.32466271562879

References and Notes

1. R. A. Moss, M. S. Platz, M. Jones Jr., Eds., *Reactive Intermediate Chemistry* (Wiley, 2004).

2. J. Stöhr, H. C. Siegmann, Eds., *Magnetism: From Fundamentals to Nanoscale Dynamics* (Springer, 2006).

3. E. König, G. König, Eds., *Magnetic Properties of Coordination and Organometallic Transition-Metal Compounds* (Springer, 1981).

4. M. Gomberg, Triphenylmethyl, ein Fall von dreiwerthigem Kohlenstoff. *Ber. Dtsch. Chem. Ges.* **33**, 3150–3163 (1900). doi:10.1002/cber.19000330369

5. M. Gomberg, An instance of trivalent carbon: Triphenylmethyl. *J. Am. Chem. Soc.* **22**, 757–771 (1900). doi:10.1021/ja02049a006

6. P. P. Power, Persistent and stable radicals of the heavier main group elements and related species. *Chem. Rev.* **103**, 789–810 (2003). doi:10.1021/cr020406p Medline

7. R. G. Hicks, Ed., *Stable Radicals: Fundamentals and Applied Aspects of Odd-Electron Compounds* (Wiley, 2010).

8. M. Abe, Diradicals. *Chem. Rev.* **113**, 7011–7088 (2013). doi:10.1021/cr400056a Medline

9. K. Hirai, T. Itoh, H. Tomioka, Persistent triplet carbenes. *Chem. Rev.* **109**, 3275–3332 (2009). doi:10.1021/cr800518t Medline

10. C. Wentrup, Carbenes and nitrenes: Recent developments in fundamental chemistry. *Angew. Chem. Int. Ed.* **57**, 11508–11521 (2018). doi:10.1002/anie.201804863 Medline

11. L. Dostál, Quest for stable or masked pnictinidenes: Emerging and exciting class of group 15 compounds. *Coord. Chem. Rev.* **353**, 142–158 (2017). doi:10.1016/j.ccr.2017.10.009

12. H. Tomioka, E. Iwamoto, H. Itakura, K. Hirai, Generation and characterization of a fairly stable triplet carbene. *Nature* **412**, 626–628 (2001). doi:10.1038/35088038 Medline

13. E. Iwamoto, K. Hirai, H. Tomioka, A triplet carbene surviving a week in solution at room temperature. *J. Am. Chem. Soc.* **125**, 14664–14665 (2003). doi:10.1021/ja038423z Medline

14. F. Dielmann, O. Back, M. Henry-Ellinger, P. Jerabek, G. Frenking, G. Bertrand, A crystalline singlet phosphinonitrene: A nitrogen atom-transfer agent. *Science* **337**, 1526–1528 (2012). doi:10.1126/science.1226022 Medline

15. L. Liu, D. A. Ruiz, D. Munz, G. Bertrand, A singlet phosphinidene stable at room temperature. *Chem* **1**, 147–153 (2016). doi:10.1016/j.chempr.2016.04.001

16. J. Sun, J. Abbenseth, H. Verplancke, M. Diefenbach, B. de Bruin, D. Hunger, C. Würtele, J. van Slageren, M. C. Holthausen, S. Schneider, A platinum(II) metallonitrene with a triplet ground state. *Nat. Chem.* **12**, 1054–1059 (2020). doi:10.1038/s41557-020-0522-4 Medline

17. H. W. Moon, J. Cornella, Bismuth redox catalysis: An emerging main-group platform for organic synthesis. *ACS Catal.* **12**, 1382–1393 (2022). doi:10.1021/acscatal.1c04897 Medline

18. A. Heimer, E. Hulthén, Band spectrum of bismuth hydride. *Nature* **127**, 557 (1931). doi:10.1038/127557a0

19. G. Herzberg, *Molecular Spectra and Molecular Structure, I. Spectra of Diatomic Molecules* (Van Nostrand, 1950).

20. D. P. Mukhopadhyay, D. Schleier, S. Wirsing, J. Ramler, D. Kaiser, E. Reusch, P. Hemberger, T. Preitschopf, I. Krummenacher, B. Engels, I. Fischer, C. Lichtenberg, Methylbismuth: An organometallic bismuthinidene biradical. *Chem. Sci.* **11**, 7562–7568 (2020). doi:10.1039/D0SC02410D Medline

21. N. Tokitoh, Y. Arai, R. Okazaki, S. Nagase, Synthesis and characterization of a stable dibismuthene: Evidence for a Bi-Bi double bond. *Science* **277**, 78–80 (1997). doi:10.1126/science.277.5322.78

22. B. Twamley, C. D. Sofield, M. M. Olmstead, P. P. Power, Homologous series of heavier element dipnictenes 2,6-$Ar_2H_3C_6E{=}EC_6H_3$-2,6-Ar_2 (E = P, As, Sb, Bi; Ar = Mes = C_6H_2-2,4,6-Me_3; or Trip = C_6H_2-2,4,6-$^iPr_3$) stabilized by *m*-terphenyl ligands. *J. Am. Chem. Soc.* **121**, 3357–3367 (1999). doi:10.1021/ja983999n

23. H. J. Breunig, R. Rösler, E. Lork, The first organobismuth rings: $(RBi)_3$ and $(RBi)_4$, R=$(Me_3Si)_2CH$. *Angew. Chem. Int. Ed.* **37**, 3175–3177 (1998). doi:10.1002/(SICI)1521-3773(19981204)37:22<3175:AID-ANIE3175>3.0.CO;2-M Medline

24. P. Šimon, F. de Proft, R. Jambor, A. Růzicka, L. Dostál, Monomeric organoantimony(I) and organobismuth(I) compounds stabilized by an NCN chelating ligand: Syntheses and structures. *Angew. Chem. Int. Ed.* **49**, 5468–5471 (2010). doi:10.1002/anie.201002209 Medline

25. G. Wang, L. A. Freeman, D. A. Dickie, R. Mokrai, Z. Benkő, R. J. Gilliard Jr., Isolation of cyclic(alkyl)(amino) carbene-bismuthinidene mediated by a beryllium(0) complex. *Chem. Eur. J.* **25**, 4335–4339 (2019). doi:10.1002/chem.201900458 Medline

26. M. M. Siddiqui, S. K. Sarkar, M. Nazish, M. Morganti, C. Köhler, J. Cai, L. Zhao, R. Herbst-Irmer, D. Stalke, G. Frenking, H. W. Roesky, Donor-stabilized antimony(I) and bismuth(I) ions: Heavier valence isoelectronic analogues of carbones. *J. Am. Chem. Soc.* **143**, 1301–1306 (2021). doi:10.1021/jacs.0c12084 Medline

27. T. Matsuo, K. Suzuki, T. Fukawa, B. Li, M. Ito, Y. Shoji, T. Otani, L. Li, M. Kobayashi, M. Hachiya, Y. Tahara, D. Hashizume, T. Fukunaga, A. Fukazawa, Y. Li, H. Tsuji, K. Tamao, Synthesis and structures of a series of bulky "Rind-Br" based on a rigid fused-ring *s*-hydrindacene skeleton. *Bull. Chem. Soc. Jpn.* **84**, 1178–1191 (2011). doi:10.1246/bcsj.20110090

28. M. Mantina, A. C. Chamberlin, R. Valero, C. J. Cramer, D. G. Truhlar, Consistent van der Waals radii for the whole main group. *J. Phys. Chem. A* **113**, 5806–5812 (2009). doi:10.1021/jp8111556 Medline

29. P. Pyykkö, M. Atsumi, Molecular single-bond covalent radii for elements 1–118. *Chem. Eur. J.* **15**, 186–197 (2009). doi:10.1002/chem.200800987 Medline

30. I. Vránová, M. Alonso, R. Lo, R. Sedlák, R. Jambor, A. Růžička, F. De Proft, P. Hobza, L. Dostál, From dibismuthenes to three- and two-coordinated bismuthinidenes by fine

ligand tuning: Evidence for aromatic BiC_3N rings through a combined experimental and theoretical study. *Chem. Eur. J.* **21**, 16917–16928 (2015). doi:10.1002/chem.201502724 Medline

31. Y. Pang, M. Leutzsch, N. Nöthling, J. Cornella, Catalytic activation of N_2O at a low-valent bismuth redox platform. *J. Am. Chem. Soc.* **142**, 19473–19479 (2020). doi:10.1021/jacs.0c10092 Medline

32. Y. Pang, M. Leutzsch, N. Nöthling, F. Katzenburg, J. Cornella, Catalytic hydrodefluorination via oxidative addition, ligand metathesis, and reductive elimination at Bi(I)/Bi(III) centers. *J. Am. Chem. Soc.* **143**, 12487–12493 (2021). doi:10.1021/jacs.1c06735 Medline

33. J. D. Queen, A. Lehmann, J. C. Fettinger, H. M. Tuononen, P. P. Power, The monomeric alanediyl :$AlAr^{iPr8}$ (Ar^{iPr8} = C_6H-2,6-(C_6H_2-2,4,6-Pr^i_3)$_2$-3,5-Pr^i_2): An organoaluminum(I) compound with a one-coordinate aluminum atom. *J. Am. Chem. Soc.* **142**, 20554–20559 (2020). doi:10.1021/jacs.0c10222 Medline

34. H. Fujii, ^{13}C NMR signal detection of iron-bound cyanide ions in ferric cyanide complexes of heme proteins. *J. Am. Chem. Soc.* **124**, 5936–5937 (2002). doi:10.1021/ja025737y Medline

35. Y. Hiraoka, T. Ikeue, H. Sakiyama, F. Guégan, D. Luneau, B. Gillon, I. Hiromitsu, D. Yoshioka, M. Mikuriya, Y. Kataoka, M. Handa, An unprecedented up-field shift in the ^{13}C NMR spectrum of the carboxyl carbons of the lantern-type dinuclear complex TBA[$Ru_2(O_2CCH_3)_4Cl_2$] (TBA^+ = tetra(*n*-butyl)ammonium cation). *Dalton Trans.* **44**, 13439–13443 (2015). doi:10.1039/C5DT01680K Medline

36. J. Ví Cha, J. Novotný, S. Komorovsky, M. Straka, M. Kaupp, R. Marek, Relativistic heavy-neighbor-atom effects on NMR shifts: Concepts and trends across the periodic table. *Chem. Rev.* **120**, 7065–7103 (2020). doi:10.1021/acs.chemrev.9b00785 Medline

37. M. O. Krause, J. H. Oliver, Natural widths of atomic *K* and *L* levels, *K*α x-ray lines and several *KLL* Auger lines. *J. Phys. Chem. Ref. Data* **8**, 329–338 (1979). doi:10.1063/1.555595

38. F. Neese, F. Wennmohs, U. Becker, C. Riplinger, The ORCA quantum chemistry program package. *J. Chem. Phys.* **152**, 224108 (2020). doi:10.1063/5.0004608 Medline

39. F. Neese, Software update: The ORCA program system—Version 5.0. *Wiley Interdiscip. Rev. Comput. Mol. Sci.* **12**, e1606 (2022). doi:10.1002/wcms.1606

40. M. Wu, H. Li, W. Chen, D. Wang, Y. He, L. Xu, S. Ye, G. Tan, A triplet stibinidene. *Chem* 10.1016/j.chempr.2023.05.005 (2023). doi:10.1016/j.chempr.2023.05.005

41. R. Evans, Z. Deng, A. K. Rogerson, A. S. McLachlan, J. J. Richards, M. Nilsson, G. A. Morris, Quantitative interpretation of diffusion-ordered NMR spectra: Can we rationalize small molecule diffusion coefficients? *Angew. Chem. Int. Ed.* **52**, 3199–3202 (2013). doi:10.1002/anie.201207403 Medline

42. R. Evans, G. Dal Poggetto, M. Nilsson, G. A. Morris, Improving the interpretation of small molecule diffusion coefficients. *Anal. Chem.* **90**, 3987–3994 (2018). doi:10.1021/acs.analchem.7b05032 Medline

43. Y. He, C. Dai, D. Wang, J. Zhu, G. Tan, Phosphine-stabilized germylidenylpnictinidenes as synthetic equivalents of heavier nitrile and isocyanide in cycloaddition reactions with alkynes. *J. Am. Chem. Soc.* **144**, 5126–5135 (2022). doi:10.1021/jacs.2c00305 Medline

44. E. Welter, R. Chernikov, M. Herrmann, R. Nemausat, A beamline for bulk sample x-ray absorption spectroscopy at the high brilliance storage ring PETRA III. *AIP Conf. Proc.* **2054**, 040002 (2019). doi:10.1063/1.5084603

45. S. Diaz-Moreno, S. Hayama, M. Amboage, A. Freeman, J. Sutter, G. Duller, I20; the versatile x-ray absorption spectroscopy beamline at Diamond Light Source. *J. Phys. Conf. Ser.* **190**, 012038 (2009). doi:10.1088/1742-6596/190/1/012038

46. S. Hayama, G. Duller, J. P. Sutter, M. Amboage, R. Boada, A. Freeman, L. Keenan, B. Nutter, L. Cahill, P. Leicester, B. Kemp, N. Rubies, S. Diaz-Moreno, The scanning four-bounce monochromator for beamline I20 at the Diamond Light Source. *J. Synchrotron Radiat.* **25**, 1556–1564 (2018). doi:10.1107/S1600577518008974 Medline

47. M. Newville, Larch: An analysis package for XAFS and related spectroscopies. *J. Phys. Conf. Ser.* **430**, 012007 (2013). doi:10.1088/1742-6596/430/1/012007

48. M. Newville, T. Stensitzki, D. B. Allen, A. Ingargiola, LMFIT: Non-linear least-square minimization and curve-fitting for Python. Zenodo (2014); https://doi.org/10.5281/zenodo.11813.

49. E. van Lenthe, J. G. Snijders, E. J. Baerends, The zero-order regular approximation for relativistic effects: The effect of spin–orbit coupling in closed shell molecules. *J. Chem. Phys.* **105**, 6505–6516 (1996). doi:10.1063/1.472460

50. C. van Wüllen, Molecular density functional calculations in the regular relativistic approximation: Method, application to coinage metal diatomics, hydrides, fluorides and chlorides, and comparison with first-order relativistic calculations. *J. Chem. Phys.* **109**, 392–399 (1998). doi:10.1063/1.476576

51. A. D. Becke, A new mixing of Hartree–Fock and local density-functional theories. *J. Chem. Phys.* **98**, 1372–1377 (1993). doi:10.1063/1.464304

52. P. J. Stephens, F. J. Devlin, C. F. Chabalowski, M. J. Frisch, Ab initio calculation of vibrational absorption and circular dichroism spectra using density functional force fields. *J. Phys. Chem.* **98**, 11623–11627 (1994). doi:10.1021/j100096a001

53. F. Weigend, R. Ahlrichs, Balanced basis sets of split valence, triple zeta valence and quadruple zeta valence quality for H to Rn: Design and assessment of accuracy. *Phys. Chem. Chem. Phys.* **7**, 3297–3305 (2005). doi:10.1039/b508541a Medline

54. D. A. Pantazis, F. Neese, All-electron scalar relativistic basis sets for the 6p elements. *Theor. Chem. Acc.* **131**, 1292 (2012). doi:10.1007/s00214-012-1292-x

55. S. Grimme, J. Antony, S. Ehrlich, H. Krieg, A consistent and accurate ab initio parametrization of density functional dispersion correction (DFT-D) for the 94 elements H-Pu. *J. Chem. Phys.* **132**, 154104 (2010). doi:10.1063/1.3382344 Medline

56. D. Bykov, T. Petrenko, R. Izsák, S. Kossmann, U. Becker, E. Valeev, F. Neese, Efficient implementation of the analytic second derivatives of Hartree–Fock and hybrid DFT

energies: A detailed analysis of different approximations. *Mol. Phys.* **113**, 1961–1977 (2015). doi:10.1080/00268976.2015.1025114

57. C. Angeli, R. Cimiraglia, S. Evangelisti, T. Leininger, J. P. Malrieu, Introduction of *n*-electron valence states for multireference perturbation theory. *J. Chem. Phys.* **114**, 10252–10264 (2001). doi:10.1063/1.1361246

58. W. Kutzelnigg, W. Liu, Quasirelativistic theory equivalent to fully relativistic theory. *J. Chem. Phys.* **123**, 241102 (2005). doi:10.1063/1.2137315 Medline

59. P. Pollak, F. Weigend, Segmented contracted error-consistent basis sets of double- and triple-ζ valence quality for one- and two-component relativistic all-electron calculations. *J. Chem. Theory Comput.* **13**, 3696–3705 (2017). doi:10.1021/acs.jctc.7b00593 Medline

60. Y. J. Franzke, R. Treß, T. M. Pazdera, F. Weigend, Error-consistent segmented contracted all-electron relativistic basis sets of double- and triple-zeta quality for NMR shielding constants. *Phys. Chem. Chem. Phys.* **21**, 16658–16664 (2019). doi:10.1039/C9CP02382H Medline

61. B. A. Heß, C. M. Marian, U. Wahlgren, O. Gropen, A mean-field spin-orbit method applicable to correlated wavefunctions. *Chem. Phys. Lett.* **251**, 365–371 (1996). doi:10.1016/0009-2614(96)00119-4

62. F. Neese, Efficient and accurate approximations to the molecular spin-orbit coupling operator and their use in molecular *g*-tensor calculations. *J. Chem. Phys.* **122**, 34107 (2005). doi:10.1063/1.1829047 Medline

63. F. Neese, E. I. Solomon, Calculation of zero-field splittings, g-values, and the relativistic nephelauxetic effect in transition metal complexes. Application to high-spin ferric complexes. *Inorg. Chem.* **37**, 6568–6582 (1998). doi:10.1021/ic980948i Medline

64. D. Ganyushin, F. Neese, First-principles calculations of zero-field splitting parameters. *J. Chem. Phys.* **125**, 24103 (2006). doi:10.1063/1.2213976 Medline

65. F. Neese, T. Petrenko, D. Ganyushin, G. Olbrich, Advanced aspects of ab initio theoretical optical spectroscopy of transition metal complexes: Multiplets, spin-orbit coupling and resonance Raman intensities. *Coord. Chem. Rev.* **251**, 288–327 (2007). doi:10.1016/j.ccr.2006.05.019

66. M. Atanasov, D. Ganyushin, K. Sivalingam, F. Neese, "A modern first-principles view on ligand field theory through the eyes of correlated multireference wavefunctions" in *Molecular Electronic Structures of Transition Metal Complexes II*, vol. 143 of Structure and Bonding series, D. M. P. Mingos, P. Day, J. P. Dahl, Eds. (Springer, 2012), pp. 149–220.

67. M. Atanasov, D. Aravena, E. Suturina, E. Bill, D. Maganas, F. Neese, First principles approach to the electronic structure, magnetic anisotropy and spin relaxation in mononuclear 3d-transition metal single molecule magnets. *Coord. Chem. Rev.* **289-290**, 177–214 (2015). doi:10.1016/j.ccr.2014.10.015